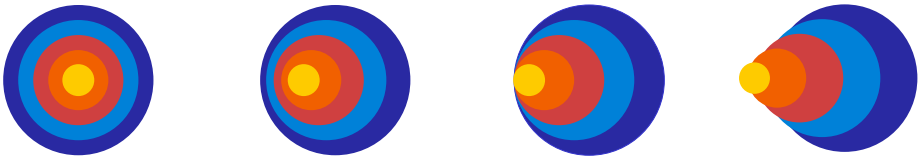
arXiv:0711.4416v1 [gr-qc] 28 Nov 2007

Emergent spacetimes

Silke Christine Edith Weinfurtner



Department of Mathematics, Statistics and Computer Science — Te Kura Tatau

VICTORIA UNIVERSITY OF WELLINGTON
Te Whare Wānanga o te Ūpoko o te Ika a Māui



Thesis submitted for the degree of Doctor of Philosophy
at the Victoria University of Wellington.

In Memory of
Johann Weinfurtner

Abstract

In this thesis we discuss the possibility that spacetime geometry may be an emergent phenomenon. This idea has been motivated by the Analogue Gravity programme. An “effective gravitational field” dominates the kinematics of small perturbations in an Analogue Model. In these models there is no *obvious* connection between the “gravitational” field tensor and the Einstein equations, as the emergent spacetime geometry arises as a consequence of linearising around some classical field. After a brief survey of the most relevant literature on this topic, we present our contributions to the field.

First, we show that the spacetime geometry on the equatorial slice through a rotating Kerr black hole is formally equivalent to the geometry felt by phonons entrained in a rotating fluid vortex. The most general acoustic geometry is compatible with the fluid dynamic equations in a collapsing/ expanding perfect-fluid line vortex. We demonstrate that there is a suitable choice of coordinates on the equatorial slice through a Kerr black hole that puts it into this vortex form; though it is not possible to put the entire Kerr spacetime into perfect-fluid “acoustic” form.

We then discuss an analogue spacetime based on the propagation of excitations in a 2-component Bose–Einstein condensate. This analogue spacetime has a very rich and complex structure, which permits us to provide a mass-generating mechanism for the quasi-particle excitations. Additionally, we show that the analogue spacetime based on 2-component Bose–Einstein condensates provides models not just for standard general relativistic spacetimes, but also for the more general bi-metric, and even more general pseudo–Finsler spacetimes.

Furthermore, at short distances, where microscopic corrections due to the substructure (*i.e.*, the fundamental Bosons) can no longer be neglected, and even in the mono-metric regime, one begins to see deviations from “Lorentz invariance” — these deviations are qualitatively of the type encountered in “quantum gravity phenomenology”, with the interesting property that the Lorentz violating physics is naturally suppressed by powers of the quasi-particle mass divided by the mass of the fundamental bosons that form the condensate.

A completely different issue can be probed in a single component BEC. This system naturally exhibits a microscopic mechanism allowing us to perform controlled signature change between

Lorentzian and Riemannian geometries. We calculate the number of particles produced from a finite-duration Euclidean signature event, focussing on its impact on particle production in the ultraviolet regime, and the possibility of using the proposed signature change event as an amplifier for pre-existing fluctuations in condensed matter experiments.

Last but not least, we investigate cosmological particle production in a Bose–Einstein condensate with tunable microscopic interaction strength. Here Lorentz invariance emerges in the infrared limit, but is explicitly broken in the ultraviolet regime. Thus these models are similar to many (but not all) models of quantum gravity, where a breakdown of Lorentz invariance is expected for ultraviolet physics around the Planck/ string scale. Motivated by previous studies on spacetimes emerging from a microscopic substrate, we show how these modifications naturally lead to momentum-dependent rainbow metrics. In detail we investigate the robustness of the particle production process against the model-specific modifications, and also encounter cosmological particle production in "rainbow inflation".

We conclude with a brief discussion of lessons learned from these emergent spacetime models.

Contents

Abstract i

Contents iii

List of Figures vii

List of Tables ix

Acknowledgments xi

1 Introduction 1
- 1.1 Spacetime geometry . . . 1
 - 1.1.1 Einstein field equations . . . 2
 - 1.1.2 Analogue spacetime geometry . . . 3
- 1.2 Quantum aspects of analogue gravity . . . 7
 - 1.2.1 Semi-classical quantum gravity . . . 8
 - 1.2.2 Quantum gravity phenomenology . . . 15
 - 1.2.3 Gravity as an emergent phenomenon? . . . 16

2 Acoustic analogues of the Kerr black hole 19
- 2.1 Geometrical and physical acoustics . . . 19
 - 2.1.1 The role of dimension . . . 20
 - 2.1.2 Various coordinate systems . . . 22
- 2.2 Acoustic non-rotating black holes . . . 23
 - 2.2.1 Geometrical acoustics and the Painléve–Gullstrand geometry . . . 24
 - 2.2.2 Acoustic isotropic version of the Schwarzschild geometry . . . 24
 - 2.2.3 Acoustic spherically symmetric geometries . . . 26
 - 2.2.4 The problem with acoustic rotating black holes . . . 26
- 2.3 General vortex flow in fluids . . . 27

2.3.1 General framework . . . 27
2.3.2 Zero radial flow . . . 28
2.3.3 General analysis with radial flow . . . 30
2.4 Rotating black holes . . . 34
2.4.1 Kerr black holes . . . 34
2.4.2 The ergosphere . . . 37
2.4.3 The Kerr equator . . . 38
2.5 Acoustic Kerr equator . . . 40
2.6 Discussion . . . 43

3 Emergent particle masses in Lorentzian and Finslerian geometries 47
3.1 Theory of the 2-component BEC . . . 47
3.1.1 Gross–Pitaevskii equation . . . 49
3.1.2 Dynamics . . . 49
3.1.3 Healing length . . . 52
3.2 Emergent spacetime at low energies . . . 54
3.2.1 Pseudo-Finsler geometry . . . 55
3.2.2 Bi-metric geometry . . . 58
3.2.3 Mono-metric geometry . . . 61
3.2.4 Merging spacetime geometry with mass eigenmodes . . . 61
3.2.5 Special case: $\Xi =$ constant. . . . 62
3.3 Outlook, summary and discussion . . . 65

4 Analogue quantum gravity phenomenology 67
4.1 Application to quantum gravity phenomenology . . . 68
4.1.1 Specializing the wave equation . . . 70
4.1.2 Hydrodynamic approximation . . . 71
4.1.3 Beyond the hydrodynamic approximation . . . 74
4.1.4 The relevance for quantum gravity phenomenology . . . 78

5 Early universe cosmology in emergent spacetime 85
5.1 Introduction and Motivation . . . 85
5.2 Emergent geometry from a Bose gas . . . 87
5.2.1 Ultra-cold, weakly interacting Bose gas . . . 88
5.2.2 Analogue spacetime . . . 91
5.3 Sudden changes in spacetime geometry . . . 92
5.3.1 Quantum fields as harmonic oscillators . . . 92
5.3.2 Particle production . . . 94
5.4 Signature change events . . . 98

5.4.1 Classical aspects . . . 98
5.4.2 Particle production from a finite-duration Euclidian region . . . 99
5.5 Ultraviolet corrections . . . 101
5.5.1 Rainbow geometries . . . 101
5.5.2 Lorentz symmetry violation and Particle Production . . . 103
5.6 Particle Amplifier for Cosmological Particle Production . . . 104
5.6.1 Main concept . . . 105
5.6.2 Simple example . . . 106
5.7 Conclusions . . . 107

6 Cosmological inflation in emergent rainbow spacetime 113
6.1 Introduction . . . 114
6.2 Emergent spacetimes . . . 117
6.2.1 Ultraviolet non-perturbative corrections . . . 117
6.2.2 FRW-rainbow geometries . . . 124
6.3 Quantum field theory in rainbow geometries . . . 127
6.3.1 Particle production . . . 128
6.3.2 Finiteness of particle production in emergent spacetimes . . . 135
6.4 FRW-rainbow spacetimes in $(2+1)$ dimensions . . . 138
6.4.1 $(2+1)$ dimensional FRW-rainbow spacetimes . . . 138
6.4.2 Inflation in emerging universe . . . 139
6.4.3 Quantum field theory and rainbow inflation . . . 143
6.5 Conclusions and outlook . . . 160

7 Summary & Conclusions 163

A Publications not included in the thesis 167
A.1 Generating perfect fluid spheres in general relativity . . . 168
A.2 Solution generating theorems for the TOV equation . . . 169
A.3 Analogue model of a FRW universe in *realistic* Bose–Einstein condensates . . . 170
A.4 Effective refractive index tensor for weak field gravity . . . 171

B Klein–Gordon equation and exterior derivatives 173
B.1 Differential forms and exterior derivatives in brief . . . 173
B.2 Index-free Klein–Gordon equation . . . 174

C Finsler and co–Finsler geometries 175
C.1 Basics . . . 175
C.2 Connection with the quasi-particle PDE analysis . . . 177
C.3 Lorentzian signature Finsler geometries . . . 179

C.4 Summary 181

D Some matrix identities **183**
D.1 Determinants 183
D.2 Hamilton–Cayley theorems 184

E Junction conditions **185**
E.1 Basics 185
E.2 The two non-overlapping simple regions 186
E.3 Normalization 187
E.4 Applying the junction conditions 188
E.5 Using “canonical time” 189

F Numerical results for rainbow inflation **193**
F.1 Quasi-particle production during rainbow inflation for $t_s = 1 \times 10^{-4}$ 194
F.2 Qualitative particle production in Bose gas 195

Curriculum Vitae **199**

Publications **201**

Bibliography **204**

List of Figures

1.1 Sound waves in acoustic black hole spacetime. 11

2.1 Non-collapsing vortex geometry. 29
2.2 Collapsing vortex geometry. 30
2.3 Rotating Kerr black hole. 36
2.4 Penrose Process. 37
2.5 Sound speed and rotational background velocity in acoustic Kerr geometry. 44
2.6 Fluid density in acoustic Kerr geometry. 44
2.7 Conformal factor in acoustic Kerr geometry. 45

3.1 Energy levels for Rb^{87}. 48
3.2 Overview of fine tuning. 54
3.3 Mass generation in n-component system. 66

4.1 Emergent Lorentz symmetry. 68

5.1 Schematic outline for sudden Lorentzian changes. 97
5.2 Schematic outline for sudden Euclidean changes. 99
5.3 Particle Amplifier for quantum fluctuations. 105
5.4 Particle spectra for sudden Lorentzian and Euclidean changes in emergent geometry. 108

6.1 Rainbow scale factor for effective inflation in Bose gas. 141
6.2 Quasi-particle production during rainbow inflation — I. 145
6.3 Qualitative particle production in Bose gas. 150
6.4 Long lasting rainbow inflation. 157
6.5 Final particle spectra. 159
6.6 Final particle spectra. 160

F.1 Quasi-particle production during rainbow inflation — II. 194

F.2 Qualitative particle production in Bose gas — A. 195
F.3 Qualitative particle production in Bose gas — B. 196
F.4 Qualitative particle production in Bose gas — C. 196
F.5 Qualitative particle production in Bose gas — D. 197

List of Tables

3.1 Tuning conditions. 60

Acknowledgments

Dear Matt, I cannot thank you enough for your tremendous support during the last three years. In endless conversations, discussions and explanations you have helped me to find my way through analogue models for gravity. With your infectious passion for science, you have motivated and encouraged me to pursue my scientific career. Rather than imposing your ideas, you helped me find my own way, and supported a (guided) scientific independence. You kept on pushing me to another level, the $(3+1)$-sentence "Finish the paper, now!", will always be indelibly branded in my mind. Also on Martin's behalf, I thank you for your friendliness, many interesting conversations and numerous excursions around New Zealand. I am looking forward to hosting you in Vancouver, to continue our lunch time conversations and collaborations.

Next I would like to thank Dr. Stefano Liberati, with his infectious passion for the analogue model programme. Over the last three years you were a source of knowledge and inspiration, and this thesis would not be the same without you. Someone whose opinion I regard highly once told me, that the transformation from an undergraduate student to a Postdoctoral fellow is similar to the metamorphosis that is involved turning a caterpillar into a butterfly. As a matter of fact, you never treated me like a graduate student, more as a collaborator and friend. I always felt very welcome when I stayed with you and your wife Paola. I would like to thank you both, for your support and friendship.

A couple of years ago Dr. Susan Scott and Dr. Craig Savage suggested a collaboration between their PhD student Angela White and myself, to work on issues related to analogue models in Bose–Einstein-condensates. I would like to thank Susan and Craig for their scientific and financial support. In both visits I felt warmly welcomed and enjoyed working at the Australian National University (ANU). Dear Angela, thank you for your hospitality and your friendship.

I also would like to thank my New Zealand collaborators Prof. Crispin Gardiner and his PhD student Piyush Jain. In many stimulating and fruitful conversations I had the opportunity to gain a deeper and different insight into condensed matter physics, and I would like to thank you both for that. Dear Piyush, thank you for your friendship which made the initial time in New Zealand so much

easier.

I also would like to thank my colleagues Petarpa Boonserm and Celine Cattoën for sharing an office with me, and especially their support during the last few weeks. I wish you both good luck with your future careers, and I am looking forward to seeing you again. Dear Petarpa, whenever you feel a longing to revisit the Bavarian Forest, my mother and I will always welcome you as our special guest.

I shall not forget to thank the staff at the Department for Mathematics, Statistics and Computer Science for providing an ideal working environment. I really enjoyed studying for my PhD at Victoria University, and generally the time I spent in Aotearoa (the land of the long white cloud).

CHAPTER 1

Introduction

This chapter is an introduction to *Analogue Models of (and possibly for) Gravity*. We shall review important issues of general relativity and quantum aspects of gravity, that are necessary to derive the notion of emergent spacetime geometry, without *obvious* connection with the Einstein field equations.

1.1 | Spacetime geometry

In 1915 Albert Einstein presented to the world a theory of gravitation where gravity is not a force but a consequence of *spacetime geometry* [65, 66, 67]. This theory is based on the unification of d dimensional space *and* time, such that time is playing the role of an "extra" dimension in a $n = (d+1)$ dimensional *spacetime*. The geometry of spacetime — in 3 spatial dimensions — is characterized by the metric tensor

$$g_{ab} = \begin{bmatrix} g_{00} & g_{01} & g_{02} & g_{03} \\ g_{01} & g_{11} & g_{12} & g_{13} \\ g_{02} & g_{12} & g_{22} & g_{23} \\ g_{03} & g_{13} & g_{23} & g_{33} \end{bmatrix}, \tag{1.1}$$

a symmetric covariant rank 2 tensor. Without any further specification, *e.g.*, the Einstein equations, coordinate conditions, or spacetime symmetries, the *metric tensor* (1.1) has $n(n+1)/2$ independent — here 10 — components. Each component may be a function of time and space $g_{ab} = g_{ab}(t, \mathbf{r})$.

In general relativity *free* particles are *freely falling* particles; they are free from any external force but remain under the influence of the spacetime geometry. Under the assumption that the mass of the object is small enough not to interfere with the gravitational field g_{ab}, the *kinematic* equations of

motion are obtained by the principle of least action. The world line for a *free test particle* connecting two points A and B in the n dimensional spacetime extremizes the "distance"

$$s_{AB} = \int_A^B ds = \int_A^B \left[-g_{ab}\, dx^a\, dx^b \right]^{1/2} , \tag{1.2}$$

between them. The world lines are called geodesics; we are dealing with a curved spacetime geometry, as opposed to Newtonian gravity where the three dimensional space is considered to be *Euclidean* and flat. [► The *signature* of flat or curved n dimensional spacetime differs from that of a flat or curved n dimensional space. We study this topic in greater detail in Chapter 5.]

This geometrical interpretation of the gravitational field is only one aspect of Einstein's theory of general relativity.

1.1.1 | Einstein field equations

The second aspect of general relativity is to identify — in a coordinate covariant manner — the density and flux of energy and momentum in the n dimensional spacetime as the source of the gravitational field g_{ab}, in a manner similar to the way that mass is the source for the gravitational force in Newtonian gravity.

The *Einstein field equations*,

$$G_{ab} = 8\pi G_{\rm N}\, T_{ab} , \tag{1.3}$$

relate (part of) the local curvature in the gravitational field G_{ab} to the matter energy density T_{ab}. The current value — provided by the Committee on Data for Science and Technology (CODATA) — for the universal *Newtonian constant of gravitation* is $G_{\rm N} = 6.67428(67) \times 10^{-11}\ m^3\, kg^{-1}\, s^{-2}$.

The covariant tensor G_{ab}, referred to as the Einstein tensor,

$$G_{ab} = R_{ab} - \tfrac{1}{2} R\, g_{ab} , \tag{1.4}$$

depends on second derivatives of the gravitational field, the Ricci tensor $R_{ab} = R^c{}_{acb}$, and Ricci scalar $R = R^{bc}{}_{bc}$. [1] On the right hand side of Eq. (1.3) we have the stress-energy tensor, defined as

$$T^{ab} = \left[\begin{array}{c|c} \text{energy density} & \text{energy fluxes} \\ \hline \text{momentum densities} & \text{stress tensor} \end{array} \right] . \tag{1.6}$$

[1] In general the Riemann tensor

$$R^a{}_{bcd} = -\left(\partial_d \Gamma^a{}_{bc} - \partial_b \Gamma^a{}_{bd} + \Gamma^a{}_{md} \Gamma^m{}_{bc} - \Gamma^a{}_{mc} \Gamma^m{}_{bd} \right) , \tag{1.5}$$

is given in terms of first derivatives and quadratic combinations of *Christoffel symbols*, $\Gamma^a{}_{bc} = \frac{1}{2}\, g^{ad} \left(\partial_b g_{cd} + \partial_c g_{bd} - \partial_d g_{bc} \right)$. Note, that $\Gamma^a{}_{bc}$ is *not* a tensor. In Riemann normal coordinates, $\Gamma^a{}_{(bc,d)}|_p = 0$ at the point p, the Ricci tensor simplifies to $R_{ab} = \frac{1}{2}\, g^{cd} \left(g_{cd,b,a} - g_{db,c,a} + g_{ab,c,d} - g_{ac,b,d} \right)$.

The stress-energy tensor is a covariantly conserved entity, such that $\nabla_b T^{ab} = 0$. [2]

Automatically, the Einstein equations are such that they fulfill the contracted Bianchi identities

$$\nabla_b G^{ab} = 0\,. \tag{1.8}$$

The contracted Bianchi identities reflect the coordinate freedom and impose n conditions on the n-dimensional gravitational field. (So in $3+1$ dimensions the metric effectively has 6 free components.)

There are three different approaches to the Einstein field equations: (1) For any given metric tensor we can calculate the stress-energy density (and then check to see if it is "physically reasonable"), (2) for any given stress-energy density we can calculate the corresponding gravitational field (possibly up to a few integration constants), and (3) the Einstein field equations can be viewed as *dynamical* equations for the gravitational field, correlating changes in the stress-energy density (the cause of gravitation) with changes in the local spacetime curvature (the effect of gravitation).

[► In [32] we study exact solutions for perfect fluid spheres. Based on known solutions we show how to generate new solutions without explicitly solving the Einstein equation. For the abstract of this article see Appendix A.1. In the subsequent paper [33] we connected the differences in the gravitational field between "old" and "new" solutions with changes in the stress-energy density; for abstract see Appendix A.2]

Thus at first glance it seems that the notion of spacetime geometry is inevitably associated with the Einstein field equations. However, in the following we present a model for an effective $(d+1)$ dimensional spacetime geometry, where the metric tensor g_{ab} is *not* obtained by solving the Einstein equations. In the literature this phenomenon is referred to as an *analogue model for gravity* or an *analogue spacetime*.

1.1.2 | Analogue spacetime geometry

The first modern paper on analogue spacetime geometry was published in 1981 by *Bill Unruh* [173], followed by *Matt Visser* [178] in 1993. The authors demonstrated that the effective propagation of *sound waves* in a fluid flow is given in terms of geodesics in an *acoustic* "spacetime geometry". Since then an increasing number of articles have been published on this subject, now commonly

[2] As pointed out in the beginning of this section, the tensorial structure of the Einstein equations is maintained in any coordinatization. This has been achieved by the replacement of partial derivatives ∂ with *covariant* derivatives ∇. The covariant derivative ∇_a acting on an arbitrary tensor field $T^{b_1\cdots b_k}{}_{c_1\cdots c_l}$ is

$$\nabla_a T^{b_1\cdots b_k}{}_{c_1\cdots c_l} = \partial_a T^{b_1\cdots b_k}{}_{c_1\cdots c_l} + \sum_{\alpha=1}^{k} \Gamma^{b_\alpha}{}_{\sigma a} T^{b_1\cdots\sigma\cdots b_k}{}_{c_1\cdots c_l} + \sum_{\beta=1}^{l} \Gamma^{\sigma}{}_{c_\beta a} T^{b_1\cdots b_k}{}_{c_1\cdots\sigma\cdots c_l}\,, \tag{1.7}$$

a combination of partial derivatives and Christoffel symbols.

referred to as “Analogue Gravity” [18]. In the following sections we briefly summarize aspects of analogue gravity relevant for this thesis, and refer the reader interested in more details to the review article “Analogue Gravity”, freely available online through *Living Reviews in Relativity* [18].

A simple example: Sound waves in a fluid flow

The *kinematic* equations for small — classical or quantum — perturbations (*i.e.*, sound waves) in a barotropic, inviscid and irrotational fluid are given by

$$\frac{1}{\sqrt{-g}}\,\partial_a\left(\sqrt{-g}g^{ab}\partial_b\phi\right)=0\,, \tag{1.9}$$

which represents a massless minimally coupled scalar field in an *effective* curved spacetime. The sound waves experience an acoustic metric,

$$g_{ab}\propto\begin{bmatrix}-(c^2-v^2) & -v_j\\ -v_i & \delta_{ij}\end{bmatrix}\,, \tag{1.10}$$

whose entries include the purely collective variables $c=c(t,\mathbf{x})$, the sound speed, and $\mathbf{v}=\mathbf{v}(t,\mathbf{x})$, the background velocity. Here the indices run from 1 to d, where d is the spatial dimension of the fluid. For a detailed derivation of this result see Refs. [173, 178, 144, 18].

Therefore it is possible to read off the metric components from the “covariant” classical ϕ or quantum $\hat{\phi}$ field equation (1.9). In a broader sense we are dealing effectively with a semi-classical model, where the matter fields are quantized $\hat{\phi}$, but the entries in the *acoustic* metric remain classical. We will elaborate on this in Section 1.2.1.

Vorticity. The macroscopic fluid parameters can easily be chosen to design emergent non-rotating black holes [173, 112, 178]. [▶ In Chapter 2 we analyzed the possibility of developing acoustic rotating Kerr black hole geometries, where we analyze the most general vortex flow in fluids.] Since many “real” fluids exhibit vortices, it is — *not only* from a gravity point of view, see Chapter 2 — desirable to extend the concept of acoustic metrics to rotational fluids. First attempts to derive the acoustic metric in a (barotropic and inviscid) fluid with vorticity have been carried out in [149].

Substantive derivative. The *substantive* derivative (also referred to as *fluid following*, or *material*, or *advective* derivative) in a fluid is defined as

$$\frac{D\star}{Dt}=\frac{\partial\star}{\partial t}+\vec{v}\cdot\nabla\,\star\,. \tag{1.11}$$

[▶ The material derivative plays an important role in quantum field theory in effective curved spacetimes, as we show explicitly in 5.2.2 and in 6.2.1, where we relate the material derivative to the conjugate momentum on the emergent spacetime geometry; see also [176].]

Geometrical and physical acoustics. In Eq. (1.10) we give an expression for the acoustic metric up to an overall conformal factor. This representation is referred to as the *geometrical acoustics approximation*, which is good enough to describe how sound rays propagate in the fluid. Since the overall conformal factor can in general be a function of space and time, and also explicitly depending on the spatial dimensions, we require — for the full kinematic equations — the "complete" metric, this is referred to as the *physical acoustics approximation*. [► In Chapter 2 we discuss geometrical and physical acoustics in detail, and outline some of the consequences of the overall conformal factor.]

Zero background velocity For $\vec{v} = \vec{0}$ we obtain

$$g_{ab} \rightarrow \eta_{ab} \propto \begin{bmatrix} -c^2 & 0 \\ 0 & \delta_{ij} \end{bmatrix} , \tag{1.12}$$

an acoustic Lorentzian flat spacetime (or acoustic Minkowski) geometry, as long as $c^2 > 0$. In general we notice that the acoustic metric for 2 and 3 spatial dimensions describes a Lorentzian (pseudo-Riemannian) geometry. [► In Chapter 5 we present a specific analogue model, that exhibits a natural mechanism to change between Lorentzian $(-,+++)$, and Riemannian $(+,+++)$ *effective* spacetime geometries.]

A catalogue of models

Over the last 25 years the basic concept of analogue models has been transferred to many different media. There is a broad class of systems that possess an emergent spacetime in the low-energy regime. We would like to list some of the different models that have been studied in the past. More background information and current developments can be found in [144, 18].

Sound in moving fluids The fluid can be any barotropic, inviscid and irrotational fluid. As mentioned above, the first (modern) papers on this subject were written by *Bill Unruh* [172, 173, 175] and *Matt Visser* [178, 181, 180, 179]. (For more details see above, or in Refs. [144, 18]. We will revisit these models below when we discuss the quantum aspects of analogue spacetime geometry.)

Shallow water waves (gravity waves) The natural occurrence of an acoustic metric governing the propagation of ripples in a basin filled with liquid has been pointed out by *Ralf Schützhold* and *Bill Unruh* in 2002 [166]. The acoustic line element is given in terms of the background velocity parallel to the basin $\vec{v}_B^{\,II}$, as

$$ds^2 = \frac{1}{c^2} \left[-(c^2 - (v_B^{II})^2)\, dt^2 - 2\, \vec{v}_B^{\,II} \cdot d\vec{x}\, dt + d\vec{x}^{\,T} \cdot d\vec{x} \right] . \tag{1.13}$$

Noticeable in this model is the extreme ease with which the velocity of the surface waves,

$$c^2 = g\, h_B \,, \tag{1.14}$$

can be adjusted by changing the depth h_B of the basin. (The variations in the gravity waves at the surface of the fluid in the basin are caused by the presence of Earth's gravity.)

Classical refractive index The Maxwell equations inside a dielectric material in flat 4 dimensional Minkowski spacetime can be written in a very condensed way,

$$\partial_b \left(Z^{abcd} F_{cd} \right) = 0. \tag{1.15}$$

As usual $F_{cd} = -2 A_{[c,d]}$ is the electromagnetic tensor, and Z^{abcd} is a rank 4 tensor whose components are functions of the components of the 3×3 permittivity tensor ϵ, and the 3×3 permeability tensor μ of the dielectric.

The dielectric can be adjusted such that the equations for the electric field (in flat spacetime inside the dielectric) are similar to the equation for an electric field in an *effective* curved spacetime inside vacua. [► In [31] we have shown the reverse analogy, how weak-field gravity can be interpreted in terms of an *effective* refractive index. For abstract see A.4.]

Electromagnetic wave-guide In 2006 *Ralf Schützhold* and *Bill Unruh* [161] showed the possibility of manipulating electromagnetic waves in a wave-guide so that they experience an effective curved spacetime (in the form of a $(2+1)$ dimensional Painléve–Gullstrand–Lemaître geometry).

The wave-guide consists of a ladder circuit with a time-dependent capacitance $C_n(t)$ at each rung of the ladder, while the coil in each loop has inductance $L_n = L =$ constant. The rungs are spatially separated by equal distances Δx. The current in each circuit is given by I_n, and we can define an effective potential A_n, such that $I_n = A_{n+1} - A_n$. For wave-length with $\lambda \gg \Delta x$ the discreteness of the x-axis is negligibly small, $A_n \to A(x)$, and in the continuum limit the wave equation is given by

$$\left[(\partial_t + v\,\partial_x)\; 1/c^2\; (\partial_t + v\,\partial_x) - \partial_x^2 \right] A(x) = 0\,. \tag{1.16}$$

Here the spacetime dependent propagation velocity can be arranged to be

$$c_n(t) = \Delta x / \sqrt{L\, C_n(t)} \to c(x + v\,t)\,, \tag{1.17}$$

a function of time and space, and the constant velocity v. (For smaller wavelengths the sound speed will be momentum-dependent, in a manner similar to Lattice field theory. We will turn back to this issue shortly, when we discuss the quantum aspects of analogue spacetime geometries, and also in the section about quantum gravity phenomenology.)

Condensed matter systems To the best of our knowledge the first to point out the analogy between curved spacetimes and condensed matter systems such as superfluid Helium, was *Grisha Volovik* in 1995 [191]. This was followed (2000/01) by *Luis Garay et al.* [81, 82], and

Carlos Barceló and *Matt Visser* [12] focussing on analogue models arising from Bose–Einstein condensates. Both systems are prime models for superfluids (zero viscosity), and yield similar kinematics to sound waves in a flowing fluid — as explained above.

In Chapers 3-6 we have focused on the latter, on spacetimes emerging from Bose gases. A derivation of the effective spacetime geometry starting from the many-body Hamiltonian for an ultra-cold weakly interacting gas of Bosons can be found in those chapters. Before we jump to the main part of this thesis, we would like to briefly summarize the (for this work) relevant applications and properties of analogue spacetime geometries. (While many of the presented topics are valid far beyond the specific model we discuss, the main focus of this thesis is on *emergent spacetime geometries* from Bose gases.)

We would like to comment on the *incompleteness* of the list we have just presented. To do justice to all existing models would go far beyond the scope of this thesis, to give a brief introduction to the field. We refer the interested reader to [144, 18] for more detail, for example to see a study on analogue models in quantum dielectrics [122, 176].

1.2 | Quantum aspects of analogue gravity

After more than 80 years of devoted research, the quest to unify quantum mechanics and gravity (general relativity) continues. While remarkable progress has been achieved in the unification of three out of the four forces of nature — the Weak force (Electroweak theory), the Electromagnetic force (Quantum Electrodynamics), and the Strong force (Quantum Chromodynamcis) — the Gravitational force (General Relativity) remains excluded. All direct attempts to quantize general relativity have been in vain, for example see [97, 96]. (However, limited progress has been made in other quantum gravity candidates, *e.g.*, string models.)

(From an emergent spacetime point of view any attempt to quantize the “emergent gravitational field” cannot be successful in reproducing the overall quantum theory of the analogue model. A quantization of the macroscopic fluid variables (*e.g.*, the Bose–Einstein condensate) will *not* reveal the microscopic degrees of freedom of the underlying substructure (*e.g.*, the ultra-cold weakly interacting gas of Bosons); for example see [19, 93, 195].)

From a general standpoint the question has to be asked if there is anything at all we can say about the occurrence of quantum phenomena in gravitational fields. Especially important for the analogue model programme is the demand for quantum effects where the (fully interacting) dynamical behavior in the gravitational field can be approximated by kinematical equations (no back-reaction). Only for those cases we can guarantee the *obvious* validity of the analogy, and employ the analogue for mimicking quantum field theory phenomena in *effective* curved spacetimes.

1.2.1 | Semi-classical quantum gravity

One particular approximation that circumvents the problem of quantizing the gravitational field itself is that called *semi-classical* quantum gravity. Here the gravitational field is treated as being a classical field, while the matter fields are treated as being quantum fields.

The stress-enery tensor of a matter field is given in terms of

$$T_{ab}(\mathbf{x}) = \frac{2}{\sqrt{-g}} \frac{\delta S^{\text{matter}}[g_{ab}, \phi]}{\delta g^{ab}(x)} , \tag{1.18}$$

the functional derivative of the matter action S^{matter} with respect to metric tensor. Therefore the quantization of the right hand side of the Einstein field equations (1.3) is relatively straightforward. It can be shown that the coupling of the matter fields to the gravitational field yields

$$G_{ab} = 8\pi G_{\text{N}} \langle \hat{T}_{ab} \rangle . \tag{1.19}$$

These are *semi-classical Einstein equations*, where vacuum fluctuations in the matter fields contribute to the gravitational field via the expectation value for the quantized stress-energy tensor. (A derivation of the semi-classical Einstein equations can be found *inter alia* in [29, 77, 141].)

Below we will focus on cases where back-reaction effects are negligibly small, and quantum field theory in curved spacetime is a sufficiently good approximation. In Chapters 5 and 6 we study quantum effects in a covariant *free* field, where no *external* forces act on the field, and the "gravitational force" is encoded in the spacetime geometry, $\eta_{ab} \rightarrow g_{ab}$. Within this approximation (semi-classical quantum gravity for small quantum effects), which only involves the kinematics of the gravitational field, analogue models for gravity can be employed for mimicking quantum aspects of "gravity".

Semi-classical quantum geometry

While it is relatively straightforward to derive semi-classical quantum gravity, the situation is much more difficult in the analogue gravity programme. Here the fundamental equations for the effective spacetime geometry are obtained from various media.

However, in [13, 18] the authors showed that the phenomenon of quantum field theory in *effective* curved spacetimes can be generalized in the following way. Small perturbations around some background solution $\phi_0(t, \mathbf{x})$,

$$\phi(t, \mathbf{x}) = \phi_0(t, \mathbf{x}) + \epsilon\, \phi_1(t, \mathbf{x}) + \frac{\epsilon^2}{2}\, \phi_2(t, \mathbf{x}) , \tag{1.20}$$

in a generic Lagrangian $\mathcal{L}(\partial_a\phi, \phi)$, depending only on a single scalar field and its first derivatives yields an effective spacetime geometry,

$$g_{ab}(\phi_0) = \left[-\det \left(\frac{\partial^2 \mathcal{L}}{\partial(\partial_a\phi)\, \partial(\partial_b\phi)} \right) \right]^{\frac{1}{d-1}} \Bigg|_{\phi_0} \left(\frac{\partial^2 \mathcal{L}}{\partial(\partial_a\phi)\, \partial(\partial_b\phi)} \right)^{-1} \Bigg|_{\phi_0} , \tag{1.21}$$

for the classical / quantum fluctuations. The equation of motion for small perturbations around the background ϕ_0 are then given by

$$\left(\Delta_{g(\phi_0)} - V(\phi_0)\right)\phi_1 = 0\,, \tag{1.22}$$

where $\Delta_{g(\phi_0)}$ is the d'Alembertian operator associated with the metric $g(\phi_0)$ and $V(\phi_0)$ is potential depending on the background. That is, we have derived an *effective* curved-spacetime quantum field theory description of the linearization process, under the premise that back-reaction effects are negligibly small. [► In Chapter 3 we show that multi-scalar fields yield interesting extensions of this framework for the analogue gravity programme. There we show that a 2-component Bose–Einstein condensate can be used for mimicking massive scalar fields in mono- and bi-metric Lorentzian, or even Finslerian spacetimes. A more general study on this topic has been carried out in [14, 186] by *Carlos Barceló*, *Matt Visser* and *Stefano Liberati*.]

Before we address specific quantum aspects of gravity, we wish to add a few comments regarding the quantum aspects of emergent spacetimes arising from condensed matter systems. The entries in the emergent spacetime metric are collective variables associated with the expectation value of the macroscopic mean-field description of the superfluid. In momentum space the condensate itself represents the (large) occupation number of the lowest energy state in the system. In some sense the Bose–Einstein condensate itself is quantum fluctuation where $k = 0$. Any change in the occupation number depletes the condensate, and therefore yields changes in the emergent gravitational field. So strictly speaking we are dealing with a *semi-classical quantum geometry*.

First attempts to include the back-reaction effects (here due to the Hawking effect, see below) of quantum fluctuations into the analogue gravity programme have been made 2004 by *Roberto Balbinot et al.*, where the authors assumed the validity of the Einstein equations for the acoustic spacetime geometry, see [7, 5, 6]. (While there is no *obvious* connection between the analogue models and the Einstein equations, there are some tentative indications in favor of emergent Einstein field equations, see Section 1.2.3.)

A completely different point of view on this topic has been presented 2005 by *Ralf Schützhold et al.* [164], where the back-reaction effects of quantum fluctuations (here Hawking radiation, see below) have been derived at the level of the fundamental Hamiltonian for the Bose gas. In this approach the quantum fluctuations are not necessarily expected to be small; so that significant corrections to the linearization process can be obtained.

[► In [113] we have taken an alternative route. We have employed *Classical Phase Space Methods* [83] to numerically simulate quantum effects (here Cosmological Particle Production, see below) in a "realistic" Bose–Einstein condensate, where (besides other deviations) back-reaction effects are automatically included. From our simulation it can be seen that indeed (as expected) back-reaction effects are negligibly small in the semi-classical quantum geometry picture.]

After a brief discussion of the validity of both theories, "usual" quantum field theory and *emergent* quantum field theory, we present three different cases where non-trivial gravitational / effective gravitational effects in quantum fields are expected.

Quantum aspects of black holes

We expect serious disturbances for quantum fields in the vicinity of a black hole, for field modes whose wavelengths are comparable or larger than the black hole radius. The first semi-classical treatment of quantum field theory in a black hole geometry has been carried out by *Stephen Hawking* in 1974 [91, 40]. Hawking showed that a Schwarzschild black hole emits a thermal radiation at a temperature T proportional to the surface gravity κ at the horizon,[3]

$$T = \frac{\kappa}{2\pi} \,. \tag{1.23}$$

Unfortunately, the surface temperature for example of a solar mass black hole, $\sim 10^{-7}$ Kelvin,[4] when compared to the 2.7 Kelvin of the surrounding cosmic background radiation is far too small for experimental verification. (The only hope is the existence of "primordial" black holes, relics of the early universe, that are expected to have masses of order 10^{15} gm.)

On this account analogue black hole geometries are of great interest, since they might be the only chance for experimentally measuring *effective* Hawking radiation. Indeed, the first modern analogue model, by *Bill Unruh*, explicitly discussed the possibility of "Experimental black hole evaporation" [173].

The acoustic metric for sound waves in a fluid, as given in Eq. (1.10), shows that we expect an *apparent horizon* — a locally definable horizon — at $c(t,\mathbf{x}) = |\vec{v}(t,\mathbf{x})|$, where g_{00} vanishes. In the region denoted by $c(t,\mathbf{x}) > |\vec{v}(t,\mathbf{x})|$ the sound waves are propagating faster than the background velocity, and the fluid is said to be *subsonic*. On the other hand, for $c(t,\mathbf{x}) < |\vec{v}(t,\mathbf{x})|$ the sound waves propagate with less speed than the background flow. Here the fluid flow dominates and the flow is said to be *supersonic*. Thus sound waves in the supersonic region are not free to propagate in any direction, they get dragged along with the fluid flow. In Figure 1.1 we illustrated sound waves at different parts of a lake that flows into a river via a waterfall. Let us further assume that the waterfall splits the stream into a subsonic and a supersonic part. This is in analogy to a black hole, where the supersonic region corresponds to the region bounded by the *apparent* horizon. Here sound rays behave like light rays inside black holes, they are trapped. Sound waves in our gedanken-experiment

[3] Here we use natural units, where $G = c = \hbar = 1$.

[4] The temperature of a black hole is inverse proportional to its mass m,

$$T = \frac{\hbar\, c^3}{8\pi\, G_{\mathrm{N}}\, k_{\mathrm{B}}\, m} \,. \tag{1.24}$$

Here k_B is the Boltzmann constant, and $\hbar$ the Planck constant.

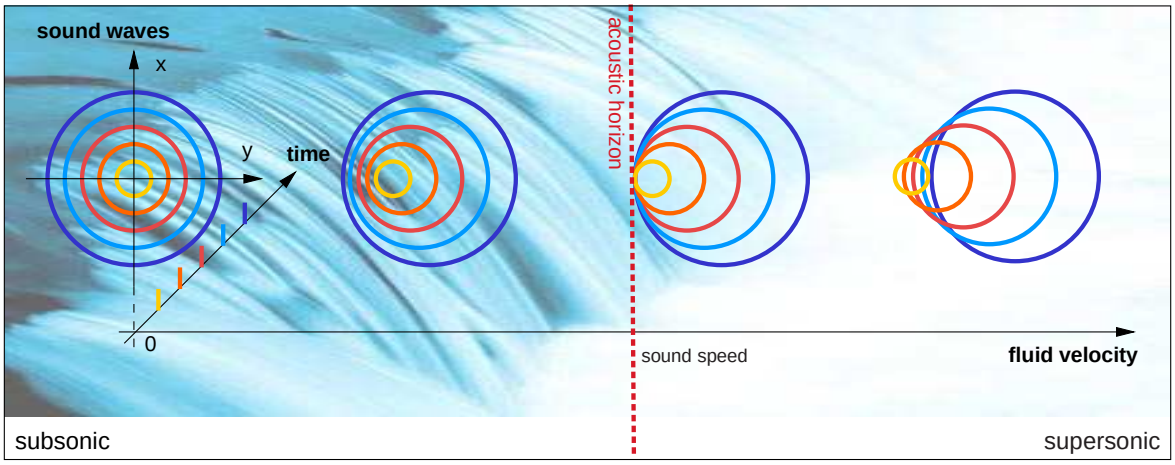


Figure 1.1: We illustrate the propagation of sound waves in convergent fluid flow.

can only cross the horizon from one direction, from subsonic to supersonic.

As pointed out above, Hawking radiation is a semi-classical quantum gravity effect, that does not directly involve the validity of the Einstein equations. This is in contrast to the notion of *Bekenstein entropy*, a geometrical entropy formulated in 1973 [25, 26]. The derivation for Bekenstein entropy *directly* involves the Einstein equations. In the context of the analogue model programme the issue of the "Essential and inessential features of Hawking radiation" has been summarized by *Matt Visser* [184].

Hawking radiation requires — besides the existence of a Lorentzian metric — (1) an apparent horizon (at least asymptotically), (2) non-zero "surface gravity",

$$\kappa(t)\Big|_{\text{Horizon}} = c_{\text{sound}}\, \frac{d\left[c(t,\mathbf{x}) - |\vec{v}(t,\mathbf{x})|\right]}{d\mathbf{x}}\Bigg|_{\text{Horizon}}, \tag{1.25}$$

and (3) a relatively slow evolution of the geometry,

$$\frac{d\left[c(t,\mathbf{x}) - |\vec{v}(t,\mathbf{x})|\right]}{d\mathbf{x}} \gg \frac{\dot{c}_{\text{sound}}}{c_{\text{sound}}}\Bigg|_{\text{Horizon}}. \tag{1.26}$$

The latter is important to guarantee the dominance of spatial gradients over temporal gradients. The slower the geometry evolves, the closer the *apparent* horizon sits to the *event* horizon (absolute horizon), and the closer the actual spectrum is to a quasi-thermal spectrum [184]. (More recently, in [11, 17] the authors argued that the presence of a pre-existing apparent horizon can be further relaxed.)

Acoustic Hawking radiation from analogue models. Quantum aspects of analogue black holes have been studied in various media: For example in fluids [174, 173, 166], slow light [176, 122], and in electro-magnetic wave-guides [176], in Bose–Einstein condensates [81, 82, 13, 11, 17], in superfluid Helium [109, 103, 191].

Robustness of Hawking radiation. Besides all the reasons mentioned above, there is another property of the Hawking process that makes the analogue model programme both useful and interesting. That is the fact that the Hawking effect is largely independent of the choice for the high-frequency cutoff. This is important for any analogue model — as it has per definition nothing to do with "real" gravity — its "true" nature reveals itself in terms of a high-frequency cutoff. The cutoff is related to the microscopic physics of the media. [► We show this explicitly in Chapter 4, where we study Lorentz symmetry breaking in spacetimes emerging from a Bose gas.]

The first author to study the *robustness* of Hawking radiation against the introduction of a high-frequency cutoff was *Ted Jacobson* in 1991 [112, 104]. Subsequently this topic has been further investigated in [174, 177, 36]. [► In Chapter 6 we study the robustness of cosmological particle production for inflation in a Bose gas.]

Rotating black holes. The quantum aspects of rotating black holes are interesting in two regards. Firstly, we also expect Hawking radiation related to the outer event horizon, and secondly the *ergoregion* (see Chapter 2.4.2) yields *superradiant scattering* [148, 204, 206, 86, 205, 123, 84, 116]. [► In Chapter 2 we study the possibility of setting up analogue models for Kerr black holes.]

The superradiance from analogue black holes has been studied in [22, 23, 21, 168]. However, we are still lacking a complete derivation of the most general vortex geometry / collapsing vortex geometry, as it involves fluids with vorticity [149].

Quantum aspects of cosmology

Similarly, we also expect a time-dependent gravitational field to have a non-trivial effect on quantum field modes, if the time-scale t_s over which the gravitational field varies is faster than the oscillation frequency of the mode, $t_s^{-1} \gtrsim \omega_k$. Pioneer work on the theory of cosmological particle production in time-dependent universes has been carried out in 1969 by *Leonard Parker* [145, 146, 146, 147].

An expanding / collapsing universe is described by the Friedmann–Robertson–Walker line-element, representing a time-dependent conformally flat metric tensor. [► In Chapter 6 we study a special sub-case that is of particular interest for cosmology, the *de Sitter* universe, where the scale factor is given by an exponentially expanding (or contracting) universe. In the relevant chapter we also explain why a rapidly exponentially changing universe is believed to account for the large-scale structure of

our universe, as seen in our microwave background [88, 134, 2, 92, 20, 170, 35, 158, 51].]

The de Sitter universe contains so-called *cosmological horizons* [158], such that every point in a de Sitter geometry is surrounded by a boundary that can *never* be crossed. In 1977 [85] *Gibbons* and *Hawking* were able to show that the thermal spectrum — as expected from cosmological particle production in an infinitely-long lasting expanding de Sitter universe — is equivalent to the temperature calculated from the surface gravity at the cosmological horizon, compare with Eq. (1.25). An extensive treatment of both quantum effects, the Hawking radiation and cosmological particle production, can be found in [29, 77, 141]. [► In Chapter 6 we discuss the existence of cosmological horizons in emergent spacetimes.]

In Chapter 2.2.3 we show that is is always possible to cast the acoustic metric, see Eq. (1.10) into Friedman–Robertson–Walker (FRW) form, and consequently reproduce cosmological particle production for any time-dependent FRW geometry.

Analogue FRW spacetimes and cosmological particle production. While the Hawking effect could in principle occur in many different media — *e.g.*, ordinary fluids, electromagnetic wave-guide and superfluids — the only *available* analogues for FRW geometries are superfluids.

The first to point out the analogy in superfluid Helium was *Grisha Volovik* [192, 195] in 1996. A few years later the analogy was transfered to sound waves in *freely expanding* Bose–Einstein condensates, by *Luis Garay* [80] and *Uwe Fischer* and his student in 2003 [76, 70, 74, 75, 72, 71]. An alternative route of achieving FRW geometry in a Bose–Einstein condensate was suggested by *Carlos Barceló*, *Stefano Liberati* and *Matt Visser* shortly afterwards in [15, 16, 18]. Here the authors showed that in a Bose–Einstein condensate with time-dependent atomic interaction strength the sound waves propagate with a time-dependent speed of sound, and consequently experience an *effective* FRW universe. [► Our analysis in Chapter 6 is based on the latter approach.] In [171] *Michael Uhlmann*, *Yan Xu*, and *Ralf Schützhold* focused on the approach suggested by *Uwe Fischer*, and calculated the density-density fluctuations during *effective* inflation based on a freely expanding condensate.

Trans-Planckian physics and cosmological particle production. In [143, 137, 139, 24] the authors analyzed the dependence of the particle spectra on *ad-hoc* artificially imposed *Lorentz symmetry breaking* modifications to the dispersion relation. This question is particularly interesting for the analogue model programme, where the Lorentz symmetry only emerges for the low-energy perturbations in the system. [► In Chapter 6 we study the model-dependent high-energy deviations for the particle production during *effective* inflation in a Bose–Einstein condensate. We show that the full picture, including non-perturbative corrections in the dispersion relation, relates to momentum-dependent rainbow geometries, see also [113].]

Quantum aspects of signature changes

A different problem that can be treated by similar mathematical methods is short sudden signature change — from Lorentzian $(-,+++)$ to Euclidean $(+,+++)$ — in the spacetime geometry. The particle production process can be understood in terms of the drastic change in the behavior of the quantum field modes. In the Euclidean region the dispersion relation of the modes turns imaginary, and thus the modes are exponentially growing and decaying. This is similar to the behavior of "frozen" modes in the de Sitter universe, after the frequency of the mode drops below the scaling time of the surrounding universe, see also [94, 38, 39]. The quantum mode then gets "dragged along" with the spacetime fabric. [► We explain this effect in depth in Chapter 6.]

A thorough treatment of signature change events in general relativity has been carried out by *Tevian Dray et al.*, and can be found in [55, 54, 62, 60, 63, 56, 61, 59, 58, 57]. Here the authors (in a slightly different context) not only studied the particle production from a finite Euclidean region, they also studied the behavior of the Einstein equations for Euclidean geometries, and how to patch geometries with different signature together.

A more physical motivation for signature change events has been suggested in 1983 by *James Hartle* and *Steven Hawking* [90] — they consider a signature change at extremely early times, in the very early stages of the big bang. Consequently the existence of physical time, and hence the existence of our universe, is associated with a signature change event from Euclidean to Lorentzian geometry (the "no boundary" proposal).

Analogue signature change events from Bose gas In 2001 *Donley et al.* carried out a Bose–Einstein condensate experiment that can be viewed as the first analogue model experiment. In the experiment the atomic interactions were driven — for a finite time duration — into a weakly attractive regime. This triggered a controlled condensate collapse [52, 156]. Two years later, the theoretical work of *Esteban Calzetta* and *Bei-Lok Hu* [38, 39], connected the so-called Bose-nova phenomenon with the amplification, mixing of positive and negative modes, and squeezing of vacuum fluctuations due to a signature change event. [► In Chapter 5 we study the influence of the "trans-Planckian" cutoff in this analogue model for the quantum effects in the "signature change event".]

Next we would like to focus on the "trans-Planckian", or model-dependent modifications that *must* arise in any analogue model — that in some sense makes the analogue model programme vulnerable in in the ultraviolet regime. The key questions have to be asked: "Is it possible to classify the type of Lorentz symmetry violation in a specific model?" Can we find similar Lorentz symmetry breaking mechanisms motivated by various candidates for quantum gravity?

1.2.2 | Quantum gravity phenomenology

So-called "quantum gravity phenomenology" summarizes all possible phenomenological consequences from quantum gravity. While different quantum gravity candidates may have completely distinct physical motivation, they can yield similar *observable* consequences. One example is that in many quantum gravity models the fundamental symmetry of Lorentz invariance is *not* an exact symmetry. The investigation of the possible consequences, and detectability of Lorentz symmetry breaking has been reviewed by *David Mattingly* in [138], (freely available online through *Living Reviews in Relativity*). In the following we would like to summarize some relevant aspects of Lorentz symmetry breaking.

There are many different quantum gravity models that suggest the violation of Lorentz symmetry at ultraviolet scales, for example string theory [119, 69], wraped brane worlds [37], and loop quantum gravity [78]. (For more references herein please consult [138].) If Lorentz symmetry is not an exact symmetry, we expect due to the tight experimental constraints that the violations have to take place around the Planck-scale $\approx 10^{19} GeV$ or higher.

There are two fundamentally different frameworks for Lorentz violation: (1) due to the presence of a preferred frame of observers or background field that decouples from the notion of spacetime metric, and (2) all frames remain equal, but transformation laws between the frames are modified (*e.g.*, see "Doubly special" relativity (DSR) [117, 129]).

It is possible to analyze kinematic effects for testing Lorentz symmetry [3, 136, 133, 157] in a way similar to analyzing curved-spacetime quantum-field-theory — where full (dynamical) quantum gravity is not *necessarily* required.

Analogue Lorentz symmetry breaking It is easy to see that the symmetry breaking mechanism in different analogue models will lead to model-specific modifications in the dispersion relation. For example it is common knowledge that the "full" dispersion relation for perturbations in a Bose–Einstein condensate is given by

$$\omega_k^2 = c_0^2\, k^2 + \epsilon_{\text{qp}}^2\, k^4\,, \tag{1.27}$$

the so-called Bogoliubov dispersion relation [151, 178], while the dispersion relation for the specific "lumped element" electromagnetic wave-guide considered in [161] is given by

$$\omega_k^2 = \frac{4}{L\,C}\,\sin^2\left(\frac{k\,\Delta x}{2}\right) \approx c^2\,k^2 - \frac{\Delta x^4}{12\,L\,C}\,k^4\,. \tag{1.28}$$

Both models are capable of mimicking *effective* black hole geometries within the infrared limit, but already start to deviate at the kinematic level, since the Bose–Einstein condensate yields a *su-*

personic dispersion relation, while the electromagnetic wave-guide exhibits a *subsonic* dispersion relation. (However, the robustness of the Hawking effect [112, 104, 174, 177, 36] assures us that there will be similar quantum effects.) It also demonstrates, that despite all the fundamental differences both models exhibit very similar Lorentz symmetry breaking mechanisms in terms of a quartic modification in $\Delta\omega_k^2 \sim \pm k^4$.

A possible explanation might be related to the fact that *any* emergent spacetimes based on analogue models *per definition* have a preferred frame. This is the frame of the *external observer*. At high energies the "microscopic" substructure starts to reveal itself, and all the fundamental particles the microscopic substructure are compared to the *external* frame. On the other hand, low-energy perturbations experience an *emergent Lorentz symmetry*.[5] Thus we conclude that analogue models of gravity are classified under type (1) Lorentz symmetry breaking, see discussion above. [► In Chapter 3 we introduce a specific model for an emergent massive scalar field. In the subsequent Chapter 4 we employ this model to analyze the "Lorentz symmetry breaking" in the presence of "massive particles".]

1.2.3 | Gravity as an emergent phenomenon?

In 1968 *Andrei Sakharov* [160] proposed the concept of "induced gravity" providing a natural framework for the emergence of "effective geometrodynamics". His ideas have been revisited by *Matt Visser et al.* in [13, 19, 183], and below we would like to summarize the key points of "induced gravity".

In Section 1.2.1 we briefly pointed out that the notion of an "effective metric" generally arises for linear perturbations around some classical background field described by a generic Lagrangian $\mathcal{L}(\partial_a\phi, \phi)$ depending only on a single scalar field and its first derivatives. The emergent spacetime geometry therefore can be derived under the application of classical physics.

Sakharov's "induced gravity" instead is based on the quantum nature of the system. Here we explicitly focus on small *quantum fluctuations* $\phi_1 \to \hat{\phi}_1$ (compare with Eq. (1.20)) around the background field, employing Feynman path integral methods [29, 77, 150, 207, 141] to calculate the one-loop effective action. After regularization and renormalization, the one-loop effective action

$$\begin{aligned}\Gamma[g(\phi_0),\phi_0] &= S[\phi_0] + \hbar \int \sqrt{-g}\,\kappa\,[-2\Lambda + R(g) - 6V(\phi_0)]\,d^{d+1}x \\ &\quad + \hbar\, X[g(\phi_0),\phi_0] + \mathcal{O}(\hbar^2)\,, \end{aligned} \tag{1.29}$$

induces an Einstein–Hilbert term, [6] and the cosmological constant Λ. [7] The term $X[g(\phi_0),\phi_0]$ is a finite contribution to the renormalized one-loop effective action. For more details see [13, 19, 183].

[5] A nice explanation for *External and inner observers* can be found in [195], in Chapter (4.3.2).

[6] Variations of the Einstein–Hilbert action with respect to the metric field tensor g^{ab} yields the Einstein tensor, for an explicit derivation see [153].

[7] The cosmological constant has been introduced by *Albert Einstein* as a generalization of the Einstein field equations.

Note that, explicitly through ϕ_0 and implicitly through $g(\phi_0)$, the emergent "Einstein-Hilbert term" depends on the background field. Since the "effective metric" only depends on the single scalar field ϕ_0 it *seems* not possible to reproduce full Einstein gravity.

Altogether we notice that Sakharov's "induced gravity" provides us with Einstein-*like* equations. In this context it does not seem to be completely hopeless to expect that Einstein gravity itself may not a be "fundamental theory", instead it *might* emerge from "some other" more fundamental theory.

For alternative viewpoints on emergent gravity consult [93, 195, 194, 105].

Summary

We trust that this introduction has provided sufficient guidance to place the various topics to be discussed in this thesis into a wider perspective. Briefly, analogue spacetimes are a generic tool for probing the interface between gravity and quantum physics, and *might* ultimately point to a deeper fundamental theory.

The cosmological constant can be viewed as an intrinsic energy density of the vacuum, and is considered to be related to expansion rate of the recent expanding universe, for example see [51].

CHAPTER 2

Acoustic analogues of the Kerr black hole

The spacetime geometry on the equatorial slice through a Kerr black hole is formally equivalent to the geometry felt by phonons entrained in a rotating fluid vortex. We analyse this example of "analogue gravity" in some detail: First, we find the most general acoustic geometry compatible with the dynamical equations for the fluid flow in a collapsing or expanding perfect-fluid line vortex. Secondly, we demonstrate that there is a suitable choice of coordinates on the equatorial slice through a Kerr black hole that puts the spacetime geometry into this vortex form; though it is not possible to put the entire Kerr spacetime into perfect-fluid "acoustic" form. Finally, we discuss the implications of this formal equivalence; both with respect to gaining insight into the Kerr spacetime and with respect to possible vortex-inspired experiments, and indicate ways in which more general analogue spacetimes might be constructed.

2.1 | Geometrical and physical acoustics

In the geometrical acoustics approximation, spacetime geometry emerges in a straightforward manner by considering the way the "sound cones" are dragged along by the fluid flow, thereby obtaining the conformal class of metrics (see, for instance, [144]) given by,

$$g_{\mu\nu} \propto \left[\begin{array}{c|c} -(c^2 - h^{mn}\, v_n\, v_n) & -v_j \\ \hline -v_i & h_{ij} \end{array}\right] . \tag{2.1}$$

Here c is the velocity of sound, v is the velocity of the fluid, and h_{ij} is the 3-metric of the ordinary Euclidean space of Newtonian mechanics (possibly in curvilinear coordinates).

Previously in Section 1.1.2 we have indicated how that the wave-equation for sound can be derived by linearizing and combining the Euler equation, the continuity equation, and a barotropic equation of state [173, 175, 178, 180]. For irrotational flow this process leads to the curved-space d'Alembertian equation (or, Klein–Gordon equation) and in particular now fixes the overall conformal factor. The resulting acoustic metric in (3+1) dimensions is (see, for instance, [173, 175, 178, 180, 144, 10], and references therein):

$$g_{\mu\nu} = \left(\frac{\rho}{c}\right) \left[\begin{array}{c|c} -(c^2 - h^{mn}\, v_n\, v_n) & -v_j \\ \hline -v_i & h_{ij} \end{array}\right]. \tag{2.2}$$

Here, in physical acoustics, the density of the fluid, ρ, is entering the emergent metric. Sound is then described by a massless minimally coupled scalar field propagating in this acoustic geometry.
In the presence of vorticity, a more complicated wave equation may still be derived [152, 149]. Then for frequencies large compared to the local vorticity,

$$c\,k \gg ||\nabla \times \vec{v}|| \tag{2.3}$$

this wave equation reduces to the d'Alembertian and the acoustic geometry can be identified in the usual manner. For more details see [149].

The overall conformal factor derived in the physical acoustics approximation (2.2) depends explicitly on the dimension d of the spatial slice.

2.1.1 | The role of dimension

The role of spacetime dimension in these acoustic geometries is sometimes a bit surprising and potentially confusing. There is a real physical distinction between truly two-dimensional systems and systems that are effectively two dimensional, such as three-dimensional systems with cylindrical symmetry. We emphasize that in cartesian coordinates the wave equation is given by

$$\frac{\partial}{\partial x^\mu}\left(f^{\mu\nu}\frac{\partial}{\partial x^\nu}\,\psi\right) = 0\,, \tag{2.4}$$

where

$$f^{\mu\nu} = \left[\begin{array}{c|c} -\rho/c^2 & -\rho\, v^j/c^2 \\ \hline -\rho\, v^i/c^2 & \rho\,\{\delta^{ij} - v^i v^j/c^2\} \end{array}\right], \tag{2.5}$$

holds *independent* of the dimensionality of spacetime. It depends only on the Euler equation, the continuity equation, a barotropic equation of state, and the assumption of irrotational flow [178].

Introducing the acoustic metric $g^{\mu\nu}$, defined by

$$f^{\mu\nu} = \sqrt{-g}\, g^{\mu\nu}; \qquad g = \frac{1}{\det(g^{\mu\nu})} \tag{2.6}$$

the wave Eq. (2.4) corresponds to the massless Klein–Gordon equation (d'Alembertian wave equation) in a curved space-time with contravariant metric tensor:

$$g^{\mu\nu} = \left(\frac{\rho}{c}\right)^{-2/(d-1)} \left[\begin{array}{c|c} -1/c^2 & -\vec{v}^{\,T}/c^2 \\ \hline -\vec{v}/c^2 & \mathbf{I}_{d\times d} - \vec{v}\otimes\vec{v}^{\,T}/c^2 \end{array}\right], \tag{2.7}$$

where d is the dimension of *space* (not spacetime).

The covariant acoustic metric is

$$g_{\mu\nu} = \left(\frac{\rho}{c}\right)^{2/(d-1)} \left[\begin{array}{c|c} -\left(c^2 - v^2\right) & -\vec{v}^{\,T} \\ \hline -\vec{v} & \mathbf{I}_{d\times d} \end{array}\right]. \tag{2.8}$$

$d = 3$

The acoustic line-element for three space and one time dimension reads

$$g_{\mu\nu} = \left(\frac{\rho}{c}\right) \left[\begin{array}{c|c} -\left(c^2 - v^2\right) & -\vec{v}^{\,T} \\ \hline -\vec{v} & \mathbf{I}_{3\times 3} \end{array}\right]. \tag{2.9}$$

This is the primary case of interest in this chapter.

$d = 2$

The acoustic line-element for two space and one time dimension reads

$$g_{\mu\nu} = \left(\frac{\rho}{c}\right)^2 \left[\begin{array}{c|c} -\left(c^2 - v^2\right) & -\vec{v}^{\,T} \\ \hline -\vec{v} & \mathbf{I}_{2\times 2} \end{array}\right]. \tag{2.10}$$

This situation would be appropriate when dealing with surface waves or excitations confined to a particular substrate, for example at the surface between two superfluids. An important physical point is that, due to the fact that one can always find a conformal transformation to make the two-dimensional spatial slice flat [196], essentially all possible 2+1 metrics can in principle be reproduced by acoustic metrics [195]. (The only real restriction is the quite physical constraint that there be no closed timelike curves in the spacetime.)

$d = 1$

The naive form of the acoustic metric in (1+1) dimensions is ill-defined, because the conformal factor is raised to a formally infinite power — this is a side effect of the well-known conformal invariance of the Laplacian in 2 dimensions. The wave equation in terms of $f^{\mu\nu}$ continues to make good sense — it is only the step from $f^{\mu\nu}$ to the effective metric that breaks down.

Note that this issue only presents a difficulty for physical systems that are intrinsically one-dimensional. A three-dimensional system with plane symmetry, or a two-dimensional system with

line symmetry, provides a perfectly well behaved model for (1+1) dimensions, as in the cases $d = 3$ and $d = 2$ above.

Before we go ahead with our programme, we present explicit expressions for the acoustic line-element in cylindrical polar coordinates and spherical polar coordinates.

2.1.2 | Various coordinate systems

The acoustic line element for d dimensions in cartesian coordinates, see Eq. (2.7), is defined by

$$ds^2 = \left(\frac{\rho}{c}\right)^{2/(d-2)} \left[-(c^2 - v^2)\, dt^2 - 2\,\vec{v}\cdot d\vec{r}\, dt + dx^2 + dy^2 + dz^2\right] , \tag{2.11}$$

where $d\vec{r}^T = [dx,\, dy,\, dz]^T$. For computational convenience it is advantageous to change to cylindrical coordinates.

Cylindrical polar coordinates

The coordinate transformation from cartesian to cylindrical coordinates is specified by $x = r\,\cos\phi$, $y = r\,\sin\phi$, and $z = z$, where ϕ is the angle between the position vector $\mathbf{r}$ and the x-axis, and r the length of the position vector. In acoustic cylindrical polar coordinates we get [1] ,

$$ds^2 = \left(\frac{\rho}{c}\right)^{2/(d-2)} \left[-(c^2 - v^2)\, dt^2 - 2\left(v_{\hat{r}}\, dr + v_{\hat{\phi}}\, r\, d\phi + v_z dz\right)\, dt + dr^2 + r^2\, d\phi^2 + dz^2\right] . \tag{2.12}$$

If we take the cylindrical polar coordinate system and simply drop the z direction, setting $dz = 0$, everything reduces to a $(2+1)$ dimensional problem. However, the acoustic metric depends on the total spacetime dimension so there is a physical difference between a $(3+1)$ dimensional problem that has cylindrical symmetry (*e.g.*, a line vortex), and an intrinsically $(2+1)$ dimensional system. For surface phonons trapped on a two-dimensional substrate, and so living in $(2+1)$ dimensional spacetime we have to use the appropriate conformal factor resulting from $d = 2$.

Spherical polar coordinates

In similar manner we obtain the acoustic line element in spherical polar coordinates. The mapping between cartesian to spherical polar coordinates is given by $x = r\,\sin\theta\,\cos\phi$, $y = r\,\sin\theta\,\sin\phi$, and

[1] Here we used the formal replacement,

$$d\vec{r} = \begin{pmatrix} \cos\phi\, dr - r\,\sin\phi\, d\phi \\ \sin\phi\, dr + r\,\cos\phi\, d\phi \\ dz \end{pmatrix} \quad \rightarrow \quad \begin{pmatrix} dr \\ r\, d\phi \\ dz \end{pmatrix} = \begin{pmatrix} \cos\phi\, dx + \sin\phi\, dy \\ -\sin\phi\, dx + \cos\phi\, dy \\ dz \end{pmatrix} .$$

$z = r\,\cos\theta$, where ϕ represents the angle between the position vector $\vec{r}$ and the x-axis, and θ the angle between the position vector $\vec{r}$ and the z-axis. Altogether we get [2]

$$ds^2 = \left(\frac{\rho}{c}\right)^{\frac{2}{d-2}} \left[-(c^2 - v^2)\,dt^2 - 2\left(v_{\hat{r}}\,dr + v_{\hat{\phi}}\,r\,\sin\phi\,d\phi + v_{\hat{\theta}}\,r\,d\theta\right)\,dt + dr^2 + r^2\left(\sin^2(\theta)\,d\phi^2 + d\theta^2\right)\right]. \tag{2.14}$$

Please note, that for $\theta = \pi/2$, that is if we are in the $r-\phi$-plane, the spherical polar coordinates are identical to the reduced, that is $z = 0$, cylindrical polar coordinates.

Now because the ordinary Euclidean space (h_{ij}) appearing in these perfect fluid acoustic geometries is Riemann flat, the 3-dimensional space (given by the constant-time slices) in any acoustic geometry is forced to be conformally flat, with 3-metric $g_{ij} = (\rho/c)\,h_{ij}$. This constraint places very strong restrictions on the class of (3+1)-dimensional geometries that can be cast into perfect fluid acoustic form. While many of the spacetime geometries of interest in general relativity can be put into this acoustic form, there are also important geometries that *cannot* be put into this form; at least for a literal interpretation in terms of flowing perfect fluid liquids and physical sound. In the following we briefly summarize the situation for non-rotating acoustic black holes in ordinary fluids.

2.2 | Acoustic non-rotating black holes

In particular, the Schwarzschild geometry can, at the level of geometrical acoustics, certainly be cast into this perfect fluid acoustic form [180]. However, at the level of physical acoustics (and working within the context of the Painléve–Gullstrand coordinates) there is a technical difficulty in that the Euler and continuity equations applied to the background fluid flow yield a nontrivial and unwanted (3+1) conformal factor ρ/c [180]. This overall conformal factor is annoying, but it does not affect the sound cones, and so does not affect the "causal structure" of the resulting analogue spacetime [10]. Furthermore any overall conformal factor will not affect the surface gravity [108], so it will not directly affect the acoustic analogue of Hawking radiation [173, 180]. So for most of the interesting questions one might ask, the Schwarzschild geometry can for all practical purposes be cast into acoustic form.

To begin with we illustrate in detail the problems involved with the "acoustic Painléve–Gullstrand coordinates". Alternatively, we demonstrate how the Schwarzschild geometry can also be put into acoustic form in different manner by using isotropic coordinates.

[2] Here we used the formal replacement,

$$d\vec{r} = \begin{pmatrix} \sin\theta\,\cos\phi\,dr + r\,\cos\theta\,\cos\phi\,d\theta - r\,\sin\theta\,\sin\phi\,d\phi \\ \sin\theta\,\sin\phi\,dr + r\,\cos\theta\,\sin\phi\,d\theta + r\,\sin\theta\,\cos\phi\,d\phi \\ \cos\theta\,dt - r\,\sin\theta\,d\theta \end{pmatrix}$$

$$\rightarrow \qquad \begin{pmatrix} dr \\ r\,\sin\theta\,d\phi \\ r\,d\theta \end{pmatrix} = \begin{pmatrix} \sin\theta\,\cos\phi\,dx + \sin\theta\,\sin\phi\,dy + \cos\theta\,dz \\ -\sin\phi\,dx + \cos\phi\,dy \\ \cos\theta\,\cos\phi\,dx + \cos\theta\,\sin\phi\,dy - \sin\theta\,dz \end{pmatrix}. \tag{2.13}$$

2.2.1 | Geometrical acoustics and the Painléve–Gullstrand geometry

We consider a time-independent fluid flow with a velocity profile as a function of r. The continuity equation (2.35) in this situation implies

$$\rho(r)\, v(r) = \text{constant}\,, \tag{2.15}$$

thus we have a fixed relationship between the velocity and density profile. The physical acoustic geometry for this case is given by

$$ds^2 = \left(\frac{\text{constant}}{v(z)\, c(z)}\right)^{\frac{2}{d-1}} \left[-\left(c(r)^2 - v(r)^2\right)\, dt^2 + 2\, v(r)\, dt\, dr + dr^2 + r^2\, \left(d\theta^2 + \sin^2(\theta)\, d\phi^2\right)\right]\,. \tag{2.16}$$

The Painléve–Gullstrand, also often called the Lemaître, line element is

$$ds^2 = -dt^2 + \left(dr \pm \sqrt{\frac{2m}{r}}\, dt\right)^2 + r^2\, \left(d\theta^2 + \sin^2(\theta)\, d\phi^2\right)\,, \tag{2.17}$$

where the $+/-$ represent ingoing / outgoing coordinates.

Comparing the two line-elements, one might be tempted to simply adjust the density, $\rho(r) = \rho_0$ (*i.e.*, an incompressible fluid), and sound speed, $c(r) = c_0$, to be position independent constants, and simultaneously set $v = 2m/r$. The crux is that this violates the continuity equation.

Alternatively, if we pick $c = 1$, and $v = \frac{2\,m}{r}$, the continuity equation (in spherical coordinates),

$$\nabla\, (\rho \cdot \vec{v}) = \frac{1}{r^2}\, \frac{1}{\partial r}\, \left(r^2\, \rho\, \vec{v}\right) = 0\,, \tag{2.18}$$

can only be satisfied for

$$\rho(r) = \frac{\text{constant}}{\sqrt{2\, m}}\, r^{-3/2}\,, \tag{2.19}$$

a compressible fluid.

The resulting physical acoustic line-element,

$$ds^2 = \left(\frac{\text{constant}}{\sqrt{2\, m}}\right)^{\frac{2}{1-d}}\, r^{-\frac{3}{1-d}}\, \left[-dt^2 + \left(dr \pm \sqrt{\frac{2m}{r}}\, dt\right)^2 + r^2\, \left(d\theta^2 + \sin^2(\theta)\, d\phi\right)\right]\,, \tag{2.20}$$

is *up to a conformal factor* equivalent to the black hole geometry in Painléve–Gullstrand coordinates. Thus the analogy only holds at the level of geometrical acoustics, since the light-cone structure is unchanged by any overall conformal factor.

2.2.2 | Acoustic isotropic version of the Schwarzschild geometry

The isotropic version of the Schwarzschild geometry can be cast *exactly* into acoustic form, without any extraneous conformal factors. Since this is not the standard way of viewing the acoustic analogue of the Schwarzschild geometry [180], and since the algebra is simple enough to be done in

closed form, it is worthwhile taking a small detour.

In isotropic coordinates the Schwarzschild geometry reads

$$ds^2 = -\frac{(1-\frac{m}{2r})^2}{(1+\frac{m}{2r})^2}\,dt^2 + \left(1+\frac{m}{2r}\right)^4 \left[dr^2 + r^2\left(d\theta^2 + \sin^2\theta\, d\phi^2\right)\right], \tag{2.21}$$

and so in these coordinates the acoustic analogue in $(3+1)$ dimensions corresponds to

$$v = 0; \tag{2.22}$$

$$\rho = \rho_\infty \left(1 - \frac{m^2}{4r^2}\right); \tag{2.23}$$

$$c^2 = c_\infty^2\, \frac{(1-\frac{m}{2r})^2}{(1+\frac{m}{2r})^6}. \tag{2.24}$$

The external force required to hold this configuration in place against the pressure gradient is

$$f_{\hat{r}} = \frac{dp}{dr} = c^2\,\frac{d\rho}{dr} = \rho_\infty\, c_\infty^2\, \frac{(1-\frac{m}{2r})^2}{(1+\frac{m}{2r})^6}\, \frac{m^2}{2r^3}. \tag{2.25}$$

The pressure itself (normalizing $p_\infty \to 0$) is then

$$p(r) = -\rho_\infty\, c_\infty^2\, m^2 \left(\frac{120r^3 - 20r^2 m + 10m^2 r + m^3}{480\, r^5\, (1+\frac{m}{2r})^5}\right), \tag{2.26}$$

and by eliminating r in favour of ρ using

$$r = \frac{m}{2\sqrt{1-\rho/\rho_\infty}} \tag{2.27}$$

we can deduce the equation of state

$$p(\rho) = -(\rho_\infty - \rho)\, c_\infty^2 \left(\frac{20 - 5\rho/\rho_\infty - 4\sqrt{1-\rho/\rho_\infty} - \rho/\rho_\infty\sqrt{1-\rho/\rho_\infty}}{15\,(1+\sqrt{1-\rho/\rho_\infty})^5}\right). \tag{2.28}$$

At the horizon, which occurs at $r_H = m/2$ in these coordinates, both $\rho = 0$ and $c = 0$ in the acoustic analogue, while

$$p_H = -\frac{\rho_\infty\, c_\infty^2}{30} \tag{2.29}$$

is finite, so there is a finite pressure drop between asymptotic infinity and the horizon. Everything is now simple enough to be fully explicit, and although we now have an analogue model that reproduces the *exterior* part of the Schwarzschild geometry *exactly*, we can also clearly see the two forms in which fine tuning arises — in specifying the external force, and in the equation of state.

More generally, any spherically symmetric geometry (static or otherwise) can be put into acoustic form, as we shall see now.

2.2.3 | Acoustic spherically symmetric geometries

It is a standard result that *any* spherically symmetric geometry can be put into isotropic form

$$ds^2 = -\exp(-2\Phi)\, dt^2 + \exp(-2\Psi)\left[dr^2 + r^2\left(d\theta^2 + \sin^2\theta\, d\phi^2\right)\right]. \tag{2.30}$$

This can be put into acoustic form in a particularly simple manner by setting

$$v(r) = 0; \tag{2.31}$$

$$\rho(r) = \rho_\infty \exp(-\Phi - \Psi); \tag{2.32}$$

$$c(r) = c_\infty \exp(\Psi - \Phi). \tag{2.33}$$

The pressure can now be formally evaluated as

$$p(r) = \rho_\infty\, c_\infty^2 \int_r^\infty \exp(\Psi - 3\Phi)\, \partial_r(\Phi + \Psi)\, dr, \tag{2.34}$$

and comparison with $\rho(r)$ can be used to construct a formal equation of state, $\rho(p)$.

This of course implies that the Reissner–Nordström geometry can be put into acoustic form. In particular, the FRW cosmologies can also be put into acoustic form, both at the level of physical acoustics and at the level of geometrical acoustics. In fact there are two rather different routes for doing so: Either by causing the fluid to explode or by adjusting the speed of sound [15, 16, 71, 70, 72, 132, 198, 199].

2.2.4 | The problem with acoustic rotating black holes

There is however a fundamental restriction preventing the Kerr geometry [and Kerr–Newman geometry] from being cast into perfect fluid acoustic form. It has recently been established [79, 121, 120] that no possible time-slicing of the full Kerr geometry can ever lead to conformally flat spatial 3-slices. Faced with this fact, we ask a more modest question: Can we at least cast a *subspace* of the Kerr geometry into perfect fluid acoustic form? Specifically, since we know that the effective geometry of a generalized line vortex (a "draining bathtub" geometry) contains both horizons and ergosurfaces [180, 144], one is prompted to ask: If we look at the equatorial slice of the Kerr spacetime can we at least put that into acoustic form? If so, then this opens the possibility of finding a physically reasonable analogue model based on a vortex geometry that might mimic this important aspect of the Kerr geometry. Thus we have three independent physics questions to answer:

Sec. 2.3 | What is the most general perfect fluid acoustic metric that can (even in principle) be constructed for the most general (translation invariant) line vortex geometry?

Sec. 2.4 | Can the equatorial slice of Kerr then be put into this form?
(And if not, how close can one get?)

Sec. 2.5 | By generalizing the analogue model to something more complicated than a perfect fluid, can we do any better?

We shall now explore these three issues in some detail.

2.3 | General vortex flow in fluids

The Euler (zero-viscosity Navier–Stokes) equation for fluids sets tight constraints on the currents in moving fluids. In the following we derive the most general (translation invariant) line vortex geometry in a barotropic fluid.

2.3.1 | General framework

The background fluid flow (on which the sound waves are imposed) is governed by three key equations, the continuity equation, the Euler equation, and a barotropic equation of state;

$$\frac{\partial \rho}{\partial t} + \nabla \cdot (\rho\, \vec{v}) = 0\,; \tag{2.35}$$

$$\rho \left[\frac{\partial \vec{v}}{\partial t} + (\vec{v} \cdot \nabla)\vec{v} \right] = -\nabla p + \vec{f}\,; \tag{2.36}$$

$$p = p(\rho)\,. \tag{2.37}$$

Here we have included for generality an arbitrary external force $\vec{f}$, possibly magneto-hydrodynamic in origin, that we can in principle think of imposing on the fluid flow to shape it in some desired fashion. From an engineering perspective the Euler equation is best rearranged as

$$\vec{f} = \rho \left[\frac{\partial \vec{v}}{\partial t} + (\vec{v} \cdot \nabla)\vec{v} \right] + \nabla p, \tag{2.38}$$

with the physical interpretation being that $\vec{f}$ is now telling you what external force you would need in order to set up a specified fluid flow.

Magneto-hydrodynamic fluids

Magneto-hydrodynamic (MHD) fluids are conductive fluids (*e.g.*, plasmas, liquid metals, or salt water), where under the application of an external magnetic field controlled currents in the fluid are induced. MHD fluids are described by a combination of the Navier–Stokes equation of the fluid and Maxwell's equation of electromagnetism.

MHD fluids allow a sophisticated manipulation of the fluid flow, and as we shall see shortly, are a necessity to set up an acoustic analogue for a rotating back hole.

2.3.2 | Zero radial flow

Assuming now a cylindrically symmetric time-independent fluid flow without any sinks or sources we have a line vortex aligned along the z axis with fluid velocity $\vec{v}$:

$$\vec{v}(r) = v_{\hat{\theta}}(r)\,\hat{\theta}\,. \tag{2.39}$$

The continuity equation (2.35) for this geometry is trivially satisfied and we write the fluid acceleration $(\mathbf{v}\cdot\nabla)\,\mathbf{v}$ in cylindrical polar coordinates. The gradient vector is $\nabla^T = (\partial_r, r^{-1}\partial_\phi)^T$, and the unit vectors $\hat{r}$ and $\hat{\theta}$ are

$$\hat{r} = d\vec{r}\,|dr|^{-1} = \cos\theta\,\hat{x} + \sin\theta\,\hat{y}\,; \tag{2.40}$$

$$\hat{\phi} = d\vec{\phi}\,|d\phi|^{-1} = -\sin\theta\,\hat{x} + \cos\theta\,\hat{y}\,. \tag{2.41}$$

Further calculations show that

$$\partial_t\hat{r} = 0; \quad \partial_\theta\hat{r} = \hat{\theta}; \quad \partial_r\hat{\theta} = 0; \quad \partial_\theta\hat{\theta} = -\hat{r}\,, \tag{2.42}$$

and we get

$$\vec{a} = (\vec{v}\cdot\nabla)\vec{v} = -\frac{v_{\hat{\phi}}(r)^2}{r}\,\hat{r}\,, \tag{2.43}$$

for the fluid acceleration. A substitution into the rearranged Euler equation(2.38) yields

$$\vec{f} = f_{\hat{r}}\,\hat{r} = \left\{-\rho(r)\,\frac{v_{\hat{\phi}}(r)^2}{r} + c^2(r)\,\partial_r\rho(r)\right\}\hat{r}\,. \tag{2.44}$$

Physical interpretation

The external force $\vec{f}_{\hat{r}}$ must be chosen to precisely cancel against the combined effects of centripetal acceleration and pressure gradient. The angular-flow is not completely controlled by this external force, but is instead an independently specifiable quantity. (There is only *one* relationship between $f_r(r)$, $\rho(r)$, $c(r)$, and $v_\phi(r)$, which leaves *three* of these quantities as arbitrarily specifiable functions.)

We are now considering the equation of state to be an *output* from the problem, rather than an *input* to the problem. If for instance $\rho(r)$ and $c^2(r)$ are specified then the pressure can be evaluated from

$$p(r) = \int c^2(r)\,\frac{d\rho}{dr}\,dr, \tag{2.45}$$

and then by eliminating r between $p(r)$ and $\rho(r)$, the EOS $p(\rho)$ can in principle be determined.

For zero external force (and no radial flow), which arguably is the most natural system to set up in the laboratory, we have

$$\frac{v_\phi^2(r)}{c^2(r)} = r\,\partial_r \ln\rho(r), \tag{2.46}$$

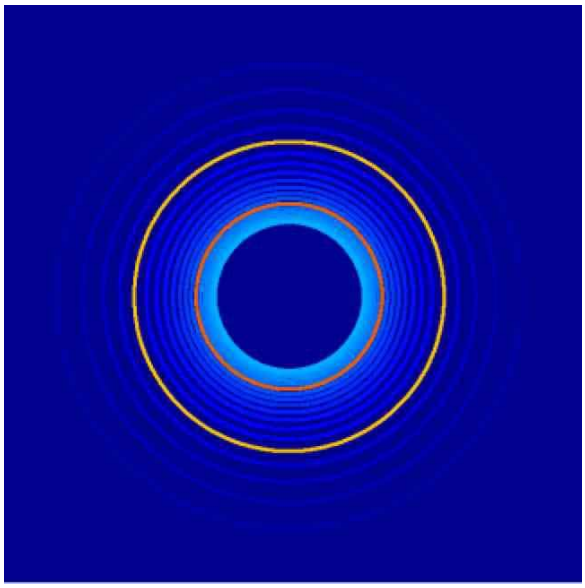


Figure 2.1: A simple non-collapsing vortex geometry: The orange colored circles denote the streamlines of the fluid flow. The brighter the circles the faster the angular velocity of the fluid. The outer golden circle represents the ergosurface, where the fluid velocity reaches the speed of sound. The inner orange circle (which need not exist in general) represents a possible (outer) horizon where the speed of sound goes to zero.

which still has two arbitrarily specifiable functions.

In the geometric acoustics regime the acoustic line-element for this zero-source / zero-sink line vortex is

$$ds^2 \quad \propto \quad -\left(c^2 - v_{\hat{\phi}}^2\right) dt^2 - 2v_{\hat{\phi}}\, r\, d\phi\, dt + dr^2 + r^2 d\phi^2 + dz^2. \tag{2.47}$$

In the physical acoustics regime the acoustic line-element is

$$ds^2 = \left(\frac{\rho}{c}\right)\left[-\left(c^2 - v_{\hat{\phi}}^2\right) dt^2 - 2v_{\hat{\phi}}\, r d\phi\, dt + dr^2 + r^2 d\phi^2 + dz^2\right]. \tag{2.48}$$

The vortex quite naturally has an ergosurface where the speed of the fluid flow equals the speed of sound in the fluid. This vortex geometry may or may not have a horizon — since $v_{\hat{r}}$ is identically zero the occurrence or otherwise of a horizon depends on whether or not the speed of sound $c(r)$ exhibits a zero. [3] We shall later see that this class of acoustic geometries is the most natural for building analogue models of the equatorial slice of the Kerr geometry.

[3] The vanishing of $c(r)$ at a horizon is exactly what happens for Schwarzschild black holes (or their analogues) in either Schwarzschild or isotropic coordinate systems. This is rather different from the behavior in Painleve–Gullstrand coordinates, but is a quite standard signal for the presence of a horizon.

2.3.3 | General analysis with radial flow

For completeness we now consider the situation where the vortex contains a sink or source at the origin. (A concrete example might be the "draining bathtub" geometry where fluid is systematically extracted from a drain located at the centre.) Assuming now a cylindrically symmetric time-independent fluid flow with a line vortex aligned along the z axis, the fluid velocity $\vec{v}$ is

$$\vec{v} = v_{\hat{r}}(r)\,\hat{r} + v_{\hat{\phi}}(r)\,\hat{\phi}. \tag{2.49}$$

Wherever the radial velocity $v_{\hat{r}}(r)$ is nonzero the entire vortex should be thought of as collapsing or expanding.

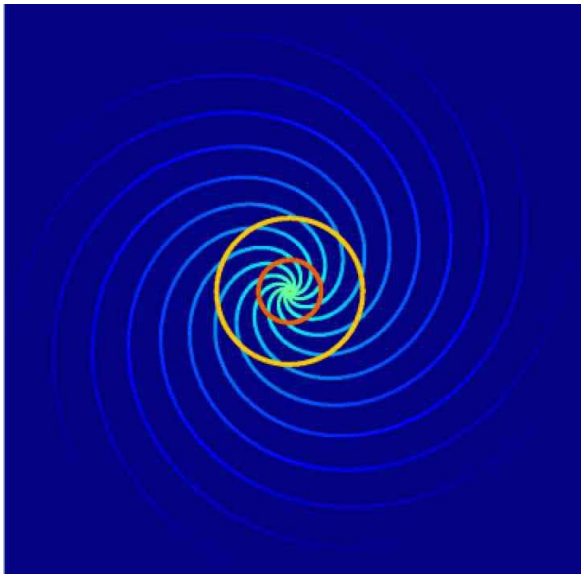


Figure 2.2: A collapsing vortex geometry (draining bathtub): The multi-colored spirals denote streamlines of the fluid flow. Following a streamline towards the center of the vortex the velocity increases. (The brighter the blue, the faster the velocity on the streamline.) The outer golden circle represents the ergosurface while the inner orange circle represents the (outer) event horizon.

The continuity equation (2.35) for this cylindrically symmetric problem is

$$\nabla \cdot (\rho\ \vec{v}) = 0, \tag{2.50}$$

and the rearranged Euler equation (2.38) for a pressure p which depends only on the radial-coordinate r is

$$\vec{f} = \rho\,(\vec{v}\cdot\nabla)\vec{v} + c^2\ \partial_r\rho\ \hat{r}. \tag{2.51}$$

At this stage we note that ρ is in general not an independent variable. Because Eq. (2.50) corresponds to a divergence-free field, integration over any closed circle in the two-dimensional plane yields

$$\oint \rho(r)\ \vec{v}(r)\cdot\hat{r}\ ds = 2\pi\ \rho(r)\ v_{\hat{r}}(r)\ r = 2\pi\ k_1. \tag{2.52}$$

Then *provided* $v_{\hat{r}} \neq 0$,

$$\rho(r) = \frac{k_1}{r\ v_{\hat{r}}(r)}. \tag{2.53}$$

Substituting into the rearranged Euler equation gives

$$\vec{f} = \frac{k_1}{r v_{\hat{r}}}\ (\vec{v}\cdot\nabla)\vec{v} + c^2\ \partial_r\left(\frac{k_1}{r v_{\hat{r}}}\right)\ \hat{r}, \tag{2.54}$$

where c is a function of ρ, and thus a function of $v_{\hat{r}}$. This now completely specifies the force profile in terms of the desired velocity profile, $v_{\hat{r}}$, $v_{\hat{\phi}}$, the equation of state, and a single integration constant k_1. Calculating the fluid acceleration leads to

$$(\vec{v}\cdot\nabla)\vec{v} = \left\{ v_{\hat{r}}(r)\partial_r v_{\hat{r}}(r) - \frac{v_{\hat{\phi}}(r)^2}{r}\right\}\hat{r} + \left\{ v_{\hat{r}}(r)\partial_r v_{\hat{\phi}}(r) + \frac{v_{\hat{r}}(r)\ v_{\hat{\phi}}(r)}{r}\right\}\hat{\phi}, \tag{2.55}$$

which can be rearranged to yield

$$(\vec{v}\cdot\nabla)\vec{v} = \left\{ \frac{1}{2}\partial_r[v_{\hat{r}}(r)^2] - \frac{v_{\hat{\phi}}(r)^2}{r}\right\}\hat{r} + \left\{ \frac{v_{\hat{r}}(r)}{r}\partial_r[r\ v_{\hat{\phi}}(r)]\right\}\hat{\phi}. \tag{2.56}$$

Finally, decomposing the external force into radial and tangential (torque-producing directions) we have

$$f_{\hat{r}} = \vec{f}\cdot\hat{r} = k_1\left\{ \frac{1}{r v_{\hat{r}}}\ \left[\frac{1}{2}\partial_r[v_{\hat{r}}(r)^2] - \frac{v_{\hat{\phi}}(r)^2}{r}\right] + c^2\ \partial_r\left(\frac{1}{r v_{\hat{r}}}\right)\right\}, \tag{2.57}$$

and

$$f_{\hat{\phi}} = \vec{f}\cdot\hat{\phi} = k_1\left\{\frac{1}{r^2}\partial_r[r\ v_{\hat{\phi}}(r)]\right\}. \tag{2.58}$$

The radial equation can undergo one further simplification to yield

$$f_{\hat{r}} = k_1\left\{\frac{1}{r}\ \left[1 - \frac{c_s^2}{v_{\hat{r}}^2}\right]\ \partial_r v_{\hat{r}} - \frac{c_s^2 + v_{\hat{\phi}}^2}{r^2\ v_{\hat{r}}}\right\}. \tag{2.59}$$

Summary

In the geometric acoustics regime the acoustic line-element for the most general (time-independent cylindrically symmetric collapsing / expanding) line vortex is

$$ds^2 \quad \propto \quad -\left(c^2 - v_{\hat{r}}^2 - v_{\hat{\phi}}^2\right) dt^2 - 2v_{\hat{r}}\ dr\ dt - 2v_{\hat{\phi}}\ r\ d\phi\ dt + dr^2 + r^2 d\phi^2 + dz^2. \tag{2.60}$$

We again reiterate that — given a barotropic equation of state $p(\rho)$ — once the velocity profile $v_{\hat{r}}$ and $v_{\hat{\phi}}$ is specified, then up to a single integration constant k_1, the density and speed of sound are no longer free but are fixed by the continuity equation and the equation of state respectively. Furthermore, the Euler equation then tells you exactly how much external force is required to set up the fluid flow. There are still *two* freely specifiable functions which we can take to be the two components of velocity.

In the physical acoustics regime the acoustic line-element is

$$ds^2 \;=\; \left(\frac{\rho}{c}\right)\left[-\left(c^2-v_{\hat{r}}^2-v_{\hat{\phi}}^2\right)dt^2-2v_{\hat{r}}\,dr\,dt-2v_{\hat{\phi}}\,r\,d\phi\,dt+dr^2+r^2d\phi^2+dz^2\right]. \quad (2.61)$$

The major difference for physical acoustics is that for technical reasons the massless curved-space Klein–Gordon equation (d'Alembertian wave equation) can only be derived if the flow has zero vorticity. This requires $v_{\hat{\phi}}(r) = k_2/r$ and hence $f_{\hat{\phi}} = 0$, so that the flow would be un-torqued. More precisely, the d'Alembertian wave equation is a good approximation as long as the frequency of the wave is high compared to the vorticity. However, in the presence of significant torque and vorticity, a more complicated wave equation holds [149], but that wave equation requires additional geometrical structure beyond the effective metric, and so is not suitable for developing general relativity analogue models. (Though this more complicated set of coupled PDEs is of direct physical interest in its own right.) [4]

Special cases

There are several special cases of particular interest:

- No vorticity, $\nabla \times \vec{v} = 0$;
- No angular torque, $f_{\hat{\phi}} = 0$;
- No radial flow $v_{\hat{r}} = 0$;
- No radial force, $f_{\hat{r}} = 0$;
- No external force, $\vec{f} = 0$;

which we will now explore in more detail.

Zero vorticity / zero torque If we assume zero vorticity, $\nabla \times \vec{v} = 0$, the above calculation simplifies considerably, since then

$$v_{\hat{\phi}} = \frac{k_2}{r}\,, \quad (2.62)$$

[4] We shall subsequently see that the "equivalent Kerr vortex" is not irrotational — but the vorticity is proportional to the angular momentum, so there is a large parameter regime in which the effect of vorticity is negligible.

which implies $f_{\hat{\phi}} = 0$. Conversely, if we assume zero torque, then (assuming $k_1 \neq 0$) the vorticity is zero.

But note that the simple relationship *zero torque* $\iff$ *zero vorticity* requires the assumption of nonzero radial flow. With zero radial flow the torque is always zero for a time independent flow, regardless of whether or not the flow is vorticity free.

Zero radial force: Assuming zero radial force, $f_{\hat{r}} = 0$, and assuming $k_1 \neq 0$, one finds

$$\frac{1}{r v_{\hat{r}}} \left[\frac{1}{2} \partial_r [v_{\hat{r}}(r)^2] - \frac{v_{\hat{\phi}}(r)^2}{r} \right] + c^2(r)\, \partial_r \left(\frac{1}{r v_{\hat{r}}} \right) = 0. \tag{2.63}$$

Thus the radial and angular parts of the background velocity are now dependent on each other. Once you have chosen, *e.g.*, $v_{\hat{\theta}}(r)$ and $c(r)$, a differential equation constrains $v_{\hat{r}}$:

$$v_{\hat{r}}\, \partial_r v_{\hat{r}} \left[1 - \frac{c^2}{v_r^2} \right] = \frac{c^2 + v_{\hat{\theta}}^2}{r} \,. \tag{2.64}$$

Zero external force: If we assume zero external force, $\vec{f} = 0$, both the radial and angular external forces are zero. Then assuming $k_1 \neq 0$

$$v_{\hat{r}}\, \partial_r v_{\hat{r}} \left[1 - \frac{c^2}{v_r^2} \right] = \frac{c^2}{r} + \frac{k_2^2}{r^3} \,. \tag{2.65}$$

Since c depends on ρ via the barotropic equation, and ρ depends on v_r via the continuity equation, this is actually a rather complicated nonlinear ODE for $v_r(r)$. (For zero radial flow this reduces to the tautology $0 = 0$ and we must adopt the analysis of the previous subsection.)

In general the ergosurface is defined by the location where the flow goes supersonic

$$v_{\hat{r}}^2 + v_{\hat{\phi}}^2 = c^2 \tag{2.66}$$

while the horizon is defined by the location where

$$v_{\hat{r}}^2 = c^2 \tag{2.67}$$

Note that horizons can form in three rather different ways:

- $v_{\hat{r}} = -c \neq 0$ — a black hole horizon.
- $v_{\hat{r}} = +c \neq 0$ — a white hole horizon.
- $v_{\hat{r}} = \pm c = 0$ — a bifurcate horizon.

In analogue models it is most usual to keep $c \neq 0$ and use fluid flow to generate the horizon, this is the case for instance in the Painléve–Gullstrand version of the Schwarzschild geometry [180,

144]. The alternate possibility of letting both $v_{\hat{r}} \to 0$ and $c \to 0$ to obtain a horizon is not the most obvious construction from the point of view of acoustic geometries, but cannot *a priori* be excluded on either mathematical or physical grounds. Indeed, it is this less obvious manner of implementing the acoustic geometry that most closely parallels the analysis of Schwarzschild black holes in curvature coordinates or isotropic coordinates, and we shall soon see that this route is preferred when investigating the Kerr spacetime.

2.4 | Rotating black holes

To begin with we briefly summarize some aspects of rotating black holes, *e.g.*, the line element for a rotating black hole in Boyer–Lindquist coordinates, the similarities and differences compared to non-rotating black holes (in Schwarzschild coordinates), and finally we point out some classical and quantum effects in the vicinity of rotating black holes that makes them interesting for the analogue model programme.

2.4.1 | Kerr black holes

The *Kerr black hole*, named after the New Zealand mathematician / physicist Roy Kerr, is a solution for the vacuum Einstein equations for a rotating black hole. The Kerr black hole only depends on *two* physical parameters, the total mass m, and the angular momentum J. From an astrophysical point of view the Kerr black hole is of immense importance, since any *realistic* gravitational collapse is not spherically symmetric, and therefore leads to the formation of a black hole with non-zero angular momentum. An observer collapsing with the matter very rapidly approaches the "center" of the black hole, where a singularity is expected. From the perspective of a distant observer, the remnant of a collapsed star is a black hole only characterized by m and J. Thus any information about the collapse, or the original star, is lost. It has been conjectured that the singularity resulting from either spherical or non-spherical collapse is concealed by the event horizon, and therefore the formation of naked singularities is conjectured to be prohibited, see the discussion of *cosmic censorship* in Refs [196, 140, 50].

The line element for a rotating black hole of mass m and angular momentum J in Boyer–Lindquist coordinates is given by

$$ds^2 = - \left(1 - \frac{2\,m\,r}{\rho^2}\right) c^2\,dt^2 - \frac{4\,m\,a\,r\sin^2\theta}{\rho^2}\,d\phi\,dt \tag{2.68}$$

$$+ \frac{\rho^2}{\Delta}\,dr^2 + \rho^2\,d\theta^2 + \left(r^2 + a^2 + \frac{2\,m\,r\,a^2\,\sin^2\theta}{\rho^2}\right)\sin^2\theta\,d\phi^2\,. \tag{2.69}$$

Here a represents the specific angular momentum of the black hole,

$$a = J/m\,, \tag{2.70}$$

the ratio between the angular momentum J, and the total mass m, and we also define the two quantities ρ and Δ as functions of a, m, r and θ:

$$\rho^2 = r^2 + a^2 \cos^2\theta\,; \tag{2.71}$$

$$\Delta = r^2 - 2\,m\,r + a^2\,. \tag{2.72}$$

As already pointed out in the beginning of the section, from the perspective of an observer following the collapse all matter will fall towards the *intrinsic* singularity. Evaluating

$$R^{abcd}R_{abcd} = \frac{48\,m^2\left(r^2 - a^2\,\cos^2\theta\right)\left[\rho^2 - (4\,r\,a\,\cos\theta)^2\right]}{\rho^{12}} \tag{2.73}$$

explicitly, it can be seen that the Riemann invariant is infinite at $\rho^2 = 0$. Thus the singularity for a Kerr black hole is associated with

$$\rho^2 \equiv r^2 + a^2\cos^2\theta = 0\,. \tag{2.74}$$

While for non-rotating black holes the singularity lies at a particular point $r = 0$, we now encounter a *ring singularity* at $r = 0$, $\theta = \pi/2$. In terms of "cartesian" coordinates

$$x = \sqrt{r^2 + a^2}\,\sin\theta\,\cos\phi\,, \tag{2.75}$$

$$y = \sqrt{r^2 + a^2}\,\sin\theta\,\sin\phi\,, \tag{2.76}$$

$$z = r\,\cos\theta\,, \tag{2.77}$$

the ring singularity is in the $z = 0$ plane for $x^2 + y^2 = a^2$, in the $z = 0$ plane for $x^2 + y^2 = a^2$. Note, in cases where $a \to 0$ the ring singularity is shrinking to a point singularity at $r = 0$, in agreement with the non-rotating case.

The coordinate singularity, $g_{11} = \infty$ is related to

$$\Delta \equiv r^2 - 2\,m\,r + a^2 = 0\,, \tag{2.78}$$

such that we obtain from $\Delta = 0$ two surfaces of infinite red-shift,

$$r_\pm = m \pm \sqrt{m^2 - a^2}. \tag{2.79}$$

Here $r_H = r_+$ denotes the *outer event horizon*, and $r_{\tilde{H}} = r_-$ the *inner event horizon*. Notice that for $a \to 0$ the outer event horizon simplifies to $r_H \to 2m$ and $r_{\tilde{H}} \to 0$. This is also in agreement with a non-rotating black hole, where we expect a single event horizon at $2m$.

It can be seen that for $a \to 0$

$$ds^2 = -\left(1 - \frac{2m}{r}\right)\,dt^2 + \left(1 - \frac{2m}{r}\right)^{-1}\,dr^2 + r^2\,\left(d\theta^2 + \sin^2\theta\,d\phi^2\right)\,, \tag{2.80}$$

the Kerr solution takes the form of a non-rotating black hole in Schwarzschild coordinates. Note also that for $m \to 0$ both — the Schwarzschild and the Kerr — line elements represent flat Minkowski

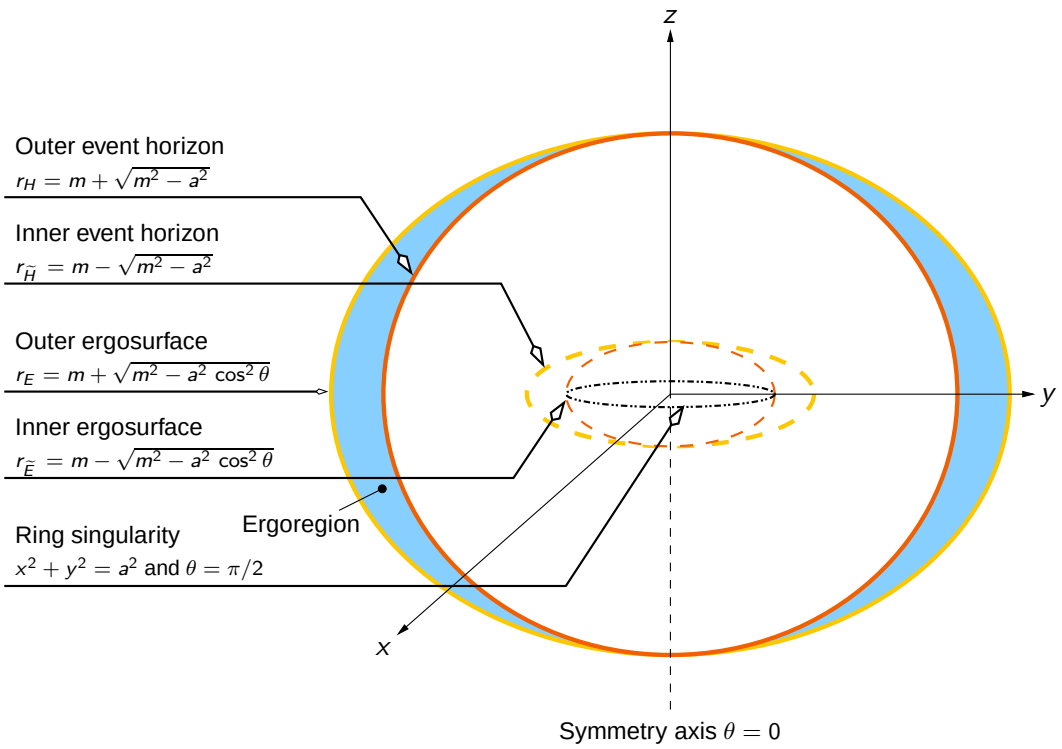


Figure 2.3: The Kerr solution for a rotating black hole exhibits various surfaces of interest [50].

spacetimes. While this is obvious for the Schwarzschild line element, it is less obvious for the Kerr solution, unless we consider the limit $m \to 0$ of the Riemann invariant (2.73), $R^{abcd}R_{abcd} \to 0$, or more precisely not that in an orthonormal frame $R_{\hat{a}\hat{b}\hat{c}\hat{d}} \to 0$.

As the Kerr solution is an extension of the non-rotating black hole, we expect similar classical and quantum effects to appear. However, the Kerr black hole also offers one completely *new* feature that does not appear in non-rotating black holes, the *ergosurface*.

The *ergoregion* is the region bounded between the outer event horizon and the *ergosurface*. The latter is determined by the coordinate condition $g_{00} = 0$, therefore at

$$r_{\pm} = m \pm \sqrt{m^2 - a^2 \cos^2\theta}. \tag{2.81}$$

Again, we obtain two surfaces, the *outer ergosphere* at $r_E = r_+$, and the *inner ergosphere* at $r_{\widetilde{E}} = r_-$. The relationship between the event horizons and ergospheres is as follows $r_{\widetilde{E}} < r_{\widetilde{H}} < r_H \leq r_E$, see Eq. (2.79). We illustrated the different layers of a rotating black hole in Fig. 2.3. (Note, that for $a \to 0$ the outer event horizon and the ergosurface are on top of each other, consequently a non-rotating

black hole *cannot* exhibit an ergoregion.)

While from an astrophysical point of view the Kerr black hole is of immense interest as the remnant of a collapsed star, the acoustic analogue focuses on the classical and quantum effects in the vicinity of the *ergoregion*.

2.4.2 | The ergosphere

The *ergosphere* represents a spacetime region where the angular velocity of the rotating black hole is high enough to "drag the surrounding space along with the velocity of light". Any observer or particle entering this region can no longer remain in a non-rotating orbit — regardless of how much force is applied. It will be dragged along with the rotating spacetime. However, as the observer / object is still outside the event horizon $r \geq r_+$, it is in principle possible to escape to infinity.

In 1969 Roger Penrose [148] discovered that it is possible to extract energy from rotating black holes. This mechanism is referred to as the *Penrose effect* (its field theory analogue is referred to as *superradiant scattering*) and can be understood as follows [196].

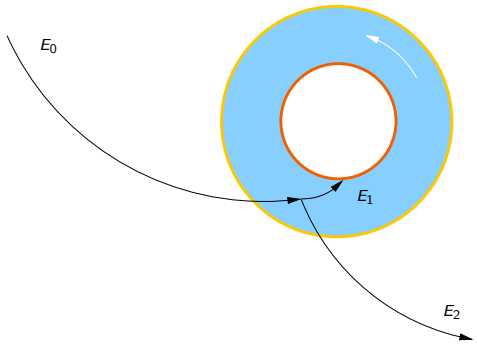


Figure 2.4: Illustration of the superradiance scattering in the ergoregion of a rotating black hole. (The figure shows a projection of the black hole onto some $\theta =$ constant plane, for $\theta = \pi/2$.)

Consider a particle — starting far away from the rotating black hole — that is freely falling into the ergoregion. The Kerr geometry is time-independent, and therefore posesses a time like Killing vector field ξ^a. It is possible to establish a relationship between time translation in the Kerr geometry, and a conserved and well-defined energy far away (due to asymptotic flatness) from the black hole, such that $E_0 = -p_a\xi^a$; see Noether's theorem for example in [150] . Here p^a is the 4-momentum of the test particle. As pointed out in the introduction, there are no forces acting on a freely falling particle, so that the energy remains constant when the particle is approaching the black hole. The particle has been prepared such that it will be broken up into two fragments (*e.g.*, employing explosives and a timing device), once it enters the ergoregion. Conservation of energy-momentum $p_0^a = p_1^a + p_2^a$,

shows that $E_0 = E_1 + E_2$. The break-up is arranged so that, $J_{\text{particle}}/m_{\text{particle}} < J/m$, implying that one piece has negative energy, $E_1 < 0$, and the corresponding particle falls into the black hole (crosses the event horizon), see Fig. 2.4. The remaining piece will leave the ergoregion with greater energy than it entered, $E_0 > E_2$. The difference $|E_1|$ has been subtracted from the black hole. In [196] it is also explained how much energy can be subtracted, and that this process will not convert the Kerr black hole into a naked singularity.

The Penrose effect describes the behavior of classical objects in the vicinity of ergosphere. *Superradiance* describes the corresponding quantum process. In some sense the Penrose effect occurs already at the level of classical wave-packets, while the superradiance effect shows particle enhancement already for a single-mode analysis in terms of non-interacting vacuum fluctuations.

Altogether the rotating black hole exhibits two interesting quantum effects. The existence of the outer horizon at r_H guaranties Hawking radiation. Similar to the Hawking radiation from non-rotating black holes, the Kerr black hole has a thermal radiation associated with the surface gravity at r_H. Beyond that rotating black holes feature the Penrose process and superradiance [204, 206, 86, 205, 123, 84, 116].

In many cases Hawking radiation and superradiance are expected to be small enough not to back-react significantly with the gravitational field, so that curved-spacetime quantum-field-theory is a sufficiently good approximation to cover the quantum effects without (explicitly) invoking the Einstein equation. Effective superradiant scattering has been studied in the context of analogue spacetime in [22, 23, 21, 168].

To conclude the introduction, we notice that *in principle* both effects are expected to occur at the level of the acoustic analog for a rotating black hole.

Before we turn to study the possibility of finding an acoustic analogue for the Kerr black hole, we would like to stress that a special slicing, where we take $\theta =$ constant, but $\theta \neq 0$, contains all the important features — ergosurfaces and horizons — of the rotating black hole. (Best is to choose $\theta = \pi/2$, where the radial distance between the ergosurface and outer horizon, $r_E - r_H$, is maximal.)

2.4.3 | The Kerr equator

To compare the vortex acoustic geometry to the physical Kerr geometry of a rotating black hole [118], consider the equatorial slice $\theta = \pi/2$ in Boyer–Lindquist coordinates [34]:

$$(ds^2)_{(2+1)} = -dt^2 + \frac{2m}{r}(dt - a\, d\phi)^2 + \frac{dr^2}{1 - 2m/r + a^2/r^2} + (r^2 + a^2)\, d\phi^2. \tag{2.82}$$

We would like to put this into the form of an "acoustic metric"

$$g_{\mu\nu} = \left(\frac{\rho}{c}\right) \left[\begin{array}{c|c} -\{c^2 - h^{mn}\, v_n\, v_n\} & -v_j \\ \hline -v_i & h_{ij} \end{array}\right]. \tag{2.83}$$

If we look at the 2-d r-ϕ plane, the metric is

$$(ds^2)_{(2)} = \frac{dr^2}{1 - 2m/r + a^2/r^2} + \left(r^2 + a^2 + \frac{2ma^2}{r}\right) d\phi^2. \tag{2.84}$$

Now it is well-known that any 2-d geometry is locally conformally flat [196], though this fact is certainly not manifested in these particular coordinates. Introduce a new radial coordinate $\tilde{r}$ such that:

$$\frac{dr^2}{1 - 2m/r + a^2/r^2} + \left(r^2 + a^2 + \frac{2ma^2}{r}\right) d\phi^2 = \Omega(\tilde{r})^2\, [d\tilde{r}^2 + \tilde{r}^2\, d\phi^2]. \tag{2.85}$$

This implies

$$\left(r^2 + a^2 + \frac{2ma^2}{r}\right) = \Omega(\tilde{r})^2\, \tilde{r}^2, \tag{2.86}$$

and

$$\frac{dr^2}{1 - 2m/r + a^2/r^2} = \Omega(\tilde{r})^2\, d\tilde{r}^2, \tag{2.87}$$

leading to the differential equation

$$\frac{1}{\tilde{r}(r)}\, \frac{d\tilde{r}(r)}{dr} = \frac{1}{\sqrt{1 - 2m/r + a^2/r^2}\sqrt{r^2 + a^2 + 2ma^2/r}}, \tag{2.88}$$

which is formally solvable as

$$\tilde{r}(r) = \exp\left\{\int \frac{dr}{\sqrt{1 - 2m/r + a^2/r^2}\sqrt{r^2 + a^2 + 2ma^2/r}}\right\}. \tag{2.89}$$

The normalization is most easily fixed by considering the $m = 0 = a$ case, in which case $\tilde{r} = r$, and then using this to write the general case as

$$\tilde{r}(r) = r \exp\left[-\int_r^\infty \left\{\frac{1}{\sqrt{1 - 2m/\bar{r} + a^2/\bar{r}^2}\sqrt{\bar{r}^2 + a^2 + 2ma^2/\bar{r}}} - \frac{1}{\bar{r}}\right\} d\bar{r}\right], \tag{2.90}$$

where $\bar{r}$ is simply a dummy variable of integration. If $a = 0$ this integral can be performed in terms of elementary functions

$$\int \frac{dr}{r\sqrt{1 - 2m/r}} = \ln\left(\sqrt{r^2 - 2mr} + r - m\right) \qquad [r > 2m], \tag{2.91}$$

so that

$$\tilde{r}(r) = \tfrac{1}{2}\left(\sqrt{r^2 - 2mr} + r - m\right), \tag{2.92}$$

though for $m \neq 0$ and general a no simple analytic form holds. Similarly, for $m = 0$ and $a \neq 0$ it is easy to show that

$$\tilde{r}(r) = \sqrt{r^2 + a^2}, \tag{2.93}$$

though for $a \neq 0$ and general m no simple analytic form holds.

Nevertheless, since we have an exact [if formal] expression for $\tilde{r}(r)$ we can formally invert it to assert the existence of a function $r(\tilde{r})$. It is most useful to write $\tilde{r} = r\ F(r)$, with $\lim_{r\to\infty} F(r) = 1$, and to write the inverse function as $r = \tilde{r}\ H(\tilde{r})$ with the corresponding limit $\lim_{\tilde{r}\to\infty} H(\tilde{r}) = 1$. Even if we cannot write explicit closed form expressions for $F(r)$ and $H(\tilde{r})$ there is no difficulty in calculating them numerically, or in developing series expansions for these quantities, or even in developing graphical representations.

We now evaluate the conformal factor as

$$\Omega(\tilde{r})^2 = \frac{r^2 + a^2 + 2ma^2/r}{\tilde{r}^2} = H(\tilde{r})^2 \left(1 + \frac{a^2}{r^2} + \frac{2ma^2}{r^3}\right), \tag{2.94}$$

with r considered as a function of $\tilde{r}$, which now yields

$$(ds^2)_{(2+1)} = -dt^2 + \frac{2m}{r}(dt^2 - 2a\ d\phi\ dt) + \Omega(\tilde{r})^2\ [d\tilde{r}^2 + \tilde{r}^2\ d\phi^2]. \tag{2.95}$$

Equivalently

$$(ds^2)_{(2+1)} \quad = \quad \Omega(\tilde{r})^2 \left\{ -\Omega(\tilde{r})^{-2} \left[1 - \frac{2m}{r}\right] dt^2 - \Omega(\tilde{r})^{-2} \frac{4am}{r}\ d\phi\ dt + [d\tilde{r}^2 + \tilde{r}^2\ d\phi^2] \right\}. \tag{2.96}$$

2.5 | Acoustic Kerr equator

This now lets us pick off the coefficients of the equivalent acoustic metric. For the overall conformal factor

$$\frac{\rho}{c} = \Omega(\tilde{r})^2 = H^2(\tilde{r}) \left(1 + \frac{a^2}{r^2} + \frac{2ma^2}{r^3}\right). \tag{2.97}$$

For the azimuthal "flow"

$$v_\phi = \Omega(\tilde{r})^{-2}\ \frac{2am}{r} = \frac{2am}{r}\ H^{-2}(\tilde{r}) \left(1 + \frac{a^2}{r^2} + \frac{2ma^2}{r^3}\right)^{-1}. \tag{2.98}$$

In terms of orthonormal components

$$v_{\hat{\phi}} = \frac{v_\phi}{\tilde{r}} = \frac{2am}{r^2}\ H^{-1}(\tilde{r}) \left(1 + \frac{a^2}{r^2} + \frac{2ma^2}{r^3}\right)^{-1}. \tag{2.99}$$

This is, as expected, a vortex geometry. Finally for the "coordinate speed of light", corresponding to the speed of sound in the analogue geometry

$$c^2 = \Omega(\tilde{r})^{-2}\left[1-\frac{2m}{r}\right]+\Omega(\tilde{r})^{-4}\,\frac{4a^2m^2}{\tilde{r}^2\,r^2}, \tag{2.100}$$

$$= \Omega(\tilde{r})^{-4}\left\{\Omega(\tilde{r})^2\left[1-\frac{2m}{r}\right]+\frac{4a^2m^2}{\tilde{r}^2\,r^2}\right\}. \tag{2.101}$$

The speed of sound can be rearranged a little

$$c^2=\Omega(\tilde{r})^{-4}\,H^2(\tilde{r})\,\left\{\left[1+\frac{a^2}{r^2}+\frac{2ma^2}{r^3}\right]\left[1-\frac{2m}{r}\right]+\frac{4a^2m^2}{r^4}\right\}. \tag{2.102}$$

This can now be further simplified to obtain

$$c^2=\Omega(\tilde{r})^{-4}\,H^2(\tilde{r})\,\left\{1-\frac{2m}{r}+\frac{a^2}{r^2}\right\}, \tag{2.103}$$

and finally leads to

$$\rho = H(\tilde{r})\,\sqrt{1-\frac{2m}{r}+\frac{a^2}{r^2}}, \tag{2.104}$$

with r implicitly a function of $\tilde{r}$. Note that the velocity field of the "equivalent Kerr vortex" is not irrotational. Application of Stokes' theorem quickly yields

$$\omega=\frac{1}{2\pi\tilde{r}}\frac{\partial}{\partial\tilde{r}}\left(2\pi\tilde{r}\;v_{\hat{\phi}}\right)=\frac{1}{\tilde{r}}\frac{\partial}{\partial\tilde{r}}\left(v_\phi\right)=\frac{1}{\tilde{r}}\frac{\partial}{\partial\tilde{r}}\left[\frac{2am\tilde{r}^2}{r^3}\,\left(1+\frac{a^2}{r^2}+\frac{2ma^2}{r^3}\right)^{-1}\right]. \tag{2.105}$$

which we can somewhat simplify to

$$\omega=\frac{4am}{r^3}\,\left(1+\frac{a^2}{r^2}+\frac{2ma^2}{r^3}\right)^{-1}+\Omega\,\tilde{r}\,\sqrt{1-2m/r+a^2/r^2}\,\frac{\partial}{\partial r}\left[\frac{2am}{r^3}\,\left(1+\frac{a^2}{r^2}+\frac{2ma^2}{r^3}\right)^{-1}\right]. \tag{2.106}$$

Note that (as should be expected), the vorticity is proportional to an overall factor of a, and so is proportional to the angular momentum of the Kerr geometry we are ultimately interested in.

Note that $\tilde{r}$ is the radial coordinate in which the space part of the acoustic geometry is conformally flat, so that $\tilde{r}$ is the "physical" radial coordinate that corresponds to distances measured in the laboratory where the vortex has been set up. Unfortunately this particular radial coordinate is also mathematically rather difficult to work with. For some purposes it is more useful to present the coefficients of the acoustic metric as functions of r, using the relationship $F(r)=1/H(\tilde{r})$. Then we have:

$$\frac{\rho(r)}{c(r)}=\Omega^2(r)=F^{-2}(r)\,\left(1+\frac{a^2}{r^2}+\frac{2ma^2}{r^3}\right). \tag{2.107}$$

$$v_{\hat{\phi}}(r)=\frac{2am}{r^2}\,F(r)\,\left(1+\frac{a^2}{r^2}+\frac{2ma^2}{r^3}\right)^{-1}. \tag{2.108}$$

$$c(r) = \sqrt{1 - \frac{2m}{r} + \frac{a^2}{r^2}}\; F(r)\; \left(1 + \frac{a^2}{r^2} + \frac{2ma^2}{r^3}\right)^{-1}. \tag{2.109}$$

Finally this yields

$$\rho(r) = F^{-1}(r)\, \sqrt{1 - \frac{2m}{r} + \frac{a^2}{r^2}}, \tag{2.110}$$

and the explicit if slightly complicated result that

$$F(r) = \exp\left[- \int_r^\infty \left\{ \frac{1}{\sqrt{1 - 2m/\bar{r} + a^2/\bar{r}^2}\sqrt{\bar{r}^2 + a^2 + 2ma^2/\bar{r}}} - \frac{1}{\bar{r}} \right\} d\bar{r} \right]. \tag{2.111}$$

One of the advantages of writing things this way, as functions of r, is that it is now simple to find the locations of the horizon and ergosphere.

The ergo-surface is defined by $c^2 - v^2 = 0$, equivalent to the vanishing of the g_{tt} component of the metric. This occurs at

$$r_E = 2m. \tag{2.112}$$

The horizon is determined by the vanishing of c, (recall that $v_{\hat{r}} \equiv 0$), this requires solving a simple quadratic with the result

$$r_H = m + \sqrt{m^2 - a^2} < r_E. \tag{2.113}$$

These results agree, as of course they must, with standard known results for the Kerr metric. It is easy to check that $F(r_H)$ is finite (the function inside the exponential is integrable as long as the Kerr geometry is non-extremal), and that $F(r_E)$ is finite. This then provides some simple consistency checks on the geometry:

$$\rho(r_H) = 0 = c(r_H); \tag{2.114}$$

$$\Omega(r_H) = \text{finite}; \tag{2.115}$$

$$F(r_H) = G(r_H)^{-1} = \text{finite}; \tag{2.116}$$

$$\Omega(r_H)\; v_{\hat{\phi}}(r_H) = \frac{a}{r_H}; \tag{2.117}$$

$$\omega(r_H) = \frac{a}{2mr_H}; \tag{2.118}$$

$$c(r_E) = |v_{\hat{\phi}}(r_E)|. \tag{2.119}$$

In particular if we compare the vorticity at the horizon, $\omega(r_H) = a/(2mr_H)$, with the surface gravity

$$\kappa_H = \frac{2m}{r_H^2} - \frac{2a^2}{r_H^3}, \tag{2.120}$$

we find a large range of parameters for which the peak frequency of the Hawking spectrum is high compared to the frequency scale set by the vorticity — this acts to suppress any complications specifically coming from the vorticity. (Of course in the extremal limit, where $r_H \to 0$, the vorticity at

the horizon becomes infinite. In the extremal limit one would need to make a more careful analysis of the effect of nonzero vorticity on the Hawking radiation.)

From the point of view of the acoustic analogue the region inside the horizon is unphysical. In the unphysical region the density of the fluid is zero and the concept of sound meaningless. In the physical region outside the horizon the flow has zero radial velocity, and zero torque, but is *not* irrotational. Since by fitting the equatorial slice of Kerr to a generic acoustic geometry we have fixed $\rho(r)$ and $c^2(r)$ as functions of r [and so also as functions of $\tilde{r}$] it follows that $p(r)$ is no longer free, but is instead determined by the geometry. From there, we see that the EOS $p(\rho)$ is determined, as is the external force $f_{\hat{r}}(r)$. The net result is that we can [in principle] simulate the Kerr equator exactly, but at the cost of a very specific *fine-tuning* of both the equation of state $p(\rho)$ and the external force $f_{\hat{r}}(r)$.

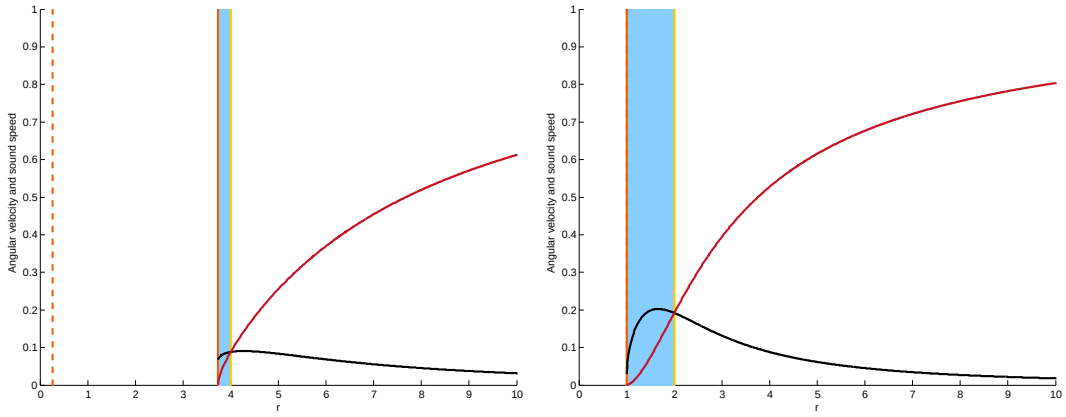
In Fig. 2.5 we present an illustrative graph of the speed of sound and velocity of the fluid. Key points to notice are that the speed of sound (red curve) and velocity of flow (black curve) intersect on the ergosurface (golden line), that the speed of sound goes to zero at the horizon (orange line), and that the velocity of fluid flow is finite on the horizon. Finally the inner horizon is represented by the dashed orange vertical line. While the region inside the outer horizon is not physically meaningful, one can nevertheless mathematically extend some (not all) of the features of the flow inside the horizon. This is another example of the fact that analytic continuation across horizons, which is a standard tool in general relativity, can sometimes fail for physical reasons when one considers Lorentzian geometries based on physical models that differ from standard general relativity. This point is more fully discussed in [10, 102, 109].

In Fig. 2.6 we present an illustrative graph of the fluid density. Note that the density asymptotes to a constant at large radius, and approaches zero at the horizon. Finally, in figure 2.7 we present an illustrative graph of the conformal factor Ω, which remains finite at the horizon and ergosurface, and asymptotes to unity at large distances from the vortex core. Figures 2.5–2.7 all correspond to (a) a "normal" rotating black hole for $m = 2$ and $a = 1$ and (b) an *extremal* black hole, where $m = 2 = a$.

2.6 | Discussion

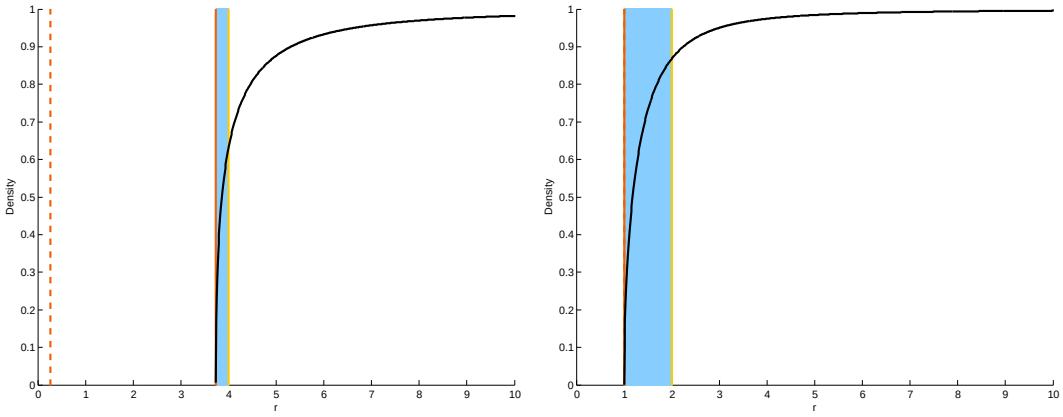
We have shown that the Kerr equator can [in principle] be exactly simulated by an acoustic analogue based on a vortex flow with a very specific equation of state and subjected to a very specific external force. Furthermore we have as a result of the analysis also seen that such an analogue would have to be very specifically and deliberately engineered. Thus the results of this investigation are to some extent mixed, and are more useful for theoretical investigations, and for the gaining of insight into the nature of the Kerr geometry, than they are for actual laboratory construction of a vortex simulating the Kerr equator.

One of the technical surprises of the analysis was that the Doran [53, 89] coordinates (the natural generalization of the Painléve–Gullstrand coordinates that worked so well for the Schwarzschild ge-



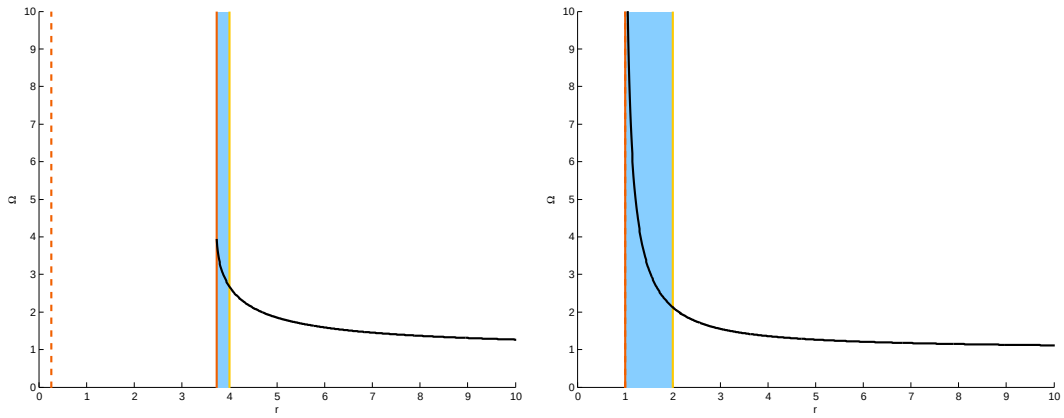
(a) $a = 1$; $m = 2$. (b) $a = 2$; $m = 2$.

Figure 2.5: Illustrative graph of the speed of sound (red) and rotational velocity (black) of the vortex as a function of r.



(a) $a = 1$; $m = 2$. (b) $a = 2$; $m = 2$.

Figure 2.6: Illustrative graph of the fluid density as a function of r.



(a) $a = 1$; $m = 2$. (b) $a = 2$; $m = 2$.

Figure 2.7: Illustrative graph of the conformal factor Ω as a function of r.

ometry) did not lead to a useful acoustic metric even on the equator of the Kerr spacetime. Ultimately, this can be traced back to the fact that in Doran coordinates the space part of the Kerr metric is non-diagonal, even on the equator, and that no simple coordinate change can remove the off-diagonal elements. In Boyer–Lindquist coordinates however the space part of the metric is at least diagonal, and the $\tilde{r}$ coordinate introduced above makes the spatial part of the equatorial geometry conformally flat. This $\tilde{r}$ coordinate is thus closely related to the radial coordinate in the isotropic version of the Schwarzschild solution and $\tilde{r}$ in fact reduces to that isotropic radial coordinate as $a \to 0$.

However, in a more general physical setting the Doran [53, 89] coordinates might still be useful for extending the acoustic analogue away from the equator, and into the bulk of the domain of outer communication. To do this we would have to extend and modify the notion of acoustic geometry. The fact that the spatial slices of the Kerr geometry are *never* conformally flat [79, 121, 120] forces any attempt at extending the acoustic analogy to consider a more general class of acoustic spacetimes. A more general physical context that may prove suitable in this regard is anisotropic fluid media, and we are currently investigating this possibility. The simplest anisotropic fluid media are the classical liquid crystals [44, 45], which in the present context suffer from the defect that they possess considerable viscosity and exist chiefly at room temperature — this makes them unsuitable for the construction of analogue horizons, and particularly unsuitable for the investigation of quantum aspects of analogue horizons. Much more promising in this regard are the quantum liquid crystals. These are anisotropic superfluids such as, in particular, 3He–A [195, 193]. The anisotropic superfluids are generally characterized by the presence of a non-scalar order parameter; they behave as superfluid liquid crystals, with zero friction at $T = 0$. The premier example of an anisotropic superfluid is fermionic 3He–A, where the effective gravity for fermions is described by vierbeins, though several types of Bose and Fermi condensates of cold atoms also exhibit similar behavior [195, 193].

In the system we have presented above we have found that two of the main features of the Kerr geometry appear: the horizon (outer horizon) and ergo-region. By slight modification of standard arguments, these geometric features are expected to lead to the quantum phenomena of super-radiance and Hawking radiation [173, 175, 178, 180, 144]. The super-radiance corresponds to the reflection and amplification of a wave packet at the ergo surface [168]. (See also [23, 22].) The model, because it contains a horizon, also satisfies the basic requirements for the existence of Hawking radiation, which would now be a thermal bath of phonons emitted from the horizon [173]. These are two of the most fundamental physics reasons for being interested in analogue models [144] [5]. A subtlety in the argument that leads to Hawking radiation arises from the way that the choice of coordinates *seems* to influence the choice of quantum vacuum state. In the presence of a horizon, the choice of quantum vacuum is no longer unique, and standard *choices* for the quantum vacuum are the Unruh, Hartle–Hawking, and Boulware states. It is the Unruh vacuum that corresponds (for either static or stationary black holes) to Hawking radiation into an otherwise empty spacetime, while the Hartle–Hawking vacuum (for a static black hole) corresponds to a black hole in thermal equilibrium with its environment (at the Hawking temperature). For a stationary [non-static] black hole the Hartle–Hawking vacuum state does not strictly speaking exist [197], but there are quasi-Hartle–Hawking quantum states that possess most of the relevant features [98]. In general relativity, because physics is coordinate independent, the choice of vacuum state is manifestly independent of the choice of coordinate system. In the analogue spacetimes considered in this article, because the preferred choice of coordinate system is intimately tied to the flowing medium, the situation is perhaps less clear. The coordinate system we have adopted is invariant under combined time reversal and parity, which might tempt one to feel that a pseudo-Hartle–Hawking vacuum is the most natural one. On the other hand, if we think of building up the vortex from a fluid that is initially at rest, then there is clearly a preferred time direction, and the "white hole" component of the maximally extended horizon would exist only as a mathematical artifact. In this physical situation the Unruh vacuum is the most natural one. We feel that there is an issue worth investigating here, to which we hope to return in some future article.

Finally, since astrophysically all black holes are expected to exhibit some degree of rotation, it is clear that an understanding of the influence of rotation on analogue models is important if one wishes to connect the analogue gravity programme back to astrophysical observations. [6] In conclusion, there are a number of basic physics reasons for being interested in acoustic analogues of the Kerr geometry, and a number of interesting directions to which the present analysis might be extended.

[5] Furthermore, there is a strong feeling that the cosmological constant problem in elementary particle physics might be related to a mis-identification of the fundamental degrees of freedom [195, 193].

[6] An interesting attempt in the opposite direction [48, 49] is the recent work that analyzes accretion flow onto a black hole in terms of a dumb hole superimposed upon a general relativity black hole.

CHAPTER 3

Emergent particle masses in Lorentzian and Finslerian geometries

In this chapter we will discuss an analogue spacetime based on the propagation of excitations in a 2-component Bose–Einstein condensate (BEC) [188, 189, 130, 202, 202, 131]. This analogue spacetime has a very rich and complex structure. The 2-BEC system permits us to provide a mass-generating mechanism for the quasi-particle excitations [188, 189]. Additionally, in certain portions of parameter space the most natural interpretation of the geometry is in terms of a specific class of pseudo–Finsler spacetimes, and indeed we will see how more generally it is possible to associate a pseudo–Finsler spacetime with the leading symbol of a wide class of hyperbolic partial differential equations. In other parts of parameter space, the most natural interpretation of the geometry is in terms of a bi-metric spacetime, where one has a manifold that is simultaneously equipped with two distinct pseudo-Riemannian metric tensors. Further specialization in parameter space leads to a region where a single pseudo-Riemannian metric tensor is encountered — this mono-metric regime corresponds to Lorentzian spacetimes of the type encountered in standard general relativity and cosmology [162, 75, 199, 15]. Thus the analogue spacetime based on 2-component BECs provides models not just for standard general relativistic spacetimes, but also for the more general bi-metric , and even more general pseudo–Finsler spacetimes.

3.1 | Theory of the 2-component BEC

The basis for our analogue model is an ultra-cold dilute atomic gas of N bosons, which exist in two single-particle states $|\mathrm{A}\rangle$ and $|\mathrm{B}\rangle$. For example, we consider two different hyperfine states, $|F = 1, m_F = -1\rangle$ and $|F = 2, m_F = 1\rangle$ of ^{87}Rb [114, 169]. They have different total angular momenta

F and therefore slightly different energies. That permits us, from a theoretical point of view, to keep $m_A \neq m_B$, even if they are very nearly equal (to about one part in 10^{16}). At the assumed ultra-cold temperatures and low densities the atoms interact only via low-energy collisions, and the 2-body atomic potential can be replaced by a contact potential. That leaves us with with three atom-atom coupling constants, U_{AA}, U_{BB}, and U_{AB}, for the interactions within and between the two hyperfine states. For our purposes it is essential to include an additional laser field, that drives transition between the two single-particle states.

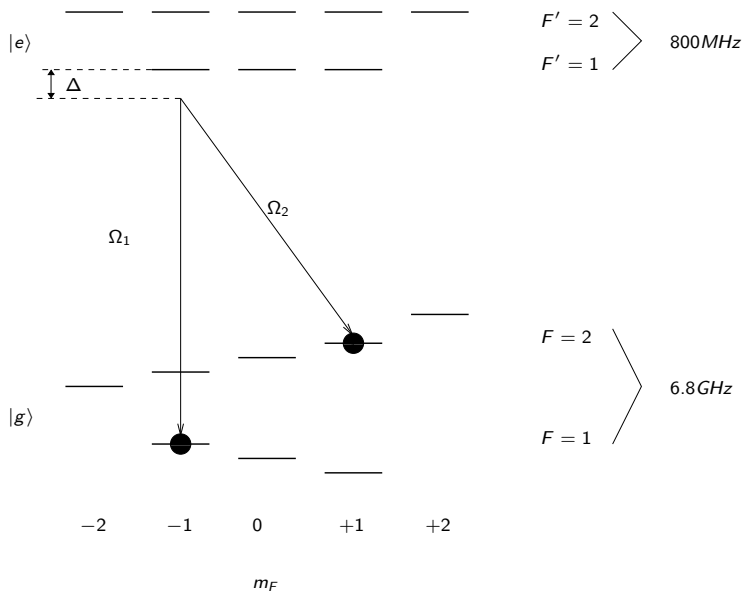


Figure 3.1: The horizontal lines indicate the hyperfine states of ^{87}Rb. The arrows represent two laser fields — with the two frequencies Ω_1 and Ω_2 — necessary to drive transitions between the two trapped states $|F = 1, m_F = -1\rangle$ and $|F = 2, m_F = 1\rangle$, where the frequency difference corresponds to the energy difference of the two hyperfine states. This is realized by a three-level atomic system, because the hyperfine states must be coupled over an intermediate level, that has to lie somewhat below the excited $|e\rangle$ states, as indicated by Δ.

In Fig. 3.1 the energy levels for different hyperfine states of ^{87}Rb, and possible transitions involving three-level processes, are schematically explained. A more detailed description on how to set up an external field driving the required transitions can be found in [30].

3.1.1 | Gross–Pitaevskii equation

The rotating-frame[1] Hamiltonian for our closed 2-component system is given by: [2]

$$\hat{H} = \int d\mathbf{r} \left\{ \quad \sum_{i=\mathrm{A,B}} \quad \left(-\hat{\Psi}_i^\dagger \frac{\hbar^2 \nabla^2}{2m_i} \hat{\Psi}_i + \hat{\Psi}_i^\dagger V_{ext,i}(\mathbf{r}) \hat{\Psi}_i \right) \right.$$
$$\left. + \frac{1}{2} \quad \sum_{i,j=\mathrm{A,B}} \quad \left(U_{ij} \hat{\Psi}_i^\dagger \hat{\Psi}_j^\dagger \hat{\Psi}_i \hat{\Psi}_j + \lambda \hat{\Psi}_i^\dagger (\sigma_x)_{ij} \hat{\Psi}_j \right) \right\}, \tag{3.1}$$

with the transition rate λ between the two hyperfine states. Here $\hat{\Psi}_i(\mathbf{r})$ and $\hat{\Psi}_i^\dagger(\mathbf{r})$ are the usual boson field annihilation and creation operators for a single-particle state at position $\mathbf{r}$, and σ_x is the usual Pauli matrix. For temperatures at or below the critical BEC temperature, almost all atoms occupy the spatial modes $\Psi_\mathrm{A}(\mathbf{r})$ and $\Psi_\mathrm{B}(\mathbf{r})$. The mean-field description for these modes,

$$i\,\hbar\,\partial_t \Psi_i = \left[-\frac{\hbar^2}{2\,m_i} \nabla^2 + V_i - \mu_i + U_{ii}\ |\Psi_i|^2 + U_{ij}\,|\Psi_j|^2 \right] \Psi_i + \lambda\,\Psi_j\,, \tag{3.2}$$

are a pair of coupled Gross–Pitaevskii equations (GPE): $(i,j) \to (\mathrm{A},\mathrm{B})$ or $(i,j) \to (\mathrm{B},\mathrm{A})$.

3.1.2 | Dynamics

In order to use the above 2-component BEC as an analogue model, we have to investigate small perturbations (sound waves) in the condensate cloud.[3] The excitation spectrum is obtained by linearizing around some background densities ρ_{i0} and phases θ_{i0}, using:

$$\Psi_i = \sqrt{\rho_{i0} + \varepsilon\,\rho_{i1}}\; e^{i(\theta_{i0} + \varepsilon\,\theta_{i1})} \quad \text{for} \quad i = \mathrm{A},\,\mathrm{B}\,. \tag{3.3}$$

To keep the analysis as general as possible, we allow the two initial background phases to be independent from each other, and define

$$\delta_\mathrm{AB} \equiv \theta_\mathrm{A0} - \theta_\mathrm{B0}, \tag{3.4}$$

as their difference.

A tedious calculation [188, 189, 130] shows that it is convenient to introduce the following 2×2 matrices: An effective coupling matrix,

$$\hat{\Xi} = \Xi + \hat{X}, \tag{3.5}$$

[1] A rotation in state-space.

[2] In general, it is possible that the collisions drive coupling to other hyperfine states. Strictly speaking the system is not closed, but it is legitimate to neglect this effect [115].

[3] The perturbations amplitude has to be small compared to the overall size of the condensate could, so that the system remains in equilibrium.

where we introduced the energy-independent matrix

$$\Xi \equiv \frac{1}{\hbar}\begin{bmatrix} \tilde{U}_{\mathrm{AA}} & \tilde{U}_{\mathrm{AB}} \\ \tilde{U}_{\mathrm{AB}} & \tilde{U}_{\mathrm{BB}} \end{bmatrix}. \tag{3.6}$$

This matrix contains the quantities

$$\tilde{U}_{\mathrm{AA}} \equiv U_{\mathrm{AA}} - \frac{\lambda\cos\delta_{\mathrm{AB}}\,\sqrt{\rho_{\mathrm{A0}}\rho_{\mathrm{B0}}}}{2}\frac{1}{\rho_{\mathrm{A0}}^2}, \tag{3.7}$$

$$\tilde{U}_{\mathrm{BB}} \equiv U_{\mathrm{BB}} - \frac{\lambda\cos\delta_{\mathrm{AB}}\,\sqrt{\rho_{\mathrm{A0}}\rho_{\mathrm{B0}}}}{2}\frac{1}{\rho_{\mathrm{B0}}^2}, \tag{3.8}$$

$$\tilde{U}_{\mathrm{AB}} \equiv U_{\mathrm{AB}} + \frac{\lambda\cos\delta_{\mathrm{AB}}\,\sqrt{\rho_{\mathrm{A0}}\rho_{\mathrm{B0}}}}{2}\frac{1}{\rho_{\mathrm{A0}}\,\rho_{\mathrm{B0}}}. \tag{3.9}$$

A second matrix, denoted $\hat{X}$, contains differential operators $\hat{Q}_{X1}$ — these are the second-order differential operators obtained from linearizing the quantum potential:

$$V_{\mathrm{Q}}(\rho_X) \equiv -\frac{\hbar^2}{2m_X}\left(\frac{\nabla^2\sqrt{\rho_X}}{\sqrt{\rho_X}}\right) = -\frac{\hbar^2}{2m_X}\left(\frac{\nabla^2\sqrt{\rho_{X0}+\varepsilon\rho_{X1}}}{\sqrt{\rho_{X0}+\varepsilon\rho_{X_1}}}\right) \tag{3.10}$$

$$= -\frac{\hbar^2}{2m_X}\left(\hat{Q}_{X0}(\rho_{X0}) + \varepsilon\;\hat{Q}_{X1}(\rho_{X1})\right). \tag{3.11}$$

The quantity $\hat{Q}_{X0}(\rho_{X0})$ corresponds to the background value of the quantum pressure, and contributes only to the background equations of motion — it does not affect the fluctuations. Now in a general background

$$\hat{Q}_{X1}(\rho_{X1}) = \frac{1}{2}\left\{\frac{(\nabla\rho_{X0})^2 - (\nabla^2\rho_{X0})\rho_{X0}}{\rho_{X0}^3} - \frac{\nabla\rho_{X0}}{\rho_{X0}^2}\nabla + \frac{1}{\rho_{X0}}\nabla^2\right\}\rho_{X1}, \tag{3.12}$$

and we define the matrix $\hat{X}$ to be

$$\hat{X} \equiv -\frac{\hbar}{2}\begin{bmatrix} \frac{\hat{Q}_{\mathrm{A1}}}{m_{\mathrm{A}}} & 0 \\ 0 & \frac{\hat{Q}_{\mathrm{B1}}}{m_{\mathrm{B}}} \end{bmatrix}. \tag{3.13}$$

Given the background homogeneity that will be appropriate for later parts of the current discussion, this will ultimately simplify to

$$\hat{Q}_{X1}(\rho_{X1}) = \frac{1}{2\rho_{X0}}\nabla^2\rho_{X1}, \tag{3.14}$$

in which case

$$\hat{X} = -\frac{\hbar}{4}\begin{bmatrix} \frac{1}{m_{\mathrm{A}}\,\rho_{\mathrm{A0}}} & 0 \\ 0 & \frac{1}{m_{\mathrm{B}}\,\rho_{\mathrm{B0}}} \end{bmatrix}\nabla^2 = -X\,\nabla^2\,. \tag{3.15}$$

Without transitions between the two hyperfine states, when $\lambda = 0$, the matrix Ξ only contains the coupling constants $\Xi_{ij} \to U_{ij}/\hbar$. While Ξ is independent of the energy of the perturbations,

the importance of $\hat{X}$ increases with the energy of the perturbation. In the so-called hydrodynamic approximation $\hat{X}$ can be neglected, effectively $\hat{X} \to 0$ and $\hat{\Xi} \to \Xi$.

Besides the interaction matrix, we also introduce a transition matrix,

$$\Lambda \equiv -\frac{2\lambda \cos\delta_{AB} \sqrt{\rho_{i0}\,\rho_{j0}}}{\hbar} \begin{bmatrix} +1 & -1 \\ -1 & +1 \end{bmatrix} \tag{3.16}$$

and a mass-density matrix,

$$D \equiv \hbar \begin{bmatrix} \frac{\rho_{A0}}{m_A} & 0 \\ 0 & \frac{\rho_{B0}}{m_B} \end{bmatrix} \equiv \hbar \begin{bmatrix} d_A & 0 \\ 0 & d_B \end{bmatrix}. \tag{3.17}$$

The final step is to define two column vectors,

$$\bar{\theta} \equiv [\theta_{A1}, \theta_{B1}]^T, \tag{3.18}$$

and

$$\bar{\rho} \equiv [\rho_{A1}, \rho_{B1}]^T. \tag{3.19}$$

We then obtain two compact equations for the perturbation in the phases and densities:

$$\dot{\bar{\theta}} = -\hat{\Xi}\,\bar{\rho} - \vec{V}\cdot\nabla\bar{\theta} + \Theta\,\bar{\theta}, \tag{3.20}$$

$$\dot{\bar{\rho}} = -\nabla\cdot\left(D\,\nabla\bar{\theta} + \bar{\rho}\,\vec{V}\right) - \Lambda\,\bar{\theta} - \Theta^{\mathsf{T}}\bar{\rho}\,. \tag{3.21}$$

Here the background velocity matrix simply contains the two background velocities of each condensate,

$$\vec{V} = \begin{bmatrix} \vec{v}_{A0} & 0 \\ 0 & \vec{v}_{B0} \end{bmatrix}, \tag{3.22}$$

with two possibly distinct background velocities,

$$\begin{aligned} \vec{v}_{A0} &= \frac{\hbar}{m_A}\nabla\theta_{A0}, \\ \vec{v}_{B0} &= \frac{\hbar}{m_B}\nabla\theta_{B0}. \end{aligned} \tag{3.23}$$

Additionally we also introduce the matrix Θ, which depends on the difference of the initial phases and is defined as

$$\Theta \equiv \frac{\lambda \sin\delta_{AB}}{\hbar} \begin{bmatrix} +\sqrt{\frac{\rho_{B0}}{\rho_{A0}}} & -\sqrt{\frac{\rho_{B0}}{\rho_{A0}}} \\ +\sqrt{\frac{\rho_{A0}}{\rho_{B0}}} & -\sqrt{\frac{\rho_{A0}}{\rho_{B0}}} \end{bmatrix}. \tag{3.24}$$

Now combine these two equations into one:

$$\begin{aligned} \partial_t(\hat{\Xi}^{-1}\,\dot{\bar{\theta}}) = &- \partial_t\left(\hat{\Xi}^{-1}\,\vec{V}\cdot\nabla\bar{\theta}\right) - \nabla(\vec{V}\,\hat{\Xi}^{-1}\,\dot{\bar{\theta}}) + \nabla\cdot\left[\left(D - \vec{V}\,\hat{\Xi}^{-1}\,\vec{V}\right)\nabla\bar{\theta}\right] + \Lambda\,\bar{\theta} \\ &+ \mathsf{K}\,\bar{\theta} + \frac{1}{2}\left\{\Gamma^a\partial_a\bar{\theta} + \partial_a(\Gamma^a\bar{\theta})\right\}, \end{aligned} \tag{3.25}$$

where the index a runs from 0–3 (that is, over both time and space), and we now define

$$\Gamma^t = \hat{\Xi}^{-1}\Theta - \Theta^{\mathsf{T}}\hat{\Xi}^{-1}, \tag{3.26}$$

$$\Gamma^i = \vec{V}\hat{\Xi}^{-1}\Theta - \Theta^{\mathsf{T}}\hat{\Xi}^{-1}\vec{V}, \tag{3.27}$$

and

$$\mathsf{K} = \Theta^{\mathsf{T}}\hat{\Xi}^{-1}\Theta + \frac{1}{2}\partial_t\left(\hat{\Xi}^{-1}\Theta + \Theta^{\mathsf{T}}\hat{\Xi}^{-1}\right) + \frac{1}{2}\nabla\left(\vec{V}\hat{\Xi}^{-1}\Theta + \Theta^{\mathsf{T}}\hat{\Xi}^{-1}\vec{V}\right). \tag{3.28}$$

Note that the Γ^a matrices are antisymmetric in field-space ($\mathsf{A} \leftrightarrow \mathsf{B}$), while the matrix K is symmetric. Also, both $\Gamma^a \to 0$ and $\mathsf{K} \to 0$ as $\delta_{\mathsf{AB}} \to 0$.

Our first goal is to show that Eqs. (3.25), which fundamentally describes quasi-particle excitations interacting with a condensed matter system in the mean-field approximation, can be given a physical and mathematical interpretation in terms of a classical background geometry for massless and massive particles propagating through an analogue spacetime [13, 14, 186, 12]. This analogy only holds (at least in its cleanest form) in the so-called hydrodynamic limit $\hat{\Xi} \to \Xi$, which limit is directly correlated with the healing length which we shall now introduce.

3.1.3 | Healing length

The differential operator $\hat{Q}_{X1}$ that underlies the origin of the $\hat{X}$ contribution above is obtained by linearizing the quantum potential

$$V_{\mathsf{Q}}(\rho_X) \equiv -\frac{\hbar^2}{2m_X}\left(\frac{\nabla^2\sqrt{\rho_X}}{\sqrt{\rho_X}}\right) \tag{3.29}$$

which appears in the Hamilton–Jacobi equation of the BEC flow. This quantum potential term is suppressed by the smallness of $\hbar$, the comparative largeness of m_X, and for sufficiently uniform density profiles. But of course in any real system the density of a BEC must go to zero at the boundaries of its electro-magnetic trap (given that $\rho_X = |\psi_X(\vec{x}, t)|^2$). In a 1-component BEC the healing length characterizes the minimal distance over which the order parameter goes from zero to its bulk value. If the condensate density grows from zero to ρ_0 within a distance ξ the quantum potential term (non local) and the interaction energy (local) are respectively $E_{\mathsf{kinetic}} \sim \hbar^2/(2m\xi^2)$ and $E_{\mathsf{interaction}} \sim 4\pi\hbar^2 a\rho_0/m$. These two terms are comparable when

$$\xi = (8\pi\rho_0 a)^{-1/2}, \tag{3.30}$$

where a is the s-wave scattering length defined as

$$a = \frac{m\ U_0}{4\pi\hbar^2}. \tag{3.31}$$

Note that what we call U_0 in the above expression is just the coefficient of the non-linear self-coupling term in the Gross–Pitaevskii equation, *i.e.*, just U_{AA} or U_{BB} if we completely decouple the 2 BECs ($U_{AB} = \lambda = 0$).

Only for excitations with wavelengths much larger than the healing length is the effect of the quantum potential negligible. This is called the hydrodynamic limit because the single–BEC dynamics is then described by the continuity and Hamilton–Jacobi equations of a super-fluid, and its excitations behave like massless phononic modes. In the case of excitations with wavelengths comparable with the healing length this approximation is no longer appropriate and deviations from phononic behavior will arise.

Such a simple discrimination between different regimes is lost once one considers a system formed by two coupled Bose–Einstein condensates. One is forced to introduce a generalization of the healing ξ length in the form of a "healing matrix". If we apply the same reasoning used above for the definition of the "healing length" to the 2-component BEC system we again find a functional form like that of Eq. (3.30) however we now have the crucial difference that both the density and the scattering length are replaced by matrices. In particular, we generalize the scattering length a to the matrix $\mathcal{A}$:

$$\mathcal{A} = \frac{1}{4\pi\hbar^2} \begin{bmatrix} \sqrt{m_A} & 0 \\ 0 & \sqrt{m_B} \end{bmatrix} \begin{bmatrix} \tilde{U}_{AA} & \tilde{U}_{AB} \\ \tilde{U}_{AB} & \tilde{U}_{BB} \end{bmatrix} \begin{bmatrix} \sqrt{m_A} & 0 \\ 0 & \sqrt{m_B} \end{bmatrix}. \tag{3.32}$$

Furthermore, from (3.30) a healing length matrix Y can be defined by

$$Y^{-2} = \frac{2}{\hbar^2} \begin{bmatrix} \sqrt{\rho_{A0} m_A} & 0 \\ 0 & \sqrt{\rho_{B0} m_B} \end{bmatrix} \begin{bmatrix} \tilde{U}_{AA} & \tilde{U}_{AB} \\ \tilde{U}_{AB} & \tilde{U}_{BB} \end{bmatrix} \begin{bmatrix} \sqrt{\rho_{A0} m_A} & 0 \\ 0 & \sqrt{\rho_{B0} m_B} \end{bmatrix}. \tag{3.33}$$

That is, in terms of the matrices we have so far defined:

$$Y^{-2} = \frac{1}{2}\, X^{-1/2}\, \Xi\, X^{-1/2}; \qquad Y^2 = 2\, X^{1/2}\, \Xi^{-1}\, X^{1/2}. \tag{3.34}$$

Define "effective" scattering lengths and healing lengths for the 2-BEC system as

$$a_{\text{eff}} = \frac{1}{2}\,\text{tr}[\mathcal{A}] = \frac{m_A \tilde{U}_{AA} + m_B \tilde{U}_{BB}}{8\pi\hbar^2}, \tag{3.35}$$

and

$$\xi^2_{\text{eff}} = \frac{1}{2}\,\text{tr}[Y^2] = \text{tr}[X\Xi^{-1}] = \frac{\hbar^2[\tilde{U}_{BB}/(m_A\rho_{A0}) + \tilde{U}_{AA}/(m_B\rho_{B0})]}{4(\tilde{U}_{AA}\tilde{U}_{BB} - \tilde{U}^2_{AB})}. \tag{3.36}$$

That is

$$\xi^2_{\text{eff}} = \frac{\hbar^2[m_A\rho_{A0}\tilde{U}_{AA} + m_B\rho_{B0}\tilde{U}_{BB}]}{4m_A m_B \rho_{A0}\rho_{B0}\,(\tilde{U}_{AA}\tilde{U}_{BB} - \tilde{U}^2_{AB})}. \tag{3.37}$$

Note that if the two components are decoupled and tuned to be equivalent to each other, then these effective scattering and healing lengths reduce to the standard one-component results.

3.2 | Emergent spacetime at low energies

The basic idea behind analogue models is to re-cast the equation for excitations in a fluid into the equation describing a massless or massive scalar field embedded in a pseudo–Riemannian geometry. Starting from a two component superfluid we are going to show that it is not only possible to obtain a massive scalar field from such an analogue model, in addition we are also able to model much more complex geometries. In Fig. 3.2 we illustrate how excitations in a 2-component BEC are associated with various types of emergent geometry.

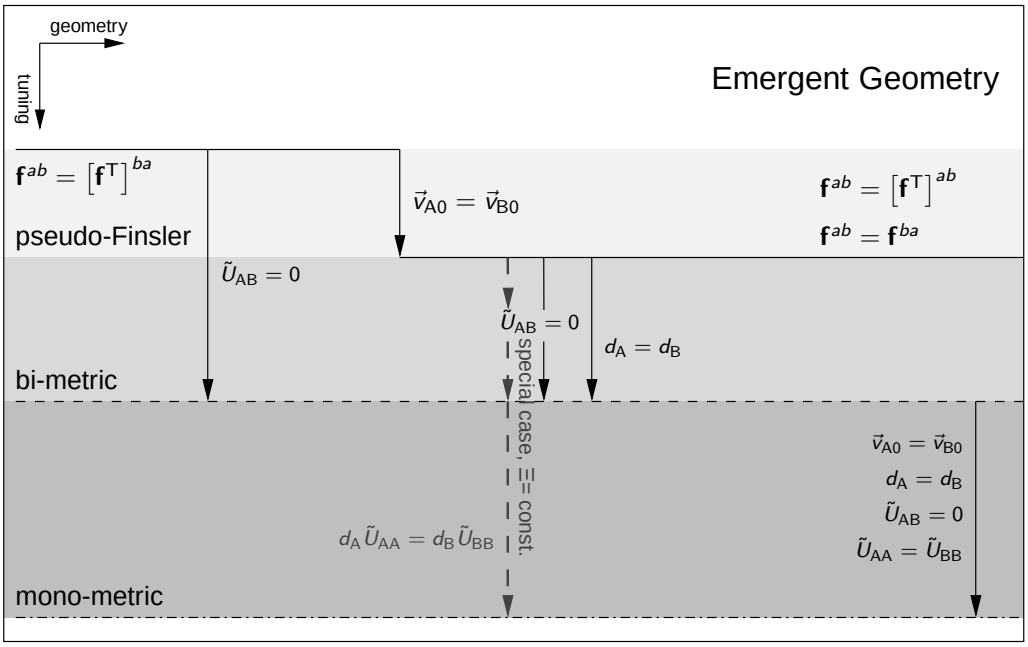


Figure 3.2: The dependence of the emergent geometry on the 2-component BEC parameters.

Most generally, we show that excitations in a 2-component BEC (in the hydrodynamic limit) can be viewed as propagating through a specific class of pseudo–Finsler geometry. As additional constraints are placed on the BEC parameter space, the geometry changes from pseudo–Finsler , first to bi-metric, and finally to mono-metric (pseudo–Riemannian, Lorentzian) geometry. This can be accomplished by tuning the various BEC parameters, such as the transition rate λ, the background velocities $\vec{v}_{\mathrm{A}0}$, $\vec{v}_{\mathrm{B}0}$, the background densities $\rho_{\mathrm{A}0}$, $\rho_{\mathrm{B}0}$, and the coupling between the atoms U_{AA}, U_{BB} and U_{AB}.

At first, it might seem to be quite an artificial thing to impose such constraints onto the system. But if one considers that the two macroscopic wave functions represent two interacting classical

fields, it is more or less obvious that this is the *only* way in which to enforce physical constraints onto the fields themselves, and on the way they communicate with each other.

3.2.1 | Pseudo-Finsler geometry

In the hydrodynamic limit ($\hat{\Xi} \to \Xi$), it is possible to simplify Eq. 3.25 — without enforcing any constraints on the BEC parameters — if we adopt a (3+1)-dimensional "spacetime" notation by writing $x^a = (t, x^i)$, with $i \in \{1, 2, 3\}$ and $a \in \{0, 1, 2, 3\}$. Then Eq. (3.25) can be very compactly rewritten as [13, 14]:

$$\partial_a \left(\mathbf{f}^{ab}\, \partial_b \bar{\theta} \right) + (\Lambda + \mathsf{K})\ \bar{\theta} + \frac{1}{2} \left\{ \Gamma^a\, \partial_a \bar{\theta} + \partial_a (\Gamma^a \bar{\theta}) \right\} = 0. \tag{3.38}$$

The object $\mathbf{f}^{ab}$ is a 4×4 spacetime matrix (actually a tensor density), each of whose components is a 2×2 matrix in field-space — equivalently this can be viewed as a 2×2 matrix in field-space each of whose components is a 4×4 spacetime tensor density. By inspection this is a self-adjoint second-order linear system of PDEs. The spacetime geometry is encoded in the leading-symbol of the PDEs, namely the $\mathbf{f}^{ab}$, without considering the other subdominant terms. That this is a sensible point of view is most easily seem by considering the usual curved-spacetime d'Alembertian equation for a charged particle interacting with a scalar potential in a standard pseudo–Riemannian geometry

$$\frac{1}{\sqrt{-g}} [\partial_a - iA_a] \left(\sqrt{-g} g^{ab} [\partial_b - iA_b] \theta \right) + V\theta = 0 \tag{3.39}$$

from which it is clear that we want to make the analogy

$$\mathbf{f}^{ab} \sim \sqrt{-g}\ g^{ab} \tag{3.40}$$

as the key quantity specifying the geometry. In addition

$$\Gamma^a \sim iA^a \qquad \text{and} \qquad \Lambda + \mathsf{K} \sim V - g^{ab} A_a A_b \tag{3.41}$$

so that Γ^a is analogous to a vector potential and Λ (plus corrections) is related to the scalar potential V — in a translation invariant background this will ultimately provide a mass term.

Specifically in the current 2-BEC system we have

$$\mathbf{f}^{ab} = \left(\begin{array}{c|c} -\Xi^{-1} & -(\vec{V}\Xi^{-1})^{\mathsf{T}} \\ \hline -\vec{V}\Xi^{-1} & D - \vec{V}\Xi^{-1}\vec{V}^{\,T} \end{array} \right), \tag{3.42}$$

where

$$\vec{V}^{\,\mathsf{T}} = \begin{bmatrix} \vec{v}_{\mathrm{A0}}^{\mathsf{T}} & 0 \\ 0 & \vec{v}_{\mathrm{B0}}^{\mathsf{T}} \end{bmatrix} \tag{3.43}$$

is a 2×2 matrix in field space that is also a row vector in physical 3-space. Overall, this does look like a rather complicated object. However, it is possible to re-write the 4×4 geometry containing

2×2 matrices as its elements, in form of a single $(2 \cdot 4) \times (2 \cdot 4)$ matrix.[4] Explicitly we have[5]

$$\mathbf{f}^{ab} = \left[\begin{array}{c|c} \Xi_{11}^{-1}\left(\begin{array}{c|c} -1 & -\vec{v}_{\mathrm{A0}}^{\mathsf{T}} \\ \hline -\vec{v}_{\mathrm{A0}} & \frac{d_{\mathrm{A}}}{\Xi_{11}^{-1}}\delta_{ij} - \vec{v}_{\mathrm{A0}}\vec{v}_{\mathrm{A0}}^{\mathsf{T}} \end{array}\right) & \Xi_{12}^{-1}\left(\begin{array}{c|c} 1 & \vec{v}_{\mathrm{B0}}^{\mathsf{T}} \\ \hline \vec{v}_{\mathrm{A0}} & \vec{v}_{\mathrm{A0}}\vec{v}_{\mathrm{B0}}^{\mathsf{T}} \end{array}\right) \\ \hline \Xi_{21}^{-1}\left(\begin{array}{c|c} 1 & \vec{v}_{\mathrm{A0}}^{\mathsf{T}} \\ \hline \vec{v}_{\mathrm{B0}} & \vec{v}_{\mathrm{B0}}\vec{v}_{\mathrm{A0}}^{\mathsf{T}} \end{array}\right) & \Xi_{22}^{-1}\left(\begin{array}{c|c} -1 & -\vec{v}_{\mathrm{B0}}^{\mathsf{T}} \\ \hline -\vec{v}_{\mathrm{B0}} & \frac{d_{\mathrm{B}}}{\Xi_{22}^{-1}}\delta_{ij} - \vec{v}_{\mathrm{B0}}\vec{v}_{\mathrm{B0}}^{\mathsf{T}} \end{array}\right) \end{array}\right], \tag{3.44}$$

which we can re-write as

$$\mathbf{f} = \left[\begin{array}{c|c} -\Xi_{11}^{-1}\,\mathcal{V}_1\mathcal{V}_1^{\mathsf{T}} + D_{11}h & -\Xi_{12}^{-1}\,\mathcal{V}_1\mathcal{V}_2^{\mathsf{T}} + D_{12}h \\ \hline -\Xi_{21}^{-1}\,\mathcal{V}_2\mathcal{V}_1^{\mathsf{T}} + D_{21}h & -\Xi_{22}^{-1}\,\mathcal{V}_2\mathcal{V}_2^{\mathsf{T}} + D_{22}h \end{array}\right], \tag{3.45}$$

where

$$\mathcal{V}_1^a := \left(1, \vec{v}_{\mathrm{A0}}^{\,i}\right), \tag{3.46}$$

$$\mathcal{V}_2^a := \left(1, \vec{v}_{\mathrm{B0}}^{\,i}\right), \tag{3.47}$$

and

$$h^{ab} := \mathrm{diag}(0, 1, 1, 1). \tag{3.48}$$

Even simpler is the form

$$\mathbf{f} = \left[\begin{array}{c|c} -\Xi_{11}^{-1}\,\mathcal{V}_1\mathcal{V}_1^{\mathsf{T}} & -\Xi_{12}^{-1}\,\mathcal{V}_1\mathcal{V}_2^{\mathsf{T}} \\ \hline -\Xi_{21}^{-1}\,\mathcal{V}_2\mathcal{V}_1^{\mathsf{T}} & -\Xi_{22}^{-1}\,\mathcal{V}_2\mathcal{V}_2^{\mathsf{T}} \end{array}\right] + D \otimes h. \tag{3.49}$$

The key point is that this allows us to write

$$\mathbf{f}^{ab} = \left[\begin{array}{cc} f_{11}^{ab} & f_{12}^{ab} \\ f_{21}^{ab} & f_{22}^{ab} \end{array}\right], \tag{3.50}$$

where

$$\begin{aligned} f_{11}^{ab} &= -\,\Xi_{11}^{-1}\,\mathcal{V}_1^a\mathcal{V}_1^b + D_{11}h^{ab}, \\ f_{12}^{ab} &= -\,\Xi_{12}^{-1}\,\mathcal{V}_1^a\mathcal{V}_2^b, \\ f_{21}^{ab} &= -\,\Xi_{12}^{-1}\,\mathcal{V}_2^a\mathcal{V}_1^b, \\ f_{22}^{ab} &= -\,\Xi_{22}^{-1}\,\mathcal{V}_2^a\mathcal{V}_2^b + D_{22}h^{ab}. \end{aligned} \tag{3.51}$$

[4] This result can be generalized for n-component systems. Any 4×4 geometry obtained from a n-component system can be re-written as a single $(n \cdot 4) \times (n \cdot 4)$ matrix.

[5] Note $\Xi_{12} = \Xi_{21}$, so $\Xi_{12}^{-1} = \Xi_{21}^{-1}$.

It is also possible to separate the representation of $\mathbf{f}^{ab}$ into field space and position space as follows

$$\begin{aligned}\mathbf{f}^{ab} = &\begin{bmatrix} \Xi_{11}^{-1} & 0 \\ 0 & 0 \end{bmatrix} \mathcal{V}_1^a \mathcal{V}_1^b + \begin{bmatrix} 0 & 0 \\ 0 & \Xi_{22}^{-1} \end{bmatrix} \mathcal{V}_2^a \mathcal{V}_2^b \\ &+ \begin{bmatrix} 0 & \Xi_{12}^{-1} \\ 0 & 0 \end{bmatrix} \mathcal{V}_1^a \mathcal{V}_2^b + \begin{bmatrix} 0 & 0 \\ \Xi_{21}^{-1} & 0 \end{bmatrix} \mathcal{V}_2^a \mathcal{V}_1^b + Dh^{ab}.\end{aligned} \tag{3.52}$$

Why do we assert that the quantity $\mathbf{f}^{ab}$ defines a pseudo–Finsler geometry? (Rather than, say, simply a 2×2 matrix of ordinary Lorentzian geometries?) To see the reason for this claim, recall the standard result [47] that the leading symbol of a system of PDEs determines the "signal speed" (equivalently, the characteristics, or the causal structure) [14]. Indeed if we consider the eikonal approximation (while still remaining in the realm of validity of the hydrodynamic approximation) then the causal structure is completely determined by the leading term in the Fresnel equation

$$\det[\mathbf{f}^{ab} k_a k_b] = 0, \tag{3.53}$$

where the determinant is taken in field space. (The quantity $\mathbf{f}^{ab} k_a k_b$ is exactly what is called the leading symbol of the system of PDEs, and the vanishing of this determinant is the statement that high-frequency modes can propagate with wave vector k_a, thereby determining both characteristics and causal structure.) In the 2-BEC case we can explicitly expand the determinant condition as

$$(f_{11}^{ab} k_a k_b)(f_{22}^{cd} k_c k_d) - (f_{12}^{ab} k_a k_b)(f_{21}^{cd} k_c k_d) = 0. \tag{3.54}$$

Define a completely symmetric rank four tensor

$$Q^{abcd} \equiv f_{11}^{(ab} f_{22}^{cd)} - f_{12}^{(ab} f_{21}^{cd)}, \tag{3.55}$$

then the determinant condition is equivalent to

$$Q^{abcd} k_a k_b k_c k_d = 0, \tag{3.56}$$

which now defines the characteristics in terms of the vanishing of the pseudo-co–Finsler structure

$$Q(k) = Q^{abcd} k_a k_b k_c k_c, \tag{3.57}$$

defined on the cotangent bundle. As explained in Appendix C, this pseudo-co–Finsler structure can be Legendre transformed to provide a pseudo–Finsler structure, a Finslerian notion of distance

$$ds^4 = g_{abcd}\, dx^a dx^b dx^c dx^d. \tag{3.58}$$

Here the completely symmetric rank 4 tensor g_{abcd} determines the "sound cones" through the relation $ds = 0$. It is interesting to note that a distance function of the form

$$ds = \sqrt[4]{g_{abcd}\, dx^a dx^b dx^c dx^d} \tag{3.59}$$

first made its appearance in Riemann's inaugural lecture of 1854 [154, 155], though he did nothing further with it, leaving it to Finsler to develop the branch of geometry now bearing his name [73]. The present discussion is sufficient to justify the use of the term "pseudo–Finsler" in the generic 2-BEC situation, but we invite the more mathematically inclined reader to see Appendix C for a sketch of how much further these ideas can be taken.

The pseudo–Finsler geometry implicit in (3.50) is rather complicated compared with the pseudo-Riemannian geometry we actually appear to be living in, at least as long as one accepts standard general relativity as a good description of reality. To mimic real gravity, we need to simplify our model. It is now time to use the major advantage of our analogue model, the ability to tune the BEC parameters, and with it the 2-field background configuration. The first order of business is to decouple $\mathbf{f}^{ab}$ in field space.

3.2.2 | Bi-metric geometry

The reduction of Eq. 3.52 to a diagonal representation in field space (via an orthogonal rotation on the fields),

$$\mathbf{f}^{ab} \to \mathrm{diag}\left[f_{11}^{ab}, f_{22}^{ab}\right] = \mathrm{diag}\left[\sqrt{-g_{11}}\, g_{11}^{ab}, \sqrt{-g_{22}}\, g_{22}^{ab}\right], \tag{3.60}$$

enforces a bi-metric structure onto the condensate. There are two ways to proceed.

Distinct background velocities

For

$$\mathcal{V}_1 \neq \mathcal{V}_2, \tag{3.61}$$

we require all five 2×2 matrices appearing in (3.52) to commute with each other. This has the unique solution $\Xi_{12}^{-1} = 0$, whence

$$\tilde{U}_{\mathrm{AB}} = 0. \tag{3.62}$$

We then get

$$\mathbf{f}^{ab} = \begin{bmatrix} \Xi_{11}^{-1} & 0 \\ 0 & 0 \end{bmatrix} \mathcal{V}_1^a \mathcal{V}_1^b + \begin{bmatrix} 0 & 0 \\ 0 & \Xi_{22}^{-1} \end{bmatrix} \mathcal{V}_2^a \mathcal{V}_2^b + D h^{ab}. \tag{3.63}$$

Since D is a diagonal matrix this clearly represents a bi-metric geometry. The relevant parameters are summarized in Table 3.1.

Equal background velocities

For

$$\mathcal{V}_1 = \mathcal{V}_2 \equiv \mathcal{V}, \tag{3.64}$$

we are still dealing with a pseudo–Finsler geometry, one which is now independently symmetric in field space ($\mathbf{f}^{ab} = [\mathbf{f}^{\mathsf{T}}]^{ab}$), and position space $\mathbf{f}^{ab} = \mathbf{f}^{ba}$.[6] In terms of the BEC parameters that means we must set equal the two background velocities, $\vec{v}_{\mathrm{A}0} = \vec{v}_{\mathrm{B}0} \equiv \vec{v}_0$, and Eq. (3.52) is simplified to:

$$\mathbf{f}^{ab} = -\Xi^{-1}\mathcal{V}^a\mathcal{V}^b + Dh^{ab}. \tag{3.65}$$

From the above, diagonalizability in field space now additionally requires the commutator of the interaction and mass-density matrix to vanish:

$$[\Xi, D] = 0 \quad \Rightarrow \quad \tilde{U}_{\mathrm{AB}}(d_{\mathrm{A}} - d_{\mathrm{B}}) = 0. \tag{3.66}$$

Here, we have a choice between two tuning conditions that do the job:

$$\tilde{U}_{\mathrm{AB}} = 0 \qquad \text{or} \qquad d_{\mathrm{A}} = d_{\mathrm{B}}. \tag{3.67}$$

Under the first option, where $\tilde{U}_{\mathrm{AB}} = 0$, the two off-diagonal elements in Eq. (3.65) are simply zero, and we get the desired bi-metricity in the form[7]

$$\mathbf{f}^{ab} = \begin{bmatrix} \Xi_{11}^{-1} & 0 \\ 0 & \Xi_{22}^{-1} \end{bmatrix} \mathcal{V}^a\mathcal{V}^b + Dh^{ab}. \tag{3.68}$$

Under the second option, for $d_{\mathrm{A}} = d_{\mathrm{B}} \equiv d$, we have $D = d\,\mathbf{I}$. The situation is now a bit trickier, in the sense that one has to diagonalize Ξ^{-1}:

$$\begin{aligned} \tilde{\Xi}^{-1} &= O^{\mathsf{T}}\Xi^{-1}O \qquad (3.69)\\ &= \mathrm{diag}\left[\frac{\tilde{U}_{\mathrm{AA}} + \tilde{U}_{\mathrm{BB}} + \sqrt{(\tilde{U}_{\mathrm{AA}} - \tilde{U}_{\mathrm{BB}})^2 + 4\tilde{U}_{\mathrm{AB}}^2}}{2\,(\tilde{U}_{\mathrm{AA}}\tilde{U}_{\mathrm{BB}} - \tilde{U}_{\mathrm{AB}}^2)}, \frac{\tilde{U}_{\mathrm{AA}} + \tilde{U}_{\mathrm{BB}} - \sqrt{(\tilde{U}_{\mathrm{AA}} - \tilde{U}_{\mathrm{BB}})^2 + 4\tilde{U}_{\mathrm{AB}}^2}}{2\,(\tilde{U}_{\mathrm{AA}}\tilde{U}_{\mathrm{BB}} - \tilde{U}_{\mathrm{AB}}^2)} \right]. \end{aligned}$$

Once this is done, the way to proceed is to use the elements of $\tilde{\Xi}^{-1}$ instead of Ξ^{-1} in Eq. (3.68). The relevant parameters are summarized in Table 3.1.

There is a subtlety implicit in setting the background velocities equal that should be made explicit. If $\mathcal{V}_1 = \mathcal{V}_2$ so that $\vec{v}_{\mathrm{A}0} = \vec{v}_{\mathrm{B}0}$, then since the masses appear in the relationship between phase and velocity we deduce

$$m_{\mathrm{B}}\theta_{\mathrm{A}0}(t, \vec{x}) - m_{\mathrm{A}}\theta_{\mathrm{B}0}(t, \vec{x}) = f(t). \tag{3.70}$$

If $m_{\mathrm{A}} \neq m_{\mathrm{B}}$, and if the background velocity is nonzero, we must deduce that $\delta_{\mathrm{AB}}(t, x)$ will be at the very least be position dependent, and we will be unable to set it to zero. Alternatively, if we demand $\delta_{\mathrm{AB}} = 0$, and have $\nabla\theta_{\mathrm{A}0}(t, \vec{x}) = \nabla\theta_{\mathrm{B}0}(t, \vec{x}) \neq 0$, then we cannot set $\vec{v}_{\mathrm{A}0} = \vec{v}_{\mathrm{B}0} \neq 0$. Fortunately this will not seriously affect further developments.

Last, but certainly not least, we present the conditions for a mono-metric geometry in a 2-component BEC.

[6] The most general pseudo–Finsler geometry is symmetric under simultaneous exchange of field space and position space: $\mathbf{f}^{ab} = [\mathbf{f}^{\mathsf{T}}]^{ba}$.

[7] We would like to stress that this constraint can be easily fulfilled, at least in the special case $\delta_{\mathrm{AB}} = 0$, by tuning the transition rate λ, see Eq. (3.9).

Bi-metric tuning scenarios			
	$\vec{v}_{A0} \neq \vec{v}_{B0}$	$\vec{v}_{A0} = \vec{v}_{B0}$	
	$\tilde{U}_{AB} = 0$	$\tilde{U}_{AB} = 0$	$d_A = d_B$
$f_{11}^{ab} \propto$	$\left(\begin{array}{c\|c} -1 & -\vec{v}_{A0}^{\,T} \\ \hline -\vec{v}_{A0} & \tilde{U}_{AA} d_A h^{ij} - \vec{v}_{A0}\vec{v}_{A0}^{\,T} \end{array}\right)$	$\left(\begin{array}{c\|c} -1 & -\vec{v}_{0}^{\,T} \\ \hline -\vec{v}_{0} & \tilde{U}_{AA} d_A h^{ij} - \vec{v}_{0}\vec{v}_{0}^{\,T} \end{array}\right)$	$\left(\begin{array}{c\|c} -1 & -\vec{v}_{0}^{\,T} \\ \hline -\vec{v}_{0} & \tilde{\Xi}_{11}^{-1} d\, h^{ij} - \vec{v}_{0}\vec{v}_{0}^{\,T} \end{array}\right)$
$f_{22}^{ab} \propto$	$\left(\begin{array}{c\|c} -1 & -\vec{v}_{B0}^{\,T} \\ \hline -\vec{v}_{B0} & \tilde{U}_{BB} d_B h^{ij} - \vec{v}_{B0}\vec{v}_{B0}^{\,T} \end{array}\right)$	$\left(\begin{array}{c\|c} -1 & -\vec{v}_{0}^{\,T} \\ \hline -\vec{v}_{0} & \tilde{U}_{BB} d_B h^{ij} - \vec{v}_{0}\vec{v}_{0}^{\,T} \end{array}\right)$	$\left(\begin{array}{c\|c} -1 & -\vec{v}_{0}^{\,T} \\ \hline -\vec{v}_{0} & \tilde{\Xi}_{22}^{-1} d\, h^{ij} - \vec{v}_{0}\vec{v}_{0}^{\,T} \end{array}\right)$
$g_{11\,ab} \propto$	$\left(\begin{array}{c\|c} -(c_{11}^2 - v_{A0}^2) & -\vec{v}_{A0}^{\,T} \\ \hline -\vec{v}_{A0} & h^{ij} \end{array}\right)$	$\left(\begin{array}{c\|c} -(c_{11}^2 - v_{0}^2) & -\vec{v}_{0}^{\,T} \\ \hline -\vec{v}_{0} & h^{ij} \end{array}\right)$	
$g_{22\,ab} \propto$	$\left(\begin{array}{c\|c} -(c_{22}^2 - v_{B0}^2) & -\vec{v}_{B0}^{\,T} \\ \hline -\vec{v}_{B0} & h^{ij} \end{array}\right)$	$\left(\begin{array}{c\|c} -(c_{22}^2 - v_{0}^2) & -\vec{v}_{0}^{\,T} \\ \hline -\vec{v}_{0} & h^{ij} \end{array}\right)$	
$c_{11}^2 =$	$\tilde{U}_{AA} d_A = \frac{U_{AA}\rho_{A0} + U_{AB}\rho_{B0}}{m_A}$		$\tilde{\Xi}_{11}^{-1}\, d$
$c_{22}^2 =$	$\tilde{U}_{BB} d_B = \frac{U_{BB}\rho_{B0} + U_{AB}\rho_{A0}}{m_B}$		$\tilde{\Xi}_{22}^{-1}\, d$

Table 3.1: If the pseudo–Finsler geometry decouples into two independent Lorentzian geometries $f_{11}^{ab} = \sqrt{-g_{11}} g_{11}$ and $f_{11}^{ab} = \sqrt{-g_{11}} g_{11}$, with two distinct speed of sounds c_{11} and c_{22}, we are effectively dealing with a bi-metric Lorentzian metric. The table shows the results from three different tuning scenarios, that are sufficient to drive the 2-component BEC from Finsler to bi-Lorentzian spacetime. The rightmost column $d_A = d_B$ is addressed in [75] where the authors analyze cosmic inflation in such a bi-metric system.

3.2.3 | Mono-metric geometry

Despite the fact that there are three different routes to bi-metricity, once one demands mono-metricity, where

$$\mathbf{f}^{ab} = \mathrm{diag}\left[f_{11}^{ab}, f_{11}^{ab}\right] = \mathrm{diag}\left[\sqrt{-g_{11}}\, g_{11}^{ab}, \sqrt{-g_{11}}\, g_{11}^{ab}\right], \tag{3.71}$$

then one ends up with one set of unique constraints to reduce from pseudo–Finsler to a single-metric Lorentzian geometry, namely:

$$\begin{aligned} &\vec{v}_{\mathrm{A}0} = \vec{v}_{\mathrm{B}0} = \vec{v}_0; \\ &\tilde{U}_{\mathrm{AB}} = 0; \\ &\tilde{U}_{\mathrm{AA}} = \tilde{U}_{\mathrm{BB}} = \tilde{U}; \\ &d_{\mathrm{A}} = d_{\mathrm{B}} = d. \end{aligned} \tag{3.72}$$

This tuning completely specifies the spacetime geometry, in that

$$f_{11}^{ab} = f_{22}^{ab} \propto \left(\begin{array}{c|c} -1 & -\vec{v}_0^{\,\mathsf{T}} \\ \hline -\vec{v}_0 & \tilde{U} d\, h^{ij} - \vec{v}_0 \vec{v}_0^{\,\mathsf{T}}, \end{array} \right) \tag{3.73}$$

and after a small calculation we get

$$g_{11}{}^{ab} = g_{22}{}^{ab} \propto \left(\begin{array}{c|c} -(c^2 - v_0^2) & -\vec{v}_0^{\,\mathsf{T}} \\ \hline -\vec{v}_0 & h^{ij}, \end{array} \right) \tag{3.74}$$

where we have defined

$$c^2 = \tilde{U}\, d, \tag{3.75}$$

as the speed of sound.[8]

Throughout the preceding few pages we have analyzed in detail the first term in Eq. (3.38), and identified different condensate parameters with different emergent geometries. Since there is more than one term in the wave equation describing excitations in a two-component system, this is not the end of the story. The remaining terms in Eq. (3.38), which we might generically view as “mass” and “vector potential” terms, do not directly affect the spacetime geometry as such. But when an excitation propagates through a specific analogue spacetime geometry, these terms will contribute to the kinematics. It then becomes useful to consider the “mass eigenmodes” in field-space.

3.2.4 | Merging spacetime geometry with mass eigenmodes

The eigenmodes we are interested in are eigenmodes of the field-space matrices occurring in the sub-dominant terms of the wave equation. These eigenmodes (when they exist) do not notice the presence of multiple fields — in our specific case a 2-field system — and therefore propagate nicely

[8] The speed of sound for quasi-particle excitations is of course our analogue for the speed of light in real gravity.

through the effective curved spacetime. As promised in the abstract and the motivation, we are striving for an analogue model representing a massive scalar field in a mono-metric Lorentzian structure. By using the results from section 3.2.3 we are able to decouple the first term of equation (3.38).

In the following we are focusing on two issues: First, we decouple the remaining terms in Eq. (3.38), and subsequently we check that these eigenmodes do not recouple the geometric term. There is however one more (technical) problem, and that is the fact that the terms we want to associate with the effective mass of the scalar field still contain partial derivatives in time and space, which ultimately implies a dependence on the energy of the propagating modes.[9] Luckily, this problem can be easily circumvented, for equal background phases,[10]

$$\theta_{\mathrm{A}0} = \theta_{\mathrm{B}0}, \tag{3.76}$$

in which case

$$\mathrm{K} = \Gamma^{t} = \Gamma^{i} = 0. \tag{3.77}$$

This has the effect of retaining only the matrix Λ among the sub-dominant terms, so that the wave equation becomes

$$\partial_a(\mathbf{f}^{ab}\partial_b\bar{\theta}) + \Lambda\,\bar{\theta} = 0. \tag{3.78}$$

Due to the fact that the structure of the coupling matrix Λ cannot be changed, its eigenmodes determine the eigenmodes of the overall wave equation. The eigenvectors of Λ are given by

$$\begin{aligned} \mathrm{EV1} &:= [+1, +1] \\ \mathrm{EV2} &:= [-1, +1] \end{aligned} \tag{3.79}$$

The final step is to make sure that our spacetime geometry commutes with the eigenvectors of Λ, that is

$$\left[\mathbf{f}^{ab}, \Lambda\right] = 0. \tag{3.80}$$

This constraint is only fulfilled in the mono-metric case, where we are dealing with two identical classical fields, that effectively do not communicate with each other.[11] That is, all field matrices are proportional to the identity matrix.

3.2.5 | Special case: $\Xi =$ constant.

There is one specific class of geometries we are particularly interested it, and that is when Ξ is a position independent and time independent constant. In the next section we will focus exclusively

[9] This can be easily be seen by going to the eikonal approximation where $\nabla \to -i\vec{k}$ and $\partial_t \to i\omega$.

[10] Note that $\delta_{\mathrm{AB}} = 0$ plus mono-metricity implies either $m_{\mathrm{A}} = m_{\mathrm{B}}$ with arbitrary $\vec{v}_0 \neq 0$, or $m_{\mathrm{A}} \neq m_{\mathrm{B}}$ with zero $\vec{v}_0 = 0$. These are exactly the two situations we shall consider below.

[11] While $\tilde{U}_{\mathrm{AB}} = 0$, $U_{\mathrm{AB}} \neq 0$.

on this case, and apply it to quantum gravity phenomenology. This case is however, also of interest as an example of an alternate interplay between fine tuning and emergent geometry. Under the assumption that Ξ is position and time independent, we are able to directly manipulate the overall wave equation for the excitations and as a consequence obtain slightly milder tuning conditions for mono-metricity.

Let us define

$$\tilde{\theta} = \Xi^{-1/2}\,\bar{\theta}, \tag{3.81}$$

and multiply the whole wave equation (3.38) with $\Xi^{1/2}$ from the left. What we are doing is a transformation in field space onto a new basis $\tilde{\theta}$, and in the new basis the wave equation is given by,

$$\partial_a\left(\tilde{\mathbf{f}}^{ab}\,\partial_b\tilde{\theta}\right) + \left(\tilde{\Lambda} + \tilde{\mathsf{K}}\right)\,\tilde{\theta} + \frac{1}{2}\left\{\tilde{\Gamma}^a\,\partial_a\tilde{\theta} + \partial_a(\tilde{\Gamma}^a\tilde{\theta})\right\} = 0, \tag{3.82}$$

where the matrices in field space transform as: $\tilde{\Lambda} = \Xi^{1/2}\Lambda\Xi^{1/2}$, $\tilde{\mathsf{K}} = \Xi^{1/2}\mathsf{K}\Xi^{1/2}$, $\tilde{\Gamma}^a = \Xi^{1/2}\Gamma^a\Xi^{1/2}$, and the tensor-density as

$$\tilde{\mathbf{f}}^{ab} = \Xi^{1/2}\,\mathbf{f}^{ab}\,\Xi^{1/2}. \tag{3.83}$$

In general, the transformation matrix $\Xi^{1/2}$ is non-diagonal, though always symmetric:[12]

$$\Xi^{1/2} = \frac{\Xi + \sqrt{\det\Xi}\;\mathbf{I}}{\sqrt{\mathrm{tr}[\Xi] + 2\sqrt{\det\Xi}}}. \tag{3.84}$$

A close look at Eq. (3.52), now using the tensor-density $\tilde{\mathbf{f}}^{ab}$, makes it obvious that for

$$\tilde{U}_{\mathsf{AB}} = 0, \tag{3.85}$$

the geometry reduces from pseudo-Finsler to bi-metric. For the sake of keeping the discussion short and easy to follow, we set the background velocities equal, and now get

$$\tilde{\mathbf{f}}^{ab} = \mathcal{V}^a\mathcal{V}^b + \tilde{D}h^{ab}. \tag{3.86}$$

In view of the tuning, $\tilde{U}_{\mathsf{AB}} = 0$, we see

$$\tilde{D} = \mathrm{diag}(\tilde{U}_{\mathsf{AA}}\,d_{\mathsf{A}}, \tilde{U}_{\mathsf{BB}}\,d_{\mathsf{B}}). \tag{3.87}$$

The new mass-density matrix, and therefore the overall geometry, is diagonal in field space, hence we are now dealing with the required bi-metric structure.

So far we are in complete agreement with what we have obtained in our previous analysis, see Fig. 3.2. However, if we now ask for mono-metricity, we obtain a slightly milder constraint:

$$\tilde{U}_{\mathsf{AA}}\,d_{\mathsf{A}} = \tilde{U}_{\mathsf{BB}}\,d_{\mathsf{B}}. \tag{3.88}$$

[12] See Appendix D.

Last but not least, we show in detail the results we obtain for this tuning scenario when including the Λ term (the mass term). To avoid confusion, we re-define a few matrices,

$$C_0^2 = \Xi^{1/2}\, D\, \Xi^{1/2}\,; \qquad \text{and} \qquad \Omega^2 = \Xi^{1/2}\, \Lambda\, \Xi^{1/2}. \tag{3.89}$$

Both C_0^2 and Ω^2 are symmetric matrices. If $[C_0^2,\ \Omega^2] = 0$, which is equivalent to the matrix equation $D\ \Xi\ \Lambda = \Lambda\ \Xi\ D$, and is certainly satisfied in view of the above constraint, then they have common eigenvectors. Decomposition onto the eigenstates of the system results in a pair of independent Klein–Gordon equations

$$\frac{1}{\sqrt{-g_{\text{I/II}}}}\,\partial_a\left\{\sqrt{-g_{\text{I/II}}}\,(g_{\text{I/II}})^{ab}\,\partial_b\tilde{\theta}_{\text{I/II}}\right\} + \omega^2_{\text{I/II}}\,\tilde{\theta}_{\text{I/II}} = 0\ , \tag{3.90}$$

where the "acoustic metrics" are given by

$$(g_{\text{I/II}})_{ab} \propto \left[\begin{array}{c|c} -\left(c^2 - v_0^2\right) & -\vec{v_0}^{\,T} \\ \hline -\vec{v_0} & \mathbf{I}_{d\times d} \end{array}\right]. \tag{3.91}$$

The metric components depend only on the background velocity $\vec{v}_0$ and the common speed of sound c. It is also possible to calculate the eigenfrequencies of the two phonon modes,

$$\omega_I^2 = 0; \qquad \omega_{II}^2 = \text{tr}[\Omega^2]\,. \tag{3.92}$$

A zero / non-zero eigenfrequency corresponds to a zero / non-zero mass for the phonon mode.

In the eikonal limit we see that the in-phase perturbation will propagate with the speed of sound,

$$\vec{v}_s = \vec{v}_0 + \hat{k}\ c\,, \tag{3.93}$$

while the anti-phase perturbations propagates with a lower group velocity given by:

$$\vec{v}_g = \frac{\partial\omega}{\partial\vec{k}} = \vec{v}_0 + \hat{k}\ \frac{c^2}{\sqrt{\omega_{II}^2\ + c^2\ k^2}}. \tag{3.94}$$

Here k is the usual wavenumber. The dispersion relation we obtain for the mono-metric structure is Lorentz invariant.

The fact that we have an analogue model representing both massive and massless particles is promising for quantum gravity phenomenology if we now extend the analysis to high-energy phonon modes where the quantum pressure term is significant, and where we consequently expect a breakdown of Lorentz invariance. For the following, we concentrate on the generalization of flat Minkowski spacetime, which implies a constant Ξ and zero background velocities, $\vec{v}_0$. In the language of condensed matter physics, we are thinking of a uniform condensate at rest.

3.3 | Outlook, summary and discussion

So where can (and should) we go from here? If 2-component BECs provide such a rich mathematical and physical structure, are 3-component BECs, or general multi-component BECs even better? That depends on what you are trying to do:

- If one wishes to actually *build* such an analogue spacetime in the laboratory, and perform actual experiments, then iteration through 1-BEC and 2-BEC systems seems the most promising route in terms of our technological capabilities.

- For n-component BECs we sketch the situation in figure 3.3. The key point is that due to overall translation invariance one again expects to find one massless quasi-particle, with now $n-1$ distinct massive modes. Unfortunately the matrix algebra is now considerably messier — not intrinsically difficult (after all we are only dealing with $n \times n$ matrices in field space) — but extremely tedious. Physical insight remains largely intact, but (except in some specific particularly simple cases), computations rapidly become lost in a morass of technical detail.

- However, if one wishes to draw general theoretical lessons from the analogue spacetime programme, then multi-component systems are definitely the preferred route — though in this case it is probably better to be even more abstract, and to go beyond the specific details of BEC-based systems to deal with general hyperbolic systems of PDEs.

- In Appendix C we have sketched some of the key features of the pseudo–Finsler spacetimes that naturally emerge from considering the leading symbol of a hyperbolic system of PDEs. While it is clear that much more could be done based on this, and on extending the field theory "normal modes" of [13, 14], such an analysis would very much move outside the scope of the current thesis.

In short the 2-BEC system is a good compromise between a system complex enough to exhibit a mass-generating mechanism, and still simple enough to be technologically tractable, with good prospects for laboratory realization of this system in the not too distant future.

The key features we have emphasised in this chapter have been:

- A general analysis of the 2-BEC system to see how perturbations on a 2-BEC background lead to a system of coupled wave equations.

- Extraction of the geometric notion of pseudo–Finsler spacetime from this wave equation, coupled with an analysis of how to specialize pseudo–Finsler geometry first to a bi-metric Lorentzian geometry and finally to the usual mono-metric Lorentzian geometry of most direct interest in general relativity and cosmology.

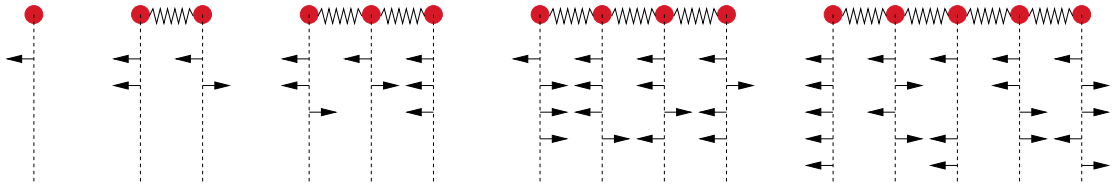


Figure 3.3: The figure captures the key features of possible eigenmodes for a small perturbation (circles) in a 1 (left side), 2, 3, 4, and 5-component (right side) BEC. In a 1-component system only one kind of perturbation is allowed, which corresponds to a massless particle propagating through an effective curved spacetime, while in the 2-component case two different kinds of mode appear, the one in-phase (massless particle) and one in anti-phase (massive particle). For a three-component system we again expect to find one massless particle, when all perturbations are in phase, and now in addition to that two massive particles.

- The mass-generating mechanism we have identified in suitably coupled 2-component BECs is an essential step in making this analogue spacetime more realistic; whatever one's views on the ultimate theory of "quantum gravity", any realistic low-energy phenomenology must contain *some* mass-generating mechanism.
- Use of the "quantum pressure" term in the 2-BEC system to mimic the sort of Lorentz violating physics that (based on the relatively young field of "quantum gravity phenomenology") is widely expected to occur at or near the Planck scale.
- Intriguingly, we have seen that in our specific model the mass-generating mechanism interacts with the Lorentz violating mechanism, naturally leading to a situation where the Lorentz violations are suppressed by powers of the quasi-particle mass scale divided by the analogue of the Planck scale.

In summary, while we do not personally believe that the real universe *is* an analogue spacetime, we are certainly intrigued by the fact that so much of what is normally viewed as being specific to general relativity and/or particle physics can be placed in this much wider context. We should also be forthright about the key weakness of analogue models as they currently stand: As we have seen, obtaining an analogue spacetime geometry (including spacetime curvature) is straightforward — but what is not straightforward is obtaining the Einstein equations. The analogue models are currently analogue models of quantum field theory on curved spacetime, but not (yet?) true analogue models of Einstein gravity. Despite this limitation, what can be achieved through the analogue spacetime programme is quite impressive, and we expect interest in this field, both theoretical and hopefully experimental, to continue unabated.

CHAPTER 4

Analogue quantum gravity phenomenology

As we have seen in the previous chapter, the 2-BEC system permits us to provide a mass-generating mechanism for the quasi-particle excitations [188, 189]. The specific mass-generating mechanism arising herein is rather different from the Higgs mechanism of the standard model of particle physics, and provides an interesting counterpoint to the more usual ways that mass-generation is achieved. Furthermore, at short distances, where the "quantum pressure" term can no longer be neglected, then even in the mono-metric regime one begins to see deviations from "Lorentz invariance" — and these deviations are qualitatively of the type encountered in "quantum gravity phenomenology", with the interesting property that the Lorentz violating physics is naturally suppressed by powers of the quasi-particle mass divided by the mass of the fundamental bosons that form the condensate [130, 200, 202, 131]. So in these analogue systems the mass-generating mechanism is related to the "hierarchy problem" and the suppression of Lorentz-violating physics. The 2-BEC model also allows us to probe the "universality" (or lack thereof) in the Lorentz violating sector [130, 200, 202, 131]. More generally, as one moves beyond the hydrodynamic limit in generic pseudo–Finsler parts of parameter space, one can begin to see hints of geometrical structure even more general than the pseudo–Finsler geometries.

While we do not wish to claim that the 2-BEC analogue spacetime of this chapter is necessarily a good model for the real physical spacetime arising from the putative theory of "quantum gravity" (be it string-model, loop-variable, or lattice based), it is clear that the 2-BEC analogue spacetime is an extraordinarily rich mathematical and physical structure that provides many interesting hints regarding the sort of kinematics and dynamics that one might encounter in a wide class of models for "quantum gravity phenomenology". This is the fundamental reason for our interest in this model, and we hope we can likewise interest the reader in this system and its relatives.

4.1 | Application to quantum gravity phenomenology

In using this 2-BEC model to probe issues of interest to the "quantum gravity phenomenology" community it behooves us to simplify as much as possible the parts of the model not of direct interest for current considerations. Specifically, we wish to use the "quantum pressure" term as a model for the type of Lorentz violating physics that might occur in the physical universe at or near the Planck scale [185]. Since we are then interested in high energies, and consequently short distances, one might expect the average spacetime curvature to be negligible — that is, we will be interested in looking for "quantum pressure" induced deviations from special relativity, and can dispense with the notion of curved spacetimes for now. ("Flat" pseudo–Finsler spaces are already sufficiently complicated to lead to interesting physics.) In terms of the BEC condensates this means that in this section of the chapter we will concentrate on a spatially-homogeneous time-independent background, so that in particular all the matrices $\mathbf{f}^{ab}$ will be taken to be position-independent. (And similarly, Ξ, Λ, D, *etc.* are taken to be position independent and we set $\vec{v}_0 = 0$, so the background is at rest.) We now consider Lorentz invariance breakdown in a flat mono-metric spacetime geometry as indicated in Fig. 4.1. This greatly simplifies the calculations (though they are still relatively messy), but without sacrificing the essential pieces of the physics we are now interested in.

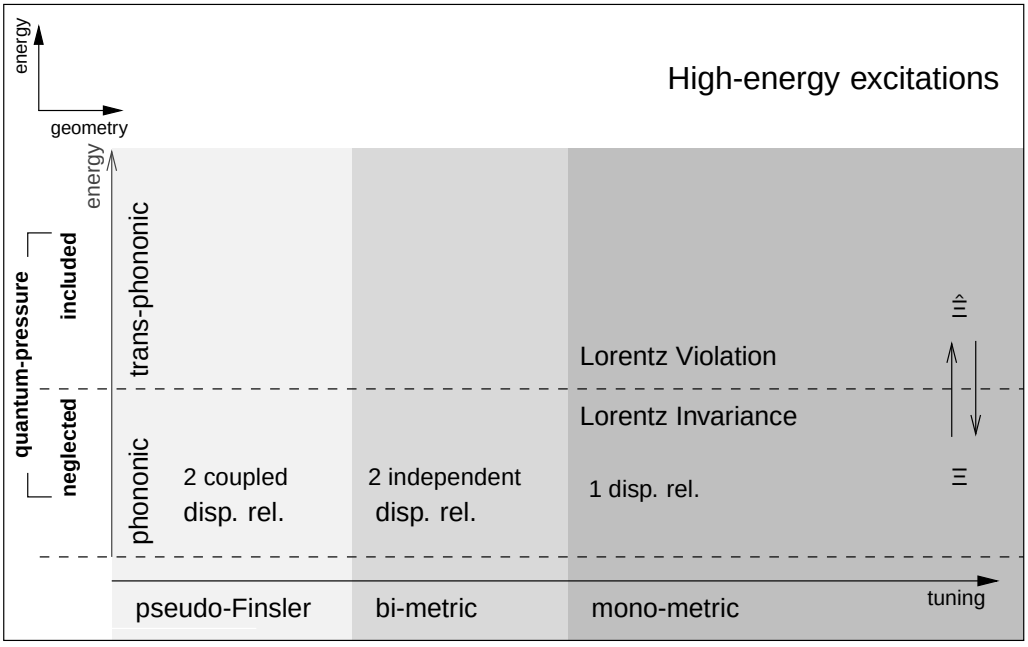


Figure 4.1: How to tune the system to exhibit breakdown of Lorentz symmetry.

Now the purpose of quantum gravity phenomenology is to analyze the physical consequences arising from various models of quantum gravity. One hope for obtaining an experimental grasp on quantum gravity is the generic prediction arising in many (but not all) quantum gravity models that ultraviolet physics at or near the Planck scale, $M_{\text{Planck}} = 1.2 \times 10^{19}\ \text{GeV}/c^2$, (or in some models the string scale), typically induces violations of Lorentz invariance at lower scales [138, 111]. Interestingly most investigations, even if they arise from quite different fundamental physics, seem to converge on the prediction that the breakdown of Lorentz invariance can generically become manifest in the form of modified dispersion relations

$$\omega^2 = \omega_0^2 + (1 + \eta_2)\ c^2\ k^2 + \eta_4 \left(\frac{\hbar}{M_{\text{Lorentz violation}}} \right)^2 k^4 + \dots\ , \tag{4.1}$$

where the coefficients η_n are dimensionless (and possibly dependent on the particle species considered), and we have restricted our expansion to CPT invariant terms (otherwise one would also get odd powers in k). The particular inertial frame for these dispersion relations is generally specified to be the frame set by the cosmological microwave background, and $M_{\text{Lorentz violation}}$ is the scale of Lorentz symmetry breaking which furthermore is generally assumed to be of the order of M_{Planck}.

Although several alternative scenarios have been considered in the literature in order to justify the modified kinematics discussed above, to date the most commonly explored avenue is an effective field theory (EFT) approach. In the present chapter we focus on the class of non-renormalizable EFTs with Lorentz violations associated to dispersion relations like equation (4.1). Relaxing our CPT invariance condition this class would include the model developed in [142], and subsequently studied by several authors, where an extension of quantum electrodynamics including only mass dimension five Lorentz-violating operators was considered. (That ansatz leads to order k^3 Lorentz and CPT violating terms in the dispersion relation.) Very accurate constraints have been obtained for this model using a combination of experiments and observations (mainly in high energy astrophysics). See *e.g.* [111, 110, 100, 101, 99]. In spite of the remarkable success of this framework as a "test theory", it is interesting to note that there are still significant open issues concerning its theoretical foundations. Perhaps the most pressing one is the so called *naturalness problem* which can be expressed in the following way: Looking back at our ansatz (4.1) we can see that the lowest-order correction, proportional to η_2, is not explicitly Planck suppressed. This implies that such a term would always be dominant with respect to the higher-order ones and grossly incompatible with observations (given that we have very good constraints on the universality of the speed of light for different elementary particles). Following the observational leads it has been therefore often assumed either that some symmetry (other than Lorentz invariance) enforces the η_2 coefficients to be exactly zero, or that the presence of some other characteristic EFT mass scale $\mu \ll M_{\text{Planck}}$ (*e.g.*, some particle physics mass scale) associated with the Lorentz symmetry breaking might enter in the lowest order dimensionless coefficient η_2 — which will be then generically suppressed by appropriate ratios of this characteristic mass to the Planck mass: $\eta_2 \propto (\mu/M_{\text{Planck}})^\sigma$ where $\sigma \geq 1$ is some positive power (often taken as one or two). If this is the case then one has two distinct regimes: For low momenta

$p/(M_{\text{Planck}}c) \ll (\mu/M_{\text{Planck}})^{\sigma}$ the lower-order (quadratic in the momentum) deviations in (4.1) will dominate over the higher-order ones, while at high energies $p/(M_{\text{Planck}}c) \gg (\mu/M_{\text{Planck}})^{\sigma}$ the higher order terms will be dominant.

The naturalness problem arises because such a scenario is not well justified within an EFT framework; in other words there is no natural suppression of the low-order modifications in these models. In fact we implicitly assumed that there are no extra Planck suppressions hidden in the dimensionless coefficients η_n with $n > 2$. EFT cannot justify why *only* the dimensionless coefficients of the $n \leq 2$ terms should be suppressed by powers of the small ratio μ/M_{Planck}. Even worse, renormalization group arguments seem to imply that a similar mass ratio, μ/M_{Planck} would implicitly be present also in *all* the dimensionless $n > 2$ coefficients — hence suppressing them even further, to the point of complete undetectability. Furthermore it is easy to show [46] that, without some protecting symmetry, it is generic that radiative corrections due to particle interactions in an EFT with only Lorentz violations of order $n > 2$ in (4.1) for the free particles, will generate $n = 2$ Lorentz violating terms in the dispersion relation, which will then be dominant. Observational evidence [138] suggests that for a variety of standard model particles $|\eta_2| \lesssim 10^{-21}$. Naturalness in EFT would then imply that the higher order terms are at least as suppressed as this, and hence beyond observational reach.

A second issue is that of "universality", which is not so much a "problem", as an issue of debate as to the best strategy to adopt. In dealing with situations with multiple particles one has to choose between the case of universal (particle-independent) Lorentz violating coefficients η_n, or instead go for a more general ansatz and allow for particle-dependent coefficients; hence allowing different magnitudes of Lorentz symmetry violation for different particles even when considering the same order terms (same n) in the momentum expansion. The two choices are equally represented in the extant literature (see *e.g.* [4] and [100] for the two alternative ansätze), but it would be interesting to understand how generic this universality might be, and what sort of processes might induce non-universal Lorentz violation for different particles.

4.1.1 | Specializing the wave equation

For current purposes, where we wish to probe violations of Lorentz invariance in a flat analogue spacetime, we start with our basic wave equation (3.25) and make the following specializations: $\delta_{\text{AB}} \to 0$ (so that $\Gamma^a \to 0$ and $K \to 0$). We also set all background fields to be homogeneous (space and time independent), and use the formal operators $\hat{\Xi}^{1/2}$ and $\hat{\Xi}^{-1/2}$ to define a new set of variables

$$\tilde{\theta} = \hat{\Xi}^{-1/2}\, \bar{\theta}, \tag{4.2}$$

in terms of which the wave equation becomes

$$\partial_t^2 \tilde{\theta} = \left\{ \hat{\Xi}^{1/2}\, [D\nabla^2 - \Lambda]\, \hat{\Xi}^{1/2} \right\} \tilde{\theta}, \tag{4.3}$$

or more explicitly

$$\partial_t^2 \tilde{\theta} = \left\{ [\Xi - X\nabla^2]^{1/2} \, [D\nabla^2 - \Lambda] \, [\Xi - X\nabla^2]^{1/2} \right\} \tilde{\theta}. \tag{4.4}$$

This is now a (relatively) simple PDE to analyze. The objects $\hat{\Xi}^{1/2}$ and $\hat{\Xi}^{-1/2}$ are 2×2 matrices whose elements are pseudo-differential operators, but to simplify things it is computationally efficient to go directly to the eikonal limit where[1]

$$\hat{\Xi} \to \Xi + X \, k^2. \tag{4.5}$$

This finally leads to a dispersion relation of the form

$$\det\left\{ \omega^2 \, \mathbf{I} - [\Xi + Xk^2]^{1/2} \, [Dk^2 + \Lambda] \, [\Xi + Xk^2]^{1/2} \right\} = 0 \,, \tag{4.6}$$

and "all" we need to do for the purposes of this chapter, is to understand this quasiparticle excitation spectrum in detail.

4.1.2 | Hydrodynamic approximation

The hydrodynamic limit consists of formally setting $\hat{X} \to 0$ so that $\hat{\Xi} \to \Xi$. (That is, one is formally setting the healing length matrix to zero: $Y \to 0$. More precisely, all components of the healing length matrix are assumed small compared to other length scales in the problem.) The wave equation (4.4) now takes the form:

$$\partial_t^2 \tilde{\theta} = \left\{ \Xi^{1/2} \, [D\nabla^2 - \Lambda] \, \Xi^{1/2} \right\} \tilde{\theta}. \tag{4.7}$$

Since this is second-order in both space and time derivatives, we now have at least the possibility of obtaining an exact "Lorentz invariance". We can now define the matrices

$$\Omega^2 = \Xi^{1/2} \, \Lambda \, \Xi^{1/2}; \qquad C_0^2 = \Xi^{1/2} \, D \, \Xi^{1/2}; \tag{4.8}$$

so that after Fourier transformation

$$\omega^2 \tilde{\theta} = \left\{ C_0^2 \, k^2 + \Omega^2 \right\} \, \tilde{\theta} \equiv H(k^2) \, \tilde{\theta}, \tag{4.9}$$

leading to the Fresnel equation

$$\det\{\omega^2 \, \mathbf{I} - H(k^2)\} = 0. \tag{4.10}$$

That is

$$\omega^4 - \omega^2 \, \mathrm{tr}[H(k^2)] + \det[H(k^2)] = 0, \tag{4.11}$$

whence

$$\omega^2 = \frac{\mathrm{tr}[H(k^2)] \pm \sqrt{\mathrm{tr}[H(k^2)]^2 - 4 \, \det[H(k^2)]}}{2}. \tag{4.12}$$

[1] Once we are in the eikonal approximation the pseudo-differential operator $\hat{\Xi}^{1/2} \to \sqrt{\Xi + k^2 X}$ can be given a simple and explicit meaning in terms of the Hamilton–Cayley theorems of Appendix D.

Note that the matrices Ω^2, C_0^2, and $H(k^2)$ have now carefully been arranged to be *symmetric*. This greatly simplifies the subsequent matrix algebra. Also note that the matrix $H(k^2)$ is a function of k^2; this will forbid the appearance of odd powers of k in the dispersion relation — as should be expected due to the parity invariance of the system.

Masses

We read off the "masses" by looking at the special case of space-independent oscillations for which

$$\partial_t^2 \bar{\theta} = -\Omega^2 \, \bar{\theta}, \tag{4.13}$$

allowing us to identify the "mass" (more precisely, the natural oscillation frequency) as

$$\text{"masses"} \propto \text{eigenvalues of } (\Xi^{1/2} \, \Lambda \, \Xi^{1/2}) = \text{eigenvalues of } (\Xi \, \Lambda). \tag{4.14}$$

Since Λ is a singular 2×2 matrix this automatically implies

$$\omega_I^2 = 0; \qquad \omega_{II}^2 = \text{tr}\,(\Xi \, \Lambda). \tag{4.15}$$

So we see that one mode will be a massless phonon while the other will have a non zero mass. Explicitly, in terms of the elements of the underlying matrices

$$\omega_I^2 = 0; \qquad \omega_{II}^2 = -\frac{2\sqrt{\rho_{A0}\,\rho_{B0}}\,\lambda}{\hbar^2}\{\tilde{U}_{AA} + \tilde{U}_{BB} - 2\tilde{U}_{AB}\} \tag{4.16}$$

so that (before any fine-tuning or decoupling)

$$\omega_{II}^2 = -\frac{2\sqrt{\rho_{A0}\,\rho_{B0}}\,\lambda}{\hbar^2} \times \left\{ U_{AA} + U_{BB} - 2U_{AB} - \frac{\lambda}{2\sqrt{\rho_{A0}\,\rho_{B0}}} \left[\sqrt{\frac{\rho_{A0}}{\rho_{B0}}} + \sqrt{\frac{\rho_{B0}}{\rho_{A0}}} \right]^2 \right\}. \tag{4.17}$$

It is easy to check that this quantity really does have the physical dimensions of a frequency.

Mono-metricity conditions

In order for our system to be a perfect analogue of special relativity:

- we want each mode to have a quadratic dispersion relation;
- we want each dispersion relation to have the same asymptotic slope.

Let us start by noticing that the dispersion relation (4.12) is of the form

$$\omega^2 = [\text{quadratic}_1] \pm \sqrt{[\text{quartic}]}. \tag{4.18}$$

The first condition implies that the quartic must be a perfect square

$$[\text{quartic}] = [\text{quadratic}_2]^2, \tag{4.19}$$

but then the second condition implies that the slope of this quadratic must be zero. That is

$$[\text{quadratic}_2](k^2) = [\text{quadratic}_2](0), \tag{4.20}$$

and so

$$[\text{quartic}](k^2) = [\text{quartic}](0) \tag{4.21}$$

must be constant independent of k^2, so that the dispersion relation is of the form

$$\omega^2 = [\text{quadratic}_1](k^2) \pm [\text{quadratic}_2](0). \tag{4.22}$$

Note that this has the required form (two hyperbolae with the same asymptotes, and possibly different intercepts). Now let us implement this directly in terms of the matrices C_0^2 and M^2.
Step 1: Using the results of the Appendix D.6, specifically equation (D.6):

$$\begin{aligned} \det[H^2(k)] &= \det[\Omega^2 + C_0^2\ k^2] && (4.23)\\ &= \det[\Omega^2] - \text{tr}\left\{\Omega^2\ \bar{C}_0^2\right\}\ k^2 + \det[C_0^2]\ (k^2)^2. && (4.24)\end{aligned}$$

(This holds for any linear combination of 2×2 matrices. Note that we apply trace reversal to the squared matrix C_0^2, we do not trace reverse and then square.) Since in particular $\det[\Omega^2] = 0$, we have:

$$\det[H^2(k)] = -\text{tr}\left\{\Omega^2\ \bar{C}_0^2\right\}\ k^2 + \det[C_0^2]\ (k^2)^2. \tag{4.25}$$

Step 2: Now consider the discriminant (the quartic)

$$\begin{aligned} \text{quartic} &\equiv \text{tr}[H(k^2)]^2 - 4\ \det[H(k^2)] && (4.26)\\ &= (\text{tr}[\Omega^2] + \text{tr}[C_0^2]\ k^2)^2 - 4\big[-\text{tr}\left\{\Omega^2\ \bar{C}_0^2\right\}\ k^2 + \det[C_0^2]\ (k^2)^2\big] && (4.27)\\ &= \text{tr}[\Omega^2]^2 + \{2\text{tr}[\Omega^2]\text{tr}[C_0^2] + 4\text{tr}\left\{\Omega^2\ \bar{C}_0^2\right\}\}k^2 + \left\{\text{tr}[C_0^2]^2 - 4\det[C_0^2]\right\}(k^2)^2 && (4.28)\\ &= \text{tr}[\Omega^2]^2 + 2\{2\text{tr}\left\{\Omega^2\ C_0^2\right\} - \text{tr}[\Omega^2]\text{tr}[C_0^2]\}k^2 + \left\{\text{tr}[C_0^2]^2 - 4\det[C_0^2]\right\}(k^2)^2. && (4.29)\end{aligned}$$

So in the end the two conditions above for mono-metricity take the form

$$\text{mono-metricity} \iff \begin{cases} \text{tr}[C_0^2]^2 - 4\ \det[C_0^2] = 0; \\ 2\text{tr}\left\{\Omega^2\ C_0^2\right\} - \text{tr}[\Omega^2]\ \text{tr}[C_0^2] = 0. \end{cases} \tag{4.30}$$

Once these two conditions are satisfied the dispersion relation is

$$\omega^2 = \frac{\text{tr}[H(k^2)] \pm \text{tr}[\Omega^2]}{2} = \frac{\text{tr}[\Omega^2] \pm \text{tr}[\Omega^2] + \text{tr}[C_0^2]\ k^2}{2} \tag{4.31}$$

whence

$$\omega_1^2 = \frac{1}{2}\text{tr}[C_0^2]\ k^2 = c_0^2 k^2 \qquad \omega_2^2 = \text{tr}[\Omega^2] + \frac{1}{2}\text{tr}[C_0^2]\ k^2 = \omega_{II}^2 + c_0^2 k^2, \tag{4.32}$$

as required. One mode is massless, one massive with exactly the "mass" previously deduced. One can now define the quantity

$$m_{II} = \hbar\omega_{II}/c_0^2, \tag{4.33}$$

which really does have the physical dimensions of a mass.

Interpretation of the mono-metricity conditions

But now we have to analyse the two simplification conditions

$$C1: \qquad \mathrm{tr}[C_0^2]^2 - 4\,\det[C_0^2] = 0; \tag{4.34}$$

$$C2: \qquad 2\,\mathrm{tr}\left\{\Omega^2\ C_0^2\right\} - \mathrm{tr}[\Omega^2]\mathrm{tr}[C_0^2] = 0; \tag{4.35}$$

to see what they tell us. The first of these conditions is equivalent to the statement that the 2×2 matrix C_0^2 has two identical eigenvalues. But since C_0^2 is symmetric this then implies $C_0^2 = c_0^2\ \mathbf{I}$, in which case the second condition is automatically satisfied. (In contrast, condition $C2$ does not automatically imply condition $C1$.) Indeed if $C_0^2 = c_0^2\ \mathbf{I}$, then it is easy to see that (in order to make C_0^2 diagonal)

$$\tilde{U}_{\mathrm{AB}} = 0, \tag{4.36}$$

(which is sufficient, by itself, to imply bi-metricity) and furthermore that

$$\frac{\tilde{U}_{\mathrm{AA}}\ \rho_{\mathrm{A0}}}{m_{\mathrm{A}}} = c_0^2 = \frac{\tilde{U}_{\mathrm{BB}}\ \rho_{\mathrm{B0}}}{m_{\mathrm{B}}}. \tag{4.37}$$

Note that we can now solve for λ to get

$$\lambda = -2\sqrt{\rho_{\mathrm{A0}}\ \rho_{\mathrm{B0}}}\ U_{\mathrm{AB}}, \tag{4.38}$$

whence

$$c_0^2 = \frac{U_{\mathrm{AA}}\ \rho_{\mathrm{A0}} + U_{\mathrm{AB}}\ \rho_{\mathrm{B0}}}{m_{\mathrm{A}}} = \frac{U_{\mathrm{BB}}\ \rho_{\mathrm{B0}} + U_{\mathrm{AB}}\ \rho_{\mathrm{A0}}}{m_{\mathrm{B}}}, \tag{4.39}$$

and

$$\omega_{II}^2 = \frac{4\rho_{\mathrm{A0}}\rho_{\mathrm{B0}}U_{\mathrm{AB}}}{\hbar^2}\left\{U_{\mathrm{AA}} + U_{\mathrm{BB}} - 2U_{\mathrm{AB}} + U_{\mathrm{AB}}\left[\sqrt{\frac{\rho_{\mathrm{A0}}}{\rho_{\mathrm{B0}}}} + \sqrt{\frac{\rho_{\mathrm{B0}}}{\rho_{\mathrm{A0}}}}\right]^2\right\}. \tag{4.40}$$

Note that (4.40) is equivalent to (4.17) with (4.38) enforced. But this then implies

$$\omega_{II}^2 = \frac{4\rho_{\mathrm{A0}}\rho_{\mathrm{B0}}U_{\mathrm{AB}}}{\hbar^2}\left\{U_{\mathrm{AA}} + U_{\mathrm{BB}} + U_{\mathrm{AB}}\left[\frac{\rho_{\mathrm{A0}}}{\rho_{\mathrm{B0}}} + \frac{\rho_{\mathrm{B0}}}{\rho_{\mathrm{A0}}}\right]\right\}. \tag{4.41}$$

Interpretation: Condition $C2$ forces the two low-momentum "propagation speeds" to be the same, that is, it forces the two $O(k^2)$ coefficients to be equal. Condition $C1$ is the stronger statement that there is no $O(k^4)$ (or higher order) distortion to the relativistic dispersion relation.

4.1.3 | Beyond the hydrodynamic approximation

At this point we want to consider the deviations from the previous analogue for special relativity. Our starting point is again Eq. (4.4), now retaining the quantum pressure term, which we Fourier transform to get:

$$\omega^2\tilde{\theta} = \left\{\sqrt{\Xi + X\ k^2}\ \ [D\ k^2 + \Lambda]\ \ \sqrt{\Xi + X\ k^2}\right\}\ \tilde{\theta} \equiv H(k^2)\ \tilde{\theta}. \tag{4.42}$$

This leads to the Fresnel equation

$$\det\{\omega^2\,\mathbf{I} - H(k^2)\} = 0. \tag{4.43}$$

That is

$$\omega^4 - \omega^2\,\mathrm{tr}[H(k^2)] + \det[H(k^2)] = 0, \tag{4.44}$$

whence

$$\omega^2 = \frac{\mathrm{tr}[H(k^2)] \pm \sqrt{\mathrm{tr}[H(k^2)]^2 - 4\,\det[H(k^2)]}}{2}, \tag{4.45}$$

which is now of the form

$$\omega^2 = [\mathrm{quartic}_1] \pm \sqrt{[\mathrm{octic}]}. \tag{4.46}$$

Masses

The "masses", defined as the zero momentum oscillation frequencies, are again easy to identify. Just note that the k-independent term in the Fresnel equation is exactly the same mass matrix $\Omega^2 = \Xi^{1/2}\,\Lambda\,\Xi^{1/2}$ that was present in the hydrodynamical limit. (That is, the quantum potential term X does not influence the masses.)

Dispersion relations

Differently from the previous case, when the hydrodynamic approximation held, we now have that the discriminant of (4.45) generically can be an eighth-order polynomial in k. In this case we cannot hope to recover an exact analogue of special relativity, but instead can at best hope to obtain dispersion relations with vanishing or *suppressed* deviations from special relativity at low k; possibly with large deviations from special relativity at high momenta. From the form of our equation it is clear that the Lorentz violation suppression should be somehow associated with the masses of the atoms $m_{A/B}$. Indeed we will use the underlying atomic masses to define our "Lorentz breaking scale", which we shall then assume can be identified with the "quantum gravity scale". The exact form and relative strengths of the higher-order terms will be controlled by tuning the 2–BEC system and will eventually decide the manifestation (or not) of the naturalness problem and of the universality issue.

Our approach will again consist of considering derivatives of (4.45) in growing even powers of k^2 (recall that odd powers of k are excluded by the parity invariance of the system) and then setting $k \to 0$. We shall compute only the coefficients up to order k^4 as by simple dimensional arguments one can expect any higher order term will be further suppressed with respect to the k^4 one.

We can greatly simplify our calculations if before performing our analysis we rearrange our problem in the following way. First of all note that by the cyclic properties of trace

$$\begin{aligned}
\mathrm{tr}[H(k^2)] &= \mathrm{tr}[(Dk^2 + \Lambda)\,(\Xi + k^2 X)] && (4.47)\\
&= \mathrm{tr}[\Lambda\Xi + k^2(D\Xi + \Lambda X) + (k^2)^2 DX] && (4.48)\\
&= \mathrm{tr}[\Xi^{1/2}\Lambda\Xi^{1/2} + k^2(\Xi^{1/2}D\Xi^{1/2} + X^{1/2}\Lambda X^{1/2}) + (k^2)^2 X^{1/2} D X^{1/2}]. && (4.49)
\end{aligned}$$

Putting this all together, we can now define symmetric matrices

$$\Omega^2 = \Xi^{1/2}\Lambda\Xi^{1/2}; \tag{4.50}$$

$$C_0^2 = \Xi^{1/2}D\Xi^{1/2}; \qquad \Delta C^2 = X^{1/2}\Lambda X^{1/2}; \tag{4.51}$$

$$C^2 = C_0^2 + \Delta C^2 = \Xi^{1/2}D\Xi^{1/2} + X^{1/2}\Lambda X^{1/2}; \tag{4.52}$$

$$Z^2 = 2X^{1/2}DX^{1/2} = \frac{\hbar^2}{2}M^{-2}. \tag{4.53}$$

With all these definitions we can then write

$$\mathrm{tr}[H(k^2)] = \mathrm{tr}\left[\Omega^2 + k^2(C_0^2 + \Delta C^2) + \frac{1}{2}(k^2)^2 Z^2\right], \tag{4.54}$$

where everything has been done inside the trace. If we now define

$$H_s(k^2) = \Omega^2 + k^2(C_0^2 + \Delta C^2) + \frac{1}{2}(k^2)^2 Z^2, \tag{4.55}$$

then $H_s(k^2)$ is by definition both polynomial and symmetric and satisfies

$$\mathrm{tr}[H(k^2)] = \mathrm{tr}[H_s(k^2)], \tag{4.56}$$

while in contrast,

$$\det[H(k^2)] \neq \det[H_s(k^2)]. \tag{4.57}$$

But then

$$\omega^2 = \frac{1}{2}\left[\mathrm{tr}[H_s(k^2)] \pm \sqrt{\mathrm{tr}[H_s(k^2)]^2 - 4\det[H(k^2)]}\right]. \tag{4.58}$$

Whence

$$\frac{\mathrm{d}\omega^2}{\mathrm{d}k^2} = \frac{1}{2}\left[\mathrm{tr}[H_s'(k^2)] \pm \frac{\mathrm{tr}[H_s(k^2)]\mathrm{tr}[H_s'(k^2)] - 2\det'[H(k^2)]}{\sqrt{\mathrm{tr}[H_s(k^2)]^2 - 4\det[H(k^2)]}}\right], \tag{4.59}$$

and at $k = 0$

$$\left.\frac{\mathrm{d}\omega^2}{\mathrm{d}k^2}\right|_{k\to 0} = \frac{1}{2}\left[\mathrm{tr}[C^2] \pm \frac{\mathrm{tr}[\Omega^2]\mathrm{tr}[C^2] - 2\det'[H(k^2)]_{k\to 0}}{\mathrm{tr}[\Omega^2]}\right]. \tag{4.60}$$

But now let us consider

$$\begin{aligned}
\det[H(k^2)] &= \det[(Dk^2 + \Lambda)\,(\Xi + k^2 X)] && (4.61)\\
&= \det[Dk^2 + \Lambda]\,\det[\Xi + k^2 X] && (4.62)\\
&= \det[\Xi^{1/2}(Dk^2 + \Lambda)\Xi^{1/2}]\,\det[I + k^2\Xi^{-1/2}X\Xi^{-1/2}] && (4.63)
\end{aligned}$$

where we have repeatedly used properties of the determinant. Furthermore

$$\begin{aligned}
\det[I + k^2\Xi^{-1/2}X\Xi^{-1/2}] &= \det[I + k^2\Xi^{-1}X] && (4.64)\\
&= \det[I + k^2 X^{1/2}\Xi X^{1/2}] && (4.65)\\
&= \det[I + k^2 Y^2/2], && (4.66)
\end{aligned}$$

so that we have

$$\det[H(k^2)] = \det[\Omega^2 + C_0^2 k^2]\ \det[I + k^2 Y^2/2]. \tag{4.67}$$

Note the matrix Y^2 is the "healing length matrix" we had previously defined, and that the net result of this analysis is that the full determinant is the product of the determinant previously found in the hydrodynamic limit with a factor that depends on the product of wavenumber and healing length.

But now, given our formula (D.6) for the determinant, we see

$$\begin{aligned}\det{}'[H(k^2)] &= (-\mathrm{tr}(\Omega^2 \bar{C}_0^2) + 2k^2 \det[C_0^2])\ \det[I + k^2 Y^2/2] \\ &\quad + \det[\Omega^2 + C_0^2 k^2]\ (-\mathrm{tr}[\bar{Y}^2] + k^2 \det[Y^2])/2,\end{aligned} \tag{4.68}$$

whence

$$\det{}'[H(k^2)]_{k\to 0} = -\mathrm{tr}(\Omega^2 \bar{C}_0^2), \tag{4.69}$$

and so

$$\left.\frac{\mathrm{d}\omega^2}{\mathrm{d}k^2}\right|_{k\to 0} = \frac{1}{2}\left[\mathrm{tr}[C^2] \pm \frac{\mathrm{tr}[\Omega^2]\mathrm{tr}[C^2] + 2\mathrm{tr}(\Omega^2 \bar{C}_0^2)}{\mathrm{tr}[\Omega^2]}\right]. \tag{4.70}$$

That is:

$$\left.\frac{\mathrm{d}\omega^2}{\mathrm{d}k^2}\right|_{k\to 0} = \frac{1}{2}\left[\mathrm{tr}[C^2] \pm \left\{\mathrm{tr}[C^2] + 2\frac{\mathrm{tr}(\Omega^2 \bar{C}_0^2)}{\mathrm{tr}[\Omega^2]}\right\}\right]. \tag{4.71}$$

Note that all the relevant matrices have been carefully symmetrized. Also note the important distinction between C_0^2 and C^2. Now define

$$c^2 = \frac{1}{2}\mathrm{tr}[C^2], \tag{4.72}$$

then

$$\left.\frac{\mathrm{d}\omega^2}{\mathrm{d}k^2}\right|_{k\to 0} = c^2(1 \pm \eta_2), \tag{4.73}$$

with

$$\eta_2 = \left\{\frac{\mathrm{tr}[C^2]\mathrm{tr}[\Omega^2] + 2\mathrm{tr}(\Omega^2 \bar{C}_0^2)}{\mathrm{tr}[\Omega^2]\mathrm{tr}[C^2]}\right\} = \left\{1 + \frac{\mathrm{tr}(\Omega^2 \bar{C}_0^2)}{\omega_{II}^2\ c^2}\right\}. \tag{4.74}$$

Similarly, consider the second derivative:

$$\begin{aligned}\frac{\mathrm{d}^2\omega^2}{\mathrm{d}(k^2)^2} &= \frac{1}{2}\Bigg[\mathrm{tr}[H_s''(k^2)] \pm \frac{\mathrm{tr}[H_s(k^2)]\mathrm{tr}[H_s''(k^2)] + \mathrm{tr}[H_s'(k^2)]\mathrm{tr}[H_s'(k^2)] - 2\det{}''[H(k^2)]}{\sqrt{\mathrm{tr}[H_s(k^2)]^2 - 4\det[H(k^2)]}} \\ &\quad \mp \frac{(\mathrm{tr}[H_s(k^2)]\mathrm{tr}[H_s'(k^2)] - 2\det{}'[H(k^2)])^2}{(\mathrm{tr}[H_s(k^2)]^2 - 4\det[H(k^2)])^{3/2}}\Bigg],\end{aligned} \tag{4.75}$$

whence

$$\begin{aligned}\left.\frac{\mathrm{d}^2\omega^2}{\mathrm{d}(k^2)^2}\right|_{k\to 0} &= \frac{1}{2}\Bigg[\mathrm{tr}[Z^2] \pm \frac{\mathrm{tr}[\Omega^2]\mathrm{tr}[Z^2] + \mathrm{tr}[C^2]^2 - 2\det{}''[H(k^2)]_{k\to 0}}{\mathrm{tr}[\Omega^2]} \\ &\quad \mp \frac{(\mathrm{tr}[\Omega^2]\mathrm{tr}[C^2] - 2\det{}'[H(k^2)]_{k\to 0})^2}{\mathrm{tr}[\Omega^2]^3}\Bigg].\end{aligned} \tag{4.76}$$

The last term above can be related to $\mathrm{d}\omega^2/\mathrm{d}k^2$, while the determinant piece is evaluated using

$$\begin{aligned}\det{}''[H(k^2)] &= (2\det[C_0^2])\,\det[I + k^2 Y^2/2] \\ &\quad +(-\mathrm{tr}(\Omega^2\bar{C}_0^2) + 2k^2\det[C_0^2])\,(-\mathrm{tr}[\bar{Y}^2] + k^2\det[Y^2])/2 \\ &\quad +\det[\Omega^2 + C_0^2 k^2]\,(\det[Y^2]/2) \\ &\quad +(-\mathrm{tr}(\Omega^2\bar{C}_0^2) + 2k^2\det[C_0^2])\,(-\mathrm{tr}[\bar{Y}^2] + k^2\det[Y^2])/2.\end{aligned} \tag{4.77}$$

Therefore

$$\begin{aligned}\det{}''[H(k^2)]_{k\to 0} &= (2\det[C_0^2]) + (-\mathrm{tr}(\Omega^2\bar{C}_0^2))\,(-\mathrm{tr}[\bar{Y}^2])/2 + \det[\Omega^2]\,(\det[Y^2])/2 \\ &\quad +(-\mathrm{tr}(\Omega^2\bar{C}_0^2))\,(-\mathrm{tr}[\bar{Y}^2])/2.\end{aligned} \tag{4.78}$$

That is, (recalling $\mathrm{tr}[\bar{A}] = -\mathrm{tr}[A]$),

$$\det{}''[H(k^2)]_{k\to 0} = (2\det[C_0^2]) - (\mathrm{tr}(\Omega^2\bar{C}_0^2))\,(\mathrm{tr}[Y^2]), \tag{4.79}$$

or

$$\det{}''[H(k^2)]_{k\to 0} = -\mathrm{tr}[C_0^2\bar{C}_0^2] - \mathrm{tr}[\Omega^2\bar{C}_0^2]\,\mathrm{tr}[Y^2]. \tag{4.80}$$

Now assembling all the pieces, a little algebra yields

$$\left.\frac{\mathrm{d}^2\omega^2}{\mathrm{d}(k^2)^2}\right|_{k\to 0} = \frac{1}{2}\left[\mathrm{tr}[Z^2] \pm \mathrm{tr}[Z^2] \pm 2\frac{\mathrm{tr}[\Omega^2\bar{C}_0^2]}{\mathrm{tr}[\Omega^2]}\mathrm{tr}[Y^2] \pm \frac{\mathrm{tr}[C^2]^2 - 4\det[C_0^2]}{\mathrm{tr}[\Omega^2]} \mp \frac{\mathrm{tr}[C^2]^2}{\mathrm{tr}[\Omega^2]}\eta_2^2\right]. \tag{4.81}$$

With the above formula we have completed our derivation of the lowest-order terms of the generic dispersion relation of a coupled 2-BEC system — including the terms introduced by the quantum potential at high wavenumber — up to terms of order k^4. From the above formula it is clear that we do not generically have Lorentz invariance in this system: Lorentz violations arise both due to mode-mixing interactions (an effect which can persist in the hydrodynamic limit where $Z \to 0$ and $Y \to 0$) and to the presence of the quantum potential (signaled by $Z \neq 0$ and $Y \neq 0$). While the mode-mixing effects are relevant at all energies the latter effect characterizes the discrete structure of the effective spacetime at high energies. It is in this sense that the quantum potential determines the analogue of quantum gravity effects in our 2-BEC system.

4.1.4 | The relevance for quantum gravity phenomenology

Following this physical insight we can now easily identify a regime that is potentially relevant for simulating the typical ansätze of quantum gravity phenomenology. We demand that any violation of Lorentz invariance present should be due to the microscopic structure of the effective spacetime. This implies that one has to tune the system in order to cancel exactly all those violations of Lorentz invariance which are solely due to mode-mixing interactions in the hydrodynamic limit.

We basically follow the guiding idea that a good analogue of quantum-gravity-induced Lorentz violations should be characterized only by the ultraviolet physics of the effective spacetime. In the system at hand the ultraviolet physics is indeed characterized by the quantum potential, whereas possible violations of the Lorentz invariance in the hydrodynamical limit are low energy effects, even though they have their origin in the microscopic interactions. We therefore start by investigating the scenario in which the system is tuned in such a way that no violations of Lorentz invariance are present in the hydrodynamic limit. This leads us to again enforce the conditions $C1$ and $C2$ which corresponded to "mono-metricity" in the hydrodynamic limit.

In this case (4.71) and (4.81) take respectively the form

$$\left.\frac{\mathrm{d}\omega^2}{\mathrm{d}k^2}\right|_{k\to 0} = \frac{1}{2}\left[\mathrm{tr}[C_0^2] + (1\pm 1)\,\mathrm{tr}[\Delta C^2]\right] = c_0^2 + \frac{1\pm 1}{2}\mathrm{tr}[\Delta C^2], \tag{4.82}$$

and

$$\begin{aligned}\left.\frac{\mathrm{d}^2\omega^2}{\mathrm{d}(k^2)^2}\right|_{k\to 0} &= \frac{\mathrm{tr}[Z^2]\pm\mathrm{tr}[Z^2]}{2} \mp \mathrm{tr}[C_0^2]\mathrm{tr}[Y^2] \pm \frac{1}{2}\frac{\mathrm{tr}[\Delta C^2]^2 + 2\mathrm{tr}[C_0^2]\mathrm{tr}[\Delta C^2]}{\mathrm{tr}[\Omega^2]} \mp \frac{1}{2}\frac{\mathrm{tr}[\Delta C^2]^2}{\mathrm{tr}[\Omega^2]} \\ &= \frac{\mathrm{tr}[Z^2]\pm\mathrm{tr}[Z^2]}{2} \pm \mathrm{tr}[C_0^2]\left(-\mathrm{tr}[Y^2] + \frac{\mathrm{tr}[\Delta C^2]}{\mathrm{tr}[\Omega^2]}\right).\end{aligned} \tag{4.83}$$

Recall (see section 4.1.2) that the first of the physical conditions $C1$ is equivalent to the statement that the 2×2 matrix C_0^2 has two identical eigenvalues. But since C_0^2 is symmetric this then implies $C_0^2 = c_0^2\,\mathbf{I}$, in which case the second condition is automatically satisfied. This also leads to the useful facts

$$\tilde{U}_{\mathrm{AB}} = 0 \quad\Longrightarrow\quad \lambda = -2\sqrt{\rho_{\mathrm{A0}}\;\rho_{\mathrm{B0}}}\;U_{\mathrm{AB}}; \tag{4.84}$$

$$c_0^2 = \frac{\tilde{U}_{\mathrm{AA}}\;\rho_{\mathrm{A0}}}{m_{\mathrm{A}}} = \frac{\tilde{U}_{\mathrm{BB}}\;\rho_{\mathrm{B0}}}{m_{\mathrm{B}}}. \tag{4.85}$$

Now that we have the fine tuning condition for the laser coupling we can compute the magnitude of the effective mass of the massive phonon and determine the values of the Lorentz violation coefficients. In particular we shall start checking that this regime allows for a real positive effective mass as needed for a suitable analogue model of quantum gravity phenomenology.

Effective mass

Remember that the definition of m_{II} reads

$$m_{II}^2 = \hbar^2\omega_{II}^2/c_0^4. \tag{4.86}$$

Using equation (4.84) and equation (4.85) we can rewrite c_0^2 in the following form

$$c_0^2 = [m_{\mathrm{B}}\rho_{\mathrm{A0}}U_{\mathrm{AA}} + m_{\mathrm{A}}\rho_{\mathrm{B0}}U_{\mathrm{BB}} + U_{\mathrm{AB}}(\rho_{\mathrm{A0}}m_{\mathrm{A}} + \rho_{\mathrm{B0}}m_{\mathrm{B}})]/(2m_{\mathrm{A}}m_{\mathrm{B}}). \tag{4.87}$$

Similarly equation (4.84) and equation (4.85) when inserted in Eq. (4.41) give

$$\omega_{II}^2 = \frac{4U_{AB}(\rho_{A0}m_B + \rho_{B0}m_A)c_0^2}{\hbar^2}. \tag{4.88}$$

We can now estimate m_{II} by simply inserting the above expressions in equation (4.86) so that

$$m_{II}^2 = \frac{8U_{AB}(\rho_{A0}m_A + \rho_{B0}m_B)m_A m_B}{[m_B\rho_{A0}U_{AA} + m_A\rho_{B0}U_{BB} + U_{AB}(\rho_{A0}m_A + \rho_{B0}m_B)]}. \tag{4.89}$$

This formula is still a little clumsy but a great deal can be understood by doing the physically reasonable approximation $m_A \approx m_B = m$ and $\rho_A \approx \rho_B$. In fact in this case one obtains

$$m_{II}^2 \approx m^2\,\frac{8U_{AB}}{[U_{AA} + 2U_{AB} + U_{BB}]}. \tag{4.90}$$

This formula now shows clearly that, as long as the mixing term U_{AB} is small compared to the "direct" scattering $U_{AA} + U_{BB}$, the mass of the heavy phonon will be "small" compared to the mass of the atoms. Though experimental realizability of the system is not the primary focus of the current paper, we point out that there is no obstruction in principle to tuning a 2-BEC system into a regime where $|U_{AB}| \ll |U_{AA} + U_{BB}|$. For the purposes of this chapter it is sufficient that a small effective phonon mass (small compared to the atomic masses which set the analogue quantum gravity scale) is obtainable for some arrangement of the microscopic parameters. We can now look separately at the coefficients of the quadratic and quartic Lorentz violations and then compare their relative strength in order to see if a situation like that envisaged by discussions of the naturalness problem is actually realized.

Coefficient of the quadratic deviation

One can easily see from (4.82) that the η_2 coefficients for this case take the form

$$\eta_{2,I} = 0; \tag{4.91}$$

$$\begin{aligned}\eta_{2,II}\; c_0^2 &= \mathrm{tr}[\Delta C^2] = \mathrm{tr}[X^{1/2}\Lambda X^{1/2}] = \mathrm{tr}[X\Lambda] \\ &= -\frac{1}{2}\frac{\lambda}{m_A m_B}\left(\frac{m_A\rho_{A0} + m_B\rho_{B0}}{\sqrt{\rho_{A0}\rho_{B0}}}\right).\end{aligned} \tag{4.92}$$

So if we insert the fine tuning condition for λ, equation (4.84), we get

$$\eta_{2,II} = \frac{U_{AB}\,(m_A\rho_{A0} + m_B\rho_{B0})}{m_A m_B c_0^2}. \tag{4.93}$$

Remarkably we can now cast this coefficient in a much more suggestive form by expressing the coupling U_{AB} in terms of the mass of the massive quasi-particle m_{II}^2. In order to do this we start from Eq. (4.88) and note that it enables us to express U_{AB} in (4.93) in terms of ω_{II}^2, thereby obtaining

$$\eta_{2,II} = \frac{\hbar^2}{4c_0^4}\,\frac{\rho_{A0}m_A + \rho_{B0}m_B}{\rho_{A0}m_B + \rho_{B0}m_A}\,\frac{\omega_{II}^2}{m_A m_B}. \tag{4.94}$$

Now it is easy to see that

$$\frac{\rho_{A0} m_A + \rho_{B0} m_B}{\rho_{A0} m_B + \rho_{B0} m_A} \approx \mathcal{O}(1), \tag{4.95}$$

and that this factor is identically unity if either $m_A = m_B$ or $\rho_{A0} = \rho_{B0}$. All together we are left with

$$\eta_{2,II} = \bar{\eta} \left(\frac{m_{II}}{\sqrt{m_A m_B}} \right)^2, \tag{4.96}$$

where $\bar{\eta}$ is a dimensionless coefficient of order unity.

The product in the denominator of the above expression can be interpreted as the geometric mean of the fundamental bosons masses m_A and m_B. These are mass scales associated with the microphysics of the condensate — in analogy with our experience with a 1-BEC system where the "quantum gravity scale" is set by the mass of the BEC atoms. It is then natural to define an analogue of the scale of the breakdown of Lorentz invariance as $M_{\text{eff}} = \sqrt{m_A m_B}$. (Indeed this "analogue Lorentz breaking scale" will typically do double duty as an "analogue Planck mass".)

Using this physical insight it should be clear that equation (4.96) effectively says

$$\eta_{2,II} \approx \left(\frac{m_{II}}{M_{\text{eff}}} \right)^2, \tag{4.97}$$

which, given that $m_I = 0$, we are naturally lead to generalize to

$$\eta_{2,X} \approx \left(\frac{m_X}{M_{\text{eff}}} \right)^2 = \left(\frac{\text{mass scale of quasiparticle}}{\text{effective Planck scale}} \right)^2; \qquad X = I, II. \tag{4.98}$$

The above relation is exactly the sort of dimensionless ratio $(\mu/M)^\sigma$ that has been very often *conjectured* in the literature on quantum gravity phenomenology in order to explain the strong observational constraints on Lorentz violations at the lowest orders. (See earlier discussion.) Does this now imply that this particular regime of our 2-BEC system will also show an analogue version of the naturalness problem? In order to answer this question we need to find the dimensionless coefficient for the quartic deviations, η_4, and check if it will or won't itself be suppressed by some power of the small ratio m_{II}/M_{eff}.

Coefficients of the quartic deviation

Let us now consider the coefficients of the quartic term presented in equation (4.83). For the various terms appearing in (4.83) we get

$$\text{tr}[Z^2] = 2\text{tr}[DX] = \frac{\hbar^2}{2} \left(\frac{m_A^2 + m_B^2}{m_A^2 m_B^2} \right); \tag{4.99}$$

$$\text{tr}[\Delta C^2] = \text{tr}[X\Lambda] = -\frac{\lambda}{2} \frac{m_A \rho_{A0} + m_B \rho_{B0}}{m_A m_B \sqrt{\rho_{A0} \rho_{B0}}} = U_{AB} \frac{m_A \rho_{A0} + m_B \rho_{B0}}{m_A m_B}; \tag{4.100}$$

$$\mathrm{tr}[Y^2] = 2\mathrm{tr}[X\Xi^{-1}] = \frac{\hbar^2}{2}\frac{\rho_{A0}m_A\tilde{U}_{AA} + \rho_{B0}m_B\tilde{U}_{BB}}{\rho_{A0}m_A\rho_{B0}m_B\tilde{U}_{AA}\tilde{U}_{BB}}; \tag{4.101}$$

where in the last expression we have used the fact that in the current scenario $\tilde{U}_{AB} = 0$. Now by definition

$$\eta_4 = \frac{1}{2}(M_{\mathrm{eff}}^2/\hbar^2)\left[\frac{\mathrm{d}^2\omega^2}{(\mathrm{d}k^2)^2}\right]_{k=0} \tag{4.102}$$

is the dimensionless coefficient in front of the k^4. So

$$\eta_4 = \frac{M_{\mathrm{eff}}^2}{2\hbar^2}\left[\frac{\mathrm{tr}[Z^2] \pm \mathrm{tr}[Z^2]}{2} \pm \mathrm{tr}[C_0^2]\left(-\frac{\mathrm{tr}[Y^2]}{2} + \frac{\mathrm{tr}[\Delta C^2]}{\mathrm{tr}[\Omega^2]}\right)\right] \tag{4.103}$$

$$= \frac{M_{\mathrm{eff}}^2\, c_0^2}{\hbar^2}\left[\frac{\mathrm{tr}[Z^2] \pm \mathrm{tr}[Z^2]}{2\mathrm{tr}[C_0^2]} \pm \left(-\frac{\mathrm{tr}[Y^2]}{2} + \frac{\mathrm{tr}[\Delta C^2]}{\mathrm{tr}[\Omega^2]}\right)\right]. \tag{4.104}$$

Whence

$$\eta_{4,I} = \frac{M_{\mathrm{eff}}^2\, c_0^2}{\hbar^2}\left[\frac{\mathrm{tr}[Z^2]}{\mathrm{tr}[C_0^2]} + \left(-\frac{\mathrm{tr}[Y^2]}{2} + \frac{\mathrm{tr}[\Delta C^2]}{\mathrm{tr}[\Omega^2]}\right)\right]; \tag{4.105}$$

$$\eta_{4,II} = \frac{M_{\mathrm{eff}}^2\, c_0^2}{\hbar^2}\left[\left(\frac{\mathrm{tr}[Y^2]}{2} - \frac{\mathrm{tr}[\Delta C^2]}{\mathrm{tr}[\Omega^2]}\right)\right]. \tag{4.106}$$

Let us compute the two relevant terms separately:

$$\frac{\mathrm{tr}[Z^2]}{\mathrm{tr}[C_0^2]} = \frac{\hbar^2}{4c_0^2}\left(\frac{m_A^2 + m_B^2}{m_A^2 m_B^2}\right) = \frac{\hbar^2}{4c_0^2 M_{\mathrm{eff}}^2}\left(\frac{m_A^2 + m_B^2}{m_A m_B}\right); \tag{4.107}$$

$$-\mathrm{tr}[Y^2]/2 + \frac{\mathrm{tr}[\Delta C^2]}{\mathrm{tr}[\Omega^2]} = -\frac{\hbar^2}{4M_{\mathrm{eff}}^2}\left[\frac{\rho_{A0}m_A\tilde{U}_{AA}^2 + \rho_{B0}m_B\tilde{U}_{BB}^2}{\rho_{A0}\rho_{B0}\tilde{U}_{AA}\tilde{U}_{BB}\left(\tilde{U}_{AA} + \tilde{U}_{BB}\right)}\right]$$

$$= -\frac{\hbar^2}{4M_{\mathrm{eff}}^2\, c_0^2}\left[\frac{m_A^2\tilde{U}_{AA} + m_B^2\tilde{U}_{BB}}{m_A m_B\left(\tilde{U}_{AA} + \tilde{U}_{BB}\right)}\right]; \tag{4.108}$$

where we have used $\rho_{X0}\tilde{U}_{XX} = m_X c_0^2$ for $X = A, B$ as in equation (4.85). Note that the quantity in square brackets in the last line is dimensionless. So in the end:

$$\eta_{4,I} = \frac{1}{4}\left[\left(\frac{m_A^2 + m_B^2}{m_A m_B}\right) - \frac{m_A^2\tilde{U}_{AA} + m_B^2\tilde{U}_{BB}}{m_A m_B\left(\tilde{U}_{AA} + \tilde{U}_{BB}\right)}\right] \tag{4.109}$$

$$= \frac{1}{4}\left[\frac{m_A^2\tilde{U}_{BB} + m_B^2\tilde{U}_{AA}}{m_A m_B\left(\tilde{U}_{AA} + \tilde{U}_{BB}\right)}\right]; \tag{4.110}$$

$$\eta_{4,II} = \frac{1}{4}\left[\frac{m_A^2\tilde{U}_{AA} + m_B^2\tilde{U}_{BB}}{m_A m_B\left(\tilde{U}_{AA} + \tilde{U}_{BB}\right)}\right]. \tag{4.111}$$

Note: In the special case $m_A = m_B$ we recover identical quartic deviations $\eta_{4,I} = \eta_{4,II} = 1/4$, indicating in this special situation a "universal" deviation from Lorentz invariance. Indeed we also obtain $\eta_{4,I} = \eta_{4,II}$ if we demand $\tilde{U}_{AA} = \tilde{U}_{BB}$, even without fixing $m_A = m_B$.

Thus in the analogue spacetime we have developed, the issue of *universality* is fundamentally related to the complexity of the underlying microscopic system. As long as we keep the two atomic masses m_A and m_B distinct we generically have distinct η_4 coefficients (and the η_2 coefficients are unequal even in the case $m_A = m_B$). However we can easily recover identical η_4 coefficients, for instance, as soon as we impose identical microphysics for the two BEC systems we couple.

Avoidance of the naturalness problem

We can now ask ourselves if there is, or is not, a naturalness problem present in our system. Are the dimensionless coefficients $\eta_{4,I/II}$ suppressed below their naive values by some small ratio involving $M_{\text{eff}} = \sqrt{m_A m_B}$? Or are these ratios unsuppressed? Indeed at first sight it might seem that further suppression is the case, since the square of the "effective Planck scale" seems to appear in the denominator of both the coefficients (4.110) and (4.111). However, the squares of the atomic masses also appear in the numerator, rendering both coefficients of order unity.

It is perhaps easier to see this once the dependence of (4.110) and (4.111) on the effective coupling $\tilde{U}$ is removed. We again use the substitution $\tilde{U}_{XX} = m_X c_0^2/\rho_{X0}$ for $X = A, B$, so obtaining:

$$\eta_{4,I} = \frac{1}{4}\left[\frac{m_A\rho_{A0} + m_B\rho_{B0}}{m_A\rho_{B0} + m_B\rho_{A0}}\right]; \tag{4.112}$$

$$\eta_{4,II} = \frac{1}{4}\left[\frac{m_A^3\rho_{B0} + m_B^3\rho_{A0}}{m_A m_B\left(m_A\rho_{B0} + m_B\rho_{A0}\right)}\right]. \tag{4.113}$$

From these expressions it is clear that the $\eta_{4,I/II}$ coefficients are actually of order unity.

That is, if our system is set up so that $m_{II} \ll m_{A/B}$ — which we have seen in this scenario is equivalent to requiring $U_{AB} \ll U_{AA/BB}$ — no naturalness problem arises as for $p > m_{II}\, c_0$ the higher-order, energy-dependent Lorentz-violating terms ($n \geq 4$) will indeed dominate over the quadratic Lorentz-violating term.

It is quite remarkable that the quadratic coefficients (4.98) are *exactly* of the form postulated in several works on non-renormalizable EFT with Lorentz invariance violations (see e.g. [4]). They are indeed the squared ratio of the particle mass to the scale of Lorentz violation. Moreover we can see from (4.110) and (4.111) that there is no further suppression — after having pulled out a factor $(\hbar/M_{\text{Lorentz violation}})^2$ — for the quartic coefficients $\eta_{4,I/II}$. These coefficients are of order one and generically non-universal, (though if desired they can be forced to be universal by additional and specific fine tuning).

The suppression of η_2, combined with the *non-suppression* of η_4, is precisely the statement that the "naturalness problem" does not arise in the current model. We stress this is not a "tree level" result as the dispersion relation was computed directly from the fundamental Hamiltonian and was

not derived via any EFT reasoning. Moreover avoidance of the naturalness problem is not directly related to the tuning of our system to reproduce special relativity in the hydrodynamic limit. In fact our conditions for recovering special relativity at low energies do not *a priori* fix the the η_2 coefficient, as its strength after the "fine tuning" could still be large (even of order one) if the typical mass scale of the massive phonon is not well below the atomic mass scale. Instead the smallness of η_2 is directly related to the mass-generating mechanism.

The key question is now: Why does our model escape the naive predictions of dominant lowest-dimension Lorentz violations? (In fact in our model for any $p \gg m_{II}$ the k^4 Lorentz violating term dominates over the order k^2 one.) We here propose a nice interpretation in terms of "emergent symmetry": Non-zero λ *simultaneously* produces a non-zero mass for one of the phonons, *and* a corresponding non-zero Lorentz violation at order k^2. (Single BEC systems have only k^4 Lorentz violations as described by the Bogoliubov dispersion relation.) Let us now drive $\lambda \to 0$, but keep the conditions $C1$ and $C2$ valid at each stage. (This also requires $U_{\mathrm{AB}} \to 0$.) One gets an EFT which at low energies describes two non-interacting phonons propagating on a common background. (In fact $\eta_2 \to 0$ and $c_I = c_{II} = c_0$.) This system possesses a $SO(2)$ symmetry. Non-zero laser coupling λ softly breaks this $SO(2)$, the mass degeneracy, and low-energy Lorentz invariance. Such soft Lorentz violation is then characterized (as usual in EFT) by the ratio of the scale of the symmetry breaking m_{II}, and that of the scale originating the Lorentz violation in first place $M_{\text{Lorentz violation}}$. We stress that the $SO(2)$ symmetry is an "emergent symmetry" as it is not preserved beyond the hydrodynamic limit: the η_4 coefficients are in general different if $m_{\mathrm{A}} \neq m_{\mathrm{B}}$, so $SO(2)$ is generically broken at high energies. Nevertheless this is enough for the protection of the *lowest*-order Lorentz violating operators. The lesson to be drawn is that emergent symmetries are sufficient to minimize the amount of Lorentz violation in the lowest-dimension operators of the EFT. In this regard, it is intriguing to realise that an interpretation of SUSY as an accidental symmetry has indeed been considered in recent times [87], and that this is done at the cost of renouncing attempts to solve the hierarchy problem in the standard way. It might be that in this sense the smallness of the particle physics mass scales with respect to the Planck scale could be directly related to smallness of Lorentz violations in renormalizable operators of the low-energy effective field theory we live in. We hope to further investigate these issues in future work.

CHAPTER 5

Early universe cosmology in emergent spacetime

We now present an example of emergent cosmological spacetime as the hydrodynamic limit of a more fundamental microscopic theory. The low-energy, long-wavelength limit in our model is dominated by collective variables that generate an effective Lorentzian metric. This system naturally exhibits a microscopic mechanism allowing us to perform controlled signature change between Lorentzian and Riemannian geometries. We calculate the number of particles produced from a finite-duration Euclidean-signature event, where we take the position that to a good approximation the dynamics is dominated by the evolution of the linearized perturbations, as suggested by Calzetta and Hu [Phys. Rev. A **68** (2003) 043625]. We adapt the ideas presented by Dray *et al.* [Gen. Rel. Grav. **23** (1991) 967], such that the field and its canonical momentum are continuous at the signature-change event.
We investigate the interplay between the underlying microscopic structure and the emergent gravitational field, focussing on its impact on particle production in the ultraviolet regime. In general, this can be thought of as the combination of trans-Planckian physics and signature-change physics. Further we investigate the possibility of using the proposed signature change event as an amplifier for analogue "cosmological particle production" in condensed matter experiments.

5.1 | Introduction and Motivation

Emergent spacetimes [93, 18, 144] allow us to approach the subject of curved spacetime quantum field theory (CST-QFT) through the back door. This has been demonstrated in detail by using ultra-cold (non-relativistic), highly dilute Bose gases [81, 82, 12]. Under appropriate conditions the fundamental microscopic theory can be replaced by a classical mean-field, the Bose–Einstein con-

densate (BEC) [42]. Collective excitations, both classical and quantum, experience an effective spacetime whose entries are purely macroscopic mean-field variables. The kinematic equations for linearized perturbations — neglecting back-reaction and finite temperature effects — are equivalent to covariant minimally coupled scalar fields, with a d'Alembertian

$$\Delta \ldots = \frac{1}{\sqrt{-g}}\, \partial_a(\sqrt{-g}\, g^{ab}\, \partial_b \ldots) \tag{5.1}$$

defined by an effective metric g_{ab} [81, 82, 12].

Quantum field theory in curved spacetime is a good approximation for semiclassical gravity — at the level where back-reactions of the quantum fields on the gravitational field are negligible [29]. As a consequence quantum effects in curved spacetimes (CSTs) — *e.g.*, Hawking radiation [173, 178, 180] and cosmological particle production — do not require emergent Einstein gravity *per se*; the existence of an emergent spacetime, an effective gravitational field g_{ab}, is sufficient. Of course both systems, semiclassical gravity and any analogue model, must involve some dynamics — and so they will eventually diverge from each other. The only possible loophole would be if Einstein gravity were itself to be the "hydrodynamics" of some more fundamental theory (of microscopic objects, for example strings, molecules, or atoms). For our purposes a perfect match is not required, and we refer the interested reader to [160, 105, 19, 183, 195] for further details.

It has been shown that the repulsive or attractive nature of atomic interaction in a Bose gas is directly related to the signature of the low-energy emergent metric: Lorentzian $(-,+++)$ for repulsive interactions, Euclidean $(+,+++)$ for attractive interactions [12]. In 2001 a BEC experiment [52, 156] was carried out that can be viewed as the first analogue model experiment. By tuning through a Feshbach resonance [95] the atomic interactions were driven into a weakly attractive regime, and triggered a controlled condensate collapse. Two years later, the theoretical work of Calzetta and Hu [38, 39], connected the so-called Bose-nova phenomenon with the amplification, mixing of positive and negative modes, and squeezing of vacuum fluctuations due to a signature change event. Perhaps surprisingly, the calculations carried out in [38, 39] did not include background condensate dynamics and yet their theoretical predictions reflect the experimental data relatively well. For short time-intervals of attractive atom-atom interaction (*i.e.*, a brief excursion into Euclidean signature), the Bose-nova event is dominated by the evolution of the quantum perturbations, and to a good approximation independent of the background condensate dynamics.

Specifically, given that we do not as yet have any precise detailed model for emergent Einstein gravity, as opposed to emergent curved spacetime, it seems necessary to focus on quantum effects that are merely of kinematic rather than dynamic nature. However, there are ways to study the influence of possible quantum gravity candidates with CST-QFT. This branch of physics is called quantum gravity phenomenology (QGP) [138]. Emergent spacetimes can be used to analyze some portions of QGP, where Lorentz invariance violations (LIV) are present at ultraviolet scales. The LIV scale is supposed to be connected with the Planck length, where new physics is expected.

This idea is naturally implemented in any emergent spacetime model. For example, the BEC-based analogue models only recover Lorentz invariance (LI) for the low-energy, long-wavelength phonon modes. For trans-phononic modes microscopic corrections (*e.g.*, quantum pressure effects) have to be absorbed into the macroscopic picture. The borderline between the two modes can be viewed as the analogue LIV scale. Given that trans-phononic modes start to see first signs of the fundamental microscopic theory, it makes sense to speak of LIV at the analogue Planck scale. The key reason why it is interesting to study modifications in the dispersion relation is that many different effective field theories (EFTs) already predict deviations at the kinematical level. A detailed treatment of the analogue trans-Planckian model can be found in [185, 131, 130, 202, 200].

In ongoing work [113] a classical phase-space method has been used to numerically simulate cosmological particle production in BECs. There it is shown that for a consistent treatment microscopic corrections play an important role in the emergent spacetime picture. This leads to emergent "rainbow metrics", with a Planck-suppressed momentum dependence for the modes, and consequently leads to a modification in the quasi-particle spectrum.

The main aim of this chapter is to merge all of the preceding points and address the trans-Planckian problem for a signature change event in a Bose gas. We are particularly interested in the ultraviolet physics of the phonon modes and hence have chosen a specific BEC set-up where the external trapping potential does not interfere with the dynamics (*e.g.*, hard-walled box). Step-by-step, in section (5.2) we show how spacetime emerges from a Bose gas; calculate the quasi-particle production from sudden sound speed variations in section (5.3); extend this calculation to sudden variations for finite regions with different signature (Lorentzian $\leftrightarrow$ Euclidean) in section (5.4); introduce ultraviolet physics and re-calculate the quasi-particle production in section (5.5); suggest in section (5.6) to employ a finite Euclidean region as a particle amplifier for cosmological particle production in a BEC; and last but certainly not least, we address the theoretical and experimental impact of our results in section (5.7).

5.2 | Emergent geometry from a Bose gas

The intent in this section is to give readers unfamiliar with the topic some deeper understanding of BEC-based analogue spacetimes. Following the example of [18] we introduce an ultra-cold (*i.e.*, non-relativistic), highly dilute and weakly interacting gas of Bosons, using the formalism of canonical quantization, and derive the equation of motion for small quantum fluctuations around some classical background; better known as a BEC, see section (5.2.1). The Bose–Einstein condensate is a state of matter where the Bosons macroscopically occupy the lowest quantum state. In section (5.2.2) we focus on the hydrodynamic case and recover a covariant minimally coupled massless scalar field for small quantum fluctuations in the BEC. Subsequently, in section (5.5), we will revisit this derivation and include trans-phononic modes (*e.g.*, ultraviolet physics) into the emergent spacetime picture.

5.2.1 | Ultra-cold, weakly interacting Bose gas

Suppose we have a system of N Bosons. In quantum field theory the field variables are quantum operators that act on quantum states (Hilbert space of states; *e.g.*, Fock space). Field operators either create, $\hat{\psi}^\dagger(t,\mathbf{x})$, or destroy, $\hat{\psi}(t,\mathbf{x})$, an individual Boson at a particular point in space and time, and satisfy the commutators:

$$\left[\hat{\psi}(t,\mathbf{x}),\hat{\psi}(t,\mathbf{x}')\right] = \left[\hat{\psi}^\dagger(t,\mathbf{x}),\hat{\psi}^\dagger(t,\mathbf{x}')\right] = 0\,; \tag{5.2}$$

$$\left[\hat{\psi}(t,\mathbf{x}),\hat{\psi}^\dagger(t,\mathbf{x}')\right] = \delta(\mathbf{x}-\mathbf{x}')\,. \tag{5.3}$$

For a gas of trapped, ultra-cold, highly dilute and weakly interacting Bosons the Hamiltonian is given by

$$\hat{H} = \int d^d\mathrm{x}\left(-\hat{\psi}^\dagger\frac{\hbar^2}{2m}\nabla^2\hat{\psi} + \hat{\psi}^\dagger V_{\text{ext}}\hat{\psi} + \frac{U}{2}\,\hat{\psi}^\dagger\hat{\psi}^\dagger\hat{\psi}\hat{\psi}\right). \tag{5.4}$$

This is a sum of the kinetic energy of the Boson field, and the two potential energy contributions; the external trap V_{ext}, and the particle interactions. The extreme dilution of the gas (*e.g.*, $10^{13}-10^{15}\,\text{atoms}/\text{cm}^3$) suppresses more-than-two-particle interactions, and in the weakly interacting regime the actual inter-atom potential has been approximated by a pseudo-contact potential,

$$U = \frac{4\pi\hbar^2 a}{m}\,. \tag{5.5}$$

Here m is the single-Boson mass, and a the s-wave scattering length. The sign of the scattering length determines the qualitative behavior of the interactions,

$$\begin{aligned} a > 0 \qquad & \text{repulsive}\,; \\ a < 0 \qquad & \text{attractive}\,. \end{aligned} \tag{5.6}$$

Negative and positive values of a are experimentally accessible by tuning external magnetic fields, that interact with the inter-atomic potential; this process is called Feshbach resonance [95]. We would like to emphasize the importance of Eq. (5.6) for the remaining sections.

We now have all the necessary information about our system, encoded in Eqs. (5.2)–(5.4), to calculate its dynamics. We use the Heisenberg equation of motion to get the time-evolution for the field operator;

$$i\hbar\frac{\partial\hat{\psi}}{\partial t} = \left[-\frac{\hbar^2}{2m}\nabla^2 + V_{\text{ext}} + U\,\hat{\psi}^\dagger\hat{\psi}\right]\hat{\psi}\,. \tag{5.7}$$

To apply this discussion to the emergent spacetime programme, we use the macroscopic occupation of the lowest quantum state below a critical temperature (*e.g.*, for alkali gases, below 10^{-5} K). If the cooling process prohibits the gas to solidify, a new state of matter will occur, the Bose–Einstein condensate. The condensate is a complex-valued macroscopic mean-field

$$\langle\hat{\psi}(t,\mathbf{x})\rangle = \psi(t,\mathbf{x}) = \sqrt{n_0(t,\mathbf{x})}\exp\left(i\theta_0(t,\mathbf{x})\right)\,, \tag{5.8}$$

where the individual microscopic particles give way to collective variables. We will show that the condensate density, n_0, and phase, θ_0, define the analogue spacetime for small quantum fluctuations in the BEC. The essential step in deriving the kinematics for the perturbation is to separate the perturbation from the condensate:

$$\hat{\psi} \simeq \psi(t,\mathbf{x}) + \delta\hat{\psi}(t,\mathbf{x})\,; \tag{5.9}$$

$$\hat{\psi}^\dagger \simeq \psi^\dagger(t,\mathbf{x}) + \delta\hat{\psi}^\dagger(t,\mathbf{x})\,. \tag{5.10}$$

This transformation is canonical if the creation $\delta\hat{\psi}^\dagger$ and destruction $\delta\hat{\psi}$ of perturbations is consistent with the commutator Eqs. (5.2)-(5.3). Therefore, the commutators for the linearized quantum fluctuations are

$$\left[\delta\hat{\psi}(t,\mathbf{x}),\delta\hat{\psi}(t,\mathbf{x}')\right] = \left[\delta\hat{\psi}^\dagger(t,\mathbf{x}),\delta\hat{\psi}^\dagger(t,\mathbf{x}')\right] = 0\,; \tag{5.11}$$

$$\left[\delta\hat{\psi}(t,\mathbf{x}),\delta\hat{\psi}^\dagger(t,\mathbf{x}')\right] = \delta(\mathbf{x}-\mathbf{x}')\,. \tag{5.12}$$

The quantum perturbations are small perturbations which, as per Eq. (5.8), are represented by two collective parameters; the density n, and the phase θ. Clearly, any quantum perturbation should be related to variations in these two parameters; $n \simeq n_0 + \hat{n}$ and $\theta \simeq \theta_0 + \hat{\theta}$. A straightforward expansion of ψ and $\psi^\dagger$ around n_0 and θ_0 leads to

$$\delta\hat{\psi} \simeq \psi\left(\frac{1}{2}\frac{\hat{n}}{n_0} + i\hat{\theta}\right)\,, \tag{5.13}$$

$$\delta\hat{\psi}^\dagger \simeq \psi^*\left(\frac{1}{2}\frac{\hat{n}}{n_0} - i\hat{\theta}\right)\,. \tag{5.14}$$

In this way Eqs. (5.9) and (5.10) are compatible with Eq. (5.8). Thus the density, $\hat{n}$, and phase, $\hat{\theta}$, fluctuations operators are Hermitian operators:

$$\hat{n} \simeq n_0\left[\frac{\delta\hat{\psi}}{\psi} + \left(\frac{\delta\hat{\psi}}{\psi}\right)^\dagger\right]\,; \tag{5.15}$$

$$\hat{\theta} \simeq -\frac{i}{2}\left[\frac{\delta\hat{\psi}}{\psi} - \left(\frac{\delta\hat{\psi}}{\psi}\right)^\dagger\right]\,. \tag{5.16}$$

It is easy to see that the new operators are a set of canonical variables:

$$\left[\hat{n}(t,\mathbf{x}),\hat{n}(t,\mathbf{x}')\right] = \left[\hat{\theta}(t,\mathbf{x}),\hat{\theta}(t,\mathbf{x}')\right] = 0\,; \tag{5.17}$$

$$\left[\hat{n}(t,\mathbf{x}),\hat{\theta}(t,\mathbf{x}')\right] = i\delta(\mathbf{x}-\mathbf{x}')\,. \tag{5.18}$$

The latter can be further modified, and we will subsequently revisit Eq. (5.18). While the split into background plus perturbation is up to this point exact, we now linearize by assuming the perturbation

to be small, allowing us to neglect quadratic and higher-order products of the perturbation field $\delta\psi$. (There are also more sophisticated calculational techniques available based on the Hartree–Fock–Bogoliubov–Popov approximation, but they are an unnecessary complication in the present situation.)

Merging equations (5.9)–(5.10) with equations (5.13)–(5.14), applying them to Eq. (5.7), we obtain two equations,

$$\frac{\partial \hat{n}}{\partial t} + \nabla \left[\frac{n_0 \hbar}{m} \nabla \hat{\theta} + \hat{n} \cdot \mathbf{v} \right] = 0 \,; \tag{5.19}$$

$$\frac{\partial \hat{\theta}}{\partial t} + \mathbf{v} \cdot \nabla \hat{\theta} + \frac{\mathcal{U}}{\hbar} \hat{n} = 0 \,. \tag{5.20}$$

Here we introduce the background velocity of the condensate,

$$\mathbf{v} = \frac{\hbar}{m} \nabla \theta_0 . \tag{5.21}$$

The quantity $\mathcal{U}$ can be thought of as an effective atomic interaction, as seen by the collective excitations. For long-wavelength, low-energetic modes this simplifies to Eq. (5.5), the usual pseudo-contact potential;

$$\mathcal{U} \to U \quad : \quad \text{phononic modes} \,. \tag{5.22}$$

We will come back to this point in section (5.5) where we shall write down the expression for $\mathcal{U}$ in general, and in the eikonal limit, in a manner appropriate to describe trans-phononic (or, ultraviolet) modes. In the language of condensed matter physics, we include "quantum pressure" effects. Without quantum pressure we restrict our analysis to the phononic regime, and assume that all collective excitations propagate with the same speed, the sound speed c_0;

$$c_0^2 = \frac{n_0 U}{m} \,. \tag{5.23}$$

Before we continue with our program, we would like to revisit the commutator derived in Eq. (5.18). In the phononic regime, we are able to write Eq. (5.20) as follows,

$$\hat{n} = -\frac{\hbar}{U} \left(\frac{\partial}{\partial_t} + \mathbf{v} \cdot \nabla \right) \hat{\theta} = -\frac{\hbar}{U} \frac{D\hat{\theta}}{Dt} \,. \tag{5.24}$$

Thus the commutator (5.18) can be written in terms of $\hat{\theta}$ and its fluid-following derivative (or material derivative) $D\hat{\theta}/Dt$:

$$\left[\hat{\theta}(t, \mathbf{x}), \hat{\Pi}_{\hat{\theta}}(t, \mathbf{x}') \right] = i\delta(\mathbf{x} - \mathbf{x}') \,. \tag{5.25}$$

Here we have defined,

$$\hat{\Pi}_{\hat{\theta}} = \frac{\hbar}{U} \frac{D\hat{\theta}}{Dt} \,, \tag{5.26}$$

which can be viewed as the conjugate momentum of $\hat{\theta}$; see Eq. (5.33) below.

The relation (5.24) enables us to read density perturbations as fluid-following derivatives of the phase perturbations, and hence supplies us with the necessary tool to eliminate all occurrences of $\hat{n}$ from equation (5.19):

$$-\partial_t\left[\frac{\hbar}{U}\,\partial_t\hat{\theta}\right]-\partial_t\left[\frac{\hbar}{U}\,\mathbf{v}\,\nabla\hat{\theta}\right]-\nabla\left[\frac{\hbar}{U}\,\mathbf{v}\,\partial_t\hat{\theta}\right]+\nabla\left[\frac{n_0\hbar}{m}\,\nabla\hat{\theta}-\frac{\hbar}{m}\,\mathbf{v}\left(\nabla\hat{\theta}\right)\mathbf{v}\right]=0\,. \tag{5.27}$$

This equation, governing the kinematics for the phase perturbations $\hat{\theta}$, is the connection between condensed matter physics and emergent quantum field theory in curved spacetimes.

5.2.2 | Analogue spacetime

A compact and insightful way to express the evolution of phase perturbations (5.27) is

$$\frac{1}{\sqrt{|\det(g_{ab})|}}\,\partial_a\left(\sqrt{|\det(g_{ab})|}\,g^{ab}\,\partial_b\hat{\theta}\right)=0\,, \tag{5.28}$$

where we introduce

$$g_{ab}=\left(\frac{c_0}{U/\hbar}\right)^{\frac{2}{d-1}}\begin{bmatrix}-\left(c_0^2-\mathbf{v}^2\right) & -v_x & -v_y & -v_z\\ -v_x & 1 & 0 & 0\\ -v_y & 0 & 1 & 0\\ -v_z & 0 & 0 & 1\end{bmatrix}; \tag{5.29}$$

a covariant metric rank two tensor, whose entries are purely collective variables. The conformal factor depends on the spatial dimensionality, d, of the condensate cloud. To derive Eq. (5.28), we first write Eq. (5.27) as,

$$\partial_a\left(f^{ab}\,\partial_b\hat{\theta}\right)=0\,, \tag{5.30}$$

where f^{ab} is easily found to be,

$$f^{ab}:=\begin{bmatrix}-\frac{\hbar}{U} & -\frac{\hbar}{U}v_x & -\frac{\hbar}{U}v_y & -\frac{\hbar}{U}v_z\\ -\frac{\hbar}{U}v_x & \frac{n_0\hbar}{m}-\frac{\hbar}{U}v_x^2 & -\frac{\hbar}{U}v_xv_y & -\frac{\hbar}{U}v_xv_z\\ -\frac{\hbar}{U}v_y & -\frac{\hbar}{U}v_xv_y & \frac{n_0\hbar}{m}-\frac{\hbar}{U}v_y^2 & -\frac{\hbar}{U}v_yv_z\\ -\frac{\hbar}{U}v_z & -\frac{\hbar}{U}v_xv_z & -\frac{\hbar}{U}v_yv_z & \frac{n_0\hbar}{m}-\frac{\hbar}{U}v_z^2\end{bmatrix}. \tag{5.31}$$

The two equations, (5.30), and (5.28), are equivalent if

$$f^{ab}=\sqrt{|\det(g_{ab})|}\,g^{ab}. \tag{5.32}$$

Here g^{ab} is a contravariant tensor, and since $g^{ab}g_{cb}=\delta^a{}_c$, it is only a question of matrix inversion to find its covariant equivalent, (5.29). For considerably more details and a thorough derivation we suggest the following literature: [18, 187, 12, 82].

At this stage we would like to comment on the physical implications of the results presented so far. The motivation to write the differential Eq. (5.27), governing the excitation spectrum in the form

presented in (5.28), is to find an analogy for the curved spacetime Klein–Gordon equation which describes minimally coupled spin-zero Bosons in curved spacetime. It is appropriate to define an emergent Lagrange density,

$$\mathcal{L} = -\frac{1}{2} f^{ab}\, \partial_a \hat{\theta}\, \partial_b \hat{\theta}\,, \tag{5.33}$$

such that Eq. (5.28) can be obtained as the Euler-Lagrange equations justified by the principle of least action. The momentum conjugate to $\hat{\theta}$ is specified by

$$\Pi_{\hat{\theta}} := \frac{\partial \mathcal{L}}{\partial(\partial_t \hat{\theta})} = -f^{tb}\, \partial_b \hat{\theta}, \tag{5.34}$$

and hence is in agreement with equation (5.26). We see that quantum phase and density perturbations in a Bose–Einstein condensate are a canonical set of field and conjugate field operators on the emergent spacetime.

We now temporarily set aside this analogy and apply our model to particle production in non-smooth emergent geometries.

5.3 | Sudden changes in spacetime geometry

In this section we calculate the mixing of positive and negative frequencies due to "sudden" stepwise variations in the sound speed, Eq. (5.23). The initial and final emergent geometries are now flat Minkowski spacetimes, which are discontinuously connected at the step. Physically the step is generated by a very rapid change in the magnetic field, which very rapidly drives one through a Feshbach resonance, which in turn very rapidly changes the scattering length a, and so finally induces a rapid change in the speed of sound.

5.3.1 | Quantum fields as harmonic oscillators

An idealized Bose–Einstein condensate trapped in a finite quantization box of volume L^d is comparable to flat Minkowski spacetime. Here the macroscopic parameters are zero background velocity, $\mathbf{v} = \mathbf{0}$, and constant sound speed (5.23). That is, one considers a uniform number density, $n_0(t, \mathbf{x}) = \text{constant}$, and a fixed scattering length, $a(t) = \text{constant}$. Therefore the emergent metric given in (5.29) is a diagonal tensor whose entries are time- and space independent;

$$f^{ab} = \begin{bmatrix} -\frac{\hbar}{U} & 0 & 0 & 0 \\ 0 & \frac{n_0\hbar}{m} & 0 & 0 \\ 0 & 0 & \frac{n_0\hbar}{m} & 0 \\ 0 & 0 & 0 & \frac{n_0\hbar}{m} \end{bmatrix}. \tag{5.35}$$

We employ the canonical variables on our effective relativistic spacetime to write the Klein–Gordon Eq. (5.28) as

$$\partial_t \left(\frac{\hbar}{U}\, \partial_t \hat{\theta} \right) - \frac{n_0\hbar}{m} \nabla^2 \hat{\theta} = 0\,. \tag{5.36}$$

It is possible to decouple the Klein–Gordon field (5.36) into independent Harmonic oscillators. To show this, we make use of

$$\hat{\theta}(t,\mathbf{x}) = \frac{1}{L^{d/2}} \sum_k \frac{1}{\sqrt{2}} \left[\hat{a}_k v_k^*(t) e^{i\mathbf{kx}} + \hat{a}_k^\dagger v_k(t) e^{-i\mathbf{kx}} \right]. \tag{5.37}$$

Note that for a hard-walled box the modes fulfill non-periodic boundary conditions. In Minkowski spacetime there exists a natural set of mode functions,

$$v_k(t) = \sqrt{\frac{U}{\hbar}} \frac{1}{\sqrt{2\omega_k}} e^{i\omega_k t}, \tag{5.38}$$

associated with the Poincaré group, a symmetry group of the Minkowski line-element. Here ∂_t is a time-translation Killing vector which can also be thought of as a differential operator with eigenvalues $(-i\omega_k)$, where $\omega_k > 0$ are said to be positive frequency modes. Hence the vacuum is invariant under the action of the Poincaré group and all observers agree on existence, or non-existence, of particles in flat spacetime. The physics is observer-independent, as expected. For a more detailed treatment see reference [29], and the appendix below.

The decoupled equations for the mode-operators are

$$\dot{\hat{a}}_k(t) = -i\omega_k \hat{a}_k(t); \quad \text{and} \quad \dot{\hat{a}}_k^\dagger(t) = +i\omega_k \hat{a}_k^\dagger(t), \tag{5.39}$$

where $\hat{a}_k(t) = \hat{a}_k v_k^*(t)$ and $\hat{a}_k^\dagger(t) = \hat{a}_k^\dagger v_k(t)$. For now, we are working in the low-energy, long-wavelength regime and obtain a "relativistic" dispersion relation for the modes:

$$\omega_k = c\,k. \tag{5.40}$$

Later on, in section (5.5), we will include trans-phononic modes into our picture, and see how the microscopic structure induces LIV breaking terms for high-energy, short-wavelength perturbations.

The canonical creation and destruction operators obey the usual commutator

$$\left[\hat{a}_k(t), \hat{a}^\dagger_{-k'}(t) \right] = \delta_{kk'}, \tag{5.41}$$

and acting on the particle basis for the Hilbert space of states, the Fock states $|\,\rangle$, they are a powerful tool to calculate the number of particles n_k in the mode labeled by k. The normalized basis vectors can be obtained from the vacuum, or zero-particle state, $|0\rangle$. This is the state that is destroyed by operators $\hat{a}_k|0\rangle = 0$, for all modes labeled by k. In general

$$\hat{a}_k^\dagger |n_k\rangle = (n+1)^{1/2} |(n+1)_k\rangle, \tag{5.42}$$

and

$$\hat{a}_k |n_k\rangle = n^{1/2} |(n-1)_k\rangle, \tag{5.43}$$

so that we can define the number operator $\hat{N}_k$,

$$\hat{N}_k |n_k\rangle = \hat{a}_k^\dagger a_k |n_k\rangle = n_k |n_k\rangle. \tag{5.44}$$

We now use the tools we have presented above to calculate the quasi-particle production in a BEC-based emergent spacetime due to sudden changes in the sound speed; such that we patch two flat spacetimes in a step-wise fashion, by suitably changing the microscopic parameters.

5.3.2 | Particle production

From the emergent spacetime point of view step-wise changes in the microscopic parameters induce sudden variations in the collective variables, and enforce discontinuous interchanges between different Minkowski spacetimes. In terms of our emergent spacetime from a Bose gas, this can be achieved through an external magnetic field, that adjusts the atomic interactions, and consequently the scattering length a and the sound speeds $c_0^{\underline{\mathrm{i}}}$.

Following the ideas of Dray *et al.* [57, 55], we assume that the fields are continuous,

$$\hat{\theta}^{\underline{\mathrm{i}}} - \hat{\theta}^{\underline{\mathrm{j}}}\Big|_{\Sigma} = 0\,, \tag{5.45}$$

on the space like hypersurface $\sum$ at fixed time $t = t^{\underline{\mathrm{ij}}}$. Here $t = t^{\underline{\mathrm{ij}}}$ is the time at which a transition occurs from $c^{\underline{\mathrm{i}}}$ to $c^{\underline{\mathrm{j}}}$. The Klein–Gordon equation in each region can be written in terms of exterior derivatives,

$$(-1)^n \partial_a \left(f^{ab}\, \partial_b \hat{\theta}^{\underline{\mathrm{i}}} \right) = *d(*d\hat{\theta}^{\underline{\mathrm{i}}}) =: *dF^{\underline{\mathrm{i}}} = 0\,; \tag{5.46}$$

hence in each region $dF^{\underline{\mathrm{i}}} = 0$, where $F^{\underline{\mathrm{i}}}$ is an exact $(n-1)$-form. These forms are connected discontinuously;

$$F = \Theta\, F^{\underline{\mathrm{i}}} + (1-\Theta) F^{\underline{\mathrm{j}}}, \tag{5.47}$$

where Θ is the usual Heavyside function. Thus, we get

$$\begin{aligned} dF &= \Theta\, dF^{\underline{\mathrm{i}}} + (1-\Theta)\, dF^{\underline{\mathrm{j}}} + \delta(t)\, dt \wedge [F] && (5.48)\\ &= \delta(t)\, dt \wedge [F]\,, && (5.49) \end{aligned}$$

where $[F] = F^{\underline{\mathrm{i}}} - F^{\underline{\mathrm{j}}}$. This supplies us with a connection condition for the canonical momentum,

$$\delta(t)\; dt \wedge [F] = 0\,; \tag{5.50}$$

i.e.,

$$\hat{\Pi}_{\hat{\theta}^{\underline{\mathrm{i}}}} - \hat{\Pi}_{\hat{\theta}^{\underline{\mathrm{j}}}}\Big|_{\Sigma} = 0\,. \tag{5.51}$$

Thus the field and its canonical momentum must be continuously connected across the spatial hypersurface of sudden variation. In the following we apply the connection conditions we have just found, and calculate the number of quasi-particles produced by sudden sound speed variations in our BEC.

In each region $\underline{\mathrm{i}}$ the mode expansion,

$$\hat{\theta}^{\underline{\mathrm{i}}}(t, \mathbf{x}) = \frac{1}{\sqrt{2L^d}} \sum_{\mathbf{k}} e^{i\mathbf{kx}} \left[u_k^{\underline{\mathrm{i}}*}(t) \hat{a}_k^{\underline{\mathrm{i}}} + u_k^{\underline{\mathrm{i}}}(t) \hat{a}_{-k}^{\underline{\mathrm{i}}\dagger} \right] \tag{5.52}$$

involves a distinct set of creation $\hat{a}_k^{\underline{i}\dagger}$ and destruction $\hat{a}_k^{\underline{i}}$ operators. The mode functions $u_k^{\underline{i}}$ and $u_k^{\underline{i}*}$ obey the curved-spacetime Klein–Gordon equation,

$$\partial_t \left[\frac{\hbar}{U^{\underline{i}}} \, \partial_t u_k^{\underline{i}}(t) \right] - \frac{n_0 \hbar}{m} \, k^2 \; u_k^{\underline{i}}(t) = 0 \, ; \tag{5.53}$$

they form a complete basis for the two dimensional solution space. At the transition time $t^{\underline{ij}}$ we connect the mode functions and their first derivatives,

$$\vec{U}_k^{\underline{i}}(t^{\underline{ij}}) \;\; = \;\; M^{\underline{ij}} \vec{U}_k^{\underline{j}}(t^{\underline{ij}}) \, , \tag{5.54}$$

$$\frac{\hbar}{U^{\underline{i}}} \, \partial_t \vec{U}_k^{\underline{i}}(t^{\underline{ij}}) \;\; = \;\; M^{\underline{ij}} \frac{\hbar}{U^{\underline{j}}} \, \partial_t \vec{U}_k^{\underline{j}}(t^{\underline{ij}}) \, . \tag{5.55}$$

Here we have combined both mode functions into one mode vector $\vec{U}_k^{\underline{i}}$,

$$\vec{U}_k^{\underline{i}}(t) = \begin{pmatrix} u_k^{\underline{i}}(t) \\ u_k^{\underline{i}*}(t) \end{pmatrix} . \tag{5.56}$$

In the cases we are interested in the transition matrix $M^{\underline{ij}} = M(t^{\underline{ij}})$ is time-independent, and for a pair of complex conjugate mode functions in each region $\underline{\mathrm{i}}$ and $\underline{\mathrm{j}}$, the matrix is of the form

$$M^{\underline{ij}} = \begin{pmatrix} \alpha_k^{\underline{ij}} & \beta_k^{\underline{ij}} \\ \beta_k^{\underline{ij}*} & \alpha_k^{\underline{ij}*} \end{pmatrix} . \tag{5.57}$$

The Wronskian $W[u_k^{\underline{i}}, u_k^{\underline{i}*}] = (\partial_t u_k^{\underline{i}}) u_k^{\underline{i}*} - u_k^{\underline{i}*} (\partial_t u_k^{\underline{i}*})$ of the mode functions is time-independent, see Eq. (5.53), which implies a constraint on the Bogliubov coefficients $\alpha_k^{\underline{ij}}$ and $\beta_k^{\underline{ij}}$,

$$|\alpha_k^{\underline{ij}}|^2 - |\beta_k^{\underline{ij}}|^2 = 1 \, . \tag{5.58}$$

To start with, consider a no-particle state in the initial Minkowski spacetime (region $\underline{\mathrm{i}}$), such that $\hat{a}_k^{\underline{i}} |0^{\underline{i}}\rangle = 0$. The correlation between the mode operators can easily be constructed from $\hat{\theta}^{\underline{i}}(t^{\underline{ij}}) = \hat{\theta}^{\underline{j}}(t^{\underline{ij}})$, considering Eq. (5.54) and Eq. (5.58) we get

$$\hat{a}_k^{\underline{i}} \;\; = \;\; \alpha_k^{\underline{ij}} \hat{a}_k^{\underline{j}} - \beta_k^{\underline{ij}} \hat{a}_{-k}^{\underline{j}\dagger} \, , \tag{5.59}$$

$$\hat{a}_k^{\underline{i}\dagger} \;\; = \;\; \alpha_k^{\underline{ij}*} \; \hat{a}_k^{\underline{j}\dagger} - \beta_k^{\underline{ij}*} \; \hat{a}_{-k}^{\underline{j}} \, . \tag{5.60}$$

Consequently, the mean number of $\underline{\mathrm{i}}$-particles in the $\underline{\mathrm{j}}$-vacuum,

$$\langle 0^{\underline{j}} | \hat{N}_k^{\underline{i}} | 0^{\underline{j}} \rangle = |\beta_k^{\underline{ij}}|^2 \; \delta^d(0) \, , \tag{5.61}$$

depends only on $|\beta_k^{\underline{ij}}|$.

Explicitly, the elements for the transition matrix in a sudden change from region $\underline{\mathrm{i}}$ to region $\underline{\mathrm{j}}$ at a time $t^{\underline{\mathrm{i}}\,\underline{\mathrm{j}}}$ are given by:

$$\alpha_k^{\underline{\mathrm{i}}\,\underline{\mathrm{j}}} = \frac{1}{2}\left(\sqrt{X^{\underline{\mathrm{i}}\,\underline{\mathrm{j}}}} + \frac{1}{\sqrt{X^{\underline{\mathrm{i}}\,\underline{\mathrm{j}}}}}\right) e^{i(+\omega_k^{\underline{\mathrm{i}}} - \omega_k^{\underline{\mathrm{j}}})t^{\underline{\mathrm{i}}\,\underline{\mathrm{j}}}}, \tag{5.62}$$

$$\beta_k^{\underline{\mathrm{i}}\,\underline{\mathrm{j}}} = -\frac{1}{2}\left(\sqrt{X^{\underline{\mathrm{i}}\,\underline{\mathrm{j}}}} - \frac{1}{\sqrt{X^{\underline{\mathrm{i}}\,\underline{\mathrm{j}}}}}\right) e^{i(+\omega_k^{\underline{\mathrm{i}}} + \omega_k^{\underline{\mathrm{j}}})t^{\underline{\mathrm{i}}\,\underline{\mathrm{j}}}}, \tag{5.63}$$

where to simplify formulae it is convenient to introduce the ratio of change in the dispersion relations $X^{\underline{\mathrm{i}}\,\underline{\mathrm{j}}}$,

$$X^{\underline{\mathrm{i}}\,\underline{\mathrm{j}}} = \frac{\omega_k^{\underline{\mathrm{j}}}}{\omega_k^{\underline{\mathrm{i}}}} = \frac{c_0^{\underline{\mathrm{j}}}}{c_0^{\underline{\mathrm{i}}}}. \tag{5.64}$$

The last expression in (5.64) is only valid in the hydrodynamic approximation, where the number of particles produced from a single step is k-independent. The mean number of particles in each mode k is given by

$$|\beta_k^{\underline{1}\,\underline{2}}|^2 = \frac{1}{4}\left|\sqrt{\frac{c_0^{\underline{2}}}{c_0^{\underline{1}}}} - \sqrt{\frac{c_0^{\underline{1}}}{c_0^{\underline{2}}}}\right|^2 . \tag{5.65}$$

The advantage of this representation lies in the simple way that it can be extended for m sudden variations in a row

$$\vec{U}_k^{\underline{1}} = \underbrace{M^{\underline{1}\,\underline{2}} \cdot M^{\underline{2}\,\underline{3}} \cdot \cdots M^{(\underline{\mathrm{m}}-\underline{1})\,\underline{\mathrm{m}}}}_{M^{\underline{1}\,\underline{\mathrm{m}}}} \vec{U}_k^{\underline{\mathrm{m}}}, \tag{5.66}$$

and each single transition matrix $M^{\underline{\mathrm{i}}(\underline{\mathrm{i}}+\underline{1})}$ is of the form (5.57) evaluated at $t^{\underline{\mathrm{i}}(\underline{\mathrm{i}}+\underline{1})}$. The resulting matrix $M^{\underline{1}\,\underline{\mathrm{m}}}$ carries the final Bogoliubov coefficients $\alpha_k^{\underline{1}\,\underline{\mathrm{m}}}$ and $\beta_k^{\underline{1}\,\underline{\mathrm{m}}}$ for the whole chain of events. We would like to point out that the choice for the mode functions in the intermediate regimes does not have any influence on the final outcome, as can be seen in Eq. (5.66). However for the validity of our calculation it is necessary to choose a pair of complex conjugate mode functions. The rest of the chapter further investigates a particular scenario, that is two sudden variations in a row, see Figure 5.1. In this situation

$$\alpha_k^{\underline{1}\,\underline{3}} = \alpha_k^{\underline{1}\,\underline{2}}\alpha_k^{\underline{2}\,\underline{3}} + \beta_k^{\underline{1}\,\underline{2}}\beta_k^{\underline{2}\,\underline{3}*}, \tag{5.67}$$

$$\beta_k^{\underline{1}\,\underline{3}} = \alpha_k^{\underline{1}\,\underline{2}}\beta_k^{\underline{2}\,\underline{3}} + \beta_k^{\underline{1}\,\underline{2}}\alpha_k^{\underline{2}\,\underline{3}*}. \tag{5.68}$$

To obtain the Bogoliubov coefficients for a two-step process, we use the single-step results (5.62) and (5.63) to obtain:

$$\alpha_k^{\underline{1}\,\underline{3}} = \exp\left\{i\omega_k^{\underline{1}} t^{\underline{1}\,\underline{2}} - i\omega_k^{\underline{3}}(t^{\underline{1}\,\underline{2}} + T)\right\} \times \left(\frac{X^{\underline{1}\,\underline{3}}+1}{2\sqrt{X^{\underline{1}\,\underline{3}}}}\cos(\Omega_k T) - \frac{X^{\underline{1}\,\underline{2}}+X^{\underline{2}\,\underline{3}}}{i\,2\sqrt{X^{\underline{1}\,\underline{3}}}}\sin(\Omega_k T)\right), \tag{5.69}$$

and

$$\beta_k^{\underline{1}\,\underline{3}} = -\exp\left\{+i\omega_k^{\underline{1}} t_1 + i\omega_k^{\underline{3}}(t_1 + dt)\right\} \times \left(\frac{X^{\underline{1}\,\underline{3}}-1}{2\sqrt{X^{\underline{1}\,\underline{3}}}}\cos(\Omega_k T) + \frac{X^{\underline{1}\,\underline{2}}-X^{\underline{2}\,\underline{3}}}{i\,2\sqrt{X^{\underline{1}\,\underline{3}}}}\sin(\Omega_k T)\right); \tag{5.70}$$

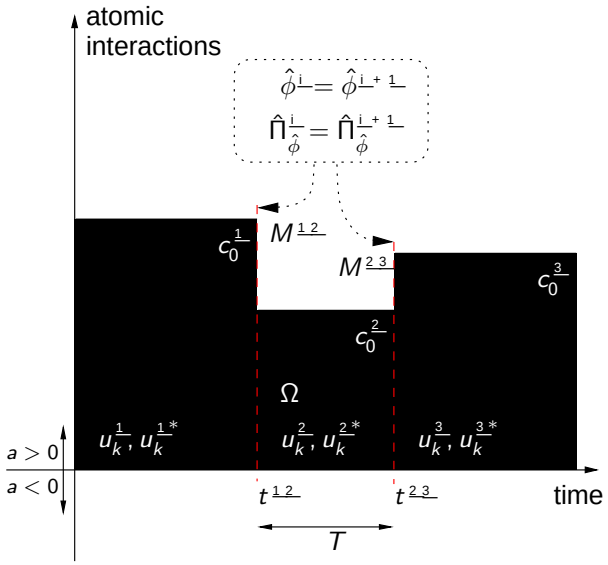


Figure 5.1: Two sudden variations in the strength of the atomic interactions is analogous to two space-like hypersurfaces connecting three different Minkowski spacetimes emerging from a Bose gas.

where for the finite duration intermediate region $\underline{2}$ we have defined the time interval $T = t^{\underline{23}} - t^{\underline{12}}$, and the dispersion relation $\Omega_k = \omega_k^{\underline{2}}$. The mean number of particles produced during this process is then given by

$$|\beta_k^{\underline{13}}|^2 = \frac{(X^{\underline{13}} - 1)^2}{4X^{\underline{13}}} - \frac{1}{4}\left[X^{\underline{12}} - \frac{1}{X^{\underline{12}}}\right]\left[X^{\underline{23}} - \frac{1}{X^{\underline{23}}}\right]\sin(\Omega_k T)^2. \tag{5.71}$$

It is easy to see that the mean number of particles produced in such a process oscillates between two single step solutions of the form

$$N_k = \frac{(X-1)^2}{4X}\,. \tag{5.72}$$

The upper bound replaces two up-down / down-up steps with a single step (here given by $X = X^{\underline{12}}/X^{\underline{23}}$), and the lower bound replaces two up-down / down-up steps with a single step (here given by $X = X^{\underline{12}}X^{\underline{23}}$). We have illustrated the quasi-particle production in the hydrodynamic limit obtained by two-sudden steps in a row in Figure 5.4(a).

In the following we show how to extend the calculations for finite intervals during which the microscopic atoms experience negative (attractive) interactions. For small negative values of the scattering length a the condensate description continues to exist for short periods of time, and hence motivates the study of Euclidean emergent geometries from a Bose gas. A sign change in the atomic

interactions corresponds to a signature change in general relativity. As a first step we investigate quasi-particle production from such an event in the hydrodynamic limit.

5.4 | Signature change events

In this section we investigate the behavior of emergent spacetimes arising from a Bose gas with variations in the principal nature of the interactions; for a finite amount of time we switch to attractive atomic interactions. For short time-scales and small absolute values of the attractive *s*-wave potential, it is possible to hold on to the concept of an emergent spacetime. With the nature of the microscopic interactions switching from repulsive to attractive, the geometric hydrodynamics also changes from Lorentzian to Riemannian. This supplies us with a toy model for signature change events, which we are going to investigate next.

We first present the standard general relativity point of view, before adapting our previous calculations for the particle production due to sudden variations on finite duration Euclidean regions.

5.4.1 | Classical aspects

Overall, we investigate manifolds that allow both Riemannian and Lorentzian regions. The latter is a generalization of Minkowski spacetimes (special relativity), while Riemannian geometries are Euclidean signature spaces including curvature (*e.g.*, the surface of an orange). Distances in Riemannian spacetimes are positive definite, while Lorentzian distances can be imaginary (time-like), zero (light-like), or positive (space-like).

In Minkowski spacetimes the signature can easily be read off as the sign of positive and negative eigenvalues of η_{ab}. From Eq. (5.35) we get Lorentzian signature $(-,+++)$. Arbitrary curved spacetimes are locally flat, and the signature can be read off from the pattern of eigenvalues of the metric tensor g_{ab} at each point on the manifold. In Lorentzian signature the "time" coordinate can be chosen to have a different sign from the "spatial" coordinates. This is in contrast to the Riemannian, or Euclidean signature $(+,+++)$, where a distinction between space and time as such does not exist [196].

We are mainly interested in the interface between these two spacetime geometries, and we investigate the physics around a space-like hypersurface $\sum$ that separates the two spaces. There are two ways to be driven through a signature change, continuously or discontinuously.

We are in favour of a non-smooth signature change, to avoid degeneracies of the effective gravitational field at the surfaces of separation. For continuous signature changes the metric volume element, and hence the existence of an orthonormal frame vanish at $\sum$; while for discontinuous signature changes the metric volume element (hence, the orthonormal frame) is well behaved [57, 59, 68].

Thus we are allowed to transfer the connection conditions, as derived in our previous calculations

for sudden changes in purely Lorentzian geometries (see Eq. (5.45), Eq. (5.51), and the discussion in the appendix), to now connect regions of Minkowskian and Euclidean spacetimes [55].

5.4.2 | Particle production from a finite-duration Euclidian region

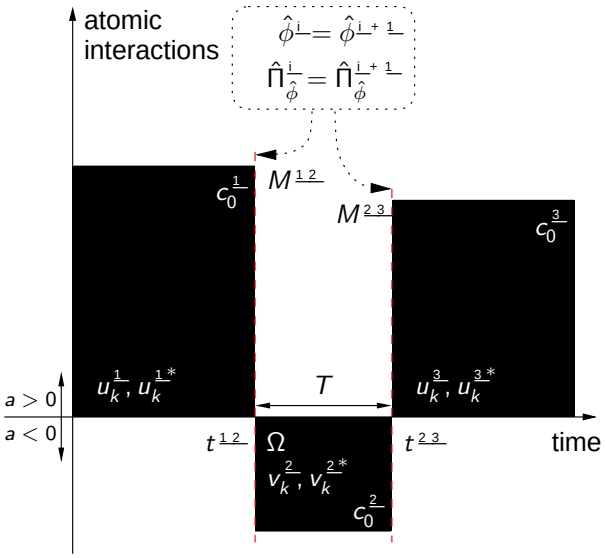


Figure 5.2: Two sudden variations in the strength of the atomic interactions are analogues to two space-like hypersurfaces connecting three different spacetimes emerging from a Bose gas. While the initial and final geometries are Lorentzian, we allow the atomic interactions to be attractive in the intermediate region, corresponding to an Euclidean geometry.

In the following we repeat our calculations from section (5.3), but this time we choose an Euclidean geometry for region $\underline{2}$; see figure (5.2). As already pointed out above, the connection conditions remain the same. We further choose the mode functions in the Lorentzian regimes $\underline{1}$, and $\underline{3}$ to be as defined in Eq. (5.38), where the sound speeds are well behaved; $(c_0^{\underline{L}})^2 \sim U > 0$. For the intermediate Euclidean region we pick a special set of mode functions for $(c_0^{\underline{E}})^2 \sim U < 0$, such that,

$$v_k^{\underline{2}} = \frac{1}{\sqrt{2|\Omega_k|}} \left(\cosh(|\Omega_k|t) + i \sinh(|\Omega_k|t)\right) ; \tag{5.73}$$

$$v_k^{\underline{2}*} = \frac{1}{\sqrt{2|\Omega_k|}} \left(\cosh(|\Omega_k|t) - i \sinh(|\Omega_k|t)\right) . \tag{5.74}$$

The two mode functions remain a complex conjugate pair. Here we make use of the purely imaginary

dispersion relation $\Omega_k = i\,|\Omega_k|$. In general, with the transformation matrix S,

$$S = \frac{\sqrt{i}}{2}\begin{pmatrix} (1-i) & (1+i) \\ (1+i) & (1-i) \end{pmatrix} \tag{5.75}$$

we can map between the two different sets of mode functions,

$$\vec{V}_k^{\,\underline{2}} = S\ \vec{U}_k^{\,\underline{2}}. \tag{5.76}$$

Notice that $S^{-1} = S^\dagger$ and $\det(S) = 1$.

It is easy to see that $M^{\underline{1\,2}}\vec{U}_k^{\,\underline{2}}$ transforms to $M^{\underline{1\,2}}S\,\vec{V}_k^{\,\underline{2}}$, while $M^{\underline{2\,3}}\vec{U}_k^{\,\underline{3}}$ transforms to $S^{-1}\,M^{\underline{2\,3}}\vec{U}_k^{\,\underline{3}}$. Altogether

$$M^{\underline{1\,3}} = M^{\underline{1\,2}}S\,S^{-1}M^{\underline{2\,3}} = M^{\underline{1\,2}}M^{\underline{2\,3}} \tag{5.77}$$

is independent of the choice for the mode functions in the intermediate regime.

Thus we are allowed to use our previous results, replacing $\Omega k \to i|\Omega k|$, and $X^{\underline{1\,2}} \to i\,|X^{\underline{1\,2}}|$ and $X^{\underline{2\,3}} \to -i\,|X^{\underline{2\,3}}|$, and keeping everything else. For the mean number of particles we now obtain

$$|\beta_k^{\underline{1\,3}}|^2 = \frac{(X^{\underline{1\,3}}-1)^2}{4X^{\underline{1\,3}}} + \frac{1}{4}\left[|X^{\underline{1\,2}}| + \frac{1}{|X^{\underline{1\,2}}|}\right]\left[|X^{\underline{2\,3}}| + \frac{1}{|X^{\underline{2\,3}}|}\right]\sinh(|\Omega_k|\ T)^2. \tag{5.78}$$

Our results are compatible with Dray *et al.* [57, 55], to the extent that the calculations and physical models overlap, but we extend the calculation for arbitrary values of the sound speeds $c_0^{\underline{i}}$. Furthermore we show that one can keep the calculations for purely sudden variation, as long as one picks a pair of complex conjugate mode functions in the intermediate regime. The standard general relativity calculation corresponds to $X^{\underline{1\,2}} = i$, $X^{\underline{2\,3}} = -i$, $X^{\underline{1\,3}} = 1$, so that

$$|\beta_k^{\underline{1\,3}}|^2 \to \sinh(|\Omega_k|\ T)^2. \tag{5.79}$$

The basic reason for this tremendous simplification is that in pure general relativity (with, by definition, a single unique spacetime metric) one always has the freedom to choose coordinates such that $c = 1$ in the Lorentzian region, and $c = i$ in the Euclidean region. This is a freedom we do not have in our BEC-based analogue spacetime — the way this shows up in our calculations is that a rapid change in the scattering length a has *two* effects in the condensed Bose gas: First the speed of sound is changed, modifying the "signal cones"; and secondly the dimension-dependent conformal factor shifts by a finite amount. This second effect is absent in the traditional general relativity calculation of Dray *et al.* — for those authors it is sufficient to *posit* a specific and simple change in the metric tensor g_{ab} and calculate the resulting particle production. In our present situation, we first *derive* a specific (dimension-independent) change in the tensor density f^{ab} induced by changing the scattering length, and then *derive* the corresponding (dimension-dependent) change in the metric tensor g_{ab}. The two situations are very closely related, but they are not quite identical.

We have plotted the mean number of particles produced in the Euclidean region in figure 5.4(c). The graph shows the quasi-particle spectrum as a function of k. The number of particles produced

depends on $\Omega_k T$. The longer the duration of Euclidian period, the more particles will be produced during this process.

However, there is a fundamental problem with the quasi-particle production in our effective spacetime. Given that it is possible to connect actual condensate excitations with the calculated quasi-particle spectrum, we expect the total number of particles produced to be finite. But in both cases, for sudden variations with and without signature changes, our results imply an infinite number for the total quasi-particle production;

$$N = 2^{d-1}\pi \int_k dk\, k^{d-1}\, N_k\,. \tag{5.80}$$

In the next section we show how this problem resolves itself once microscopic corrections to the emergent spacetime picture are taken into account.

5.5 | Ultraviolet corrections

Up to now, we have restricted our calculations to the hydrodynamic limit, which is appropriate to describe the infrared behavior of the system. Low-energy excitations in the BEC are longitudinal phonon modes approximately propagating with the same speed; see the dispersion relation given in Eq. (5.40). It is well known that so-called trans-phononic modes show a non-linear relation between excitation energy and wavelength. In references [185, 200, 131, 130, 202] it has been pointed out that this kind of behavior might be viewed as ultraviolet corrections at the “analogue Planck scale”, the borderline between phononic and trans-phononic modes.

Our next task is to use the eikonal approximation to include ultraviolet modes into the emergent spacetime picture.

5.5.1 | Rainbow geometries

Calculations up to this point were based on the assumption that spatial variations in the overall condensate are small. More specifically, variations in the kinetic energy of the condensate are considered to be negligible, compared to the internal potential energy of the Bosons,

$$\frac{\hbar^2}{2m}\,\frac{\nabla^2\sqrt{n_0+\hat{n}}}{\sqrt{n_0+\hat{n}}} \ll U\,. \tag{5.81}$$

The left hand term in relation (5.81) is the quantum pressure term and is approximated to zero in the hydrodynamic limit.

We now keep the quantum pressure term. A straightforward computation shows that it is possible to absorb all first-order corrections into:

$$\mathcal{U} = U - \frac{\hbar^2}{4mn_0}\left\{\frac{(\nabla n_0)^2 - (\nabla^2 n_0)n_0}{n_0^2} - \frac{\nabla n_0}{n_0^2}\nabla + \nabla^2\right\}\,. \tag{5.82}$$

That is, the effect of quantum pressure can be absorbed into an effective atom-atom interaction, see Eq. (5.22). For a uniform condensate this further simplifies to

$$\mathcal{U} = U - \frac{\hbar^2}{4mn_0}\nabla^2 \,. \tag{5.83}$$

In order to obtain an emergent gravitational field, we apply the eikonal approximation,

$$\mathcal{U}|_{\nabla\to -ik} \to U_k = U + \frac{\hbar^2}{4mn_0}k^2 \,. \tag{5.84}$$

Thus also the speed of sound for ultraviolet modes has to be modified

$$c_k^2 = \frac{U_k n_0}{m} = c_0^2 + \epsilon_{\rm qp}^2 k^2 \,. \tag{5.85}$$

Here we introduce,

$$\epsilon_{\rm qp} = \frac{\hbar}{2m} \,. \tag{5.86}$$

We define the borderline between the phononic and trans-phononic modes,

$$\xi^2 = \frac{1}{2}\frac{\epsilon_{\rm qp}^2}{c_0^2} \,, \tag{5.87}$$

to agree with the healing length ξ of the condensate. The healing length is the distance over which localized perturbations in the condensate tend to smooth out [151]. Phononic excitations have wavelengths that are much larger than the healing length, $k \gg \xi$. These modes are relativistic modes in the sense of an emergent relativistic dispersion relation (see Eq. (5.40)). They propagate through an emergent gravitational field, given in (5.29). Higher energy excitations around the healing scale, $k \sim \xi$, start to see deviations from the mean-field description. Such modes do not only experience collective condensate variables, they start to see the bigger picture behind the mean-field. Consequently, they exhibit a non-relativistic dispersion relation,

$$\tilde{\omega}_k = c_k k = \sqrt{c_0^2 k^2 + \epsilon_{\rm qp}^2 k^4} \,. \tag{5.88}$$

These microscopic corrections also influence the emergent spacetime, including an effective energy-dependent metric,

$$g_{ab}^k = \left(\frac{c_k}{U_k/\hbar}\right)^{\frac{2}{d-1}} \begin{bmatrix} -\left(c_k^2 - \mathbf{v}^2\right) & -v_x & -v_y & -v_z \\ -v_x & 1 & 0 & 0 \\ -v_y & 0 & 1 & 0 \\ -v_z & 0 & 0 & 1 \end{bmatrix} , \tag{5.89}$$

which results in so-called rainbow geometries.

Before we continue with our program, that is to re-calculate the mean number of particles produced including quantum pressure effects, we would like to emphasize that all the corrections are naturally small. For a detailed description of rainbow geometries, and the suppression mechanism of LIV terms in Bose gases see [131, 130, 202, 202, 200].

5.5.2 | Lorentz symmetry violation and Particle Production

As mentioned above, the spacetime description only holds in the eikonal approximation. Nevertheless, a careful analysis for the particle production can be made, where the atomic interaction is a function of differential operators, see Eq. (5.82). For an isotropic condensate, the two different approaches will lead to the same set of equations,

$$\partial_t \left(\frac{\hbar}{U_k^{\mathrm{i}}} \partial_t u_k^{\mathrm{i}}(t) \right) - \frac{n_0 \hbar}{m} k^2 \, u_k^{\mathrm{i}}(t) = 0 \, . \tag{5.90}$$

The mode functions $\tilde{u}_k^{\mathrm{i}}$ are still formally represented by Eq. (5.38), except that we replace ω^{i} with $\tilde{\omega}^{\mathrm{i}}$, which now includes the ϵ_{qp} quantum pressure term.

In the next two sections we connect those modes over three discontinuously patched spacetime geometries, and calculate the amplification and mixing of positive and negative modes living on such a manifold.

Lorentz symmetry violation and L-L-L sudden

We start with purely Lorentzian geometries, but allow two sudden variations in the speed of sound. The calculations are completely in analogy with those presented in section (5.4.2). Here, the sound speeds are given by Eq. (5.85), and from the definition for the ratio X^{ij} in the hydrodynamic approximation, we now define:

$$\tilde{X}^{\mathrm{ij}} = \frac{\tilde{\omega}_k^{\mathrm{j}}}{\tilde{\omega}_k^{\mathrm{i}}} = \frac{c_k^{\mathrm{j}}}{c_k^{\mathrm{i}}}, \tag{5.91}$$

as the sound-speed ratio for trans-phononic modes. Formally, the results for the Bogoliubov coefficients — α_k^{13} and β_k^{13}, given in Eqs. (5.69) and (5.70) — and consequently the mean number of particles produced during this two-step process as given in Eq. (5.71), all remain the same. The only effort required is to replace X^{ij} with $\tilde{X}^{\mathrm{ij}}$, and ω_k^{i} with $\tilde{\omega}_k^{\mathrm{i}}$.

We have plotted the quasi-particle spectra in figure 5.4(b). It can be seen that the quasi-particle spectrum for the two-step process is still oscillating between the two single-step processes represented by the black and green curve. Compared to the figure on the left, where we plotted the same process in the hydrodynamic limit, see figure 5.4(a), we notice that the ultraviolet particle production rapidly approaches zero.

Lorentz symmetry violation and L-E-L sudden

Finally, we are left to analyze sudden variations from Lorentzian, to Euclidean, and back to Lorentzian spacetimes for rainbow geometries. It is interesting to notice, that in the presence of quantum pressure corrections *the meaning of signature is also energy-dependent*. We distinguish between the

following cases:

$$\text{Sig. } \underline{2} \;=\; \begin{cases} |k| < c_{0}^{\underline{2}}/\epsilon_{\text{qp}} & : \quad \text{Euclidean}\,; \\ |k| > c_{0}^{\underline{2}}/\epsilon_{\text{qp}} & : \quad \text{Lorentzian}\,. \end{cases} \tag{5.92}$$

We would like to emphasize that $c_{0}^{\underline{2}}$ is the sound speed in region $\underline{2}$ for $k \to 0$.

Again, we take the previous results found in the hydrodynamic limit, see equations (5.69, 5.70, 5.71), where we need only replace $X^{\underline{i}\underline{j}}$ with $\tilde{X}^{\underline{i}\underline{j}}$, and $\omega^{\underline{i}}$ with $\tilde{\omega}^{\underline{i}}$.

Altogether we expect the mean number of particles produced for $|k| > c_{0}^{\underline{2}}/\epsilon_{\text{qp}}$ to be equivalent to those from the purely Lorentzian variations, while phononic modes, with $|k| \ll c_{0}^{\underline{2}}/\epsilon_{\text{qp}}$, should experience exponential growth similar to the result from the hydrodynamic limit. We have plotted the mean number of particles produced for the whole event, see figure 5.4(b). The plots are in agreement with our predictions.

One motivation for including microscopic corrections into our hydrodynamic calculations was to solve the problem of an infinite number of particles being produced in sudden variations; see Eq. (5.80). To estimate the total number of particles, we need only to focus on the region $|k| > c_{0}^{\underline{2}}/\epsilon_{\text{qp}}$. It can be seen that for large k the mean number of particles scales as $N_k \sim k^{-4}$. Therefore, for an isotropic emergent spacetime (with two or three spatial dimensions d), we get

$$N_{\leqslant k} \sim 2^{d-1}\pi \int dk\, k^{d-5} \sim k^{d-4}. \tag{5.93}$$

Therefore, the total number of particles produced is finite, as expected. However, it is easy to see that the total energy emitted,

$$E = 2^{d-1}\pi \int_k dk\, k^{d-1}\, N_k\, \omega_k \sim 2^{d-1}\pi \int_k dk\, k^{d-3}\,, \tag{5.94}$$

is still infinite. Note, that in the ultraviolet regime one has to use the non-linear dispersion relation $\omega_k \sim k^2$; see Eq. (5.88). We will discuss this further in the conclusion, after we investigate a possible application of signature change events for laboratory cosmology.

5.6 | Particle Amplifier for Cosmological Particle Production

In a Euclidean-signature emergent spacetime some modes (depending on the strength of the attractive interactions) grow and decay exponentially. As pointed out in [38] this behavior is in analogy to cosmological particle production, where super–Hubble horizon modes (*i.e.*, modes with frequencies that are smaller than the Hubble frequency) show similar kinematics. These modes are not free to oscillate, as they get dragged along with the spacetime fabric. This motivated us to investigate how pre-existing condensate perturbations are influenced by the existence of a short-duration Euclidean phase. To be more specific, we would like to determine whether significant amplification of a

pre-existing particle spectrum occurs from exposing it to a short finite time of attractive interactions. This might be of interest for laboratory cosmology in Bose gases. One of the outstanding problems involved with such experiments, as suggested in [70, 71, 16, 15, 72, 171], is the detectability of the quasi-particle spectrum in an emergent FRW-type universe. Due to the smallness of mode-population, common detection mechanisms would fail to measure the spectra. Recently there has been some attempt to solve this problem involving a more sophisticated detection mechanism [163]. Another way to tackle this problem is to amplify the quasi-particle spectrum so that common detection mechanisms can be applied.

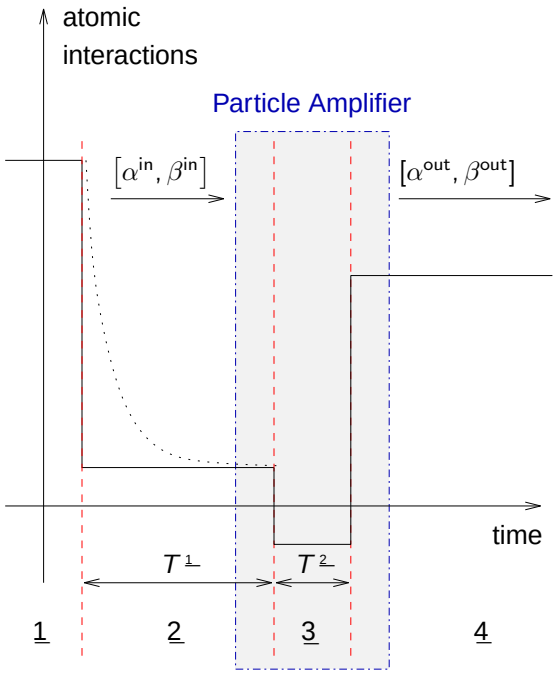


Figure 5.3: The figure shows a particle production process starting from the vacuum in region $\underline{1}$. The bold line corresponds to particles produced in a single Lorentzian step from region $\underline{1} \rightarrow \underline{2}$, while the dotted line shows particles produced during region $\underline{2}$. Region $\underline{3}$ depicts a subsequent amplification process of a finite time Euclidean interval. Altogether the OUT signal in region $\underline{4}$ can be viewed as an amplified IN signal.

5.6.1 | Main concept

In Figure (5.3) we illustrate the principle of our particle amplifier idea. The particle amplifier involves a 3-step process. Region $\underline{2}$ will create a quasi-particle spectrum $\beta_k^{\underline{1}\,\underline{2}} = \beta^{IN}$, which we wish to

amplify. The Euclidean region $\underline{3}$ is the core of our particle amplifier process with $\beta_k^{\underline{2}\,\underline{4}} = \beta^{\mathsf{PA}}$, and region $\underline{4}$ contains the amplified quasi-particle spectrum, $\beta_k^{\underline{1}\,\underline{4}} = \beta^{\mathsf{OUT}}$. For simplicity we focus on a Lorentzian sudden step process as the source of our initial quasi-particle spectrum, however we stress that this method is more general and applies to any quasi-particle spectrum in region $\underline{2}$ that is of a FRW-type universe.

We would like to determine an expression for our final amplified spectrum, in terms of the input spectrum, and the spectrum we would expect from the amplifying step. We know the connection matrix after the amplifying step can be decomposed as (see Eq. (5.66)):

$$M^{\underline{1}\,\underline{4}} = M^{\underline{1}\,\underline{2}} \cdot M^{\underline{2}\,\underline{4}} = \begin{bmatrix} \alpha_k^{\underline{2}\,\underline{4}}\alpha_k^{\underline{1}\,\underline{2}} + \beta_k^{\underline{2}\,\underline{4}*}\beta_k^{\underline{1}\,\underline{2}} & \alpha_k^{\underline{1}\,\underline{2}}\beta_k^{\underline{2}\,\underline{4}} + \beta_k^{\underline{1}\,\underline{2}}\alpha_k^{\underline{2}\,\underline{4}*} \\ \beta_k^{\underline{1}\,\underline{2}*}\alpha_k^{\underline{2}\,\underline{4}} + \alpha_k^{\underline{1}\,\underline{2}*}\beta_k^{\underline{2}\,\underline{4}*} & \beta_k^{\underline{1}\,\underline{2}*}\beta_k^{\underline{2}\,\underline{4}} + \alpha_k^{\underline{1}\,\underline{2}*}\alpha_k^{\underline{2}\,\underline{4}*} \end{bmatrix} . \tag{5.95}$$

We now look at an expression for the final output spectrum in terms of the input spectrum and particle amplifier contribution. As we already have the Bogoliubov coefficients, this is straightforward to calculate. As $\det(M^{\underline{i}\,\underline{j}}) = 1$ it follows that:

$$|\beta_k^{\underline{1}\,\underline{4}}|^2 = |\beta_k^{\underline{2}\,\underline{4}}|^2 + [2|\beta_k^{\underline{2}\,\underline{4}}|^2 + 1]|\beta_k^{\underline{1}\,\underline{2}}|^2 + 2\,\mathrm{Re}\left(\alpha_k^{\underline{2}\,\underline{4}*}\beta_k^{\underline{1}\,\underline{2}}\beta_k^{\underline{2}\,\underline{4}*}\alpha_k^{\underline{1}\,\underline{2}*}\right) . \tag{5.96}$$

This can be rewritten completely in terms of IN, OUT and PA formalism,

$$|\beta^{\mathsf{OUT}}|^2 = |\beta^{\mathsf{PA}}|^2 + [2|\beta^{\mathsf{PA}}|^2 + 1]|\beta^{\mathsf{IN}}|^2 + 2\,\sin(\gamma)\,|\alpha^{\mathsf{PA}}||\beta^{\mathsf{PA}}||\alpha^{\mathsf{IN}}||\beta^{\mathsf{IN}}| , \tag{5.97}$$

where

$$\sin(\gamma) = \mathrm{Re}\left(ph(\alpha_k^{\underline{2}\,\underline{4}*})ph(\beta_k^{\underline{1}\,\underline{2}})ph(\beta_k^{\underline{2}\,\underline{4}*})ph(\alpha_k^{\underline{1}\,\underline{2}*})\right) , \tag{5.98}$$

represents the relationship between the phases, $ph(...)$, of our Bogoliubov coefficients. Therefore the amplification process depends on γ, and it is necessary to find an explicit expression for it.

Although it would be possible to make further statements while keeping the analysis completely general, we now choose an explicit particle amplifier configuration and provide an example that demonstrates the parameters γ depends on.

5.6.2 | Simple example

For the simplest case, we look at a Euclidean amplifying step, with $X^{\underline{2}\,\underline{3}} = i$, $X^{\underline{3}\,\underline{4}} = -i$, $X^{\underline{2}\,\underline{4}} = 1$ and write $\omega_k^{\underline{3}} = i|\omega_k^{\underline{3}}|$. This describes the scenario where the speeds of sound before and after the Euclidean step are equivalent. With these replacements the Bogoliubov coefficients for the Euclidean amplifying step can be split up as follows:

$$\alpha_k^{\underline{2}\,\underline{4}} = e^{i\omega_k^{\underline{2}}(t^{\underline{1}\,\underline{2}} + T^{\underline{1}}) - i\omega_k^{\underline{4}}(t^{\underline{1}\,\underline{2}} + T^{\underline{1}} + T^{\underline{2}})}\,|\alpha_k^{\underline{2}\,\underline{4}}| , \tag{5.99}$$

$$\beta_k^{\underline{2}\,\underline{4}} = e^{+i\omega_k^{\underline{2}}(t^{\underline{1}\,\underline{2}} + T^{\underline{2}}) + i\omega_k^{\underline{4}}(t^{\underline{1}\,\underline{2}} + T^{\underline{1}} + T^{\underline{2}})}\,|\beta_k^{\underline{2}\,\underline{4}}| . \tag{5.100}$$

Using the notation for the Bogoliubov coefficients describing the input spectrum step to be;

$$\alpha_k^{\underline{1}\,2} = e^{i(\omega_k^{\underline{1}} - \omega_k^{\underline{2}})t^{\underline{1}\,2}} |\alpha_k^{\underline{1}\,2}|\,, \tag{5.101}$$

$$\beta_k^{\underline{1}\,2} = e^{i(\omega_k^{\underline{1}} + \omega_k^{\underline{2}})t^{\underline{1}\,2}} |\beta_k^{\underline{1}\,2}|\,, \tag{5.102}$$

we then find the output spectrum after amplification becomes:

$$\begin{aligned} |\beta_k^{\underline{1}\,\underline{4}}|^2 &= |\beta_k^{\underline{2}\,\underline{4}}|^2 + \left(2|\beta_k^{\underline{2}\,\underline{4}}|^2 + 1\right) |\beta_k^{\underline{1}\,2}| \\ &\quad -2\,\sin\left(2\omega_k^{\underline{2}} T^{\underline{1}}\right) \times \sqrt{(|\beta_k^{\underline{1}\,2}|^2 + 1)(|\beta_k^{\underline{2}\,\underline{4}}|^2 + 1)}\, |\beta_k^{\underline{2}\,\underline{4}}|\, |\beta_k^{\underline{1}\,2}|\,, \end{aligned} \tag{5.103}$$

where we have employed the normalization; $\det(M^{\underline{i}\,\underline{j}}) = 1$. In this particular case we found $\gamma = -2\omega_k^{\underline{2}} T^{\underline{1}}$, which therefore only depends on known parameters — the time-interval $T^{\underline{1}}$ and the dispersion relation $\omega_k^{\underline{2}}$ in region $\underline{2}$ — that are tunable (for a certain range of k-values) throughout a BEC experiment.

Depending on γ the number of OUT particles oscillates around

$$|\beta^{\mathsf{OUT}}|^2 = \left(1 + 2\,|\beta^{\mathsf{IN}}|^2 + \frac{|\beta^{\mathsf{IN}}|}{|\beta^{\mathsf{PA}}|}\right) |\beta^{\mathsf{PA}}|^2\,, \tag{5.104}$$

and thus the difference between a process with and without initial particles is given by,

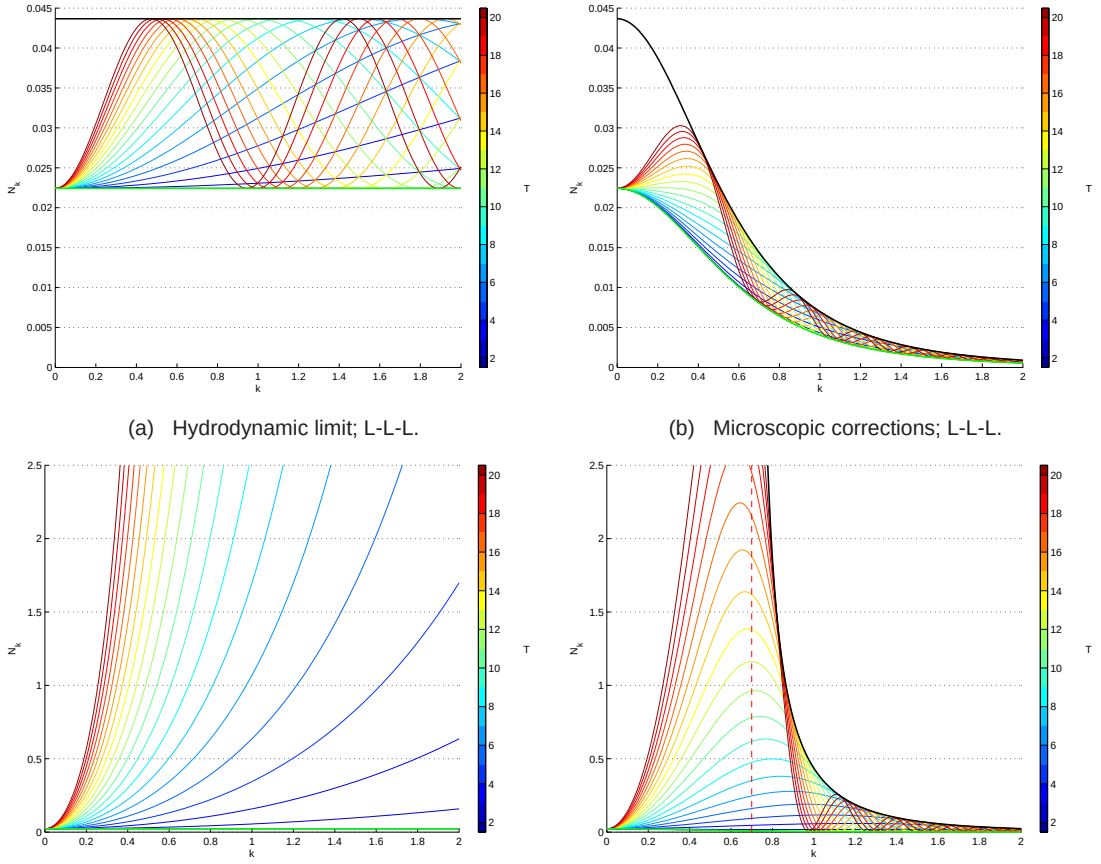
$$|\beta^{\mathsf{OUT}}|^2 \approx 2\,|\beta^{\mathsf{IN}}|^2\, |\beta^{\mathsf{PA}}|^2\,. \tag{5.105}$$

In the last step we assumed that $|\beta^{\mathsf{IN}}| \ll |\beta^{\mathsf{PA}}|$, which is plausible since we expect a much larger particle production in the Euclidean region.

Nevertheless, we have shown that for the simplest example possible the particle amplifier does indeed amplify the initial spectrum, see Eq. (5.105). However, considerably more effort is required to analyse the particle amplifier in depth. It will be important to explore the efficiency of our proposed model and how a more realistic initial particle spectrum resulting from cosmological particle production is amplified. The difference between the maximum possible particle production from the amplifying step ($\sin(\gamma) = -1$) and the minimum particles produced ($\sin(\gamma) = 1$) might be a possible way to increase the efficiency of the particle amplifier. In the next section we will review our results, connect with the existing literature, and discuss problems and open questions.

5.7 | Conclusions

In the first few pages of this chapter we introduced the reader to the concept of emergent spacetimes. Under certain conditions, the microscopic theory of an ultra-cold weakly interacting Bose gas gives way to a mean-field description, the Bose–Einstein condensate. A new state of matter has then been formed, described by a complex classical field. Its behavior is dominated by collective variables,



(a) Hydrodynamic limit; L-L-L.

(b) Microscopic corrections; L-L-L.

(c) Hydrodynamic limit; L-E-L.

(d) Microscopic corrections; L-E-L.

Figure 5.4: The figure displays the mean number of particles N_k produced from two sudden variations in the strength of the atomic interactions. The different curves (color online) correspond to the time period T for which the system is kept in the intermediate regime. The left column focusses on purely collective effects, while in the right column microscopic corrections are taken into account. The top two diagrams show variations between spacetimes emerging from a Bose gas with repulsive interactions ($a > 0$). In the bottom row of the diagrams the intermediate regime exhibits an Euclidean geometry, where the underlying Bose gas shows attractive atomic interactions ($a < 0$). (Please note the figures are *not* based on "real" condensate parameters.)

.

rather than individual atoms. A careful study of the quantum excitations around the mean-field reveals the correspondence between the condensed matter physics and quantum field theory in curved spacetimes. The quantum perturbations are massless spin-zero particles, that are controlled

by an emergent geometrical/gravitational field.

The actual excitations $\delta\hat{\psi}$ and $\delta\hat{\psi}^\dagger$ are related to perturbations in the collective Hermitian variables, the phase $\hat{\theta}$ and density $\hat{n}$ of the complex mean-field. The condensed matter description for linearized perturbations supplies commutation relations for the phase and (up to a function) its material derivatives. We were able to show that these commutators are precisely the ones for the field $\hat{\theta}$ and its canonical momentum $\hat{\Pi}_{\hat{\theta}}$ on the emergent curved spacetime.

The effective gravitational field defined on the Bose gas naturally implements a mechanism to experimentally perform signature-change events. The signature of the emergent gravitational field is directly correlated to the sign of the *s*-wave scattering amplitude of the microscopic collisions. From a gas with repulsive / attractive interaction we expect an emergent Lorentzian / Riemannian geometry. The existence of Riemannian geometries in a Bose gas is limited to short duration time intervals and weak interactions, since back-reaction and instability issues would otherwise destroy the condensate; see [93, 38, 39, 94].

Inspired by recent condensed matter experiments [52, 156], and theoretical work based on them [93, 38, 39, 94], we investigated the quasi-particle production caused by an effective gravitational field going through a sudden but finite duration transition to Euclidean signature. We compared the signature changing case with sudden variation between different Lorentzian regimes, and showed that perturbations in the Euclidean regime experience exponential growth, while for an intermediate Lorentzian regime the modes oscillate between single steps. These are given by the maxima and minima configuration of the two-step process with $T = 0$. Our results are in two ways a generalization of the existing literature, (*e.g.*, the standard general relativity calculations of Dray *et al.* [57, 55]):

1) For the right choice of mode functions (a complex conjugate pair), the calculation is formally equivalent to purely Lorentzian sudden variation between arbitrary levels. This formalism can be applied to any *n*-step process.

2) In addition, we went beyond the hydrodynamic description, which is only sufficient to account for the infrared behavior of the system, and included ultraviolet modes in our analysis. This leads to modifications in both the emergent gravitational field and the dispersion relation. For the gravitational field we obtained (in the eikonal limit) a momentum-dependent rainbow geometry; and a non-relativistic dispersion relation. The modification in the dispersion relation can be classified as being within the boost sub-group, and is of the form as suggested by some effective field theories [138, 131, 130, 202, 200].

In figure (5.4) we illustrated our four different results, namely sudden variations without (first row) or with (second row) signature change events, within the hydrodynamic limit (left column), and beyond it (right column). As a result, the total number of particles produced is finite. One way to explain the behavior of the trans-Planckian modes is to understand the physical significance of the healing length of the Bose–Einstein condensate. The healing scale defines a length scale over which quantum fluctuations in the condensate tend to smooth out. In some sense, it defines the smallest possible size for a condensate, $V > \xi^d$, see [151]. Perturbations with wavelengths that

are much larger than the healing length experience a nice smooth mean-field, here our emergent gravitational field. High energy modes, with wavelengths at the magnitude of the healing length start to see fingerprints of the microscopic structure. Note that, perturbations of sufficiently high energy are not driven by collective variables. This can also be seen in figure 5.4(d): While infrared modes behave like their hydrodynamic / relativistic neighbours to the left 5.4(c), the ultraviolet modes do not notice the change in the signature of the gravitational field. They are behaving just like their upper neighbours 5.4(b) in a purely Lorentzian geometry.

Still, not all of our concerns are yet resolved. For example, while the total number of particles produced can be made finite, the total energy remains formally infinite even beyond the hydrodynamic limit. This problem might be related to our choice of ultra-high-energy description for the fundamental Bosons. Perturbations of sufficiently high energy can excite single atoms out of the condensate, and these are (in our description) non-relativistic particles. Therefore, we suggest that to improve the ultra-high-energy behavior it might be useful to start with a fully relativistic description for the fundamental Bosons. (For a description of relativistic Bose–Einstein condensates see, *e.g.*, [28].)

Finally, we would like to comment on the possible connection between our theoretical results and the data from the Bose-nova experiment carried out by Donley *et al.* [52, 156]. There are fundamental differences between our approach, and the Bose-nova experiment. First, we have chosen a hard-walled box as an external potential, while in the experiment a harmonic trap has been used. In [93, 38, 39, 94], Hu and Calzetta have shown that the trapping energy delays the condensate collapse for a certain amount of time. Their calculations are in good accordance with the experimental values. In our case the trapping energy is zero, and hence we do not expect such a delay.

Another fundamental difference is that we kept our gravitational field non-degenerate (apart from the actual instant of signature change). In the experiment the initial scattering length was taken to be zero and held there for a finite time, and hence Donley *et al.* started with a partly *degenerate* gravitational field. (Partly degenerate gravitational field, because for a harmonic trap the quantum pressure term exhibits a k-independent contribution resulting in a position-dependent correction to the effective atomic interaction; see first term inside the curly brackets in Eq. (5.82).) In the experiment two different sequences were chosen for the sudden variations, with two different outcomes. One, where the scattering length has been driven from zero to attractive and finally to large repulsive atomic interactions. The other set-up was from zero to attractive, back to zero and then to large repulsive atomic interactions. In both cases bursts of atoms leaving the condensate were detected. But the bursts without the intermediate regime of zero interactions were much stronger. These are “jets” of atoms, while in the other case the bursts were less strong. Hu and Calzetta approached this problem without taking back-reaction effects — of the quantum perturbations onto the condensate — into account. Naturally, their description becomes less accurate with the length of the Euclidean time-interval. We would like to emphasize the difference in the behavior of the acoustic metric, the “gravitational field”, since in the first scenario it does not exhibit any finite interval of degeneracy,

while in the latter it does.

Furthermore, we would like to propose a rather different use for our L-E-L-process, as a particle amplifier for cosmological particle production in the laboratory. In our calculations so far we always started from the vacuum with zero collective excitations in the system. These calculations could easily be extended, such as to start with a non-vacuum state, *e.g.*, after cosmological particle production in an emergent Friedmann–Robertson–Walker type geometry [70, 71, 16, 15, 72, 171]. Recently this behavior has been studied numerically in a realistic Bose–Einstein condensate, where the present authors and collaborators used a classical-field-method approach, see [113]. To obtain an effective expanding universe, the scattering length has to decrease as a specific function of time. After a finite expansion time, the quasi-particle spectrum obtained — a very small number of particles — somehow has to be detected. Due to its smallness this remains a significant experimental challenge. Recently, there has been some theoretical effort regarding this problem, see [163]. That author suggests a rather complicated detection mechanism, where only perturbations of one wavelength at a time can be detected. In section (5.6) we suggested an alternative concept, that is to *amplify* the quasi-particle spectrum, *e.g.*, in a three-step process involving a brief finite-duration Euclidean region to amplify the signal, so that common detection mechanisms might be able to detect the amplified quasi-particle spectrum. For a simple example, we calculated the particle spectrum after the amplification process in terms of the initial spectrum. However, for any practical application in a real BEC experiment there are considerable technical issues that need to be explored. (For example, the possibility of using a L-L-L amplifier.)

To conclude this chapter we would like to briefly discuss the possibility of real general relativistic signature change events. In 1983, James Hartle and Steven Hawking proposed a signature change at extremely early times, in the very early stages of the big bang, when quantum gravity effects are expected to be dominant (see reference [90]). They suggested that the existence of physical time, and hence the existence of our universe, is associated with a signature change event from Euclidean to Lorentzian geometry (the “no boundary” proposal).

In some sense it is possible to consider the reverse Bose-Nova experiment (attractive to repulsive) as the creation process for our emergent spacetime. At early times the Boson interactions are strongly attractive, such that the atoms do not show any collective / mean-field behavior. If now the interactions experience a smooth, or non-smooth change for the atomic interactions, from attractive to repulsive, the individual atoms have to give way to collective / mean-field variables. Therefore the existence of our emergent gravitational field might in some sense be associated with a pre-dating signature change event caused by a change in the underlying microscopic variables.

CHAPTER 6

Cosmological inflation in emergent rainbow spacetime

We now investigate cosmological particle production in spacetimes where Lorentz invariance emerges in the infrared limit, but is explicitly broken in the ultraviolet regime. Thus these models are similar to many (but not all) models of quantum gravity, where a breakdown of Lorentz invariance is expected for ultraviolet physics around the Planck / string scale. Our specific model focuses on the boost subgroup that supports CPT invariance and results in a momentum-dependent dispersion relation. Motivated by previous studies on spacetimes emerging from a microscopic substrate, we show how these modifications naturally lead to momentum-dependent rainbow metrics.

Firstly, we investigate the possibility of reproducing cosmological particle production in spacetimes emerging from real Bose gases. Several papers have been written on the analogy between the kinematics of linearized perturbations in Bose–Einstein condensates and effective curved-spacetime quantum field theory. Recently, we have studied the influence of non-perturbative ultraviolet corrections in time-dependent analogue spacetimes, leading to momentum-dependent emergent rainbow spacetimes. We show that models involving a time-dependent microscopic interaction are suitable for mimicking quantum effects in FRW spacetimes. Within certain limits the analogy is sufficiently good to simulate relativistic quantum field theory in time-dependent classical backgrounds, and the quantum effects are approximately robust against the model-dependent modifications.

Secondly, we analyze how significantly the particle production process deviates from the common picture. While very low-energy modes do not see the difference at all, some modes “re-enter the Hubble horizon” during the inflationary epoch, and extreme ultraviolet modes are completely insensitive to the expansion. The analysis outlined here, because it is nonperturbative in the rainbow metric, exhibits features that cannot be extracted simply from the standard perturbative modification of particle dispersion relations. However, we also show how the final result, after many e-foldings,

will approach a time-independent exponentially decaying particle spectrum.

6.1 | Introduction

The use of Bose–Einstein condensates as analogue models for quantum field theory in spatially flat $k = 0$ Friedmann–Robertson–Walker (FRW) geometries

$$ds^2 = g_{ab}\, dx^a\, dx^b = -d\tau^2 + a(\tau)^2 \sum_{i=1}^{d} (dx^i)^2 \tag{6.1}$$

(in d spatial dimensions) has recently been extensively explored in [113]. The proposal [15, 16, 71, 72, 75, 171, 173] is based on the analogy between the equation of motion for collective excitations around a macroscopically occupied ground state of an ultra-cold weakly interacting gas of Bosons (*i.e.*, the novel state of matter referred to as the Bose–Einstein condensate), and

$$\frac{1}{\sqrt{|g|}}\, \partial_a \left(\sqrt{|g|}\, g^{ab}\, \partial_b \hat{\theta} \right) = 0\,, \tag{6.2}$$

the covariant free-field equation (Klein–Gordon equation) for spin-0 massless particles. (The indices a, b run from 0 to d whereas i, j run from 1 to d for the spatial coordinates only). Here g^{ab} is a symmetric covariant rank two tensor whose entries include purely collective (mean-field) variables $c = c(t, \mathbf{x})$, the speed of sound, $\mathbf{v} = \mathbf{v}(t, \mathbf{x})$, and the background velocity. Using $g^{ab}\, g_{bc} = \delta^a{}_c$ we are able to define an effective line-element for the mean-field,

$$ds^2 = \left(\frac{c}{U} \right)^{\frac{2}{d-1}} \left[-(c^2 - v^2)\, dt^2 - dt\, \mathbf{v}^{\mathsf{T}}\, d\mathbf{x} + d\mathbf{x}^{\mathsf{T}}\, d\mathbf{x} \right]. \tag{6.3}$$

Here the quantity U arises from the microscopic description of Bose–Einstein condensate, and represents the inter-atomic potential.

We have previously shown (see Chapter 5) that Eq. (6.2) is an equation for perturbations in the collective variables, the phase $\hat{\theta}$ and its conjugate momentum $\hat{\Pi}_{\hat{\theta}}$ (see also [15, 16, 71, 72, 75, 171, 173]). This kind of behavior is not restricted to Bose–Einstein condensates. Indeed the first modern paper on analogue models for gravity focussed on ordinary fluid mechanics; see [173]. Since then numerous media have been suggested as substrates to develop analogue models for gravity [18, 165, 178, 180]. Nevertheless it is sometimes difficult to isolate the fundamental principles behind the analogy.

Inspired by the Bose gas, where both the microscopic and macroscopic theory is understood to an adequate extent, we suggest that it might be useful to transfer the experience gained from the various known examples for emergent spacetimes into a more general framework:

> *Emergent spacetimes* involve (i) a microscopic system of fundamental objects (*e.g.*, strings, atoms, or molecules); (ii) a dominant mean-field regime, where the microscopic degrees of freedom give way to collective variables; (iii) a "geometrical object"

(*e.g.*, a symmetric tensor) dominating the evolution for infrared classical and quantum excitations around the mean field.

Within certain limits we are free to choose our geometrical object to mimic Einstein's theory of gravity, (*e.g.*, a symmetric rank two tensor g_{ab} that is conformal to an exact solution obtained by solving the Einstein equation for a physically reasonable stress-energy tensor).

Analogue models for gravity are emergent spacetimes that are specifically adjusted to mimic as closely as possible Einstein's geometrical theory of gravity.

The fundamental difference between emergent spacetimes and general relativity becomes obvious if we consider the following statement: Emergent spacetimes, as they appear in the analogue model programme, are "a short and simple way" to summarize the kinematics of linearized perturbations in a geometrical sense, without requiring the notion of a stress-energy tensor or the Einstein equations.

Thus, the analogy is (currently) restricted to the kinematic behavior of the system, and any back-reaction between the excitations and the mean-field might not be in analogy with Einstein's theory of gravity. Therefore it is advisable to restrict the use of analogue models for gravity as toy models for semi-classical quantum gravity at the level of curved spacetime quantum field theory, where the gravitational field is a purely classical field.

Indeed, analogue models for gravity are very idealized constructions, and require careful treatment with respect to the model-dependence to obtain the desired curved-spacetime quantum-field-theory effects. This has first been pointed out in [112, 177], where the authors analyzed the robustness of Hawking radiation against modifications in the excitation spectrum (most relevant to fluid dynamics: super- and sub- luminal dispersion).

In related previous work [113] we made use of classical phase space methods to numerically study "cosmological particle production" in a realistic BEC. In principle, there are two different ways to mimic an expanding universe in a Bose gas. In [71, 72] the authors studied a freely expanding condensate cloud, such that the density is a function of time. This idea has been further investigated in [171]. In both — our previous paper [113] and in this chapter — we pursue an alternative (more recent) idea introduced in [15, 16], where the authors achieved FRW geometry through a time-dependence in the effective atom-atom potential. A change in the inter-atomic potential is related to a change in the speed of sound, and consequently relates to a time-dependent acoustic metric. As expected our simulation verified the analogy (in the hydrodynamic limit) to a good extent. However, the ultraviolet behavior showed that it is crucial to include quantum pressure effects to understand the ultraviolet / trans-phononic part of the quasi-particle spectrum. Thus we conclude that our specific model — an ultra-cold gas of Bosons with time-varying atomic interactions — shows a specific model-dependence that interferes with the low-momentum particle production process. One lesson that can be drawn from this new insight is that a careful choice of condensate parameters is necessary in order to mimic the desired curved-spacetime quantum field theory effect.

The main focus in this chapter is to understand the differences between ordinary quantum field theory in a "real" classical FRW-background and quantum field theory in an emergent FRW-background in a Bose gas. This question has been motivated by many effective field theories, where Lorentz invariance is broken at ultraviolet energies in a similar manner as in the emergent spacetimes we are investigating.

> Emergent spacetimes exhibit an *emergent / effective Lorentz symmetry* for low-energy / infrared excitations around the macroscopic field. This symmetry will be broken in the high-energy / ultraviolet regime, that is at scales dominated by the underlying microscopic theory. These corrections are of a non-perturbative nature.

For now, we leave general questions aside, and focus on the specific emergent spacetime, investigating the influence on cosmological particle production due to ultraviolet corrections. We include quantum pressure effects — which lead to a nonlinear excitation spectrum — as nonperturbative ultraviolet corrections to the emergent geometry. We will show that this leads to momentum-dependent "rainbow spacetimes". Partly motivated by extant literature [135, 201] and our numerical results from the simulations of quantum effects in realistic Bose–Einstein condensates, we present a coherent interpretation for the quasi-particle spectrum produced in FRW rainbow spacetimes [200, 201, 130, 131, 201, 202, 185].

The "FRW rainbow metrics" recover the "ordinary" FRW type geometries in the infrared (phononic) regime, but exhibit momentum-dependent modifications in the ultraviolet (trans-phononic) regime. We show that in such a geometry the scale factor for the universe $a(t)$ is effectively momentum-dependent $a(t) \to a_k(t)$, consequently leading to a momentum-dependent Hubble parameter: $H(t) \to H_k(t)$. In addition, we are dealing with an emergent spacetime that exhibits a time-dependent effective "Planck-length". Ultimately, the particle production process in our specific analogue model will show deviations from the one expected in "standard" curved-spacetime quantum field theory.

For the "analogue gravity programme" it is important to check the robustness of cosmological particle production against those modifications. Is there a window where the analogy is good enough, for example, to use the Bose gas as a toy model for inflation?

In the following we will show that in the present model the particle process is *in general not* robust against the model-specific modifications. However, for short time duration expansion scenarios inflation can be simulated in a "realistic" Bose–Einstein condensate.

We perform a quantitative analysis to describe short time *and* long-lasting expansions. We use the ratio between the mode frequency and the Hubble frequency (the inverse of the rate of change in the size of the emergent universe), to show that our specific model indeed shows significant deviations in the ultraviolet regime, *e.g.*, both crossing *and* re-entering of the "Hubble horizon" during the inflationary epoch; $a(t) \sim \exp(t)$.

By means of our numerical analysis we are able to “read-off” the final spectrum after a sufficiently long-lasting expansion. We explain why the final particle spectrum — after an infinitely long-lasting inflationary epoch — will be time-independent and finite.

6.2 | Emergent spacetimes: Excitations in Bose–Einstein condensates

In the following we extend the calculations presented in our previous work [113]. The intent is to derive an emergent geometry that is able to simultaneously represent both the phononic and trans-phononic excitations in a Bose–Einstein condensate. It is a well established result — both in theory and experiment — that the energy-momentum relation for excitations in a Bose–Einstein condensates is given by the nonlinear Bogoliubov dispersion relation. In [131, 200, 202, 130, 201, 185] it has been shown, (within the analogue model for gravity point of view), that phononic modes are relativistic modes, since they exhibit Lorentz symmetry. The corresponding emergent geometry is a flat spacetime with Lorentzian signature (Minkowski metric). Higher energy (trans-phononic) modes break Lorentz symmetry, the excitations being “supersonic”. The full dispersion relation for excitations in a realistic Bose–Einstein condensate is similar to those expected to occur in certain effective field theories. For a more detailed description see [131, 200, 202, 130, 201, 185]. It is also known that this kind of modification is non-perturbative, since it originates in density fluctuations visible only at small scales (in the order of the healing / coherence length). These modes are trans-phononic modes, where quantum pressure effects are no longer negligible. We show that in a Bose–Einstein condensate with time-dependent condensate parameters, the borderline between phononic and trans-phononic modes is also time-dependent, and therefore requires a more accurate analysis at the level of the emergent geometry, leading to the concept of a rainbow metric. In other words we extend the treatment for ultraviolet modes from flat to curved spacetimes.

6.2.1 | Ultraviolet non-perturbative corrections: Quantum pressure effects

In [113] we derived a coupled pair of equations,

$$\partial_t \hat{n} + \nabla \cdot \left[\left(\frac{n_0 \hbar}{m} \nabla \hat{\theta} \right) + (n_0 \, \mathbf{v}) \right] = 0 \,, \tag{6.4}$$

$$\partial_t \hat{\theta} + \mathbf{v} \cdot \nabla \hat{\theta} + \frac{\widetilde{U}}{\hbar} \, \hat{n} = 0 \,; \tag{6.5}$$

for quantum fluctuations in the condensate density $\hat{n}$ and phase $\hat{\theta}$. The background velocity $\mathbf{v}$ is given by

$$\mathbf{v} = \frac{\hbar}{m}\,\nabla\theta_0\,, \tag{6.6}$$

as the gradient of the condensate phase θ_0. Here m is the mass of the fundamental Bosons, n_0 the number density, and $\hbar$ the Planck constant. The differential operator $\widetilde{U}$ has been defined as [200, 113]

$$\widetilde{U} = U - \frac{\hbar^2}{2m}\,\widetilde{D}_2\,, \tag{6.7}$$

where the differential operator

$$\widetilde{D}_2 = \frac{1}{2}\left\{\frac{(\nabla n_0)^2 - (\nabla^2 n_0)n_0}{n_0^3} - \frac{\nabla n_0}{n_0^2}\nabla + \frac{1}{n_0}\nabla^2\right\}\,, \tag{6.8}$$

accounts for the first-order correction obtained from linearizing the quantum potential term. Note the tilde notation is used to emphasize the fact that we are dealing with a differential operator.

To develop the analogy between condensed matter physics and curved-spacetime quantum field theory, see Eq. (6.2), it is necessary to combine Eq. (6.4) and Eq. (6.5) into a single equation for the phase fluctuations. For that it is important to note that we can rearrange (6.5) to make $\hat{n}$ the subject. That is

$$\hat{n} = \hbar\,\widetilde{U}^{-1}\,\left[\partial_t\hat{\theta} + \mathbf{v}\cdot\nabla\hat{\theta}\right] = \hbar\,\widetilde{U}^{-1}\,\frac{D\hat{\theta}}{Dt}\,, \tag{6.9}$$

where $D\hat{\theta}/Dt$ is the rate of change of $\hat{\theta}$ following a small volume of the fluid, the *material derivative* of $\hat{\theta}$. If the fluid is at rest, the material derivative reduces to $D\hat{\theta}/Dt \to \partial_t\hat{\theta}$, but for a moving fluid it represents a "fluid-following" derivative. The integral differential operator $\widetilde{U}^{-1}$ can *formally* be expanded as

$$\begin{aligned}\widetilde{U}^{-1} = U^{-1} \;&+\; \left[\frac{\hbar}{2m}\right]\,U^{-1}\widetilde{D}_2\,U^{-1} \\ &+\; \left[\frac{\hbar}{2m}\right]^2\,U^{-1}\widetilde{D}_2\,U^{-1}\widetilde{D}_2\,U^{-1} \\ &+\; \left[\frac{\hbar}{2m}\right]^3\,U^{-1}\widetilde{D}_2\,U^{-1}\widetilde{D}_2\,U^{-1}\widetilde{D}_2\,U^{-1} + ...\end{aligned} \tag{6.10}$$

where the *formal* series converges only on the subspace of functions spanned by the eigenfunctions whose eigenvalues satisfy

$$\lambda\left(\frac{\hbar^2}{2m}U^{-1}\widetilde{D}_2\right) < 1\,. \tag{6.11}$$

Since $\widetilde{D}_2$ and $\widetilde{U}$ are second-order linear differential operators, the inverse $\widetilde{U}^{-1}$ always exists as an integral operator (that is, in the sense of being a Green function). Expanding this Green function as in Eq. (6.10) above is a convenience that allows us to interpret $\widetilde{U}^{-1}$ as a sum of differential operators, but this is not a fundamental limitation on the formalism.

Acoustic and rainbow metrics

We use equation (6.9) to eliminate $\hat{n}$ completely in our equations of motions, by substituting it into equation (6.4). That yields a single equation for the perturbed phase

$$\partial_a \left(f^{ab}\, \partial_b \hat{\theta} \right) = 0 \,, \tag{6.12}$$

where we have introduced the matrix f^{ab} with inverse-differential-operator-valued entries:

$$f^{ab} = \hbar \left[\begin{array}{c|c} -\widetilde{U}^{-1} & -\widetilde{U}^{-1} v^j \\ \hline -v^i \widetilde{U}^{-1} & \frac{n_0}{m}\delta^{ij} - v^i \widetilde{U}^{-1} v^j \end{array} \right] . \tag{6.13}$$

Note that in general $\widetilde{U}^{-1}$ is an integral operator so Eq. (6.12) is an integro-differential equation. If we additionally require that there exists an (inverse) metric tensor g_{ab} such that

$$f^{ab} \equiv \sqrt{-g}\, g^{ab} \,, \tag{6.14}$$

where g is the determinant of the metric tensor g_{ab}, then the connection is formally made to the field equation for a minimally coupled massless scalar field in a curved spacetime; see Eq. (6.2). Now in many situations of physical interest, the differential operator $\widetilde{U}$ can be usefully approximated by a function — for instance the hydrodynamic and eikonal limits.

Hydrodynamic approximation: In the hydrodynamic limit where the *quantum pressure* is neglected one has

$$|U\, n_0| \gg |(\hbar^2/2m)\, \widetilde{D}_2\, n_0| \tag{6.15}$$

so that

$$\widetilde{U} \to U = \frac{4\pi\hbar^2 a_{\mathrm{scatt}}(t)}{m}. \tag{6.16}$$

The scattering length $a_{\mathrm{scatt}}(t)$ represents the s-wave scattering term. (See, for instance, [12, 18], and the discussion above.)

Within this approximation we obtain

$$f^{ab} = \frac{\hbar}{U} \left[\begin{array}{c|c} -1 & -v^j \\ \hline -v^i & \frac{n_0 U}{m}\delta^{ij} - v^i v^j \end{array} \right] . \tag{6.17}$$

To mimic curved spacetime classical and quantum field theory effects the acoustic metric has to be formally in agreement with Einstein's theory of gravity. For this low-momentum approximation we are able to define a common (for all wavelengths k) speed of sound in the condensate:

$$c_k^2 \to c^2 = \frac{n_0 U(t)}{m} \,. \tag{6.18}$$

Applying Eq. (6.14) we obtain,

$$g_{ab} \equiv \left(\frac{n_0\,\hbar}{c\,m}\right)^{\frac{2}{d-1}} \left[\begin{array}{c|c} -(c^2-v^2) & -v^j \\ \hline -v^i & \delta^{ij} \end{array}\right], \tag{6.19}$$

as the *acoustic metric* or *analogue metric*. In this case all collective excitations behave as sound waves with the usual linear dispersion form

$$\omega_0 = c\,k \tag{6.20}$$

and the quanta of excitations are thus phonons.

Eikonal approximation: Let us now invoke a different approximation that holds for trans-phononic modes, so that the elements of the matrix f^{ab} can be treated as (possibly momentum dependent) functions, rather than differential operators: Consider the *eikonal limit* where $\widetilde{U}$ can usefully be approximated by a function

$$\widetilde{U} \to U_k(t,\mathbf{x}) = U(t,\mathbf{x}) + \frac{\hbar^2 k^2}{4mn_0}, \tag{6.21}$$

which we shall conveniently abbreviate by writing U_k. Beyond the hydrodynamic limit we obtain

$$f^{ab} = \frac{\hbar}{U_k} \left[\begin{array}{c|c} -1 & -v^j \\ \hline -v^i & \frac{n_0 U_k}{m}\delta^{ij} - v^i v^j \end{array}\right]. \tag{6.22}$$

Note that in the eikonal approximation the k dependence hiding in U_k will make this a momentum-dependent metric, a so-called *rainbow metric*. The metric tensor is explicitly given by

$$g_{ab} \equiv \left(\frac{n_0\,\hbar}{c_k\,m}\right)^{\frac{2}{d-1}} \left[\begin{array}{c|c} -(c_k^2-v^2) & -v^j \\ \hline -v^i & \delta^{ij} \end{array}\right], \tag{6.23}$$

where we have introduced the quantity

$$c_k(t)^2 = c(t)^2 + \epsilon_{\mathrm{qp}}^2 k^2, \tag{6.24}$$

for a uniform condensate density $n_0(t,\mathbf{x}) = n_0$. It is convenient to define

$$\epsilon_{\mathrm{qp}} = \frac{\hbar}{2m}, \tag{6.25}$$

where $\epsilon_{\mathrm{qp}} \ll |c(t)/k|$ is a useful indication for the hydrodynamic limit; compare with Eq. (6.15). The dispersion relation in the eikonal limit is

$$\omega_k(t) = c_k(t)\,k = \sqrt{c(t)^2k^2 + \epsilon_{\mathrm{qp}}^2 k^4}, \tag{6.26}$$

and hence violates "*acoustic Lorentz invariance*". This is not surprising at all, since we know the quasi-particles become "atom-like", and so *non-relativistic*, at high momentum [185].

Acoustic or rainbow spacetimes? It is only in the acoustic/hydrodynamic limit that the k dependence of U_k and c_k vanish, so that the rainbow metric is reduced to an ordinary Lorentzian metric.

An interesting consequence of the Bogoliubov theory in Bose condensates is that in general the excitation spectrum displays nonlinear dispersion (see Eq. (6.26)), being linear (*i.e.*, phononic) for low $|\mathbf{k}|$ and becoming quadratic (*i.e.*, free-particle like) at large $|\mathbf{k}|$. When the nonlinear dispersion (6.26) is incorporated into analogue models of gravity it is equivalent to breaking Lorentz invariance [12, 18, 202, 130, 131, 200].

The hydrodynamic approximation is a statement about the *smallness* of the quartic term in the dispersion relation for ω_k^2 (6.26), with respect to the quadratic term. The usual line of argument is that the smallness of $\epsilon_{\rm qp}$ makes it possible to neglect the second order in Eq. (6.26) for low-energy excitations, where $\epsilon_{\rm qp}|k| \ll c(t)$. Here Lorentz invariance is an emergent symmetry. However, it is important to realise that the propagation speed can be a function of time, $c = c(t)$, and hence if $c(t) \to 0$ then one is dealing with a system that eventually violates Lorentz invariance at *all* energy scales. There are no theoretical or experimental restrictions to prevent $U(t) \propto c(t)$ becoming arbitrarily small.

In the specific cases we are interested in, we are confronted with exactly this situation, and therefore a more subtle analysis is required as to whether the acoustic metric (6.19) is a sufficient approximation, or whether we have to use the more sophisticated concept of a rainbow spacetime (6.23). We will elaborate on the point in Section 6.4.

Limitations of the rainbow analogy? It is worth reiterating the assumptions used in making the above analogy. The theory resulting from linearized quantum fluctuations leads to a *free field theory* — that is, the modes of the field $\hat{\theta}$ are non-interacting. Since we are using a linearized theory, the interactions between quantum fluctuations themselves, and between quantum fluctuations and the condensate mode are neglected. This is equivalent to assuming the metric tensor is an externally-specified classical quantity.

Our numerical simulations carried out in [113] do not require these assumptions; there all modes of the system are included and these modes are able to interact via the nonlinear interaction term. Thus we were able to explore the validity of the assumptions of the free-field theory [164].

We further note that while the present form of the analogy only holds for massless scalar (spin zero) quasi-particles, in general it is possible to modify the formalism to include massive minimally coupled scalar fields at the expense of dealing with more complex BEC configurations, *e.g.*, a two-component BEC [200, 201, 130, 131, 201, 202, 189, 188]. In BEC language one would explain this situation in terms of a dispersion relation with a gap.

Commutation relations

To derive the analogy presented above, we approximated and transformed our field operators several times, see Chapter 5 and [113]:

1. $\hat{\psi}(t,\mathbf{x})$ and $\hat{\psi}^{\dagger}(t,\mathbf{x})$: The single Boson annihilation and creation operators; where

$$[\hat{\psi}(t,\mathbf{x}),\hat{\psi}(t,\mathbf{x}')]=0\,, \tag{6.27}$$
$$[\hat{\psi}^{\dagger}(t,\mathbf{x}),\hat{\psi}^{\dagger}(t,\mathbf{x}')]=0\,, \tag{6.28}$$
$$[\hat{\psi}^{\dagger}(t,\mathbf{x}),\hat{\psi}^{\dagger}(t,\mathbf{x}')]=\delta(\mathbf{x}-\mathbf{x}')\,; \tag{6.29}$$

2. $\delta\hat{\psi}(t,\mathbf{x})$ and $\delta\hat{\psi}^{\dagger}(t,\mathbf{x})$: Decomposition into a single coherent mode $\psi(t,\mathbf{x})=\langle\hat{\psi}(t,\mathbf{x})\rangle$, and the quantum excitations $\delta\hat{\psi}(t,\mathbf{x})$ around it. Altogether, $\hat{\psi}(t,\mathbf{x})=\psi(t,\mathbf{x})+\delta\hat{\psi}(t,\mathbf{x})$ and $\hat{\psi}^{\dagger}(t,\mathbf{x})=\psi^{*}(t,\mathbf{x})+\delta\hat{\psi}^{\dagger}(t,\mathbf{x})$, where

$$[\delta\hat{\psi}(t,\mathbf{x}),\delta\hat{\psi}(t,\mathbf{x}')]=0\,, \tag{6.30}$$
$$[\delta\hat{\psi}^{\dagger}(t,\mathbf{x}),\delta\hat{\psi}^{\dagger}(t,\mathbf{x}')]=0 \tag{6.31}$$
$$[\delta\hat{\psi}^{\dagger}(t,\mathbf{x}),\delta\hat{\psi}^{\dagger}(t,\mathbf{x}')]=\delta(\mathbf{x}-\mathbf{x}')\,; \tag{6.32}$$

3. $\hat{n}$ and $\hat{\theta}$: Mapping onto Hermitian phase and density fluctuation operators, as studied (for example) in [15, 16]. Here we made use of the fact that the macroscopic field $\psi(\mathbf{x})$ is complex and so for topologically trivial regions — without zeros or singularities — one can always express it as $\psi(t,\mathbf{x})=\sqrt{n(t,\mathbf{x})}\,\exp(i\theta(t,\mathbf{x}))$. Linearizing around the two parameters of the complex-valued field, $\theta\rightarrow\theta_0+\hat{\theta}$ and $n\rightarrow n_0+\hat{n}$, we can write $\hat{\psi}\simeq\psi+\sqrt{n_0}\left(\frac{\hat{n}}{2n_0}+i\,\hat{\theta}\right)$, and its Hermitian conjugate, such that

$$[\hat{n}(t,\mathbf{x}),\hat{n}(t,\mathbf{x}')]=0\,, \tag{6.33}$$
$$\left[\hat{\theta}(t,\mathbf{x}),\hat{\theta}(t,\mathbf{x}')\right]=0\,, \tag{6.34}$$
$$\left[\hat{n}(t,\mathbf{x}),\hat{\theta}(t,\mathbf{x}')\right]=i\,\delta(\mathbf{x}-\mathbf{x}')\,. \tag{6.35}$$

4. Finally, we are able to use the equation of motion (6.9) to formally express $\hat{n}$ in terms of $\hat{\theta}$:

$$\left[\frac{1}{\widetilde{U}}\,\frac{D\hat{\theta}(t,\mathbf{x})}{Dt},\frac{1}{\widetilde{U}}\,\frac{D\hat{\theta}(t,\mathbf{x}')}{Dt}\right]=0\,, \tag{6.36}$$
$$\left[\hat{\theta}(t,\mathbf{x}),\hat{\theta}(t,\mathbf{x}')\right]=0\,, \tag{6.37}$$
$$\left[\frac{1}{\widetilde{U}}\,\frac{D\hat{\theta}(t,\mathbf{x})}{Dt},\hat{\theta}(t,\mathbf{x}')\right]=-\frac{i}{\hbar}\,\delta(\mathbf{x}-\mathbf{x}')\,; \tag{6.38}$$

There are two different ways to view the resulting commutator relations in the hydrodynamic and eikonal limit: A condensed matter point of view in terms of time-dependent commutators, or a commutator relationship for the phase perturbation $\hat{\theta}$ and its conjugate momentum $\hat{\Pi}_{\hat{\theta}}$ on the emergent spacetime.

Condensed matter point of view: First we face the problem of how to deal with the differential operator $\widetilde{D}_2$, which involves studying two interesting limits where the commutation relation takes a simpler form.

In the *hydrodynamic approximation* we get

$$\left[\frac{D\hat{\theta}(t,\mathbf{x})}{Dt}, \hat{\theta}(t,\mathbf{x}')\right] = \frac{U(t)}{i\hbar}\,\delta(\mathbf{x}-\mathbf{x}'), \tag{6.39}$$

which is now a time-dependent commutation relation.

For $U(t) = 0$ the hydrodynamic commutator vanishes completely and we are left with purely classical statements for $\hat{\theta}$. This situation changes significantly if one instead considers the eikonal approximation.

In the *eikonal approximation* we get (in momentum space)

$$\left[\frac{D\hat{\theta}(t,\mathbf{k})}{Dt}, \hat{\theta}(t,\mathbf{k}')\right] = \frac{U(t)+\frac{\hbar^2k^2}{4mn_0}}{i\hbar}\,\delta_{kk'}\,, \tag{6.40}$$

and the commutator does not vanish for $U(t) \to 0$, though it can vanish if $U(t)$ is driven negative.

This suggests that the presence of $\widetilde{D}_2$ cannot in general be neglected for a time-dependent atomic interaction $U(t)$.

Emergent spacetime point of view: An alternative insight can be gained if we define an emergent Lagrange density,

$$\mathcal{L} = -\frac{1}{2} f^{ab}\,\partial_a\hat{\theta}\,\partial_b\hat{\theta}\,, \tag{6.41}$$

in correspondence with Eq. (6.2). The momentum conjugate to $\hat{\theta}$ is given by

$$\hat{\Pi}_{\hat{\theta}} := \frac{\partial\mathcal{L}}{\partial(\partial_t\hat{\theta})} = -f^{tb}\,\partial_b\hat{\theta}, \tag{6.42}$$

and hence we evaluate the conjugate momentum to $\hat{\theta}$ as,

$$\hat{\Pi}_{\hat{\theta}} = \frac{\hbar}{\widetilde{U}} \frac{D\hat{\theta}}{Dt} \,. \tag{6.43}$$

With this new insight we are able to add another set of commutation relations, one that makes only sense after having introduced the emergent spacetime:

5. The phase and density operators are a canonical set of quantum field operators and conjugate field operators,

$$\left[\hat{\theta}(t,\mathbf{x}), \hat{\theta}(t,\mathbf{x}')\right] = 0 \,, \tag{6.44}$$

$$\left[\hat{\Pi}_{\hat{\theta}}(t,\mathbf{x}), \hat{\Pi}_{\hat{\theta}}(t,\mathbf{x}')\right] = 0 \,, \tag{6.45}$$

$$\left[\hat{\theta}(t,\mathbf{x}), \hat{\Pi}_{\hat{\theta}}(t,\mathbf{x}')\right] = i\delta(\mathbf{x}-\mathbf{x}') \,; \tag{6.46}$$

 in an effective curved spacetime represented by Eq. (6.19), for a massless spin-zero scalar field.

In the *hydrodynamic limit* $\widetilde{U} \to U$ we recover

$$\hat{\Pi}_{\hat{\theta}} = \frac{\hbar}{U} \frac{D\hat{\theta}}{Dt} \,, \tag{6.47}$$

the standard result for the conjugate momentum in curved spacetime; for more details see [29, 146].

The conjugate momentum *for ultraviolet modes* $U \to U_k$ is given by

$$\hat{\Pi}_{\hat{\theta}} = \frac{\hbar}{U_k} \frac{D\hat{\theta}}{Dt} \,, \tag{6.48}$$

as the conjugate momentum in our rainbow geometry.

This is a significant result, since it shows that knowledge of the emergent spacetime picture provides a deeper insight into the full dynamics for the density and phase perturbations, and explains the explicit time-dependence in their commutation relations.

6.2.2 | FRW-rainbow geometries: Specific time-dependence for atom-atom scattering

Clearly time dependence can enter in any of the parameters n_0, c, and $\mathbf{v}$. We now focus on the case where $\mathbf{v} = 0$, and n_0 is constant throughout space and time, so that the system is homogeneous. This choice of parameters leads to the specific class of $k = 0$ spatially flat FRW spacetimes [16, 64]. Such geometries are always conformally flat and at any particular time the spatial geometry

is simply that of flat Euclidean space. *All* the time dependence is contained entirely in the speed of sound given by Eq. (6.18). In a homogeneous condensate the sound speed and the scale factor are position independent, and within the acoustic / eikonal limit a separation of the field operators into time and position dependent parts is possible.

We introduce the dimensionless scale function $b(t)$ so that the interaction strength (or equivalently the scattering length) becomes time-dependent,

$$U(t) = U_0\, b(t)\,, \tag{6.49}$$

and under consideration of Eq. (6.7) we get

$$\widetilde{U} = U_0\, \widetilde{b}(t)\,, \tag{6.50}$$

and a time-dependent differential scaling operator $\widetilde{b}(t)$;

$$\widetilde{b}(t) = b(t) - \frac{\hbar^2}{2m\,U_0}\,\widetilde{D}_2\,. \tag{6.51}$$

It is important to realize that a change in the interaction strength, $U \to U(t)$, inevitably involves a shift in the border between the phononic and trans-phononic regime, and hence the nature of collective excitations in the condensate. To see this relationship more clearly we write down the eikonal approximation of Eq. (6.51),

$$U_k(t) = U_0\; b_k(t) = U_0\;\left(b(t) + (k/K)^2\right)\,, \tag{6.52}$$

where for further convenience it is useful to introduce K,

$$K = \frac{c_0}{\epsilon_{\mathrm{qp}}}\,. \tag{6.53}$$

We would like to stress the importance of the last two equations for the understanding of everything that follows below. Motivated by the ultraviolet deviations in our results obtained by the numerical simulation of time-dependent spacetimes in a realistic Bose–Einstein condensate [113], we set out to find a spacetime description that includes trans-phononic modes into the spacetime picture. This forced us to generalize acoustic metrics to momentum-dependent (rainbow) metrics, that cover a larger k-range. These rainbow metrics, see Eq. (6.22), show a time- and momentum-dependent scaling in the effective scale function for the interaction strength. To show this we take $b(t_0) = 1$ at some arbitrary initial time t_0. From the convergence constraint (6.11) for a uniform condensate at rest at $t = 0$, and working in the eikonal approximation,

$$|k| < |K|\,. \tag{6.54}$$

This implies that for modes $k > K$ the spacetime picture begins to break down. This strongly suggests that one should consider $1/K$ as the analogue Planck length, $\ell_{\mathrm{Planck}} = 1/K$. For modes with

wavelength $k \ll K$ we recover the "standard" geometry (*i.e.*, momentum-independent spacetimes). These modes are phononic modes. Making use of our rainbow geometries we extended the emergent spacetime picture for higher energetic (ultraviolet) modes with wavelengths $0 < k < K$. For rainbow metrics the equation of motion for modes with wavelengths $k > K$ are most easily derived in momentum space. This can immediately be seen when one Fourier transforms the initial quantum fluctuations $\delta\hat{\psi}$ and $\delta\hat{\psi}^\dagger$, since then it is not necessary to introduce g_{ab} at all. The situation is more complicated if we involve time-dependent atomic interactions. At any later time $t > 0$ we get a different convergence constraint,

$$|k| < \left|\sqrt{b(t)}\, K\right| , \tag{6.55}$$

and with it a time-dependent limit on the breakdown of the validity of the emergent geometry,

$$\ell_{\mathsf{Planck}}(t) = 1/(K\sqrt{b(t)})\,. \tag{6.56}$$

In other words, the analogue Planck volume $\ell_{\mathsf{Planck}}(t)^d$ is — depending on the form of $b(t)$ — shrinking or expanding. We will return to this point when we explain particle production in a de Sitter-like universe, with a growing Planck volume. Note that for a time dependent condensate density the problem is different, and has been studied in [71, 72, 75, 171].

It should be noted that in the acoustic approximation the scale factor,

$$U(t) = U_0\; b(t) \tag{6.57}$$

is indeed momentum-independent as expected. In practice a variation in the interaction strength is possible by using a Feshbach resonance [190, 95, 15, 16].

From Eq. (6.24) we obtain the time-dependent speed of sound in the eikonal approximation,

$$c_k(t) = c_0\, \sqrt{b(t) + k^2/K^2}\,, \tag{6.58}$$

and thus

$$\omega_k(t) = \omega_0\, \sqrt{b(t) + k^2/K^2} = \omega_0\, \sqrt{b_k(t)}\,. \tag{6.59}$$

Their acoustic counterparts are obtained in the limit $b_k(t) \to b(t)$.

The equation of motion (6.9), which depends on f^{ab}, therefore shows no explicit dependence on the spatial dimensions d of the condensate. In contrast, the emergent spacetime is given by g_{ab}, see Eq. (6.19) and Eq. (6.23), where both depend explicitly on d. In order to use a Bose–Einstein condensate (in the infrared limit) as an analogue model for Einstein's theory of gravity, we have to compare the Friedmann–Roberton–Walker universe line element given in Eq. (6.1), with the line element $g_{ab}\, dx^a\, dx^b$;

$$ds^2 = \left(\frac{n_0}{c_0}\right)^{\frac{2}{d-1}} \left[-c_0^2\, b_k(t)^\alpha\, dt^2 + b_k(t)^{\alpha-1}\, d\mathbf{x}^2\right] . \tag{6.60}$$

Here the exponent α is dimension-dependent and given as

$$\alpha = \frac{d-2}{d-1}\,. \tag{6.61}$$

This explains why the choice of $b(t)$ — to mimic a specific FRW-type universe scale factor $a(t)$ — depends on the spatial dimensions d.

6.3 | Quantum field theory in rainbow geometries: Parametric excitations

Before we address problems of interest to the programme of cosmological particle production in a specific FRW-type universe, we prepare the necessary mathematical and physical formalism. Quantum field theory in rainbow geometries requires a careful treatment of the equation of motion and the commutation relations for the quantum field operators. There are three major differences between ordinary massless spin-0 particles in real curved spacetimes and BEC quasi-particles in the particle production process. These are: (1) The numerical finiteness of the particle production in all circumstances due to the non-perturbative ultraviolet corrections, as we will show below. (2) In addition, we are taking the point of view that any Bose–Einstein condensate experiment will have a finite time duration, and therefore well-defined initial and final vacuum states. (3) Finally, there exists a preferred frame, the laboratory frame in which the experiment (or at this stage gedanken-experiment) is implemented. The laboratory time therefore has to play an important role, and can be viewed as the most relevant coordinate choice.

Conditions (1) and (2) allow us to employ the method of instantaneous Hamiltonian diagonalization to adequately calculate the particle production process. The condition (3), that our particle detector is bound to the laboratory-frame simplifies the decision as to which time coordinate to choose. However, this limitation is also very disappointing. A major awareness resulting from "conventional" curved-spacetime quantum field theory has been the observer dependence of the particle spectrum [172]: Different coordinatizations motivate different vacuum choices. One might stretch the good nature of any condensed matter experimentalist, asking for a co-moving particle detector — adjusted to a suitable vacuum in the chosen coordinate system — in an infinitely long-lasting expanding emergent spacetime. Any unambiguous measurement requires one to stop the expansion, and to project onto a positive and negative plane wave basis.

6.3.1 | Particle production

Linearized quantum excitations in condensate

The equation of motion for quantum fluctuations in such a d-dimensional condensate are given by

$$\partial_t \left(\frac{\hbar}{\widetilde{U}(t)} \, \partial_t \hat{\theta}(t, \mathbf{x}) \right) - \frac{n_0 \hbar}{m} \nabla^2 \hat{\theta}(t, \mathbf{x}) = 0 \, ; \tag{6.62}$$

compare with Eq. (6.22). In the following we are going to rewrite the equation of motion in a more suitable form, applying an auxiliary field, and simultaneously transform to momentum space.

Auxiliary field operators in Fourier space

We use the differential operator $\widetilde{R} = \widetilde{U}(t)/\hbar$ to write the field operators in terms of auxiliary field operators $\hat{\chi}$, where $\hat{\theta} = (\widetilde{R})^{1/2} \, \hat{\chi}$. As long as $\widetilde{U} = \widetilde{U}(t)$, and with it $\hat{\theta} = \hat{\theta}(t)$ and $\hat{\chi} = \hat{\chi}(t)$, is position independent, we can always write

$$\begin{aligned} \hat{\theta}(t, \mathbf{x}) &= \int \frac{d^d k}{(2\pi)^{d/2}} \sqrt{\frac{\widetilde{U}(t)}{\hbar}} \, \hat{\chi}_k(t) \, \mathrm{e}^{i \, \mathbf{kx}} \, , \\ &= \frac{1}{\sqrt{\hbar}} \int \frac{d^d k}{(2\pi)^{d/2}} \hat{\chi}_k(t) \sum_{s=0}^{\infty} \frac{(-1)^s (2s)!}{(1-2s)(s!)^2 4^s} \, (\widetilde{D}_2)^s \mathrm{e}^{i \, \mathbf{kx}} \, , \\ &= \sqrt{\frac{U_k(t)}{\hbar}} \int \frac{d^d k}{(2\pi)^{d/2}} \hat{\chi}_k(t) \, \mathrm{e}^{i \, \mathbf{kx}} \, . \end{aligned} \tag{6.63}$$

The last statement is naively based on a Taylor series which only converges for modes with wavenumbers $|k| < |K|$. Within this radius of convergence the transformation is exact, but can be extended to arbitrary k-values in the eikonal approximation, where $\widetilde{U}(t) \to U_k(t)$. The equation of motion for the mode operators $\hat{\chi}_k$,

$$\sqrt{\frac{\hbar}{U_k(t)}} \, \left(\ddot{\hat{\chi}}_k(t) + \Omega_k(t)^2 \, \hat{\chi}_k(t) \right) = 0 \, , \tag{6.64}$$

and the equal time commutation relations,

$$[\hat{\chi}_k(t), \hat{\chi}_{k'}(t)] = 0 \, , \tag{6.65}$$

$$[\partial_t \hat{\chi}_k(t), \partial_t \hat{\chi}_{k'}(t)] = 0 \, , \tag{6.66}$$

$$[\hat{\chi}_k(t), \partial_t \hat{\chi}_{k'}(t)] = i \delta_{k,k'} \, ; \tag{6.67}$$

are now slightly more convenient than (6.44)-(6.46). The function $\Omega_k(t)$ is defined as

$$\Omega_k(t)^2 = c_0^2 k^2 \, b_k(t) - \frac{3}{4} \left(\frac{\dot{b}_k(t)}{b(t)} \right)^2 + \frac{1}{2} \frac{\ddot{b}_k(t)}{b_k(t)} \, , \tag{6.68}$$

and therefore we have the connection between quantum field theory in FRW-type spacetimes and a parametrically excited harmonic oscillator. The notation $\Omega_k(t)$ will become quite obvious for time-independent cases, where it reduces to the usual dispersion relation $\Omega_k \to \omega_k$; see Eq. (6.59). Notice the overall factor, $\sqrt{\hbar/U_k(t)}$, in Eq. (6.64). This is of importance for the particle production process in cases of discontinuous, and continuous (but not differentiable) changes in $U(t)$. We will revisit this issue shortly in Section 6.3.1.

Mode expansion

The equation of motion (6.64) is a homogeneous differential equation, which can be written as

$$\widetilde{L}\,\hat{\chi}_k = 0\,, \tag{6.69}$$

where

$$\widetilde{L} = \partial_t^2 + \Omega_k(t)^2 \tag{6.70}$$

is a linear second order differential operator with a 2-dimensional solution space.

A common tool in quantum mechanics is to describe quantum states — with unknown or variable number of quasi-particles — with respect to an orthonormal occupancy number basis (*i.e.*, the Fock space basis in the infinite-dimensional function space, the Hilbert space of state). A Fock state is a quantum state consisting of an ensemble of excited non-interacting particles,

$$|n_{\mathbf{k}1}, n_{\mathbf{k}2}, ...\rangle = \frac{1}{\sqrt{n_{\mathbf{k}1}!\; n_{\mathbf{k}2}!\; ...}} \left[(\hat{a}^\dagger_{\mathbf{k}1})^{n_{\mathbf{k}1}} (\hat{a}^\dagger_{\mathbf{k}2})^{n_{\mathbf{k}2}} ...\right] |0\rangle\,, \tag{6.71}$$

with definite occupation numbers $(n_{\mathbf{k}1}, n_{\mathbf{k}2}, ...)$ in the modes $(\hat{\chi}_{\mathbf{k}1}, \hat{\chi}_{\mathbf{k}2}, ...)$. The creation, $\hat{a}^\dagger_k$, and annihilation, $\hat{a}_k$ operators create or destroy a single-particle in the mode $\chi_{\mathbf{k}}$;

$$\hat{a}^\dagger_{\mathbf{k}i}|..., n_{\mathbf{k}i} - 1, ...\rangle = \sqrt{n_{\mathbf{k}i}}\,|..., n_{\mathbf{k}i}, ...\rangle\,, \tag{6.72}$$

$$\hat{a}_{\mathbf{k}i}|..., n_{\mathbf{k}i}, ...\rangle = \sqrt{n_{\mathbf{k}i}}\,|..., n_{\mathbf{k}i} - 1, ...\rangle\,. \tag{6.73}$$

The state $|0\rangle$ — short for $|0_{\mathbf{k}1}, 0_{\mathbf{k}2}, ...\rangle$ — is a special state, the vacuum state. It is defined as the eigenstate of all annihilation operators $\hat{a}_k$ with eigenvalue 0, such that $\hat{a}_k|0\rangle = 0$. Thus any arbitrary quantum state $|\varphi\rangle$ in the Fock spaces is a linear combination of all excited states,

$$|\varphi\rangle = \sum_{n_{\mathbf{k}1}, n_{\mathbf{k}2}, ...} P_{n_{\mathbf{k}1}, n_{\mathbf{k}2}, ...}\,|n_{\mathbf{k}1}, n_{\mathbf{k}2}, ...\rangle\,, \tag{6.74}$$

that can be created out of the vacuum. Here $P_{n_{\mathbf{k}1}, n_{\mathbf{k}2}, ...}$ is the probability to measure the single Fock state with the mode occupation $(n_{\mathbf{k}1}, n_{\mathbf{k}2}, ...)$.

Within this framework we expand the mode operators in terms of destruction and creation operators,

$$\hat{\chi}_k(t) = \frac{1}{\sqrt{2}}\left[v^*_k(t)\,\hat{a}_k + v_k(t)\,\hat{a}^\dagger_{-k}\right]. \tag{6.75}$$

The coefficients v_k and v_k^* are a set of linearly-independent mode functions and any linear combination is a complete solution of

$$\widetilde{L} v_k(t) = 0\,. \tag{6.76}$$

(Due to the isotropy of the *s*-wave scattering amplitude of the atomic interactions, the mode functions are also isotropic, *i.e.*, $v_{\mathbf{k}} = v_k$ and $v_{\mathbf{k}}^* = v_k^*$. It therefore seems unlikely that we would need to extend the specific analogue set-up to mimic anisotropic expansion scenarios. The case is different for analogue models involving a changing condensate density, $n_0 = n_0(t)$; where a non-uniform density expansion can easily be achieved, for example see [71, 72, 75, 171].)

In order to obtain a "nice" canonical set of operators, which obey the common equal time commutation relations (see Eq. (6.44)-(6.45)),

$$\left[\hat{a}_k, \hat{a}_{k'}\right] = 0\,, \tag{6.77}$$

$$\left[\hat{a}_k^\dagger, \hat{a}_{k'}^\dagger\right] = 0\,, \tag{6.78}$$

$$\left[\hat{a}_k, \hat{a}_{k'}^\dagger\right] = \delta_{k,-k'}\,, \tag{6.79}$$

the Wronskian W of the mode functions has to be normalized as follows,

$$W[v_k, v_k^*] = \dot{v}_k\, v_k^* - v_k\, \dot{v}_k^* = 2i\,. \tag{6.80}$$

It is easy to see that — under the application of the equation of motion for the mode functions — the Wronskian is always time-independent. Note, a spin-zero scalar particle is its own anti-particle, where $(\hat{a}_k)^\dagger = \hat{a}_{-k}^\dagger$. We would also like to draw attention to the fact that with a particular choice of Fock space, we select a particular subspace of the Hilbert space of states (*i.e.*, the subspace that can be created out of the vacuum state, determined by our choice of $\hat{a}_k$). This will be of further interest when we discuss the validity and limitations of the Bogoliubov transformation.

Bogoliubov transformation

In Eq. (6.75) we can in principle pick some particular mode expansion, $(\vec{v}_k)^\dagger \cdot \vec{A}_k$, with a specific set of mode functions $\vec{v}_k^{\,T} = (v_k(t), v_k^*(t))$, and set of mode operators $\vec{A}_k^{\,T} = (\hat{a}_k, \hat{a}_{-k}^\dagger)$. This choice is not unique and any other mode expansion $(\vec{u}_k)^\dagger \cdot \vec{B}_k$, with mode functions $\vec{u}_k^{\,T} = (u_k(t), u_k^*(t))$, and mode operators $\vec{B}_k^{\,T} = (\hat{b}_k, \hat{b}_{-k}^\dagger)$ would have been possible. The relation between these two different representations is referred to as Bogoliubov transformation.

As mentioned above, the mode expansion $(\vec{v}_k)^\dagger \cdot \vec{A}$ corresponds to an orthonormal basis in the infinite-dimensional function space, provided the $\vec{v}_k$ are normalized; that is $W[v_k(t), v_k^*(t)] = 2i$ for all times t. If we restrict ourselves to exclusively mapping between orthonormal frames — then the mode functions fulfill the normalization constraint $W[u_k(t), u_k^*(t)] = 2i$, and the mode operators obey the commutation relations given in Eqs. (6.77-6.79) — the Bogoliubov transformation is given by

$\vec{v}_k = M \cdot \vec{u}_k$, where M must be a 2×2 matrix,

$$M = \begin{pmatrix} \alpha_k^* & \beta_k^* \\ \beta_k & \alpha_k \end{pmatrix} . \tag{6.81}$$

The complex-valued coefficients α_k and β_k are called Bogoliubov coefficients, and the transformation preserves the normalization condition if $\det(M) = 1$, that is for

$$|\alpha_k|^2 - |\beta_k|^2 = 1 . \tag{6.82}$$

At this stage we notice a minor technical subtlety when we look at summing over discreet k modes versus integrating over continuous k modes. Equation (6.82) is appropriate for summing over discreet modes whereas for continuous modes we should strictly speaking use $|\alpha_k|^2 - |\beta_k|^2 = \delta^{(d)}(\vec{0}) = V/(2\pi)^d$. Here $\delta^{(d)}(\vec{0})$ is the d-dimensional momentum space Dirac function. We will work with continuous integrals in momentum space but will suppress unnecessary occurrence of the volume V, where including it would lead to unnecessary clutter that might not aid understanding.

The relationship between the "old" and "new" mode operators, where $(\vec{v}_k)^\dagger \cdot \vec{A} = (\vec{u}_k)^\dagger \cdot \vec{B}$ and $(\vec{v}_k)^\dagger = (\vec{u}_k)^\dagger \cdot M^\dagger$, is given as $\vec{A}_k = (M^\dagger)^{-1} \cdot \vec{B}_k$ and $\vec{B}_k = (M^\dagger) \cdot \vec{A}_k$. Here

$$M^\dagger = \begin{pmatrix} \alpha_k & \beta_k^* \\ \beta_k & \alpha_k^* \end{pmatrix} \text{ and } (M^\dagger)^{-1} = \begin{pmatrix} \alpha_k^* & -\beta_k^* \\ -\beta_k & \alpha_k \end{pmatrix} , \tag{6.83}$$

and therefore

$$\hat{a}_k = \alpha_k^* \hat{b}_k - \beta_k^* \hat{b}_{-k}^\dagger, \text{ and } \hat{a}_{-k}^\dagger = \alpha_k \hat{b}_{-k}^\dagger - \beta_k \hat{b}_k^\dagger ; \tag{6.84}$$

$$\hat{b}_k = \alpha_k \hat{a}_k + \beta_k^* \hat{a}_{-k}^\dagger, \text{ and } \hat{b}_{-k}^\dagger = \alpha_k^* \hat{a}_{-k}^\dagger - \beta_k \hat{a}_k^\dagger . \tag{6.85}$$

Obviously, the two vacuum states, $\hat{a}_k \,|_{(a)}0\rangle = 0$ and $\hat{b}_k \,|_{(b)}0\rangle = 0$, are different, as $\hat{b}_k \,|_{(a)}0\rangle \neq 0$ for $\beta_k \neq 0$.

Particles and lowest energy eigenstate

Quasi-particles are excited states, and therefore they depend on the choice of (mode functions and the associated) vacuum state. Under the application of Eq. (6.85) we can *formally* calculate the mean density of b-particles, $\hat{n}^{(b)}$, the occupation number for the mode $\hat{\chi}_k$, with respect to the a-vacuum $|_{(a)}0\rangle$ as follows:

$$n_k^{(b)} = \frac{\langle_{(a)}0| \, \hat{b}_k^\dagger \hat{b}_k \,|_{(a)}0\rangle}{\text{Volume}} = |\beta_k|^2 . \tag{6.86}$$

The challenge is to find particular specified mode functions that represent physically meaningful vacuum states, that minimize the expectation value of the Hamiltonian. Only then does the chosen vacuum correspond to the "actual" physical vacuum, and its excitations describe "real" quasi-particles.

(That is, we are looking for an unambiguous measure of particles relative to some vacuum state.) The problem of finding the "right" vacuum state ("best" orthonormal frame) has been controversial from the outset. However, as we shall see, it is straightforward to find the zero-particle vacuum state for Minkowski spacetimes, and the whole controversy arises only for time-dependent cases, where the Hamiltonian $\hat{H}(t) = \int_{\mathbf{k}} \hat{\mathcal{H}}_k(t)$ is explicitly time-dependent;

$$\begin{aligned} \hat{\mathcal{H}}_k(t) &= \frac{\{[\partial_t(\sqrt{U_k(t)}\hat{\chi}_k(t))][\partial_t(\sqrt{U_k(t)}\hat{\chi}_{-k}(t))]\}}{2\,U_k(t)} \\ &\quad + \frac{1}{2}\,\omega_k(t)^2\,\chi_k(t)\,\chi_{-k}(t)\,. \end{aligned} \tag{6.87}$$

In combination with the mode expansion (6.75) the Hamiltonian in momentum space is given by

$$\begin{aligned} \hat{H}(t) &= \frac{1}{4}\int d^d\mathbf{k}\,F_k(t)\,\hat{a}_k^\dagger\hat{a}_{-k} + F_k^*(t)\,\hat{a}_k\hat{a}_{-k} \\ &\quad + E_k(t)\,(2\hat{a}_k^\dagger\hat{a}_k + \delta^{(d)}(0))\,, \end{aligned} \tag{6.88}$$

where the factor $E_k(t)$ for the diagonal terms is,

$$\begin{aligned} E_k(t) &= |\dot{v}_k(t)|^2 + \{\omega_k^2(t) + 1/4\,[\dot{U}_k(t)/U_k(t)]^2\}\,|v_k|^2 \\ &+ 1/2\,\dot{U}_k(t)/U_k(t)\,\partial_t|v_k(t)|^2\,, \end{aligned} \tag{6.89}$$

and the off-diagonal term $F_k(t)$ is given by

$$\begin{aligned} F_k(t) &= (\dot{v}_k(t))^2 + \{\omega_k^2(t) + 1/4\,[\dot{U}_k(t)/U_k(t)]^2\}\,(v_k)^2 \\ &+ 1/2\,\dot{U}_k(t)/U_k(t)\,\partial_t(v_k(t))^2\,. \end{aligned} \tag{6.90}$$

Therefore there are no time-independent eigenstates that represent the physical vacuum state, one that minimizes the expectation value for the Hamiltonian,

$$\langle_{(t)}0|\,\hat{H}_k(t)\,|_{(t)}0\rangle = \frac{1}{4}\int d^d\mathbf{k}\,E_k(t)\,, \tag{6.91}$$

for all times.

Yet somehow, in order to obtain a meaningful statement about the particle production in our effective curved spacetime, we need to deal with or circumvent this problem.

Instantaneous Hamiltonian diagonalization: One possibility to find an approximate vacuum at an instant of time — say $t = t_0$ — is to define the vacuum state $|_{(t_0)}0\rangle$ of the *instantaneous* Hamiltonian $H(\hat{t_0})$, where we project our mode functions instantaneously onto a plane-wave basis with the dispersion relation $\omega_k(t_0)$. Within this approximation we find for the coefficients in Eq. (6.88):

$$E_k = |\dot{v}_k(t)|^2 + \omega_k^2(t_0)\,|v_k|^2\,; \tag{6.92}$$

$$F_k = (\dot{v}_k(t))^2 + \omega_k^2(t_0)\,(v_k)^2\,. \tag{6.93}$$

It can be shown that the expectation value for the instantaneous Hamiltonian — up to an arbitrary phase — at $t = t_0$ is minimal for mode functions $v_k = 1/\sqrt{\omega_k(t_0)}$ and $\dot{v}_k = i\sqrt{\omega} = i\,\omega_k\,v_k(t_0)$.

Note that at t_0 the two coefficients $F_k(t_0) = 0$ and $E_k(t_0) = 2\omega_k(t_0)$, and that under this condition the instantaneous Hamiltonian (see Eq. (6.88)) is diagonal. Therefore it is referred to as the *vacuum state of instantaneous Hamiltonian diagonalization*.

In a time-dependent problem the vacuum state changes, and therefore one has to give up on this particular definition of vacuum for times $t > t_0$. The association between the $|\beta_k|^2$ Bogoliubov coefficients (as outlined above) and physical quasi-particles requires that we approach — either asymptotically or abruptly — flat initial and final state spacetimes. Only a time-independent spacetime perpetuates its vacuum state, where $\omega_k(t) = \omega_k$, and thus the normalized mode functions

$$v_k(t) = \frac{1}{\sqrt{\omega_k(t)}}\,\exp(i\,\omega_k\,t)\,, \tag{6.94}$$

$$v_k^*(t) = \frac{1}{\sqrt{\omega_k(t)}}\,\exp(-i\,\omega_k\,t)\,, \tag{6.95}$$

in this case represent a physically meaningful vacuum state for all times t.

Bogoliubov transformation in emergent spacetimes

The Bogoliubov transformation outlined in Section 6.3.1 can be applied to time-dependent problems, as long as we do not fool ourself and make any statement about the presence of "real" qusi-particles unless the expansion has started from an initial time-independent spacetime, and eventually approaches a time-independent spacetime. We also require $\omega_k^2 > 0$, such that at the beginning and the end the mode functions are simple (normalized) in- and out-going plane waves. For a constant, but imaginary frequency, $\omega_k^2 < 0$, the instantaneous Hamiltonian is still diagonal, but its expectation value no longer has a minimum, see Chapter 5.

To apply the Bogoliubov transformation (see, Section 6.3.1, and see Eqs. (6.84-6.85)) to our specific problem it is necessary to consider that the original problem was defined in terms of two linearly independent field variables, the field operator $\hat{\theta}$, and its conjugate momentum $\hat{\Pi}_{\hat{\theta}}$. The connection conditions arise from the necessity that the field operator,

$$\left[\hat{\theta}\right] = \lim_{\epsilon\to 0}\left\{\hat{\theta}(t-\epsilon) - \hat{\theta}(t+\epsilon)\right\} = 0\,, \tag{6.96}$$

and its conjugate momentum (on the emergent spacetime),

$$\left[\hat{\Pi}_{\hat{\theta}}\right] = \lim_{\epsilon\to 0}\left\{\hat{\Pi}_{\hat{\theta}}(t-\epsilon) - \hat{\Pi}_{\hat{\theta}}(t+\epsilon)\right\} = 0\,, \tag{6.97}$$

have to be continuous at all times. (A more detailed treatment of this problem in the context of emergent spacetimes from Bose gases can be found in [203].) Note, that these two conditions have to be fulfilled for any arbitrary (albeit physically reasonable) change in the contact potential $U(t)$. In

Section 6.3.1 we have already pointed out that our emergent spacetime is special in the sense that all time-dependence (in our model) has to be implemented via $U(t)$, which also shows up in the overall conformal factor in the equation of motion, see Eq. (6.64).

Bogoliubov coefficients for a time-dependent emergent spacetime: Let us consider a contact potential defined as follows,

$$U_k(t) = g_k(t)\,\Theta_{\rm HS}(t-t_0) + h_k(t)\,\Theta_{\rm HS}(t_0-t)\,. \tag{6.98}$$

We are dealing with different sets of mode functions in each region; $v_k^T = (v_k, v_k^*)$ for $t < t_0$, and $u_k^T = (u_k, u_k^*)$ for $t > t_0$. (Here $\Theta_{\rm HS}$ is the symbol for the Heaviside step function.) For the time being we do not make any further assumption except that the mode functions have to be a solution of the equation of motion (6.64) in their respective region. In particular, we do *not yet* assume the modes are normalized. The connection conditions, given in Eqs. (6.96) and (6.97), in combination with the Bogoliubov transformation — see transformation matrix (6.81), mapping between two pairs of complex-conjugate mode functions (it is always possible to choose such solutions) — provide us with two matrix equations (that is, four component equations),

$$\sqrt{\frac{g_k}{\hbar}}\,\vec{v}_k \;=\; M\sqrt{\frac{h_k}{\hbar}}\,\vec{u}_k\,, \tag{6.99}$$

$$\frac{\hbar}{g_k}\,\partial_t\left(\sqrt{\frac{g_k}{\hbar}}\,\vec{v}_k\right) \;=\; \frac{\hbar}{h_k}\,M\,\partial_t\left(\sqrt{\frac{h_k}{\hbar}}\,\vec{u}_k\right)\,, \tag{6.100}$$

for the four unknown transmission coefficients α_k, α_k^*, β_k, and β_k^*. Fortunately, due to our specific choice of complex mode functions, we only need to calculate α_k and β_k, and get the others by calculating their complex conjugate. We obtain

$$\alpha_k(t) = \frac{2\,(g\,\dot{u}_k v_k^* - h\,u_k\dot{v}_k^*) + v_k^* u_k\left(g\,\frac{\dot{h}}{h} - \frac{\dot{g}}{g}\,h\right)}{2\sqrt{g\,h}\;W[u_k, u_k^*]}\,, \tag{6.101}$$

and

$$\beta_k(t) = \frac{2\,(h\,\dot{v}_k^* u_k^* - g\,v_k^*\dot{u}_k^*) - v_k^* u_k^*\left(g\,\frac{\dot{h}}{h} - \frac{\dot{g}}{g}\,h\right)}{2\sqrt{g\,h}\;W[u_k, u_k^*]}\,. \tag{6.102}$$

A somewhat time-consuming, but trivial calculation shows that further conditions are necessary to obtain a Bogoliubov transformation in the desired normalized form (6.82), since in general (6.101) and (6.102) lead to

$$|\alpha_k(t)|^2 - |\beta_k(t)|^2 = \frac{W[v_k, v_k^*]}{W[u_k, u_k^*]} \neq 1\,. \tag{6.103}$$

Hence it is necessary to choose a consistent normalization condition, $W[v_k, v_k^*] = W[u_k, u_k^*] = \text{constant}$, so that $|\alpha_k(t)|^2 - |\beta_k(t)|^2 = 1$. Also note that for multiple-step events, meaning multiple

Bogoliubov transformations described by the compound matrix $M_n \cdot M_{n-1} \cdots M_2 \cdot M_1$, the physics is independent of the particular choice for the normalization of the intermediate mode functions, since

$$\det(M_n \cdots M_1) = \det(M_n) \cdots \det(M_1) = \frac{W[v_k^1, (v_k^1)^*]}{W[(v_k^n, v_k^n)^*]} \,. \tag{6.104}$$

Our main focus in this chapter is to calculate the particle production in a FRW-rainbow metric, and therefore we wish to restrict our problems to cases where we start and end in a physically meaningful vacuum state. This way we are able to connect $|\beta_k|^2$ with the occupation number for real condensate excitations in an effectively expanding spacetime. In our companion paper, see [113], we investigated various expansion scenarios. We will now concentrate on the most relevant expansion scenario in terms of cosmology, *i.e.*, de Sitter like inflation.

There are three principal different cases, in terms of $U(t)$, that are of interest when addressing the problem of inflation in emergent spacetimes:

Section 6.3.2: *U(t) discontinuously, connects two flat spacetime regions:* This case is indirectly interesting for inflation, since the de Sitter expansion approaches the sudden case for infinitely fast expansion [182]. But, we will show shortly that in emergent spacetimes — due to the nonperturbative ultraviolet corrections — the particle production for the extreme limit is finite, thus the Bogoliubov transformation for the de Sitter case is always well-defined.

Section 6.4.3: *U(t) continuously, but not continuously differentiably connects two flat spacetime regions with a finite de Sitter like phase in between:* This calculation can be carried out in the hydrodynamic limit, but fails to be a good approximation for infinitely long-lasting inflation in emergent spacetimes. Due to an unsolvable second order differential equation in the eikonal limit, we present a qualitative analysis, that should be compared with the numerics presented in our companion paper [113].

Section 6.4.3: *U(t) is a smooth function everywhere, such that we are left with one de Sitter like region:* The qualitative analysis shows that in our particular emergent spacetime the de Sitter expansion has, in the infinite past and in the infinite future, two distinct physical vacua, and therefore we are able to predict the existence of time-independent real (unambiguous) quasi-particles created during an infinitely long-lasting expansion. This might at first seem of less interest for the condensed matter community, but as our simulations show, this can be realized for a sufficiently long expansion time. We will see that for the right parameter choice the particle spectrum approaches a characteristic final shape, for which we can numerically determine the form of the final particle spectrum.

6.3.2 | Finiteness of particle production in emergent spacetimes

There is a relatively simple way to calculate an upper bound on the particle production in a universe that is subjected to a (finite-size) expansion, in terms of a sudden variation in the size of the

universe [182].

The case of a particle production for a sudden transition has been previously explored by Jacobson for a parametric oscillator [107]. (Though the underlying physics is rather different, there is also a model for *sonoluminescence* that is based on a rapid change in refractive index — that model shares many of the mathematical features encountered in the present calculation [125, 124, 128, 127, 27, 126, 131].) A more closely related work on sudden changes — between Lorentzian / Euclidean signatures — in emergent spacetime has recently been carried out in [203].

To calculate the particle production in the limiting case of a sudden expansion, we consider the situation where the atom-atom interaction is "instantaneously" switched from U to U/X at some time t_0. The scale function (see Eq. (6.57)) is given by

$$b(t) = 1 - \left(1 - \frac{1}{X}\right) \Theta_{\mathrm{HS}}(t - t_0)\,. \tag{6.105}$$

This corresponds to a change between two regions with distinct dispersion relations, connected at t_0. We choose as mode functions for $t < t_0$,

$$v_k(t) = \frac{\mathrm{e}^{+i\omega_k^{\mathsf{in}} t}}{\sqrt{\omega_k^{\mathsf{in}}}} \;\text{ and }\; v_k^*(t) = \frac{\mathrm{e}^{-i\omega_k^{\mathsf{in}} t}}{\sqrt{\omega_k^{\mathsf{in}}}}\,, \tag{6.106}$$

and for $t > t_0$,

$$u_k(t) = \frac{\mathrm{e}^{+i\omega_k^{\mathsf{out}} t}}{\sqrt{\omega_k^{\mathsf{out}}}} \;\text{ and }\; u_k^*(t) = \frac{\mathrm{e}^{-i\omega_k^{\mathsf{out}} t}}{\sqrt{\omega_k^{\mathsf{out}}}}\,; \tag{6.107}$$

these are normalized (see Eq. (6.80)) positive and negative frequency modes. As explained in Section 6.3.1, these mode functions represent physically meaningful vacua in flat spacetime regions.

Straightforwardly, we can apply Eqs. (6.101) and (6.102) to calculate α and β. We get for the Bogoliubov coefficients:

$$\alpha_k(t_0) \;=\; \frac{1}{2}\left[\sqrt{\frac{\omega_k^{\mathsf{out}}}{\omega_k^{\mathsf{in}}}} + \sqrt{\frac{\omega_k^{\mathsf{in}}}{\omega_k^{\mathsf{out}}}}\right] \mathrm{e}^{i\,(\omega_k^{\mathsf{out}} - \omega_k^{\mathsf{in}})\,t_0}; \tag{6.108}$$

$$\beta_k(t_0) \;=\; \frac{1}{2}\left[\sqrt{\frac{\omega_k^{\mathsf{out}}}{\omega_k^{\mathsf{in}}}} - \sqrt{\frac{\omega_k^{\mathsf{in}}}{\omega_k^{\mathsf{out}}}}\right] \mathrm{e}^{-i\,(\omega_k^{\mathsf{out}} + \omega_k^{\mathsf{in}})\,t_0}. \tag{6.109}$$

Using the transformation laws between the in and out Fock state operators, see Eq. (6.85), and Eq. (6.86), we obtain the occupation number density of out-particles in the in-vacuum,

$$n_k^{\mathsf{out}} = \frac{1}{4}\left|\frac{(\omega_k^{\mathsf{out}} - \omega_k^{\mathsf{in}})^2}{\omega_k^{\mathsf{out}}\omega_k^{\mathsf{in}}}\right|\,, \tag{6.110}$$

where we assumed that the eigenfrequencies are real. Note that this relation is valid beyond the eikonal limit, such that we are dealing with a nonlinear dispersion, see Eq. (6.58), in both regions;

$$\omega_k^{\mathsf{in}} \;=\; \omega_0^{\mathsf{in}}\sqrt{1 + k^2/K^2}\,, \tag{6.111}$$

$$\omega_k^{\mathsf{out}} \;=\; \omega_0^{\mathsf{in}}\sqrt{1/X + k^2/K^2}\,. \tag{6.112}$$

Thus we get

$$n_k^{\text{out}} = \frac{\left(\sqrt{X}\sqrt{K^2+k^2} - \sqrt{K^2+X\,k^2}\right)^2}{4\,\sqrt{X}\sqrt{K^2+k^2}\,\sqrt{K^2+X\,k^2}}\,. \tag{6.113}$$

It is perhaps surprising how simple the final result is, despite the additional technical machinery required to derive it. Of course, particle production is momentum-independent only within the hydrodynamic limit, when

$$\omega_k^{\text{in/out}} \to \omega_0^{\text{in/out}}\,. \tag{6.114}$$

The number density in the infrared limit, when $k < K$, can be simplified to

$$n_{\text{hydro}} = \frac{1}{4}\,\left|X^{1/4} - X^{-1/4}\right|^2\,, \tag{6.115}$$

and — up to an overall (thus undetectable) minus sign — is in agreement with the results obtained in "ordinary" momentum independent spacetimes with sudden jumps in the dispersion relation, instead of the scale factor; for example see [107]. Bogoliubov transformations with infinite total particle production per unit volume are ill-defined, as the out-vacuum state $|_{\text{out}}0\rangle$, can only be written in terms of a *normalizable* linear-combination of in-particle states, if $|\beta_k|^2 \to 0$ faster k^{-d} for large k. To see an explicit derivation consult, for example, Ref. [141]. We shall now show how due to non-perturbative corrections in our FRW-rainbow spacetimes, this problem does not appear. Here the total number of quasi-particles produced in the ultraviolet limit remains finite under any circumstances. At large momenta

$$\lim_{k\gg K} n_k = \frac{(X-1)^2}{X^2}\,\left(\frac{K}{2\,k}\right)^4 + O(1/k^6)\,, \tag{6.116}$$

and separately we see that for an infinitely large expansion

$$\lim_{X\to\infty} n_k = \frac{1}{4}\,\frac{(\sqrt{K^2+k^2}-k)^2}{k\,\sqrt{K^2+k^2}}\,. \tag{6.117}$$

We can also combine these two limits, and obtain $n_k \to [K/(2\,k)]^4$. The quantum pressure term supresses particle production at high momentum — effectively because at high momenta the quasi particle are free and do not "see" the evolving spacetime. (The high-momentum limit of the rainbow metric is "static".)

As a consequence the number particle production per spacetime volume,

$$N_{\leqslant k} \sim 2^{d-1}\pi \int d\mathbf{k}\; k^{d-5} \sim k^{d-4}\,, \tag{6.118}$$

for the here relevant cases of 2 or 3 spatial dimensions, is finite.

It is also possible, see Eq. (6.117), to exactly calculate the *total* number of quasi-particles produced during, $c_0 \to c_0/\sqrt{X}$, for $X \to \infty$, an *infinite* expansion:

$$N_\infty = \frac{2^{d-3}\,\pi}{d}\,K^d\,. \tag{6.119}$$

Particle production in our emergent spacetime is a good example as to how corrections — at the level of effective field theories — from the underlying microscopic structure can circumvent the problem of an infinite number density caused by a finite process. On the other hand, it seems naive to assume the validity of common quantum field theory on all scales. If spacetime is indeed the infrared limit of a more fundamental theory, the presence of ultraviolet deviations seems to be unavoidable.

6.4 | FRW-rainbow spacetimes in $(2+1)$ dimensions: Controlled parametric excitations in 2-dimensional condensate

In the following we investigate the robustness of the cosmological particle production process against model-dependent ultraviolet corrections in the dispersion relation. The modifications arise from the microscopic substructure, therefore are of non-perturbative nature and not the result of some perturbative loop-calculations. Related work on Hawking radiation from acoustic black holes has been carried out, where the various authors mainly studied the problem in media with subsonic and supersonic dispersion relations [112, 177]. In addition, similar efforts have been made in the field of "conventional" cosmology, by implementing *ad hoc* trans-Planckian modifications to the system, for example see [137, 139, 24]. This motivated us to extend our main intention — testing the analogy — to a detailed study of the deviations (from standard cosmology) in our specific model. We demonstrate this with a particular physically relevant model, a rapidly exponentially growing effective universe, how "conventional" and "modified" models naturally merge in the infrared limit at early times. Whereas, they show significant deviations at late times, yet for a sufficiently short-time expansion, the resulting particle spectra — in systems with linear and nonlinear dispersion relations — are very similar to each other.

6.4.1 | $(2+1)$ dimensional FRW-rainbow spacetimes: 2 dimensional condensates with time-dependent atomic interactions

In Eq. (6.60) we established the concept of a FRW-type rainbow universe to describe the $(2+1)$ or $(3+1)$ dimensional spacetime as seen by small quantum fluctuations in a 2 or 3 dimensional condensate. As pointed out in the text passage shortly after the line-element, besides the dimensionality, also the scale factor $b(t)$ is different for 2 and 3 dimensions. For example, if we wish to mimic the de Sitter geometry, where the scale factor in the FRW line element, see Eq. (6.1), takes the form

$$a(\tau) = \exp(H\,\tau)\,, \tag{6.120}$$

we have to choose the scale factor for the atomic interactions,

$$b(t) = \begin{cases} \exp(-t/t_s) & \text{for } d=2, \\ t_s/(t+t_s) & \text{for } d=3, \end{cases} \tag{6.121}$$

corresponding to the spatial dimension. A more detailed treatment of this problem — that originates in the discrepancy of laboratory t and proper time τ for the 3-dimensional case — can be found in [16]. In 2 spatial dimensions — where $\alpha(2) = 0$ — the effective line-element is given by

$$\mathrm{d}s^2_{d=2} = \left(\frac{n_0}{c_0}\right)^2 \left[-c_0^2\, dt^2 + b_k(t)^{-1} d\mathbf{x}^2\right] , \tag{6.122}$$

here laboratory time t and proper time τ are of the same form, and we obtain the very simple relationship,

$$a_k(t) = b_k(t)^{-1/2} = \frac{1}{\sqrt{b(t) + (k/K)^2}} , \tag{6.123}$$

between the two scale factors. To connect t_s, the scale unit in the laboratory, to the Hubble parameter H, we need to choose

$$H = \frac{1}{2\, t_s} . \tag{6.124}$$

We will soon revisit the Hubble parameter, when we discuss its physical motivation, and how the Hubble parameter applies to our de Sitter-rainbow spacetime. For practical reasons we shall be mainly interested in $(2+1)$ spacetime dimensions, that is, $d = 2$ space dimensions and 1 time dimension, simply because the numerical simulations we wish to compare the theory with are more easily carried out in 2 space dimensions.

We will always use $a(t)$ to refer to the *FRW scale factor*; if we ever really need the scattering length we will refer to it as $a_{\mathrm{scatt}}(t)$.

In what physical respect do we really have an "expanding universe", given that the condensate is physically contained in a fixed volume V? A decrease in the scattering length corresponds to a decrease in the speed of sound propagating in the condensate; therefore any acoustic excitations will propagate with decreasing speed in the condensate as time passes. To an "internal" observer at rest in the effective spacetime, and communicating by means of acoustic signals, a decrease of the speed of sound is indistinguishable from an isotropic expansion of the spatial dimensions.

6.4.2 | Inflation in emerging universe: Exponentially decreasing atomic interactions

Maybe the most interesting cosmological case to study in our emergent spacetime is the *de Sitter* universe, where the scale factor is given by an exponentially expanding (or contracting) universe. The concept of inflation was introduced simultaneously around 1981 and 1982 by Guth [88], Linde [134], and Albrecht and Steinhardt [2] to explain the homogeneity of the temperature observed in our universe, beyond casually disconnected areas. Not long after (*e.g.*, see Guth, Hawking [92], Bardeen [20], Turner [170] and Brandenburger [35]) it has been realized that inflation also accounts for the existence of the perturbations in our universe today. These perturbations in the form of a slight deviation from a uniform temperature in our cosmological microwave background (CMB) have

been measured in 2001 by Netterfield *et al*. To date, inflation — a phase of a rapid de Sitter-like expansion — seems to be the most plausible explanation for the CMB map. According to all observational evidence the inflationary epoch ends in a radiation-dominant area, where $a(t) \sim t^{1/2}$. This is due to the high temperatures after the so-called reheating process. Eventually (much later) the universe cooled down and turned into the current matter-dominated universe, with $a(t) \sim t^{2/3}$. For more details see [158, 51]. While we expect deviations from the standard picture in our emergent rainbow spacetime, it seems desirable to hold on to the concept of a thermal spectrum resulting from an exponentially expanding universe. We will come back to this point at the end of this section and show that this hope might not be in vain.

Before we focus on the particle spectrum in our de Sitter-rainbow metric, we would like to introduce some physically important parameters. They will be of great value throughout the remaining part of this chapter, and are necessary to understand the particle production process for a $2d$ analogue FRW-type universe. Let us start with the obvious question:

Why rainbow spacetimes?

The modified rainbow spacetimes owe their names to their momentum-dependence. This kind of modification can be absorbed into the time and (now also) momentum-dependent scale factor. For a de Sitter like universe (see Eqn (6.120) and (6.121)) in the hydrodynamic limit, we get

$$a_k(t) = \frac{1}{\sqrt{\exp(-2H\,t) + (k/K)^2}}\,, \tag{6.125}$$

for the modified scale factor Eq. (6.120); in 2 spatial dimensions that is. Thus the hydrodynamic,

$$\exp(-2H\,t) \gg |k/K|^2\,, \tag{6.126}$$

crossover,

$$\exp(-2H\,t) \sim |k/K|^2\,, \tag{6.127}$$

and free particle,

$$\exp(-2H\,t) \ll |k/K|^2\,, \tag{6.128}$$

limits are a matter of dividing the spectrum into appropriate energy regimes *at a particular time* t. It is interesting that for early times — when the interactions between the atoms are strong — we naturally approach the hydrodynamic case,

$$\lim_{t\to-\infty} a_k(t) \to a(t)\,, \tag{6.129}$$

in the sense that more and more modes are phononic, and therefore larger and larger k-values are covered by “conventional” FRW-type quantum-field-theory.

Quite the contrary occurs after an infinitely long-lasting expansion, where all modes behave as free particles,

$$\lim_{t\to+\infty} a_k(t) \to |K/k|\,, \tag{6.130}$$

and the universe, as seen by a mode with the wavelength k, will approach a final finite fixed size.

Due to this fundamental difference between our analogue model and the "theory" we wish to mimic, we know already that there will only be a finite time-period — its length depends on K, and therefore on the tunable initial interaction strength — beyond which the analogy breaks down. Note that the particle production process must naturally come to an end, when the expansion rate slows down to zero. That the effective expansion rate of the FRW-rainbow universe approaches zero will be shown next, but before we would like to answer the question posed in the headline of this subsection, with a simple illustration for the de Sitter-rainbow scale factor in Figure 6.1.

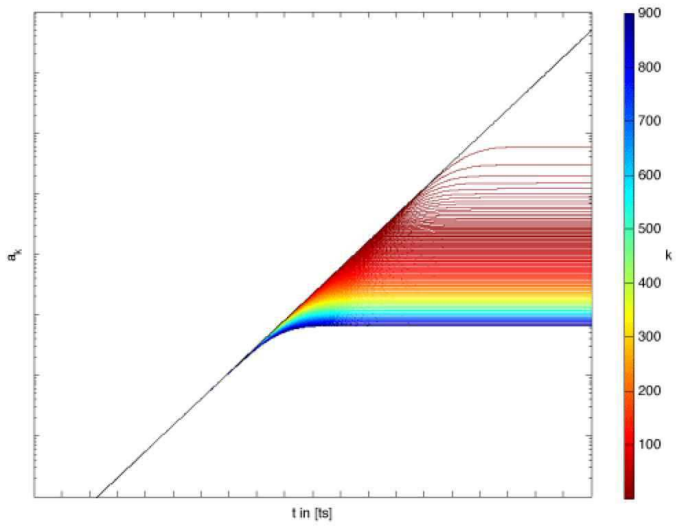


Figure 6.1: In this figure we plot the logarithm of the scale function $a_k(t)$ for each k-value — for $k \in [1, 900]$ — in a different color (colors online only). The different colors embody the energy of the modes: Gradually changing from low-energy / infrared (dark red) to high-energy / ultraviolet (dark blue). The straight black line shows the behavior of the scale function in the hydrodynamic limit. While the rainbow-scale function approaches the hydrodynamic limit for low-energy modes, the ultraviolet modes show strong deviations. Note, that in the infinite past all modes are phononic, and therefore $a_k(t) \to a(t)$.

What about the Hubble parameter?

The de Sitter universe is special in the sense that its "rate of expansion"

$$H := \frac{\dot{a}(t)}{a(t)}\,, \tag{6.131}$$

is constant. The de Sitter universe is a solution of the Einstein equations with a positive cosmological constant, Λ; *i.e.*, $H \propto \sqrt{\Lambda}$. If the acceleration of our universe can be put down to this cosmological constant, the universe will expand forever — and further dilute the matter and radiation distribution in our universe — until it approaches the de Sitter spacetime [43].

What is the situation in our emergent de Sitter universe? The rate of size change in the emergent de Sitter universe is given by,

$$H_k = H\,\frac{\exp(-2H\,t)}{\exp(-2H\,t)+(k/K)^2}\,, \tag{6.132}$$

a momentum-dependent *rainbow Hubble parameter*. At early times, or for phononic modes, when $a_k(t) \to a(t)$, the rainbow Hubble parameter,

$$\lim_{t\to-\infty} H_k(t) \to H\,, \tag{6.133}$$

reduces to the conventional Hubble parameter, while for late times,

$$\lim_{t\to+\infty} H_k(t) \to H\,K^2\,(\exp(-H\,t)/k)^2 \to 0\,. \tag{6.134}$$

This universe — mode by mode — stops expanding as the modes leave the phononic regime.

Therefore, in our particular set-up the long-time-kinematics of the particle production process is determined by the non-perturbative substructure, and not by the emergent spacetime picture. Any speculations with respect to an everlasting expanding universe are (within our model) in vain.

Characteristic value for quantum process?

To get a grasp on the cosmological particle production process, these two parameters (the effective scale function $a_k(t)$, and the effective Hubble parameter $H_k(t)$) are not quite enough. They are a good measure to describe the kinematics of the emergent gravitational field, but one also needs to know how the microscopic corrections effect the energy of the modes. Only the ratio between the mode frequency,

$$\omega_k(t) = \omega_0\,\sqrt{\exp(-2H\,t)+(k/K)^2}\,, \tag{6.135}$$

and the Hubble frequency can tell us whether the mode will be disturbed by the classical background or not. This result has been established for quantum field theory in conventional de Sitter spacetimes, and we review this point in the following section.

For now, we simply transfer the qualitative description known from conventional cosmological particle production, to our rainbow spacetimes. In this spirit we define *the ratio* between the modified dispersion relation and the effective Hubble parameter as follows:

$$\mathcal{R}_k(t) = \frac{\omega_k(t)}{H_k(t)} = \frac{\omega_0}{H}\,\frac{(\exp(-2H\,t) + (k/K)^2)^{3/2}}{\exp(-2H\,t)}\,. \tag{6.136}$$

Within the hydrodynamic limit this ratio simplifies to,

$$R_k(t) = \frac{\omega_0}{H}\,\exp(-H\,t)\,, \tag{6.137}$$

a monotone decreasing function, as time goes on. Again, we calculate limits for very early times,

$$\lim_{t\to-\infty} \mathcal{R}_k(t) \to \frac{\omega_0}{H}\,\exp(-H\,t) = R_k(t)\,, \tag{6.138}$$

and very late times,

$$\lim_{t\to+\infty} \mathcal{R}_k(t) \to \frac{\omega_0}{H}\,(k/K)^3\,\exp(+2H\,t)\,, \tag{6.139}$$

to see once again, that for late times / trans-phononic modes the deviations in our emergent spacetime play an important rule.

We will show that this ratio is sufficient to understand, and therefore predict qualitatively, the particle production process in our analogue spacetimes.

6.4.3 | Quantum field theory and rainbow inflation: Excitations from exponentially changing interaction strength

The equation of motion in the presence of time-dependent atomic interactions is given in Eq. (6.64). In the de Sitter rainbow universe, with the scale factor (6.125), and the dispersion relation (6.135), the harmonic oscillator frequency (6.68) simplifies to

$$\Omega_k(t)^2 = \omega_0^2\, b_k(t) - H^2 + \Delta_k(t)^2\,, \tag{6.140}$$

where the effective (or rainbow) scale factor is given by

$$b_k(t) = \exp[-2Ht] + (k/K)^2\,, \tag{6.141}$$

and the last term is given as

$$\Delta_k(t)^2 = H^2\,\frac{[4\,\exp(-2Ht) + (k/K)^2]\,(k/K)^2}{[\exp(-2Ht) + (k/K)^2]^2}, \tag{6.142}$$

which can be neglected in hydrodynamic approximation. Therefore the equation of motion for our rainbow de Sitter spacetime is given by a rather complicated differential equation, where common techniques for solving second-order differential equations fail.

However, this is not the end of the story, since at early times, or for phononic modes we get,

$$\lim_{t\to-\infty}\left\{\begin{array}{ccc} b_k(t) & \to & b(t) \\ \\ \Delta_k(t) & \to & 0 \end{array}\right\} \quad \Omega_k(t)^2 \to \omega_0^2\, b(t) - H^2\,, \tag{6.143}$$

where

$$b(t) = \exp(-2Ht)\,, \tag{6.144}$$

and within this limit the equation of motion simplifies to a differential equation solvable by Bessel functions. Within this regime, our emergent spacetimes can be regarded as a good toy model for quantum field theory in conventional de Sitter spacetimes. However, we need to apply special boundary conditions, that is to set limits on the time-duration and the k-range. Only then will the cosmological particle production process be robust against the model-specific non-perturbative corrections that are present in a spacetime emerging from a gas of Bosons.

As the expansion continues, the more modes will cross-over from phononic to trans-phononic, and finally for an infinitely long-lasting expansion, we get

$$\lim_{t\to+\infty}\left\{\begin{array}{ccc} b_k(t) & \to & (k/K)^2 \\ \\ \Delta_k(t) & \to & H \end{array}\right\} \quad \Omega_k(t)^2 \to \omega_0^2\,(k/K)^2\,, \tag{6.145}$$

and therefore are left with no phononic regime whatsoever. That is, in the infinite future all excitations of the fluctuations of the system are free-particle like. In this regime the quantum fluctuations are decoupled from the collective behavior, the emergent spacetime picture, and thus are static.

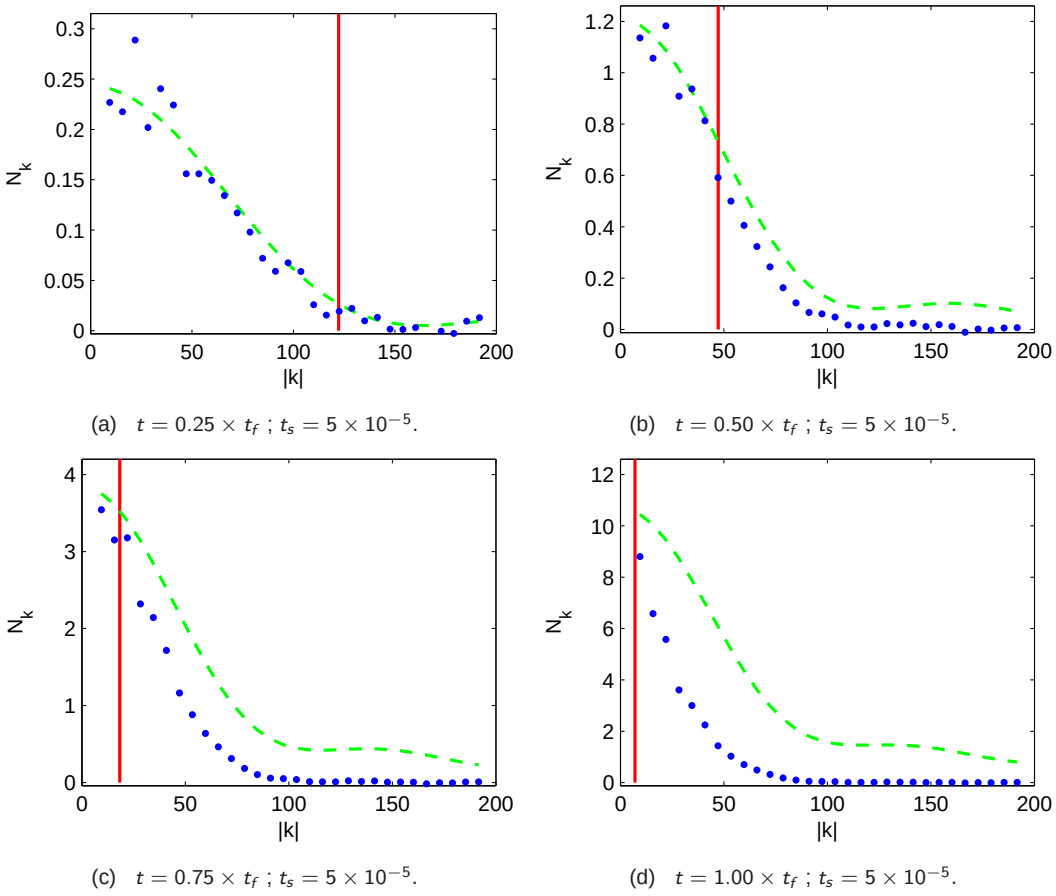
Therefore, without any further considerations, we deduce that in the infinite future we will always end up with well-defined out-states, that represent the vacuum state of instantaneous Hamiltonian diagonalization, see Sec. 6.3.1. The normalized mode functions in the infinite future are given by Eq. (6.107), where $\omega_k^{\mathrm{out}} = \omega_0|k|/K$.

We will subsequently revisit this point in Sec. 6.4.3, but for now our concern will be to focus on a regime will be to focus on a regime — the hydrodynamic limit — where the problem of particle production is tractable, and there is a straightforward description of the physics.

Toy-model for conventional inflation

To apply the method of instantaneous Hamiltonian diagonalization to particle production from a finite de Sitter phase, we assume a continuous function for all t, but at the times t_0 and t_f the function is not differentiable: In the hydrodynamic limit

$$b_k(t) \to b(t) \tag{6.146}$$



(a) $t = 0.25 \times t_f$; $t_s = 5 \times 10^{-5}$.

(b) $t = 0.50 \times t_f$; $t_s = 5 \times 10^{-5}$.

(c) $t = 0.75 \times t_f$; $t_s = 5 \times 10^{-5}$.

(d) $t = 1.00 \times t_f$; $t_s = 5 \times 10^{-5}$.

Figure 6.2: The four figures show time-slices of the "quasi-particle" production N_k in a de Sitter like spacetime, for $t_s = 5\times10^{-5}$. The blue dots represent the actual data obtained from the simulations for a realistic Bose gas with time-dependent interaction-strength [113]. The dashed green line shows the theoretical results for a finite de Sitter calculation obtained in the hydrodynamic limit, as presented in Section 6.4.3. The vertical red line indicates the borderline between the nature of the excitations: Everything to the left of the red line is phononic, while everything to right is trans-phononic / free-particle like.

.

we assume

$$b(t) = 1 + [b^{\mathrm{dS}}(t) - 1]\,\Theta_{\mathrm{HS}}(t - t_0) - [b^{\mathrm{dS}}(t) - 1/X]\,\Theta_{\mathrm{HS}}(t - t_f)\,. \tag{6.147}$$

Here $b^{\mathrm{dS}}(t) = \exp[-2H(t - t_0)]$, such that $b(t_0) = 1$, and $b(t_f) = 1/X$. In addition, we define $\omega_k(t_0) = \omega_k^{\mathrm{in}}$, and $\omega_k(t_f) = \omega_k^{\mathrm{out}}$, such that for $t < t_0$ we choose the in-mode functions, given in

Eq. (6.106), and similarly for $t > t_f$ we choose the out-mode functions, given in Eq. (6.107), for the initial and final flat regions.

Note that for any laboratory set-up the time-scales are finite, but given that this calculation is only valid for modes that are of phononic nature both before *and* after the expansion, we are not free to choose the expansion time arbitrarily.

The Bogoliubov transformation is slightly more difficult here, where two single-step processes have to be carried out:

$$\vec{v}_k(t) = M(t_f) \cdot \vec{v}_k^{dS}(t) = M(t_f) \cdot M(t_0) \cdot \vec{u}_k(t)\,. \tag{6.148}$$

For the mode functions during the de Sitter phase, which are v_k^{dS} and $(v_k^{\mathrm{dS}})^*$ for $t \in [t_0, t_f]$, we solve the harmonic oscillator equation with the time-dependent frequency given in Eq. (6.145). The solution is a linear combination of first order Hankel functions of the first $\mathrm{H}_1^{(1)}$ and second $\mathrm{H}_1^{(2)}$ kind. The normalized mode functions — with respect to the Wronskian given in Eq. (6.80) — are given by

$$v_k^{\mathrm{dS}} = \sqrt{\frac{\pi}{2H}}\,\mathrm{H}_1^{(1)}(R_k(t))\,, \tag{6.149}$$

$$(v_k^{\mathrm{dS}})^* = \sqrt{\frac{\pi}{2H}}\,\mathrm{H}_1^{(2)}(R_k(t))\,. \tag{6.150}$$

Note that in this representation the mode functions are indeed a set of complex conjugate functions, since $(\mathrm{H}^{(1)})^* = \mathrm{H}^{(2)}$; see for example [1]. The argument of the mode functions is given in terms of $R_k(t)$, the ratio between the mode frequency and the Hubble frequency, see Eq. (6.137). These mode functions are only valid within the hydrodynamic limit, that is for modes that fulfill $|k/K| \ll \exp(-H\,t)$.

To calculate the Bogoliubov coefficients at each step we again apply Eqs. (6.101) and (6.102). Below we will briefly outline the necessary steps to calculate the final Bogoliubov coefficients for the whole process. To begin with we write down the single-step Bogoliubov coefficients,

$$\alpha_k(t) = \frac{1}{4i}\left(2\,W[u_k, v_k^*] + v_k^*\,u_k(\dot{h}/h - \dot{g}/g)\right), \tag{6.151}$$

$$\beta_k(t) = \frac{1}{4i}\left(2\,W[v_k^*, u_k^*] - v_k^*\,u_k^*(\dot{h}/h - \dot{g}/g)\right), \tag{6.152}$$

appropriate to a continuous, but not continuously differentiable scale function at the time t. At the first step, where we map from plane waves onto Bessel functions, and for our specific scale factor before the step, $g(t) = 1$, and after the step, $h(t) = \exp[-2H(t - t_0)]$, we get

$$\alpha_k(t) = \frac{1}{2i}\left\{W[v_k, (v_k^{\mathrm{dS}})^*] - H\,v_k^*\,v_k^{\mathrm{dS}}\right\}, \tag{6.153}$$

$$\beta_k(t) = \frac{1}{2i}\left\{W[v_k^*, (v_k^{\mathrm{dS}})^*] + H\,v_k^*\,(v_k^{\mathrm{dS}})^*\right\}. \tag{6.154}$$

The final coefficients for our specific mode functions are given as

$$\alpha_k^{\text{in}}(t_0) = \frac{\sqrt{\pi\, R_k^{\text{in}}}}{-i\,2} \mathrm{e}^{i\,\omega^{\text{in}}\,t_0} \left\{ \mathrm{H}_0^{(1)}(R_k^{\text{in}}) + i\,\mathrm{H}_1^{(1)}(R_k^{\text{in}}) \right\} , \tag{6.155}$$

and

$$\beta_k^{\text{out}}(t_0) = \frac{\sqrt{\pi\, R_k^{\text{in}}}}{i\,2} \mathrm{e}^{i\,\omega^{\text{in}}\,t_0} \left\{ \mathrm{H}_0^{(2)}(R_k^{\text{in}}) - i\,\mathrm{H}_1^{(2)}(R_k^{\text{in}}) \right\} . \tag{6.156}$$

In the last two equations we used $R_k^{\text{in}} = R_k(t_0)$ and $\omega_k^{\text{in}} = \omega_k(t_0)$. Instead of calculating the Bogoliubov coefficients for the second step explicitly, we suggest a little shortcut. The transformation at the first step was a mapping from plane waves, represented as v_k and v_k^*, onto the de Sitter mode functions v_k^{dS} and $(v_k^{\text{dS}})^*$: $\vec{v}_k = M(t)\vec{v}_k^{\text{dS}}$. At the second step the calculation is exactly the opposite, a mapping from the de Sitter mode functions onto plane waves: $\vec{v}_k^{\text{dS}} = M(t)^{-1}\vec{v}_k$. The inverse of the transition matrix displayed in Eq. (6.81) is

$$M^{-1} = \begin{pmatrix} \alpha_k & -\beta_k^* \\ -\beta_k & \alpha_k^* \end{pmatrix} , \tag{6.157}$$

where we have employed $|\alpha_k|^2 - |\beta_k|^2 = 1$, since we map between normalized mode functions. Altogether we can formally derive the Bogoliubov coefficients at the second step as:

$$\alpha_k^{\text{out}}(t_f) \quad : \qquad \alpha_k^{\text{in}}(t_0) \xrightarrow[\text{in}\to\text{out}]{t_0\to t_f} [\alpha_k^{\text{out}}(t_f)]^* \tag{6.158}$$

$$\beta_k^{\text{out}}(t_f) \quad : \qquad \beta_k^{\text{in}}(t_0) \xrightarrow[\text{in}\to\text{out}]{t_0\to t_f} -[\beta_k^{\text{out}}(t_f)] , \tag{6.159}$$

Thus we can write down the Bogoliubov coefficients at the second step, at $t = t_f$, without any further calculation being required, as

$$\alpha_k^{\text{out}}(t_f) = \frac{\sqrt{\pi R_k^{\text{out}}}}{i\,2} \mathrm{e}^{-i\omega^{\text{out}}t_f} \left\{ \mathrm{H}_0^{(2)}(R_k^{\text{out}}) - i\,\mathrm{H}_1^{(2)}(R_k^{\text{out}}) \right\} , \tag{6.160}$$

and

$$\beta_k^{\text{out}}(t_f) = \frac{\sqrt{\pi R_k^{\text{out}}}}{-i\,2} \mathrm{e}^{-i\omega^{\text{out}}t_f} \left\{ \mathrm{H}_0^{(1)}(R_k^{\text{out}}) + i\,\mathrm{H}_1^{(1)}(R_k^{\text{out}}) \right\} . \tag{6.161}$$

Here $R_k^{\text{out}} = R_k(t_f)$ and $\omega_k^{\text{out}} = \omega_k(t_f)$.

The overall particle production, at later times $t > t_f$ can be obtained by simple matrix multiplication, since

$$M_{t>t_f} = M(t_0)\, M(t_f) = \begin{pmatrix} \alpha_k^{\text{final}} & \beta_k^{\text{final}} \\ (\beta_k^{\text{final}})^* & (\alpha_k^{\text{final}})^* \end{pmatrix} . \tag{6.162}$$

and therefore we get for the final Bogoliubov coefficients

$$\alpha_k^{\text{final}} = \alpha_k^{\text{in}}\alpha_k^{\text{out}} + \beta_k^{\text{in}}(\beta_k^{\text{out}})^* , \tag{6.163}$$

$$\beta_k^{\text{final}} = \alpha_k^{\text{in}}\beta_k^{\text{out}} + \beta_k^{\text{in}}(\alpha_k^{\text{out}})^* . \tag{6.164}$$

Note that these coefficients can in some sense be considered as time-dependent Bogoliubov coefficients, where

$$\alpha_k^{\mathsf{final}(t')} = \alpha_k^{\mathsf{in}}\alpha_k^{\mathsf{out}(t')} + \beta_k^{\mathsf{in}}(\beta_k^{\mathsf{out}(t')})^*\,, \tag{6.165}$$

$$\beta_k^{\mathsf{final}(t')} = \alpha_k^{\mathsf{in}}\beta_k^{\mathsf{out}(t')} + \beta_k^{\mathsf{in}}(\alpha_k^{\mathsf{out}(t')})^*\,, \tag{6.166}$$

where we project at any instant of time onto a plane wave basis at a particular t' with the eigenfrequency $\omega_k(t')$. But, as we pointed out in Section 6.3.1, as long as the expansion is continuing, the corresponding out-frequency modes do not represent a physically meaningful vacuum state. Nevertheless, for $t > t_f$, we stop the expansion and force the Hamiltonian of the system to become static, so that we are able to associate $n_k^{\mathsf{final}} = |\beta_k^{\mathsf{final}}|^2$ with the "real" mode occupation of a mode k per unit volume.

A lengthy but straightforward calculation now yields the mode occupation number after stopping the de Sitter like expanding phase. The number of quasi-particles produced depends only on the initial, R_k^{in}, and final R_k^{out} frequency ratio:

$$\begin{aligned} n_k^{\mathsf{dS}} = \frac{\pi^2}{64}R_k^{\mathsf{in}}R_k^{\mathsf{out}} \times \Big| & - [\mathsf{H}_1^{(1)}(R_k^{\mathsf{in}})\,\mathsf{H}_1^{(2)}(R_k^{\mathsf{out}}) - \mathsf{H}_1^{(2)}(R_k^{\mathsf{in}})\,\mathsf{H}_1^{(1)}(R^{\mathsf{out}})]^2 \\ & - [\mathsf{H}_0^{(1)}(R_k^{\mathsf{in}})\,\mathsf{H}_0^{(2)}(R_k^{\mathsf{out}}) - \mathsf{H}_0^{(2)}(R_k^{\mathsf{in}})\,\mathsf{H}_0^{(1)}(R_k^{\mathsf{out}})]^2 \\ & - [\mathsf{H}_0^{(1)}(R_k^{\mathsf{in}})\,\mathsf{H}_1^{(2)}(R_k^{\mathsf{out}}) - \mathsf{H}_1^{(2)}(R_k^{\mathsf{in}})\,\mathsf{H}_0^{(1)}(R_k^{\mathsf{out}})]^2 \\ & - [\mathsf{H}_0^{(2)}(R_k^{\mathsf{in}})\,\mathsf{H}_1^{(1)}(R_k^{\mathsf{out}}) - \mathsf{H}_1^{(1)}(R_k^{\mathsf{in}})\,\mathsf{H}_0^{(2)}(R_k^{\mathsf{out}})]^2 \\ & + 2\,\mathsf{H}_1^{(2)}(R_k^{\mathsf{out}})\,\mathsf{H}_0^{(2)}(R_k^{\mathsf{in}}) \times [\mathsf{H}_0^{(1)}(R_k^{\mathsf{in}})\,\mathsf{H}_1^{(1)}(R_k^{\mathsf{out}}) - \mathsf{H}_1^{(1)}(R_k^{\mathsf{in}})\,\mathsf{H}_0^{(1)}(R_k^{\mathsf{out}})] \\ & + 2\,\mathsf{H}_1^{(2)}(R_k^{\mathsf{in}})\,\mathsf{H}_0^{(2)}(R_k^{\mathsf{out}}) \times [\mathsf{H}_1^{(1)}(R_k^{\mathsf{in}})\,\mathsf{H}_0^{(1)}(R_k^{\mathsf{out}}) - \mathsf{H}_1^{(1)}(R_k^{\mathsf{out}})\,\mathsf{H}_0^{(1)}(R_k^{\mathsf{in}})]\Big|\,. \end{aligned} \tag{6.167}$$

At first sight this formula seems to be rather complicated, but there are two relatively simple and feasible consistency checks.

For example, we expect no particle production in the limit where the universe has not changed at all. It can easily been seen that for

$$\lim_{R_k^{\mathsf{out}}\to R_k^{\mathsf{in}}} n_k^{\mathsf{dS}} \to 0\,, \tag{6.168}$$

the occupation number indeed goes to zero.

Also interesting are limits resulting form an infinitely slow (adiabatic), that is $H \to 0$, and an infinitely fast (sudden) $H \to \infty$ expansion. In either case we replace the ratios with $R_k^{\mathsf{in}} = \omega_k^{\mathsf{in}}/H$ and $R_k^{\mathsf{out}} = \omega_k^{\mathsf{out}}/H$, hold ω_k^{out} and ω_k^{out} fixed, while we allow the Hubble parameter H to vary. Such a parameter choice requires $H\,T = \mathsf{constant}$, and therefore we expect the expansion time T to behave inverse proportional to H. The leading order, obtained from a Taylor-series-expansion around $H =$

∞,

$$\lim_{H\to\infty} n_k^{\mathrm{dS}} \to \frac{1}{4}\left|\frac{(\omega_k^{\mathrm{in}}-\omega_k^{\mathrm{out}})^2}{\omega_k^{\mathrm{in}}\omega_k^{\mathrm{out}}}\right| + O(1/H^2)\,, \tag{6.169}$$

is as expected — since $T \to 0$ — in agreement with the result from the sudden calculation within the hydrodynamic limit, see Eq. (6.110). In contrast, a Taylor-series expansion around $H = 0$ yields

$$\lim_{H\to 0} n_k^{\mathrm{dS}} \to 0\,. \tag{6.170}$$

As expected, within the limit of infinitely slow expansion, we produce zero quasi-particles, we recover adiabatic invariance. Furthermore if we consider the asymptotic expansion where $1 \ll R_k^{\mathrm{in}} \ll \sqrt{X}$, and employ the asymptotic limits of the Hankel functions [1], we get at linear order:

$$n_k \to \frac{1}{2\pi\, R_k^{\mathrm{out}}} = \frac{H}{2\pi\,\omega_k^{\mathrm{out}}}\,. \tag{6.171}$$

Of course, we cannot rely on our calculation in the case of an infinitely long-lasting expansion, since it is based on the validity of the hydrodynamic limit, which is completely inappropriate for $t \gg t_s$. However, in our previous numerical simulation of a "realistic" Bose gas [113] we compared our theoretically obtained result with short-time expansion scenarios, and were able to match them to the phononic part of the particle production spectrum, see Figs. 6.2 and F.1.

In Figure 6.2/ Figure F.1, for $t_s = 5\times10^{-5}$/ $t_s = 1\times10^{-4}$ we see an excellent agreement between our theoretical predictions (dashed green line), and the numerical data (blue dots) for the "quasi-particle" production in the phononic regime (left of the vertical red line). At the end of the expansion we see that almost all excitations are trans-phononic, hence the analogy *eventually breaks down*. But, to answer the initial question: Yes, the BEC can be used as an analogue model for cosmological particle production *within certain limits*, as our numerical results clearly affirm.

The calculations we have presented are somewhat tedious, but they are more than worth the effort since there is a fundamental lesson to be learnt from Eq. (6.167): It establishes our previous suspicion (see Section 6.4.2), that the characteristic value for the particle production is the ratio, $R_k(t)$ between the mode frequency, and the Hubble frequency. Comparison with Eq. (6.167) shows explicitly that the final quantity of particle production — for truly phononic modes before, during, and after the expansion — only depends on the initial R_k^{in} and final R_k^{out} frequency ratio. This motivated us to extend the role of the frequency ratio beyond the hydrodynamic limit, and compare our predictions with the data obtained from our simulations, where the non-perturbative corrections are included; see [113].

Qualitative behavior of quantum fluctuations

The process of cosmological particle production in an expanding / collapsing universe can be qualitatively understood by investigating one parameter, the frequency ratio $\mathcal{R}_k(t)$ as given in Eq. (6.136). First, we explain the correlation between the qualitative behavior of the particle production process

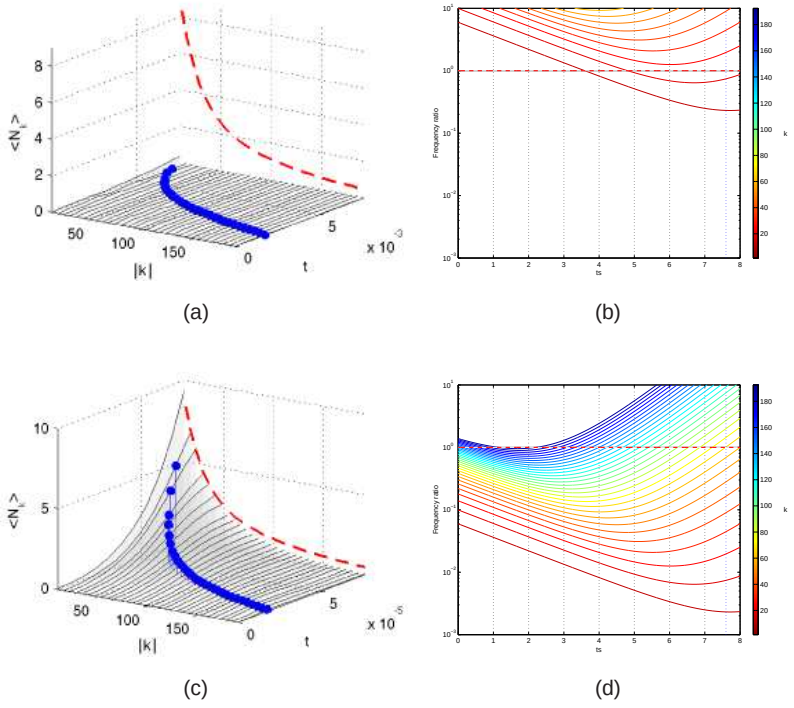


Figure 6.3: This figure compares the change in the mode occupation number in each mode on the left side, with frequency ratio $\mathcal{R}_k(t)$ of the mode on the right side. The different rows express different scaling times t_s. Each black line on the right hand side indicates the occupation number in the mode k as a function of time. (The red dashed line on the left had side indicates the sudden limit.) On the right hand side we have plotted the frequency ratio $\mathcal{R}_k(t)$ for each of those modes with a different color (online only) to indicate the energy difference of the modes; gradually changing from infrared modes (dark red), to ultraviolet modes (dark blue). The horizontal (red dashed) indicates where the frequency ratio $\mathcal{R}_k(t)$ is equal to one, while the vertical (blue dashed) line indicates end of the expansion time in our simulations. The blue dots in the figures to the left indicate when the modes cross over from phononic to trans-phononic behavior, or in other words start to decouple from the emergent spacetime. Roughly we can see that the blue dots are located where the frequency ratio has its minimum. The first row Figs. (a) and (b) correspond to a scaling time of $t_s = 1 \times 10^{-3}$, the second row Figs. (c) and (d) to $t_s = 1 \times 10^{-5}$.

and this frequency ratio (6.137) in the hydrodynamic limit, then transfer these ideas to the emergent rainbow metrics we have introduced in Section 6.2.2.

Qualitative behavior of particle production in the hydrodynamic limit There is a relatively simple way to understand the qualitative behavior of mode functions propagating through an exponentially changing universe, by checking out the effective harmonic oscillator equation for the auxiliary field. Within the hydrodynamic limit we get

$$\ddot{\hat{\chi}}_k(t) + \left(\omega_k(t)^2 - H^2\right)\hat{\chi}_k(t) = 0\,, \tag{6.172}$$

where we used the equation of motion, see Eq. (6.64), for the effective time-dependent harmonic oscillator frequency for phononic modes given in Eq. (6.143).

Above we have shown that the general solution is a linear combination of first order Hankel functions of the first and second kind, see Eqn. (6.149) and (6.150). These mode functions are a function of $R_k(t)$, and therefore in the limit of $R_k \to \infty$ the mode functions approach positive and negative frequency modes, while for $R_k \to 0$ the modes stop oscillating, and the modes exhibit exponentially growing and exponentially decaying kinematics.

A simpler way to come to the same answer is to investigate Eq. (6.172) in its obvious limits: These are $\omega_k(t) \gg H$, and $\omega_k(t) \ll H$, or in terms of the frequency ratio:

$\mathbf{R_k(t) \gg 1}$**:** It is then possible to write down an *approximate* solution for Eq. (6.172),

$$v_k^{\mathrm{dS}} = \frac{\exp(i\int_{t_0}^{t}\omega_k(t')\,dt')}{\sqrt{\omega_k t}}\,, \tag{6.173}$$

$$(v_k^*)^{\mathrm{dS}} = \frac{\exp(-i\int_{t_0}^{t}\omega_k(t')\,dt')}{\sqrt{\omega_k t}}\,. \tag{6.174}$$

These keep the shape of plane waves, but allow their amplitude and frequency to change as a function of time. This ansatz is referred to as the WKB approximation, which is valid within the *adiabatic* limit, when during one oscillation $T = 2\pi/\omega_k(t)$ the relative change in the frequency is small (see [141]),

$$\left|\frac{\omega_k(t+T)-\omega_k(t)}{\omega_k(t)}\right| \approx 2\pi\left|\frac{\dot{\omega}_k}{\omega_k^2}\right| \ll 1\,. \tag{6.175}$$

For de Sitter spacetimes this equals to

$$\left|\frac{\dot{\omega}_k^{\mathrm{dS}}}{(\omega_k^{\mathrm{dS}})^2}\right| = \left|\frac{1}{R_k(t)}\right| \ll 1\,, \tag{6.176}$$

the condition that the ratio $R_k(t)$ is much larger than one.

Hence, the particle production process goes down to zero in the infinite past, where the modes oscillations are too fast to "notice" the ongoing (relatively) slow change in the universe.

$\mathbf{R_k(t) \ll 1}$**:** Here the differential equation (6.172), reduces to

$$\ddot{\hat{\chi}}_k(t) - H^2\hat{\chi}_k(t) = 0\,. \tag{6.177}$$

The solutions of this equation are exponentially growing, $\sim \exp(Ht)$, or decaying, $\sim \exp(-Ht)$, mode functions.

Therefore, the modes are no longer free to oscillate. Instead they get dragged along with the spacetime fabric.

$\mathbf{R_k(t) = 1}$: For any mode k there is a time t_{crossing} when the frequency ratio is equal to one, and such that:

$$t < t_{\text{crossing}} \quad : \quad \Omega_k(t)^2 > 1\,, \tag{6.178}$$

$$t > t_{\text{crossing}} \quad : \quad \Omega_k(t)^2 < 1\,. \tag{6.179}$$

Therefore it is possible to associate a boundary, the so-called "*Hubble horizon*", when $\omega_k = H$. For different modes with wavelength k the Hubble horizon occurs at different times. *Subhorizon* modes, *i.e.*, $\omega_k > H$ are some sort of more or less distorted plane wave oscillations, while *superhorizon* modes, *i.e.*, $\omega_k < H$, approximately satisfy a harmonic oscillator equation with imaginary oscillator frequency, and thus they are exponentially growing or decaying. The "crossing-time" $t = t_{\text{crossing}}$ is referred to as the time of "Horizon crossing". The *superhorizon* modes are sometimes said to be frozen modes. Following this definition, if we retain the hydrodynamic approximation, then in the infinite future all modes will be frozen out.

Please bear in mind that the "Hubble horizon" is different from the cosmological horizon, see Section 6.4.3. One easy way to see this, is to remember that the Hubble horizon is associated with a point in time, which is different for each mode, while the cosmological horizon is the maximum distance for all modes.

The main lesson for the hydrodynamic limit is that it is not essential to explicitly solve the differential equation. Of course, it is much easier to investigate certain limits employing the resulting mode functions, instead of investigating the limits of the equation of motion. In the hydrodynamic limit both methods are accessible. Beyond this limit, in the eikonal approximation, we suggest a rather different strategy.

Qualitative behavior of particle production beyond the hydrodynamic limit: *Ex ante* we would like to motivate this section by the remark that while the frequency ratio in the hydrodynamic limit $R_k(t)$ is a monotone decreasing function in time, the ratio in the eikonal approximation $\mathcal{R}_k(t)$ is not. Therefore there is some freedom to obtain different results to the "conventional" particle production process. We demonstrate the correctness of this assertion by appeal to the numerical simulations reported in [113].

To obtain a rough estimate on the different qualitative regimes of particle production, we use the experience gained in the hydrodynamic limit, and simply exchange $R_k(t) \to \mathcal{R}_k(t)$. The eikonal frequency ratio has been introduced in Section 6.4.2, see Eq. (6.136), as the ratio between the modes (modified) frequency $\omega_k(t) = \omega_0\sqrt{b_k(t)}$, and the (rainbow) Hubble parameter $H_k(t)$, see Eqs. (6.141) and (6.136).

For early times, when $R_k(t) \gg 1$ the hydrodynamic and eikonal ratios are identical, therefore in both cases we are approaching the adiabatic limit, where we expect the particle production process to be negligibly small.

As intimated, the overall slope of the eikonal ratio is not a monotone decreasing function, since

$$\dot{\mathcal{R}}_k = \frac{\omega_0\,\sqrt{\exp(-2Ht)+(k/K)^2}\,[\exp(-2Ht)-2\,(k/K)^2]}{-\exp(-2Ht)}\,, \tag{6.180}$$

the time derivative of the eikonal limit changes its sign at

$$t_{\text{turn}} = \frac{\ln(K^2/(2\,k^2))}{2H}\,. \tag{6.181}$$

For $t < t_{\text{turn}}$ the slope of the ratio is negative, for $t = t_{\text{turn}}$ the ratio is given by

$$\mathcal{R}_k(t_{\text{turn}}) = \frac{3\sqrt{3}}{2}\,\frac{\epsilon_{\text{qp}}}{H}\,k^2\,, \tag{6.182}$$

and for $t > t_{\text{turn}}$ the ratio is positive. Therefore the eikonal ratio has a minimum at t_{turn}, with the maximal particle production around this point. After this point the ratio starts to increase again, and the particle production process will slow down again.

To qualitatively describe the particle production process in our specific rainbow spacetime, we suggest the following terminology:

$t \to -\infty$**:** At early times almost all modes are "sub-Hubble-horizon" modes, and the particle production process is negligible. The modes oscillate with much higher frequencies as their corresponding Hubble frequencies, that is $\mathcal{R}_k(t) \gg 1$.

$t \sim t_{\text{turn}}$**:** As time goes on the mode frequencies are decreasing, while at the same time the rainbow Hubble frequencies are decreasing as well, see Section 6.4.2. Nevertheless, the ratio between them exhibits a minimum at t_{turn}, where the particle production process is expected to be maximal. Even if the particle production process is maximal, this does not necessarily imply that the quantity of particle production is noticeable; the modes also need to be "super-Hubble-horizon" modes, or in more accurate terminology, we require $\mathcal{R}_k(t_{\text{turn}}) \ll 1$.

$t \sim t_{\text{crossing}}$**:** If there exists a time $t = t_{\text{crossing}}$, such that $R_k(t_{\text{crossing}}) \sim 1$, where a mode k is crossing the "Hubble horizon", there will be a second time $t = t_{\text{re-entering}}$, where the mode k is re-entering the "Hubble horizon", and $R_k(t_{\text{re-entering}}) \sim 1$. Altogether, we suggest that it is useful to name the behavior of the modes as follows: The "freezing of the mode k" in the time period $t_{\text{crossing}} < t < t_{\text{turn}}$, and the "melting of the mode k" during $t_{\text{turn}} < t < t_{\text{re-entering}}$.

Note, that we have used $R_k(t_{\text{crossing}}) \sim 1$ and $R_k(t_{\text{re-entering}}) \sim 1$, instead of $R_k(t_{\text{crossing}}) = 1$ and $R_k(t_{\text{re-entering}}) = 1$. This is due to the fact that the harmonic oscillator frequency in the eikonal limit, see Eq. (6.140), can be written as

$$\Omega_k(t)^2 = \omega_k(t)^2 - H_k(t)^2 \left[1 - 2\, \exp(2Ht)\, (k/K)^2\right], \tag{6.183}$$

and cannot be simplified to $\Omega_k(t)^2 = \omega_k(t)^2 - H_k(t)^2$. Here the *exact* times for the "crossing" and "re-entering" of horizons should be correlated with the sign-change in the harmonic oscillator frequency. Nevertheless, it can be seen that this does not change the qualitative description for the particle process.

Another novelty in our qualitative understanding of the particle production process in our FRW rainbow-spacetime, is the connection with the condensed matter point of view: The minimum of the ratio $\mathcal{R}_k(t_{\text{turn}})$ for a particular mode k, see Eqs. (6.180), (6.56), and (6.53), occurs at

$$\exp(-2Ht) - 2(k/K)^2 = 0 \quad \rightarrow \quad k = \ell_{\text{Planck}}(t)^2/2\,. \tag{6.184}$$

This quantity also appears in the context of conventional condensed matter physics, where it is defined as the crossover between the phonon and free-particle region. This borderline, the inverse of the healing, or coherence length ξ [151], is given by

$$\xi^{-2} = \frac{2\, m\, n_0\, U(t)}{\hbar^2} = \frac{1}{2}\, \frac{4m^2}{\hbar^2}\, \frac{n_0\, U(t)}{m} = \ell_{\text{Planck}}(t)^2/2\,, \tag{6.185}$$

which indicates where each mode starts to decouple from the spacetime. In other words, each mode can experience particle production, until it becomes free-particle like. Hence, from the BEC side we have a natural understanding of $\mathcal{R}_k(t_{\text{turn}})$.

To show the qualitative correlation between the modified frequency ratio (6.136) with particle production in our specific rainbow de Sitter spacetime, we have plotted the ratio for several k-modes as a function of time, and compared them to number occupation plots, see Figs. 6.3. (In Appendix F for the two cases we provide larger figures for $t_s = 1 \times 10^{-3}$ and $t_s = 1 \times 10^{-5}$, see Figs. F.2-F.5. In addition we also show two scaling times $t_s = 1 \times 10^{-4}$ and $t_s = 5 \times 10^{-5}$.)

For example, in Figure F.2(a) we see the "quasi-particle" production in a certain mode in the de Sitter region where $t_s = 1 \times 10^{-3}$. The negligibly small population of the modes during, and after, the expansion can be explained by means of the ratio plot to its right, in Figure F.2(b). As pointed

out above, the particle production process is large only if $\mathcal{R}_k \ll 1$, which is impossible to achieve for such a *relatively* large scaling unit t_s. We also see, that only the first two modes from the bottom of the infrared scale cross the "Hubble horizon", such that $\mathcal{R}_k < 1$, and they quickly turn around and re-enter the "Hubble horizon" after a few e-foldings. Consequently, such an experimental set-up is inappropriate for mimicking cosmological particle production.

On the contrary, Figure F.5(a) shows a noticeable "quasi-particle" production, for the first 100 modes. Here $t_s = 1 \times 10^{-5}$, and thus the expansion is two magnitudes faster than one we discussed before. The qualitative behavior is roughly in agreement with the mode frequency ratio plotted to the right in Figure F.5(b). The blue dots in the data-figure represent the point when the particular mode becomes free-particle like. The mode occupation process slows down after this point, and as we can read off the two figures, this happens for the fourth-lowest energy modes around 6 e-foldings.

While the emergent spacetime picture was necessary to understand the time-dependent commutator relations — in terms of the field operator and its conjugate momentum on a time-dependent classical background — the breakdown of the particle production process during inflation is naturally explained using condensed matter physics, as it is related to the borderline between phononic and trans-phononic particles.

Emergent cosmological horizons?

The existence of a cosmological horizon in our specific emergent spacetime can be investigated by calculating the maximum distance, r_{max}, travelled by small perturbations initiated at a certain time $t = t_0$ and certain point $\vec{r}_0$. We can associate a cosmological horizon to each point $(t_0, \vec{r}_0)$, if the maximum distance the signal — here our excitations in the Bose–Einstein condensate — can travel is finite. This naturally defines a region around the point of emission, and its boundary is the cosmological horizon. In the presence of cosmological horizons two points in spacetime can be causally disconnected if their distance is larger than r_{max}.

In "conventional" cosmology cosmological horizons are predicted for an infinitely long-lasting de Sitter universe, but what is the situation in our spacetime emerging from a Bose gas? We would like to address this problem briefly, and show that due to non-perturbative corrections there are, strictly speaking, no emergent cosmological horizons present in the system.

This can easily be shown, given that one only needs to integrate the *group* velocity of a perturbation emitted at $(t_0, \vec{r}_0)$,

$$r_{\text{max}} = \lim_{t\to\infty} \int_{t_0}^{t} c_{\text{group}}\, dt \tag{6.186}$$

from t_0 to the infinite future. In "conventional" — that is Lorentz-invariant spacetimes — *group* and *phase* velocities are identical. This is not the case for our specific analogue model, where the *phase*,

$$c_{\text{phase}} := \frac{\omega_k}{k} = c_0 \sqrt{\exp(-2Ht) + (k/K)^2}, \tag{6.187}$$

and the *group* velocity,

$$c_{\text{group}} := \frac{\partial \omega_k}{\partial k} = \frac{c_0^2 \exp(-2Ht) + 2(k/K)^2}{\sqrt{c_0^2 \exp(-2Ht) + (k/K)^2}} \tag{6.188}$$

are different.

Only within the hydrodynamic limit, when $K \to \infty$, are the two velocities equivalent, $c_{\text{group}}(t) \to c_k(t)$. Within this limit all individual signals travel with the same speed, and therefore wave packets "keep their shape", they show no dispersion. A signal — sent at $(t = 0, \vec{r}_0)$ — propagating forever will only travel a finite distance,

$$\lim_{K\to\infty} r_{\text{max}} = \lim_{t'\to\infty} \int_{t_0}^{t'} \lim_{K\to\infty} c_{\text{group}}\, dt = \frac{c_0}{H}\,. \tag{6.189}$$

In the past cosmological horizons have been repeatedly mis-interpreted, and we would like to advise the interested reader to carefully read [158].

Returning to our problem of investigating the presence of cosmological horizons in the Bose gas, the maximum distance a signal can travel is given by

$$r_{\text{max}} = \lim_{t\to\infty} \int_0^t c_{\text{group}}\, dt = \infty\,, \tag{6.190}$$

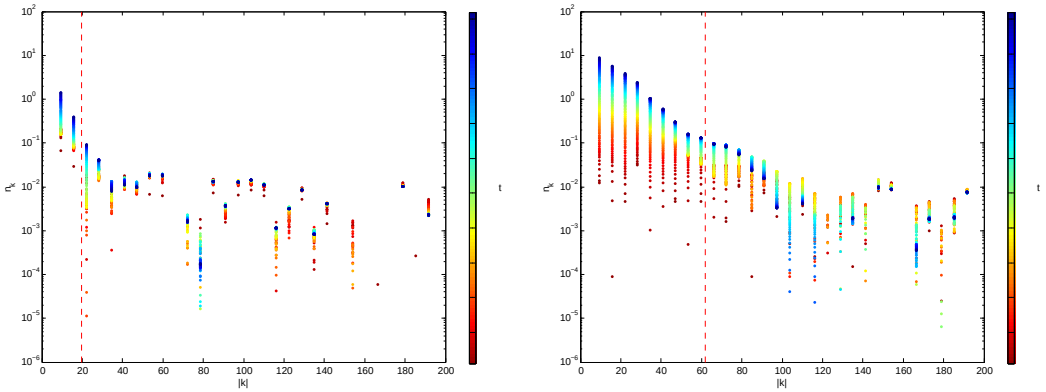
and thus is infinite. The emergent spacetime picture completely lacks the concept of (strict) cosmological horizons completely. This result can be generalized, since many super-sonic modifications in the dispersion relations will show similar behavior.

Long lasting rainbow inflation

The present analogue model does not possess horizons in the cosmological sense, consequently we cannot automatically assume that an infinitely long-lasting de Sitter phase would lead to a Planckian spectrum where the temperature is connected to the surface gravity at the horizon, see [85]. Thus there is no short-cut to calculate the overall temperature for our everlasting de Sitter rainbow spacetime.

At first, it seems to be a highly contrived question to ask for the final spectrum in our emergent rainbow spacetime after an infinitely long-lasting inflationary epoch. However, we demonstrate by means of numerical evidence — from our computer simulations [113] — that a *sufficiently long duration expansion* can be enough to reveal the characteristic final shape of the particle spectrum at the end of inflation.

Before we jump to the result, we would like to show that the final Bogoliubov coefficients are indeed time-independent, and that the mode occupation number calculated with the instantaneous



(a) $t_s = 1 \times 10^{-3}$ (b) $t_s = 1 \times 10^{-4}$

(c) $t_s = 5 \times 10^{-5}$ (d) $t_s = 1 \times 10^{-5}$

Figure 6.4: Each plot shows the time-evolution of the particle spectrum projected into one plot. As time goes on the data points become darker, changing gradually from white to black. Note that at low momenta — corresponding to those modes that twice "cross the Hubble horizon" by "freezing" and "re-entering" – the final quasi-particle density is approximately log-linear, corresponding to $n_k \sim C\ \exp(-\sigma\, k)$. Some modes never "cross the Hubble horizon", if $\mathcal{R}_k(t_{\text{turn}}) \geqslant 1$. This can be seen in our plots, where we indicated $k_{\text{static}} = [\sqrt{2}\, 3^{(-3/4)}/\sqrt{\epsilon_{\text{qp}}}] \cdot \sqrt{H}$ in each plot with a vertical (red) dashed line.

.

Hamiltonian diagonalization method represents "real" quasi-particles, due to well-defined in states in the adiabatic regime, and *also* well-defined out states in the free-particle regime. The mode functions in our rainbow spacetime interpolate between these two states.

Pair of coupled harmonic oscillators: Given that we are only dealing with one region, we can drop the prefactor in the equation of motion for the auxiliary mode operators $\hat{\chi}_k$:

$$\ddot{\hat{\chi}}_k(t) + \Omega_k(t)^2\, \hat{\chi}_k(t) = 0\,, \tag{6.191}$$

where

$$t \to +\infty \quad : \quad \ddot{\hat{\chi}}_k(t) + (\omega_k^{\mathrm{WKB}})^2\, \hat{\chi}_k(t) = 0\,, \tag{6.192}$$

$$t \to -\infty \quad : \quad \ddot{\hat{\chi}}_k(t) + (\omega_k^{\mathrm{FP}})^2\, \hat{\chi}_k(t) = 0\,. \tag{6.193}$$

In the infinite past, when the eikonal scale factor approaches the hydrodynamic ("conventional") scale factor, the mode functions approach the adiabatic regime. Thus $\omega_k^{\mathrm{WKB}} \sim \omega_k(t)$, and the mode functions are approximated by Eqs. (6.173) and (6.174). These mode functions represent positive and negative frequency modes at every instant of time, in the infinite past they represent the adiabatic vacuum, for instance see [141, 77, 29].

In the infinite future all excitations behave like free particles, since

$$\omega_k^{\mathrm{FP}} = \frac{\omega_0\, k}{K} = \frac{\hbar\, k^2}{m}\,, \tag{6.194}$$

represents the kinetic energy of an object with mass m; $E = p^2/(2m) = \hbar^2 k^2 (2m)$. The time-independence is due to the end of the effective expansion in our emergent spacetime. The mode functions are the usual positive and negative frequency modes, as given in Eq. (6.107), where $\omega_k^{\mathrm{out}} = \omega_k^{\mathrm{FP}}$.

Altogether we are dealing with well-defined *initial and final* vacua states. This kind of problem can be compared with the $\tanh$-expansion, studied for example in [77, 29]. In this case the Bogoliubov coefficients are — after an infinitely long-lasting expansion — time-independent. Please note that this analytic calculation does not by itself give any details *when and how* the mode functions change, since the Bogoliubov coefficients for a smooth scale function $b_k(t)$ for all t are given by the globally defined time-dependent quantities

$$\alpha_k(t) \;=\; \frac{1}{2i}\, W[u_k, v_k^*]\,, \tag{6.195}$$

$$\beta_k(t) \;=\; \frac{1}{2i}\, W[v_k^*, u_k^*]\,. \tag{6.196}$$

Compare with Eqs. (6.101) and (6.102). The Wronskian of the mode function is time-independent, therefore it can be evaluated at any time. (Note that the general mode functions — (theoretically) obtained from the eikonal equation of motion — are not necessarily normalized.) Again, v_k and v_k^* represent the in, and u_k and u_k^* the out mode functions.

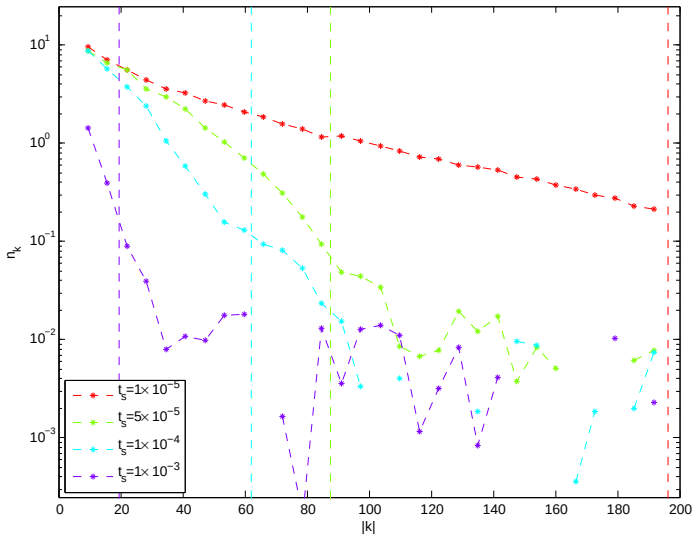


Figure 6.5: This figure shows the four different particle spectra, belonging to four different scaling times, after a finite rainbow de Sitter phase. (Please note that the "gaps" in the quasi-particle spectrum are a result of the logarithmic scale that is incapable of handling (small) negative occupation numbers, a numerical artifact arising in our simulations. For more information about the numerical tools used to obtain these results consult [113].)

By means of our numerical results, we see that the final spectrum is, after sufficiently long-lasting expansion, already *rapidly* approaching its final shape, see Figs. (6.4). We have plotted the final spectra in one figure, Figure 6.5, so that we easily see the correlation between the slope of the line and the scaling time t_s^{-1}. However the temporal duration in our previous numerical simulation for $t_s = 1 \times 10^{-5}$ has not been sufficiently long. In Figure F.5(b) we can see that at the end of the numerical simulation a good fraction of the quantum field modes (*i.e.*, roughly $|k| < 40$) are frozen. We expect particle production in those modes to contribute significantly to the infrared end of the final spectrum. We repeated the numerical simulation for $t_s = 1 \times 10^{-5}$ (so that initially all modes are sub-Hubble horizon modes) with two times the previous duration. In addition, the initial nonlinearity is now $C = 2 \times 10^7$ instead of $C = 1 \times 10^7$ so that all modes are "phononic" at the start of the simulation. As shown in Fig. (6.6), at the end of the simulation all modes are trans-phononic, and the particle production process ceases. As a result of our numerical simulations the final particle spectrum does not seem to nicely fit a straight line, but it seems conceivable to employ standard line-fitting tools to study the final particle spectrum as a function of t_s and k. (We are currently investigating this issue.)

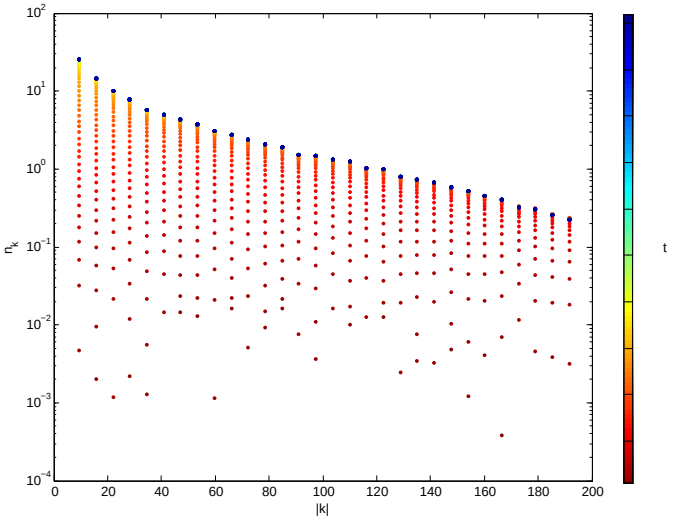


Figure 6.6: This figure shows the final particle spectra after a finite duration rainbow de Sitter phase for $t_s = 1 \times 10^{-5}$ after all modes have decoupled from the emergent spacetime geometry.

6.5 | Conclusions and outlook

In this chapter we put the analogy between a parametrically excited Bose–Einstein condensate and cosmological particle production to the test. Knowing that the analogy for mimicking a specific quantum effect in "conventional" curved-spacetime quantum-field-theory hinges on the robustness of the effect against model-specific deviations, we derived the "whole" model-dependent emergent rainbow spacetime. Similar work on the *acoustic* Hawking effect in subsonic and supersonic (super)-fluids has been carried out in [112].

There were two main lessons learnt for the analogue model community. First, the specific model we presented — a uniform gas of atoms with time-dependent atomic interactions — is in general *not* robust against the non-perturbative ultraviolet corrections. Secondly, we also showed that the analogy is sufficiently good for mimicking some aspects of cosmological particle production for finite changes in the size of the effective universe. We said "some aspects", because the analogy only holds for the low-energy part of the spectrum, and therefore the analogy is associated with a certain k-range. There are the phononic excitations, bounded by a time-dependent parameter $|k| < 1/\ell_{\text{Planck}}(t)$.

Given that we expect significant deviation from the desired quantum effect, one might ask the question "Is the analogue model we have presented a suitable candidate for laboratory experiments?" Previously in [113], as well as briefly in the current chapter, we have presented numerical

results for cosmological particle production in a "realistic" Bose gas. As a matter of fact, despite many possible sources of difficulties, for example back-reaction-effects / mode-mixing, the phononic regime shows excellent agreement with the theoretical predictions.[1] The Bose–Einstein condensate enables us to prepare and control a quantum field to such an extent, that within a few years time the technology should be able to drive "inflation" between two "natural" vacua and — that is the *outstanding* problem [163, 203, 16] — directly measure the resulting spectra. Of course, there are also other models involving a freely expanding condensate cloud, but we suspect similar problems — a growing "Planck-length" and the lack of a (strict) cosmological horizon [71] — to appear, and would like to stress that those models destroy the condensate during the expansion process. We leave it as an open problem to simulate and check the "robustness" of those models.

So much for the analogy, but what did we learn from the deviations occurring in our specific emergent spacetime? Are there conclusions to be drawn that are of relevance for the cosmology, or even quantum gravity programme? We leave this to our readers, and merely summarize our experience regarding "trans-Planckian" physics in our emergent spacetime:

The emergent spacetime we have presented is an example of emergent Lorentz-symmetry. At the infrared end of the excitation spectrum we exhibit Lorentz invariance, while non-perturbative corrections from the microscopic substructure "naturally" break the Lorentz-invariance in the ultraviolet regime [131, 202, 201, 201]. These corrections also alter the spacetime picture from "ordinary" spacetimes to the — more "unusual" but conceivable [135] — concept of *rainbow* spacetimes. These are momentum-dependent spacetimes, where the k-dependence is suppressed in the infrared regime. Further, a time-dependence in the atomic contact potential yields a FRW-type universe for phononic modes, and *rainbow FRW-type spacetimes* for higher-energy modes. The borderline that divides the energy scale into phononic and trans-phononic intervals, may be viewed as an *analogue Planck-length*. (The physical behavior changes somewhere in between the phononic and free-particle regime, in the same sense that the Planck-scale is expected to exhibit new laws of physics.) The "Planck-length" in our model is correlated with the contact potential (scattering length), and thus we are dealing with a time-dependent "Planck-length". In our expanding universe the "Planck-length" is growing as well [185], such that more and more modes are "trans-Planckian" as time goes on. Consequently they gradually decouple from the emergent spacetime picture. They behave more and more like free particles. The *rainbow* scale factor

$$a_k(t) = a(t)/\sqrt{1 + k^2\,\ell_{\text{Planck}}(t)^2}\,, \tag{6.197}$$

and the *rainbow* Hubble parameter

$$H_k(t) = H/(1 + k^2\ell_{\text{Planck}}(t)^2)\,, \tag{6.198}$$

[1] In fact, for our numerical simulations the parameters we choose (number of atoms and nonlinearity) were such that we were working in a regime where back-reaction and mode-mixing were negligible or very small effects. But in principle these effects are included by the methodology.

are both momentum-dependent. The growth in the "Planck-length" forces the *rainbow* Hubble parameter to approach zero, and therefore the universe gradually — mode by mode — effectively stops expanding [106, 143].

This leads to interesting physics for *rainbow* inflation: At early times all modes are "sub-Hubble-horizon" modes. As the expansion goes on some — not all — modes cross the "Hubble-horizon" and become "superhorizon" modes, these modes are "frozen modes" and get dragged along with the spacetime fabric. Eventually the effective expansion starts to slow down — due to the growing "Planck-length" — and a process starts that we call "*the melting of the modes*". After a while these modes "re-enter" the "Hubble-horizon" and the particle production process is finished.

However useful these results are to the general relativity and cosmology community, we would like to end our conclusion by commenting on the importance of BEC based analogue models to the condensed matter physics community. There are many aspects, *e.g.*, the time-dependent commutation relations, that really seem to require the emergent spacetime picture to fully understand the physics in our parametrically excited condensate. The emergent spacetime and the Bose–Einstein condensate are two aspects of one and the same effect, and one needs to know both points of view to appreciate the full complexity of this novel state of matter.

CHAPTER 7

Summary & Conclusions

This thesis has dealt with numerous fundamental issues related to the analogue gravity programme.

We mainly considered linearized fluctuations around some background field whose dynamics is governed by some first-order Lagrangian. In the systems (*i.e.*, fluids and superfluids) we presented in this thesis, we saw that these perturbations experience an effective gravitational field, and that the equation of motion is identical to that for spin-zero scalar fields in an effective curved-spacetime, both at the classical and quantum levels.

We gave many examples of the diversity of the emergent geometrical objects. We outlined how to obtain analogue spacetime geometries described by a fully symmetric tensor of arbitrary rank and of Lorentzian / Riemannian signature. For example, the geometry obtained from linearizing around a *single* background field is a rank two symmetric $n \times n$ tensor g_{ab} — where $n = d + 1$, for d spatial dimensions. Its signature is not necessarily pseudo-Riemannian. More specifically, we treated effective signature change events, between Riemannian and pseudo-Riemannian / Lorentzian signature, in a spacetime emerging from a *single*-component Bose–Einstein condensate. The rank of the generalized metric tensor depends on the initial background field. We also focused on small perturbations around a two-component scalar field, a Bose–Einstein condensate with atoms in two different hyperfine states. The dominant geometrical object is then a rank four symmetric tensor, a $n \times n \times n \times n$ tensor g_{abcd}, describing a *Finslerian* geometry.

Interestingly, the notion of *Finslerian* geometry also governs the equation of motion for the quasi-particle excitations around the two-component scalar field. A fine tuning of the condensate parameters is possible, such that the Finslerian structure reduces to either bi-metric, or mono-metric pseudo-Riemannian geometry. The emergent curved-spacetime quantum field theory for the pertur-

bations results in two particles, one with zero mass, and one with non-zero mass.

Bose–Einstein condensation is an example of *spontaneous symmetry breaking* as the many Body-Hamiltonian is no longer invariant under $SO(2)$ transformations, $\theta \to \tilde{\theta} = \theta \exp(i\,\alpha)$. Therefore the presence of massive excitations from a Bose–Einstein condensate naively seems to disagree with the Nambu–Goldstone theorem, which predicts massless fields whenever a continuous symmetry is broken.

However, the fundamental Hamiltonian of the two-component system is a functional of $\vec{\theta} = (\theta_A, \theta_B)$. In the absence of transitions between the two fields the Hamiltonian exhibits an extra $SO(2)$ symmetry under which $\vec{\theta}$ transforms as a 2-component vector. This symmetry is explicitly broken for interacting fields, so that $SO(2)_A \times SO(2)_B \to SO(2)_{AB}$. The coupled system is only invariant under simultaneous transformations of the form $\theta_A \to \tilde{\theta}_A = \theta_A \exp(+i\,\alpha)$, and $\theta_B \to \tilde{\theta}_B = \theta_B \exp(-i\,\alpha)$. Thus the spontaneous symmetry breaking during the Bose–Einstein condensation relates to $SO(2)_{AB}$, instead of the individual symmetries. Altogether, linearizing around both fields yields two excitations, where one *has* to be a "Nambu–Goldstone Boson" (*i.e.*, a zero-mass excitation), while there are no constraints on the mass of the second quasi-particle.

For mimicking gravity, besides the general structure of the emergent spacetime geometry, we also need to know the degrees of freedom of the metric tensor. In the case of a *single* scalar field the acoustic metric (a rank symmetric $n \times n$ two tensor) has $2\,n - 1$ non-zero components. But only three of them are functions of time and space: the density, the speed of sound, and the background velocity potential of the fluid / superfluid. The continuity equation imposes an additional constraint onto the parameters, such that we are left with effectively *two degrees of freedom*. An alternative way to get to the same result is to consider that the Bose–Einstein condensate is a complex-valued field, with only two independent parameters, the density and background phase.

The relatively low number of degrees of freedom, and the conformally flat spatial slice of the acoustic line-element, makes it impossible to mimic all features of general relativity. We have illustrated this by considering the rotating Kerr black hole, where it is not possible to cast the analogue metric into Kerr form. However it is possible to bring the acoustic metric into the form of the equatorial plane of the Kerr black hole, which is sufficient to exhibit almost all of the interesting physics, *e.g.*, apparent horizon and ergoregion.

So far we have summarized only the low-energy / long-distance regime of analogue models for gravity. However, an essential part of this thesis has been based on "extending" the analogue model programme towards an emergent spacetime picture — one that more accurately describes the high-energy / short-distance part of the excitation spectrum.

By definition Lorentz symmetry in the analogue model programme is an emergent symmetry.

The Lorentz invariant geometrical object (be it a usual metric or some Finslerian generalization) is a sufficiently good approximation to describe the long-distance behavior for linearized perturbations around the background field. At short distances non-perturbative corrections — as they are not obtained from any loop calculation — *not only* modify the dispersion relation, they also enter into the metric components. In this thesis we showed that the former, the modifications in the dispersion relation, are of interest for issues related to general framework of Lorentz symmetry breaking as a part of quantum gravity phenomenology, while the latter *may* alter the quantum aspects of the analogue model.

We explicitly calculated the modifications in the dispersion relations for perturbations in two coupled Bose–Einstein condensates. In this part of our calculations we focused on a field-configuration capable of mimicking special relativity in the infrared limit. The emergent quantum field theory yields zero mass *and* non-zero mass quasi-particles, and automatically experiences Lorentz symmetry breaking due to ultraviolet physics. The dispersion relation is of the form

$$\omega_k^2 = \omega_0^2 + (1+\eta_2)\ c^2\, k^2 + \eta_4 \left(\frac{\hbar}{M_{\mathrm{LIV}}}\right)^2 k^4 + \cdots .$$

Here $\eta_4 \approx 1$ is of order one for zero mass and non-zero mass particles. While η_4 generically shows no *further* suppression, η_2 is suppressed by the smallness of the ratio of the quasi-particle mass to the scale of the Lorentz violation. In particular the Lorentz symmetry breaking mechanism in our emergent spacetime avoids the naturalness problem that arises in the effective field theory framework.

We also included the non-perturbative corrections for single background fields: In general effective curved spacetimes the "conventional" geometry has to be replaced by a momentum-dependent "rainbow" geometry. The momentum-dependence in the metric components is suppressed by the analogue "Planck scale" / "Lorentz symmetry breaking scale". The analogue "Planck scale", $\ell_{\mathrm{Planck}} = \ell_{\mathrm{Planck}}(t, \mathbf{x})$, *may* be a function of time and space.

The notion of "rainbow" metrics has now supplied us with a more accurate description for the ultraviolet physics, and enabled us to study the robustness of "cosmological particle production in rainbow metrics" emerging from a Bose gas. We showed that the analogy is sufficiently good for mimicking parts of cosmological inflation, but in general the particle production process presented in this thesis (*i.e.*, time-dependent modifications of the microscopic interaction-strength) shows significant model-dependent effects in the particle spectrum. In our model sub-Hubble horizon quantum field modes can both cross *and* re-enter the Hubble "horizon" *during* the inflationary epoch.

This behavior of the quantum field modes is due to a time-dependent growing "Planck length", and the quantum modes gradually (*i.e.*, mode-by-mode) de-couple from the emergent spacetime picture. The *effective* expansion gradually comes to an end.

It is also noteworthy that the commutation relation for the perturbations in terms of the emergent scalar field and its conjugate momentum with respect to the preferred rest-frame — the laboratory frame — exhibits an explicit momentum-dependence:

$$\left[\partial_t \hat{\theta}_k, \hat{\theta}_k\right] \sim U + k^2 \,. \tag{7.1}$$

Consequently, the size of the quantum fluctuation is growing with the momentum of the quantum field mode. (In a sense, Planck's constant is being generalized in a momentum-dependent manner.) That is, the precision with which you can measure the macroscopic field variable $\langle \hat{\theta}_k \rangle$ decreases as momentum increases.

This behavior is related to the fact that as one goes to smaller and smaller distances the emergent spacetime picture has to be replaced by the microscopic substructure, and the notion of the field and its conjugate momentum vanish. In the high-end ultraviolet regime collective excitations are overruled by microscopic physics.

To conclude this thesis we summarize *possible* lessons to be learnt for emergent spacetimes.
Emergent spacetime geometries *involve:*

- *A microscopic system of fundamental objects (e.g. strings, atoms or molecules);*
- *a dominant mean field regime,where the microscopic degrees of freedom give way to collective variables;*
- *a geometrical object (e.g. a symmetric tensor) dominating the evolution of linearized classical and quantum excitations around the mean field;*
- *an emergent Lorentz symmetry for the long-distance behavior of the geometrical object;*

While the geometrical object supplies a measure of "distance" for excitations in the mean field limit, the fundamental microscopic objects (and their interactions) are the ones that at the same time determine both the nature of classical and quantum excitations, and the structure of the geometrical object. Independent of the specific microscopic system, we will refer to the resulting general concept as emergent spacetime. The Lorentz symmetry breaking seems to be related to existence of a preferred frame [93].

We do not wish to comment directly on the relevance of emergent spacetimes for the quantum gravity programme, as it is far beyond the scope of this thesis. However we hoped we have convinced the reader of the diversity and utility of the analogue gravity programme, that makes use of interdisciplinary approaches to investigate areas where conventional methods for quantum aspects of gravity seem not to deliver a coherent picture, or show limited progress.

"The appearance is not supported by any existent different from itself; it has its own being."
Being and Nothingness by *Jean-Paul Sartre*.

APPENDIX A

Publications not included in the thesis

A.1 | Generating perfect fluid spheres in general relativity

Petarpa Boonserm, Matt Visser, and Silke Weinfurtner

Electronic preprint gr-qc/0503007.

Published as **Physical Review D 71 (2005) 124037**

Ever since Karl Schwarzschild's 1916 discovery of the spacetime geometry describing the interior of a particular idealized general relativistic star — a static spherically symmetric blob of fluid with position independent density — the general relativity community has continued to devote considerable time and energy to understanding the general-relativistic static perfect fluid sphere. Over the last 90 years a tangle of specific perfect fluid spheres has been discovered, with most of these specific examples seemingly independent from each other. To bring some order to this chaos, in this article we develop several new transformation theorems that map perfect fluid spheres into perfect fluid spheres. These transformation theorems sometimes lead to unexpected connections between previously known perfect fluid spheres, sometimes lead to new previously unknown perfect fluid spheres, and in general can be used to develop a systematic way of classifying the set of all perfect fluid spheres.

A.2 | Solution generating theorems for the TOV equation

Petarpa Boonserm, Matt Visser, and Silke Weinfurtner

Electronic preprint gr-qc/0607001.

The Tolman–Oppenheimer–Volkov [TOV] equation constrains the internal structure of general relativistic static perfect fluid spheres. We develop several "solution generating" theorems for the TOV, whereby any given solution can be "deformed" to a new solution. Because the theorems we develop work directly in terms of the physical observables — pressure profile and density profile — it is relatively easy to check the density and pressure profiles for physical reasonableness. This work complements our previous article [Phys. Rev. **D71** (2005) 124307; gr-qc/0503007] wherein a similar "algorithmic" analysis of the general relativistic static perfect fluid sphere was presented in terms of the spacetime geometry — in the present analysis the pressure and density are primary and the spacetime geometry is secondary. In particular, our "deformed" solutions to the TOV equation are conveniently parameterized in terms of $\delta\rho_c$ and δp_c, the *shift* in the central density and central pressure.

A.3 | Analogue model of a FRW universe in Bose–Einstein condensates: Application of the classical field method

Piyush Jain, Silke Weinfurtner, Matt Visser, and C. W. Gardiner

Electronic preprint cond-mat/0705.2077

Accepted for publication in **Physical Review A**

Analogue models of gravity have been motivated by the possibility of investigating phenomena not readily accessible in their cosmological counterparts. In this paper, we investigate the analogue of cosmological particle creation in a Friedmann–Robertson–Walker universe by numerically simulating a Bose–Einstein condensate with a time-dependent scattering length. In particular, we focus on a two-dimensional homogeneous condensate using the classical field method via the truncated Wigner approximation. We show that for various forms of the scaling function the particle production is consistent with the underlying theory in the long wavelength limit. In this context, we further discuss the implications of modified dispersion relations that arise from the microscopic theory of a weakly interacting Bose gas.

A.4 | Effective refractive index tensor for weak field gravity

Petarpa Boonsern, Celine Cattoen, Tristan Faber, Matt Visser, and Silke Weinfurtner

Electronic preprint gr-qc/0411034.

Published as **Class. Quant. Grav. 22 (2006) 1905-1916**

Gravitational lensing in a weak but otherwise arbitrary gravitational field can be described in terms of a 3×3 tensor, the "effective refractive index". If the sources generating the gravitational field all have small internal fluxes, stresses, and pressures, then this tensor is automatically isotropic and the "effective refractive index" is simply a scalar that can be determined in terms of a classic result involving the Newtonian gravitational potential. In contrast if anisotropic stresses are ever important then the gravitational field acts similarly to an anisotropic crystal. We derive simple formulae for the refractive index tensor, and indicate some situations in which this will be important.

APPENDIX B

Klein–Gordon equation and exterior derivatives

We use this appendix to enable readers that are somewhat unfamiliar with the notation of exterior differential forms to relate to the alternative representation of the Klein–Gordon equation in terms of exterior differential forms: [1]

$$*d(*d\hat{\phi}) = \frac{(-1)^n}{\sqrt{-g}}\,\partial_a\left(\sqrt{-g}\,g^{ab}\,\partial_b\hat{\phi}\right)\,. \tag{B.1}$$

B.1 | Differential forms and exterior derivatives in brief

A s-form is a completely antisymmetric tensor of type T^0_s. For example a 0-form corresponds to a scalar, a 1-form to a covector, a 2-form is a covariant tensor antisymmetric in both indices, and so on. Exterior derivatives of a tensor produce covariant objects involving derivatives of the tensor, without the notation of connexions (or any parallel transport), such that completely anti-symmetrized partial derivatives of s-forms transform as tensors. The exterior derivative (denoted as d) transforms a s-form F into a $(s+1)$-form dF,

$$\{dF\}_{a_1\,a_2\,\ldots\,a_{s+1}} = (s+1)\,\partial_{[a_1}F_{a_2\,a_3\,\ldots\,a_{s+1}]}\,. \tag{B.2}$$

The Levi–Civita tensor is a n-form defined by

$$\epsilon_{a_1\,a_2\,\ldots\,a_n} = \sqrt{-\det(g_{ab})}\,\mathrm{signum}(a_1\,a_2\,\ldots\,a_n) = \sqrt{-g}\,\mathrm{sig}(a_1\,a_2\,\ldots\,a_n)\,, \tag{B.3}$$

[1] Note that "colored" indices are internal indices.

where the last step is purely cosmetic, to shorten the expressions below. We can straightforwardly write down the inverse Levi–Civita symbol as

$$\epsilon^{a_1\, a_2\, \ldots\, a_n} = \frac{1}{\sqrt{-\det(g)}}\, \mathrm{sig}(a_1\, a_2\, \ldots\, a_n)\,, \tag{B.4}$$

so that

$$\epsilon^{a\, c_1\, \ldots\, c_{n-1}}\, \epsilon_{b\, c_1\, \ldots\, c_{n-1}} = (n-1)!\, \delta^a{}_b\,. \tag{B.5}$$

Notice that sig is proportional to an anti-symmetic tensor (form), and hence

$$\mathrm{sig}(a_1\, a_2\, \ldots\, a_n) = (-1)^{n-1}\, \mathrm{sig}(a_2\, \ldots\, a_n\, a_1)\,. \tag{B.6}$$

Finally, we introduce the Hodge star operator (denoted by $*$) as the operation that transforms a s-form into a $(n-s)$-form,

$$\{*F\}_{a_1\, a_2\, \ldots\, a_{n-s}} = \frac{1}{s!}\, \epsilon_{a_1\, a_2\, \ldots\, a_{n-s}}{}^{b_1\, b_2\, \ldots b_s}\, \{F\}_{b_1\, b_2\, \ldots\, b_s}\,, \tag{B.7}$$

and are now ready to show the equivalence between the index-free version of the Klein–Gordon equation, as pointed out in Eq. (B.1).

B.2 | Index-free Klein–Gordon equation

The field operator $\hat{\phi}$ is a scalar operator, hence a 0-form, and applying Eq. (B.2) we get,

$$d\hat{\phi} = \hat{\phi}_{,a}\,. \tag{B.8}$$

We further apply the Hodge star operator and get,

$$*(d\hat{\phi}) = *\hat{\phi}_{,a} = \epsilon_{a_1\, a_2\, \ldots\, a_{n-1}}{}^{b}\, \hat{\phi}_{,b} = \sqrt{-g}\, \mathrm{sig}(a_1\, a_2\, \ldots\, a_n)\, g^{a_n\, b}\, \hat{\phi}_{,b}\,. \tag{B.9}$$

Once again we need to apply the exterior derivative,

$$\begin{aligned} d(*d\hat{\phi}) &= n\, \partial_{[c}\left(\mathrm{sig}(a_1\, a_2\, \ldots\, a_{n-1]}\, a_n)\, g^{a_n\, b_1}\, \hat{\phi}_{,b_1} \sqrt{-g}\right)\,, & \text{(B.10)}\\ &= n\,(-1)^{n-1}\, \mathrm{sig}([a_1\, a_2\, \ldots\, a_n)\, \partial_{c]}\left(g^{a_n\, b_1}\, \hat{\phi}_{,b_1} \sqrt{-g}\right)\,, & \text{(B.11)} \end{aligned}$$

and subsequently the Hodge star operator leads us to the final result:

$$\begin{aligned} *d(*d\hat{\phi}) &= \frac{n\,(-1)^{n-1}}{n!}\, \epsilon^{b_1\, b_2\, \ldots\, b_{n-1}\, b_n}\, \frac{(-1)}{\sqrt{-g}}\, \mathrm{sig}(b_1\, b_2\, \ldots\, b_{n-1}\, a_n)\, \partial_{b_n}\left(\sqrt{-g}\, g^{a_n\, b_1}\, \hat{\phi}_{,b_1}\right)\,, & \text{(B.12)}\\ &= \frac{(-1)^n}{\sqrt{-g}}\, \delta^{b_n}{}_{a_n}\, \partial_{b_n}\left(\sqrt{-g}\, g^{a_n\, b_1}\, \hat{\phi}_{,b_1}\right)\,, & \text{(B.13)}\\ &= \frac{(-1)^n}{\sqrt{-g}}\, \partial_{a_n}\left(\sqrt{-g}\, g^{a_n\, b_1}\, \hat{\phi}_{,b_1}\right)\,. & \text{(B.14)} \end{aligned}$$

Relabeling $a_n \to a$ and $b_1 \to b$ yields Eq. (B.2).

APPENDIX C

Finsler and co–Finsler geometries

Finsler geometries are sufficiently unusual that a brief discussion is in order — especially in view of the fact that the needs of the physics community are often somewhat at odds with what the mathematical community might view as the most important issues. Below are some elementary results, where we emphasise that for the time being we are working with ordinary "Euclidean signature" Finsler geometry. For general references, see [41, 159, 8, 9, 167].

C.1 | Basics

Euler theorem: If $H(z)$ is homogeneous of degree n then

$$z^i \, \frac{\partial H(z)}{\partial z^i} = n \, H(z). \tag{C.1}$$

Finsler function: Defined on the "slit tangent bundle" $T_{\neq 0}(M)$ such that $F : T_{\neq 0}(M) \to [0, +\infty)$ where

$$F(x, t): \quad F(x, \lambda t) = \lambda \, F(x, t), \tag{C.2}$$

and

$$T_{\neq 0}(M) = \bigcup_{x \in M} \left[T_x - \{\vec{0}\} \right]. \tag{C.3}$$

That is, the Finsler function is a defined only for nonzero tangent vectors $t \in [T_x - \{\vec{0}\}]$, and for any fixed direction is linear in the size of the vector.

Finsler distance:

$$d_\gamma(x, y) = \int_x^y F(x(\tau), dx/d\tau) \, d\tau; \qquad \tau = \text{ arbitrary parameter}. \tag{C.4}$$

Finsler metric:

$$g_{ij}(x,t) = \frac{1}{2}\frac{\partial^2[F^2(x,t)]}{\partial t^i\ \partial t^j}. \tag{C.5}$$

The first slightly unusual item is the introduction of co–Finsler structure:
co–Finsler function: Define a co–Finsler structure on the cotangent bundle by Legendre transformation of $F^2(x,t)$. That is:

$$G^2(x,p) = t^j(p)\ p_j - F^2(x,t(p)) \tag{C.6}$$

where $t(p)$ is defined by the Legendre transformation condition

$$\frac{\partial[F^2]}{\partial t^j}(x,t) = p_j. \tag{C.7}$$

Note

$$\frac{\partial p_j}{\partial t^k} = \frac{\partial[F^2]}{\partial t^j\ \partial t^k} = 2g_{jk}(x,t), \tag{C.8}$$

which is why we demand the Finsler metric be nonsingular.
Lemma: $G(x,p)$ defined in this way is homogeneous of degree 1.
Proof: Note

$$z^i\ \frac{\partial H(z)}{\partial z^i} = n\ H(z) \tag{C.9}$$

implies

$$z^i\ \frac{\partial}{\partial z^i}\left[\frac{\partial^m}{(\partial z)^m}H(z)\right] = (n-m)\ \left[\frac{\partial^m}{(\partial z)^m}H(z)\right]. \tag{C.10}$$

In particular:

- F^2 is homogeneous of degree 2.
- g_{ij} is homogeneous of degree 0.
- $\partial[F^2]/\partial t$ is homogeneous of degree 1.
- Therefore $p(t)$ is homogeneous of degree 1, *and* $t(p)$ is homogeneous of degree 1.
- Therefore $t(p)p - F^2(t(p))$ is homogeneous of degree 2.
- Therefore $G(p)$ is homogeneous of degree 1.

Thus from a Finsler function $F(x,t)$ we can always construct a co–Finsler function $G(x,p)$ which is homogeneous of degree 1 on the cotangent bundle.

From the way the proof is set up it is clearly reversible — if you are given a co–Finsler function $G(x,p)$ on the cotangent bundle this provides a *natural* way of extracting the corresponding Finsler function:

$$F^2(x,t) = t\ p(t) - G^2(x,p(t)). \tag{C.11}$$

C.2 | Connection with the quasi-particle PDE analysis

From the PDE-based analysis we obtain the second-order system of PDEs

$$\partial_a \left(f^{ab}{}_{\mathrm{AB}}\, \partial_b \theta^B \right) + \text{lower order terms} = 0. \tag{C.12}$$

We are now generalizing in the obvious manner to any arbitrary number n of interacting BECs, but the analysis is even more general than that — it applies to any field-theory normal-mode analysis that arises from a wide class of Lagrangian based systems [13, 14].

Going to the eikonal approximation this becomes

$$f^{ab}_{\mathrm{AB}}\, p_a p_b\, \epsilon^B + \text{lower-order terms} = 0, \tag{C.13}$$

which leads (neglecting lower order terms for now) to the Fresnel-like equation

$$\det[f^{ab}_{\mathrm{AB}}\, p_a p_b] = 0. \tag{C.14}$$

But by expanding the $n \times n$ determinant (n is the number of fields, not the dimension of spacetime) we have

$$\det[f^{ab}_{\mathrm{AB}}\, p_a p_b] = Q^{abcd\cdots}\, p_a p_b p_c p_d \ldots \tag{C.15}$$

where if there are n fields there will be $2n$ factors of p.

Now define

$$Q(x,p) = Q^{abcd\cdots}\, p_a p_b p_c p_d \ldots, \tag{C.16}$$

and

$$G(x,p) = \sqrt[2n]{Q(x,p)} = [Q(z,p)]^{1/(2n)}, \tag{C.17}$$

then

- $Q(x,p)$ is homogeneous of degree $2n$.
- $G(x,p)$ is homogeneous of degree 1, and hence is a co–Finsler function.
- We can now Legendre transform $G \to F$, providing a chain

$$Q(x,p) \to G(x,p) \to F(x,t). \tag{C.18}$$

Can this route be reversed?

Step 1: We can always reverse $F(x,t) \to G(x,p)$ by Legendre transformation.
Step 2: We can always define

$$g^{ab}(x,p) = \frac{1}{2} \frac{\partial}{\partial p_a} \frac{\partial}{\partial p_b} [G(x,p)^2], \tag{C.19}$$

this is homogeneous of degree 0, but is generically not smooth at $p = 0$.

In fact, *if* $g^{ab}(x, p)$ is smooth at $p = 0$ then there exits a limit

$$g^{ab}(x, p \to 0) = \bar{g}^{\,ab}(x), \tag{C.20}$$

but since $g^{ab}(x, p)$ is homogeneous of degree 0 this implies

$$g^{ab}(x, p) = \bar{g}^{\,ab}(x) \qquad [\forall p], \tag{C.21}$$

and so the geometry simplifies Finsler $\to$ Riemann.

This observation suggests the following definition.

Definition: A co–Finsler function $G(x, p)$ is $2n$-smooth iff the limit

$$\frac{1}{(2n)!} \lim_{p \to 0} \left(\frac{\partial}{\partial p} \right)^{2n} G(x, p)^{2n} = \bar{Q}^{\,abcd\ldots} \tag{C.22}$$

exists independent of the direction p in which you approach zero.

Lemma: If $G(x, p)$ is $2n$-smooth then

$$G(x, p)^{2n} = \bar{Q}^{\,abcd\ldots}\; p_a p_b p_c p_d \ldots, \tag{C.23}$$

and indeed

$$G(x, p) = \sqrt[2n]{\bar{Q}^{\,abcd\ldots}\; p_a p_b p_c p_d \ldots.} \tag{C.24}$$

Proof: G^{2n} is homogeneous of degree $2n$, so $(\partial/\partial p)^{2n} G^{2n}$ is homogeneous of degree 0. Therefore if the limit

$$\frac{1}{(2n)!} \lim_{p \to 0} \left(\frac{\partial}{\partial p} \right)^{2n} G(x, p)^{2n} = \bar{Q}^{\,abcd\ldots} \tag{C.25}$$

exists, it follows that

$$\frac{1}{(2n)!} \left(\frac{\partial}{\partial p} \right)^{2n} G(x, p)^{2n} = \bar{Q}^{\,abcd\ldots} \qquad [\forall p], \tag{C.26}$$

and so the result follows.

Special case $n = 1$*:* If $G(x, p)$ is 2-smooth then

$$\frac{1}{2} \frac{\partial^2}{\partial p^a\, \partial p_b} G(x, p)^2 = \bar{Q}^{\,ab} = g^{ab}(x, p), \tag{C.27}$$

and co–Finsler $\to$ Riemann.

These observations have a number of implications:

- For all those co–Finsler functions that are $2n$ smooth we *can* recover the tensor $Q^{abcd\ldots}$.
- Not all co–Finsler functions are $2n$ smooth, and for those functions we *cannot* extract $Q^{abcd\ldots}$ in any meaningful way.

- But those specific co–Finsler functions that arise from the leading symbol of a 2nd-order system of PDEs are naturally $2n$-smooth, and so for the specific co–Finsler structures we are physically interested in

$$Q(x,p) \leftrightarrow G(x,p) \leftrightarrow F(x,t). \tag{C.28}$$

- Therefore, in the physically interesting case the Finsler function $F(x,t)$ encodes all the information present in $Q^{abcd\cdots}$.

Special case $n = 2$: For two fields (appropriate for our 2-BEC system), we can follow the chain

$$\mathbf{f}^{ab} \rightarrow Q(x,p) \leftrightarrow G(x,p) \leftrightarrow F(x,t) \tag{C.29}$$

to formally write

$$ds^4 = g_{abcd}\, dx^a dx^b dx^c dx^d, \tag{C.30}$$

or

$$ds = \sqrt[4]{g_{abcd}\, dx^a dx^b dx^c dx^d}. \tag{C.31}$$

This is one of the "more general" cases Riemann alludes to in his inaugural lecture of 1854 [154, 155].

This discussion makes it clear that the general geometry in our 2-BEC system is a 4-smooth Finsler geometry. It is only for certain special cases that the Finsler geometry specializes first to "multi-metric" and then to "mono-metric" Riemannian geometries.

C.3 | Lorentzian signature Finsler geometries

The distinction between Finsler and pseudo–Finsler geometries has to do with the distinction between elliptic and hyperbolic PDEs. Elliptic PDEs lead to ordinary Finsler geometries, hyperbolic PDEs lead to *pseudo*–Finsler geometries.

Remember that in special relativity we typically define

$$d_\gamma(x,y) = \int_x^y \sqrt{g_{ab}(dx^a/d\tau)(dx^b/d\tau)}\, d\tau, \tag{C.32}$$

then

- $d_\gamma(x,y) \in \boldsymbol{R}^+$ for spacelike paths;
- $d_\gamma(x,y) = 0$ for light-like (null) paths;
- $d_\gamma(x,y) \in \boldsymbol{I}^+$ for timelike paths;

The point is that even in special relativity (and by implication in general relativity) "distances" do not have to be real numbers. This is why physicists deal with *pseudo*–Riemannian [Lorentzian] geometries, not (strictly speaking) Riemannian geometries.

To see how this generalizes in a Finsler situation let us first consider a co–Finsler structure that is multi-metric, that is:

$$Q(x,p) = \Pi_{i=1}^{n}(g_i^{ab}p_a p_b), \tag{C.33}$$

where each one of these n factors contains a Lorentzian signature matrix and so can pass through zero. Then

$$G(x,p) = \sqrt[2n]{\Pi_{i=1}^{n}(g_i^{ab}p_a p_b)}, \tag{C.34}$$

and

$$G(x,p) \in \exp\left(\frac{i\pi\ell}{2n}\right)\ \boldsymbol{R}^{+}, \tag{C.35}$$

where

- $\ell = 0 \rightarrow G(x,p) \in \boldsymbol{R}^{+} \rightarrow$ outside all n signal cones;
- $\ell = n \rightarrow G(x,p) \in \boldsymbol{I}^{+} \rightarrow$ inside all n signal cones.

So we can now define

- Spacelike $\leftrightarrow$ outside all n signal cones $\leftrightarrow$ G real;
- Null $\leftrightarrow$ on any one of the n signal cones $\leftrightarrow$ G zero;
- Timelike $\leftrightarrow$ inside all n signal cones $\leftrightarrow$ G imaginary;
- plus the various "intermediate" cases:

$$\text{"intermediate"} \leftrightarrow \text{inside } \ell \text{ of } n \text{ signal cones} \leftrightarrow G \in i^{\ell/n} \times \boldsymbol{R}^{+}. \tag{C.36}$$

Now this basic idea survives even if we do not have a multi-metric theory. The condition $Q(x,p) = 0$ defines a polynomial of degree $2n$, and so defines n nested sheets (possibly crossing in places). Compare with Courant and Hilbert's discussion of the Monge cone [47].

That is:

$$\begin{aligned} Q(x,p) = 0 \quad &\Leftrightarrow \quad Q(x,(E,\vec{p})) = 0; \\ &\Leftrightarrow \quad \text{polynomial of degree } 2n \text{ in } E \text{ for any fixed } \vec{p}; \\ &\Leftrightarrow \quad \text{in each direction } \exists\ 2n \text{ roots in } E; \\ &\Leftrightarrow \quad \text{corresponds to } n \text{ [topological] cones.} \end{aligned}$$

(These are topological cones, not geometrical cones, and the roots might happen to be degenerate.)

Question: Should we be worried by the fact that the co-metric g^{ab} is singular on the signal cone? (In fact on all n of the signal cones.) Not really. We have

$$G(x,p) = \sqrt[2n]{\bar{Q}^{\,abcd\ldots}\; p_a p_b p_c p_d \ldots}, \tag{C.37}$$

so

$$g^{ab}(x,p) = \frac{1}{2}\frac{\partial^2}{\partial p^a\, \partial p_b}\left(\sqrt[n]{Q(x,p)}\right) = \frac{1}{2n}\frac{\partial}{\partial p_b}\left\{Q^{\frac{1}{n}-1}\; Q^{abcd\ldots}\; p_b p_c p_d \ldots\right\}, \tag{C.38}$$

whence

$$\begin{aligned} g^{ab}(x,p) &= \frac{1}{2n}Q^{\frac{1}{n}-1}\; Q^{abcd\ldots}\; p_c p_d \ldots \\ &\quad + \frac{1}{2n}\left(\frac{1}{n}-1\right) Q^{\frac{1}{n}-2}\left[Q^{acde\ldots}\; p_c p_d p_e \ldots\right]\left[Q^{bfgh\ldots}\; p_f p_g p_h \ldots\right], \end{aligned} \tag{C.39}$$

which we can write as

$$\begin{aligned} g^{ab}(x,p) &= \frac{1}{2n}Q^{-(n-1)/n}\; Q^{abcd\ldots}\; p_c p_d \ldots \\ &\quad - \frac{1}{2n}\frac{n-1}{n}Q^{-(2n-1)/n}\left[Q^{acde\ldots}\; p_c p_d p_e \ldots\right]\left[Q^{bfgh\ldots}\; p_f p_g p_h \ldots\right]. \end{aligned} \tag{C.40}$$

Yes, this naively looks like it's singular on the signal cone where $Q(x,p) = 0$. But no, this is not a problem: Consider

$$g^{ab}p_a p_b = \frac{1}{2n}Q^{-(2n-1)/n}Q - \frac{1}{2n}\frac{n-1}{n}Q^{-(2n-1)/n}Q^2, \tag{C.41}$$

then

$$g^{ab}p_a p_b = \frac{1}{2n}\left(1 - \frac{n-1}{n}\right)Q^{1/n} = \frac{1}{2n^2}\; Q^{1/n} = 0, \tag{C.42}$$

and this quantity is definitely non-singular.

C.4 | Summary

In short:

- pseudo–Finsler functions arise naturally from the leading symbol of hyperbolic systems of PDEs;
- pseudo–Finsler geometries provide the natural "geometric" interpretation of a multi-component PDE before fine tuning;
- In particular the natural geometric interpretation of our 2-BEC model (before fine tuning) is as a 4-smooth pseudo–Finsler geometry.

APPENDIX D

Some matrix identities

To simplify the flow of argument in the body of the thesis, here we collect a few basic results on 2×2 matrices that are used in our analysis.

D.1 | Determinants

Theorem: For any two 2×2 matrix A:

$$\det(A) = \frac{1}{2}\left\{\mathrm{tr}[A]^2 - \mathrm{tr}[A^2]\right\}. \tag{D.1}$$

This is best proved by simply noting

$$\det(A) = \lambda_1\lambda_2 = \frac{1}{2}\left[(\lambda_1+\lambda_2)^2 - (\lambda_1^2+\lambda_2^2)\right] = \frac{1}{2}\left\{\mathrm{tr}[A]^2 - \mathrm{tr}[A^2]\right\}. \tag{D.2}$$

If we now define 2×2 "trace reversal" (in a manner reminiscent of standard GR) by

$$\bar{A} = A - \mathrm{tr}[A]\,\mathbf{I}; \qquad \bar{\bar{A}} = A; \tag{D.3}$$

then this looks even simpler

$$\det(A) = -\frac{1}{2}\mathrm{tr}[A\,\bar{A}] = \det(\bar{A}). \tag{D.4}$$

A simple implication is now:
Theorem: For any two 2×2 matrices A and B:

$$\det(A+\lambda\,B) = \det(A) + \lambda\,\{\mathrm{tr}[A]\mathrm{tr}[B] - \mathrm{tr}[A\,B]\} + \lambda^2\det(B). \tag{D.5}$$

which we can also write as

$$\det(A + \lambda\ B) = \det(A) - \lambda\ \mathrm{tr}[A\ \bar{B}\,] + \lambda^2\ \det(B). \tag{D.6}$$

Note that $\mathrm{tr}[A\ \bar{B}\,] = \mathrm{tr}[\bar{A}\ \ B]$.

D.2 | Hamilton–Cayley theorems

Theorem: For any two 2×2 matrix A:

$$A^{-1} = \frac{\mathrm{tr}[A]\ \ \mathbf{I} - A}{\det[A]} = -\frac{\bar{A}}{\det[\bar{A}\,]}. \tag{D.7}$$

Theorem: For any two 2×2 matrix A:

$$A^{1/2} = \ \pm \left\{ \frac{A \pm \sqrt{\det A}\ \ \mathbf{I}}{\sqrt{\mathrm{tr}[A] \pm 2\sqrt{\det A}}} \right\}. \tag{D.8}$$

APPENDIX E

Junction conditions

For the benefit of readers who may not wish to deal with differential forms and conjugate momenta as discussed in Chapter 5, we now present a "low-brow" calculation of the α and β coefficients — for the specific physics problem we are interested in — in two different coordinate systems. Both co-ordinate systems lead to the same physics result, and both give explicit expressions for the conserved inner product, the modes, how to normalize them, and of course the junction conditions.

E.1 | Basics

The master PDE that everything starts from is

$$\partial_t \left(-\frac{\hbar}{U}\, \partial_t \theta \right) + \frac{n_0 \hbar}{m}\, \nabla^2 \theta = 0 \tag{E.1}$$

where n_0, m and $\hbar$ are constant, while

$$U(t) = U^{1} \Theta(t^{1\,2} - t) + U^{2} \Theta(t - t^{1\,2})\,. \tag{E.2}$$

The most basic forms of the junction conditions are then that the field operators θ, and its conjugate momentum $(\hbar/U)\ \partial_t \theta$, are continuous at $t^{1\,2}$. If these conditions are not satisfied, then there is no way that the master PDE can be satisfied at $t^{1\,2}$ — there would be delta-function contributions on the LHS that would not cancel against anything on the RHS. These two junction conditions can be written as

$$[\theta] = 0; \qquad \left[\frac{\hbar}{U}\, \partial_t \theta \right] = 0. \tag{E.3}$$

Note that we are here working in terms of physical laboratory time, and will continue to do so until we get to the subsection where we explain how we could have equally well done things in terms of "canonical time". One can read the conserved inner product off by starting directly from the PDE itself — noting that this PDE is defined for all time, and then considering the quantity

$$(\theta_a, \theta_b) = \int \left(\theta_a \, \frac{\hbar}{U} \, \partial_t \theta_b - \theta_b \, \frac{\hbar}{U} \, \partial_t \theta_a \right) d^d x \,, \tag{E.4}$$

where θ_a and θ_b are solutions of the master PDE. Then by Gauss' law (or the fundamental theorem of calculus)

$$\begin{aligned} &(\theta_a, \theta_b)|_{\text{final}} - (\theta_a, \theta_b)|_{\text{initial}} \\ &\qquad = \int \partial_t \left(\theta_a \, \frac{\hbar}{U} \, \partial_t \theta_b - \theta_b \, \frac{\hbar}{U} \, \partial_t \theta_a \right) d^{d+1} x. \end{aligned} \tag{E.5}$$

Now apply Leibnitz' rule, the PDE, and an integration by parts to obtain

$$(\theta_a, \theta_b)_{\text{final}} - (\theta_a, \theta_b)_{\text{initial}} = 0. \tag{E.6}$$

So this is the correct conserved inner product for the Klein–Gordon-like PDE we are starting with. Note that this conservation law, the way we have set it up holds for any and all initial and final times, regardless of which side of the junction they are located.

E.2 | The two non-overlapping simple regions

In region $\underline{1}$ ($t < t^{\underline{1}\underline{2}}$) the master PDE reduces to

$$\partial_t \left(-\frac{\hbar}{U^{\underline{1}}} \, \partial_t \theta \right) + \frac{n_0 \hbar}{m} \, \nabla^2 \theta = 0, \tag{E.7}$$

and can be rearranged to

$$-\partial_t^2 \theta + \frac{n_0 \; U^{\underline{1}}}{m} \, \nabla^2 \theta = 0. \tag{E.8}$$

Introducing

$$(c^{\underline{1}})^2 = \frac{n_0 \; U^{\underline{1}}}{m}, \tag{E.9}$$

this becomes

$$-\partial_t^2 \theta + (c^{\underline{1}})^2 \, \nabla^2 \theta = 0, \tag{E.10}$$

with the understanding that this PDE holds only in region $\underline{1}$ (*i.e.*, $t < t^{\underline{1}\underline{2}}$). Similarly, in region $\underline{2}$ (*i.e.*, $t > t^{\underline{1}\underline{2}}$) the master PDE reduces to

$$-\partial_t^2 \theta + (c^{\underline{2}})^2 \, \nabla^2 \theta = 0. \tag{E.11}$$

The junction conditions are unchanged, though for convenience we can write them in terms of $c^2 = n_0\ U/m$ as

$$[\theta] = 0; \qquad \left[\frac{1}{c^2}\ \partial_t \theta\right] = 0. \tag{E.12}$$

In each individual region the field satisfies the usual flat spacetime Klein-Gordon equation, so solutions are of the form

$$\theta \propto \exp(i[\omega_k t - \mathbf{k}\mathbf{x}])\,, \tag{E.13}$$

where ω_k and $\mathbf{k}$ satisfy the dispersion relation

$$\omega_k = c\,k\,, \tag{E.14}$$

and we have very carefully not yet specified any normalization for these modes. (Nor is c the same in the two regions, it is either $c^{\underline{1}}$ or $c^{\underline{2}}$ as appropriate.)

One thing we can say without further calculation is this: In view of the junction condition $[\theta] = 0$, that is $\theta(t^{\underline{1}\underline{2}-}, \mathbf{x}) = \theta(t^{\underline{1}\underline{2}+}, \mathbf{x})$, the spatial position dependence of the solutions to the PDE on the two sides of the junction must be the same — this implies that in terms of the plane waves above we must enforce $\mathbf{k}$ to be the same in regions $\underline{1}$ and $\underline{2}$, and therefore

$$\frac{\omega_k^{\underline{1}}}{c^{\underline{1}}} = k = \frac{\omega_k^{\underline{2}}}{c^{\underline{2}}}\,. \tag{E.15}$$

E.3 | Normalization

Now let us compare the conserved inner product for the PDE we are physically interested in with the inner product for the naive Klein–Gordon equation. In particular, if initial is before the transition and final is after the transition, then in terms of the naive ordinary Klein–Gordon inner product the conserved inner product for our PDE is

$$(\theta_a, \theta_b)|_{\text{initial}} = \frac{\hbar}{U^{\underline{1}}}\,(\theta_a, \theta_b)_{\text{naive}}\,; \tag{E.16}$$

$$(\theta_a, \theta_b)|_{\text{final}} = \frac{\hbar}{U^{\underline{2}}}\,(\theta_a, \theta_b)_{\text{naive}}\,; \tag{E.17}$$

where $(\theta_a, \theta_b)_{\text{naive}} = \int (\theta_a\ \partial_t \theta_b - \theta_b\ \partial_t \theta_a)\ d^d x$.

This means that properly normalized modes are

$$\sqrt{\frac{U}{\hbar}}\ \frac{1}{\sqrt{2\omega_k}}\ \exp(i[\omega_k t - \mathbf{k}\mathbf{x}]), \tag{E.18}$$

which (ignoring a trivial overall constant factor, that does not change from region $\underline{1}$ to region $\underline{2}$) we might as well write as

$$\frac{c}{\sqrt{2\omega_k}}\ \exp(i[\omega_k t - \mathbf{k}\mathbf{x}]). \tag{E.19}$$

In particular in regions $\underline{1}$ and $\underline{2}$ we want to deal with

$$u_k^{\underline{1}}(t,\mathbf{x}) = \frac{c^{\underline{1}}}{\sqrt{2\omega_k^{\underline{1}}}}\ \exp(i[\omega_k^{\underline{1}}t - \mathbf{kx}]), \tag{E.20}$$

and

$$u_k^{\underline{2}}(t,\mathbf{x}) = \frac{c^{\underline{2}}}{\sqrt{2\omega_k^{\underline{2}}}}\ \exp(i[\omega_k^{\underline{2}}t - \mathbf{kx}]), \tag{E.21}$$

respectively.

E.4 | Applying the junction conditions

In regions $\underline{1}$ and $\underline{2}$ we write the solutions of the PDE as the real parts of

$$\begin{aligned}\theta^{\underline{1}} \;=\;& A\frac{c^{\underline{1}}}{\sqrt{2\omega_k^{\underline{1}}}}\ \exp(i[\omega_k^{\underline{1}}t - \mathbf{kx}]) \\ &+B\frac{c_k^{\underline{1}}}{\sqrt{2\omega_k^{\underline{1}}}}\ \exp(i[-\omega_k^{\underline{1}}t - \mathbf{kx}]),\end{aligned} \tag{E.22}$$

and

$$\begin{aligned}\theta^{\underline{2}} \;=\;& C\frac{c^{\underline{2}}}{\sqrt{2\omega_k^{\underline{2}}}}\ \exp(i[\omega_k^{\underline{2}}t - \mathbf{kx}]) \\ &+D\frac{c^{\underline{2}}}{\sqrt{2\omega_k^{\underline{2}}}}\ \exp(i[-\omega_k^{\underline{2}}t - \mathbf{kx}]).\end{aligned} \tag{E.23}$$

Note that the **x** dependence is the same in all four of these terms and so quietly factors out — this is why we asserted that **k** had to be the same in both regions.

Applying the first junction condition $[\theta] = 0$, at the transition time $t^{\underline{1}\,\underline{2}}$, and using the dispersion relation implies

$$\begin{aligned}&\sqrt{c^{\underline{1}}}\left[A\ \exp(i\omega_k^{\underline{1}}t^{\underline{1}\,\underline{2}}) + B\ \exp(-i\omega_k^{\underline{1}}t^{\underline{1}\,\underline{2}})\right] \\ &= \sqrt{c^{\underline{2}}}\left[C\ \exp(i\omega_k^{\underline{2}}t^{\underline{1}\,\underline{2}}) + D\ \exp(-i\omega_k^{\underline{2}}t^{\underline{1}\,\underline{2}})\right].\end{aligned} \tag{E.24}$$

The second junction condition, $[\partial_t\theta/c^2] = 0$, applied at the transition time $t^{\underline{1}\,\underline{2}}$, implies (after factoring out all the c's and ω's, and using the dispersion relation) that

$$\begin{aligned}&\frac{1}{\sqrt{c^{\underline{1}}}}\left[A\ \exp(i\omega_k^{\underline{1}}t^{\underline{1}\,\underline{2}}) - B\ \exp(-i\omega_k^{\underline{1}}t^{\underline{1}\,\underline{2}})\right] \\ &= \frac{1}{\sqrt{c^{\underline{2}}}}\left[C\ \exp(i\omega_k^{\underline{2}}t^{\underline{1}\,\underline{2}}) - D\ \exp(-i\omega_k^{\underline{2}}t^{\underline{1}\,\underline{2}})\right].\end{aligned} \tag{E.25}$$

These two junction conditions are enough to completely specify the transmission matrix of α's and β's. Indeed, setting $A \to 1$, $B \to 0$, $C \to \alpha$, and $D \to \beta$ and solving for α and β we find

$$\alpha = \frac{1}{2}\left(\sqrt{\frac{c^{\underline{1}}}{c^{\underline{2}}}} + \sqrt{\frac{c^{\underline{2}}}{c^{\underline{1}}}}\right) \exp(-i[c^{\underline{2}} - c^{\underline{1}}]kt^{\underline{1\,2}}); \tag{E.26}$$

$$\beta = \frac{1}{2}\left(\sqrt{\frac{c^{\underline{1}}}{c^{\underline{2}}}} - \sqrt{\frac{c^{\underline{2}}}{c^{\underline{1}}}}\right) \exp(i[c^{\underline{2}} + c^{\underline{1}}]kt^{\underline{1\,2}}); \tag{E.27}$$

which is exactly the result reported in the body of Chapter 5.

E.5 | Using “canonical time”

Let us now pick another time coordinate. Let us call it “canonical time” and define it by

$$T = \int \frac{c(t)^2}{(c_*)^2}\, dt = \int \frac{U(t)}{U_*}\, dt, \tag{E.28}$$

$$dT = \frac{c(t)^2}{(c_*)^2}\, dt = \frac{U(t)}{U_*}\, dt, \tag{E.29}$$

where we have introduced a convenient constant reference point U_* and used this to define a convenient constant reference speed

$$(c_*)^2 = \frac{n_0\, U_*}{m}. \tag{E.30}$$

The the master PDE, which was in the original laboratory time coordinate

$$\partial_t\left(-\frac{\hbar}{U}\,\partial_t\theta\right) + \frac{n_0\hbar}{m}\,\nabla^2\theta = 0, \tag{E.31}$$

now becomes

$$-\partial_T^2\theta + \frac{n_0 U_*^2}{m\, U}\,\nabla^2\theta = 0. \tag{E.32}$$

Recognizing that $n_0 U_*^2/(m\, U) = (c_*)^4/c^2$ and defining

$$c_{\text{eff}}(T) = \frac{(c_*)^2}{c(T)}, \tag{E.33}$$

this can be re-written simply in the form of a “parametrically excited oscillator”

$$-\partial_T^2\theta + c_{\text{eff}}^2(T)\,\nabla^2\theta = 0. \tag{E.34}$$

Assuming an exponential space dependence, separation of variables yields

$$\theta(t, x) = \tilde{\theta}(t)\ \exp(-i\mathbf{kx}), \tag{E.35}$$

so that

$$\partial_T^2 \tilde{\theta} = c_{\text{eff}}^2(T)\; k^2\; \tilde{\theta}. \tag{E.36}$$

The junction conditions, which were originally in terms of laboratory time (refer to equation [E.12]) now become, in terms of canonical time, the very simple:

$$[\theta] = 0; \qquad [\partial_T \theta] = 0. \tag{E.37}$$

The conserved inner product (E.4) can now be re-written

$$(\theta_a, \theta_b) = \frac{\hbar}{U_*} \int (\theta_a\, \partial_T \theta_b - \theta_b\, \partial_T \theta_a)\, d^d x, \tag{E.38}$$

that is

$$(\theta_a, \theta_b) = \frac{\hbar}{U_*}\, (\theta_a, \theta_b)_{\text{naive}}. \tag{E.39}$$

So in "canonical time" coordinates we have a particularly simple PDE, elementary junction conditions, and a trivial inner product — the only "tricky" thing is that we have to use the "effective" sound speed $c_{\text{eff}} = (c_*)^2/c$.

Now in region $\underline{1}$ the original master PDE can be cast into the form

$$-\partial_T^2 \theta + \frac{(c_*)^4}{(c^{\underline{1}})^2}\, \nabla^2 \theta = 0, \tag{E.40}$$

while in region $\underline{2}$

$$-\partial_T^2 \theta + \frac{(c_*)^4}{(c^{\underline{2}})^2}\, \nabla^2 \theta = 0. \tag{E.41}$$

In view of the form of the conserved inner product, the normalized modes are

$$\frac{1}{\sqrt{2\omega_k^{\underline{1}}}}\, \exp(i[\omega_k^{\underline{1}} T - \mathbf{kx}]); \qquad \omega_k^{\underline{1}} = \frac{(c_*)^2}{c^{\underline{1}}}\, k; \tag{E.42}$$

$$\frac{1}{\sqrt{2\omega_k^{\underline{2}}}}\, \exp(i[\omega_k^{\underline{2}} T - \mathbf{kx}]); \qquad \omega_k^{\underline{2}} = \frac{(c_*)^2}{c^{\underline{2}}}\, k. \tag{E.43}$$

Note the "odd looking" form of the dispersion relation — but this is just because $\omega_k^{\underline{1}}$ and $\omega_k^{\underline{2}}$ are not physical frequencies — they are "T-time frequencies".

In regions $\underline{1}$ and $\underline{2}$ we write the solutions of the PDE as the real parts of

$$\theta_{\underline{1}} = A \frac{1}{\sqrt{2\omega_k^{\underline{1}}}}\, \exp(i[\omega_k^{\underline{1}} T - \mathbf{kx}]) + B \frac{1}{\sqrt{2\omega_k^{\underline{1}}}}\, \exp(i[-\omega_k^{\underline{1}} T - \mathbf{kx}]); \tag{E.44}$$

$$\theta_{\underline{2}} = C \frac{1}{\sqrt{2\omega_k^{\underline{2}}}}\, \exp(i[\omega_k^{\underline{2}} T - \mathbf{kx}]) + D \frac{1}{\sqrt{2\omega_k^{\underline{2}}}}\, \exp(i[-\omega_k^{\underline{2}} T - \mathbf{kx}]). \tag{E.45}$$

The first junction condition $[\theta] = 0$, after applying the dispersion relation is

$$\begin{aligned} &\sqrt{c^{\underline{1}}}\Big[A\ \exp(i\omega_k^{\underline{1}} T^{\underline{1}\,\underline{2}}) + B\ \exp(-i\omega_k^{\underline{1}} T^{\underline{1}\,\underline{2}})\Big] \\ &= \sqrt{c^{\underline{2}}}\Big[C\ \exp(i\omega_k^{\underline{2}} T^{\underline{1}\,\underline{2}}) + D\ \exp(-i\omega_k^{\underline{2}} T^{\underline{1}\,\underline{2}})\Big]. \end{aligned} \tag{E.46}$$

The second junction condition $[\partial_T \theta] = 0$, after simplifying using the dispersion relation, now leads to

$$\begin{aligned} &\frac{1}{\sqrt{c^{\underline{1}}}}\Big[A\ \exp(i\omega_k^{\underline{1}} T^{\underline{1}\,\underline{2}}) - B\ \exp(-i\omega_k^{\underline{1}} T^{\underline{1}\,\underline{2}})\Big] \\ &= \frac{1}{\sqrt{c^{\underline{2}}}}\Big[C\ \exp(i\omega_k^{\underline{2}} T^{\underline{1}\,\underline{2}}) - D\ \exp(-i\omega_k^{\underline{2}} T^{\underline{1}\,\underline{2}})\Big]. \end{aligned} \tag{E.47}$$

Up to irrelevant phases, these are the same equations as were derived in laboratory time.

Now setting $A \to 1$, $B \to 0$, $C \to \alpha$, and $D \to \beta$ and the solving for α and β we find

$$\alpha = \frac{1}{2}\left(\sqrt{\frac{c^{\underline{1}}}{c^{\underline{2}}}} + \sqrt{\frac{c^{\underline{2}}}{c^{\underline{1}}}}\right) \exp(i[\omega_k^{\underline{1}} - \omega_k^{\underline{2}}] T^{\underline{1}\,\underline{2}}), \tag{E.48}$$

$$\beta = \frac{1}{2}\left(\sqrt{\frac{c^{\underline{1}}}{c^{\underline{2}}}} - \sqrt{\frac{c^{\underline{2}}}{c^{\underline{1}}}}\right) \exp(i[\omega_k^{\underline{1}} + \omega_k^{\underline{2}}] T^{\underline{1}\,\underline{2}}). \tag{E.49}$$

The phases on α and β are now slightly different, but this is not new physics — it has to do with the phases we picked for our “normalized modes” — these phases are now slightly different from the laboratory time calculation. Note the magnitudes are completely unambiguous:

$$|\alpha| = \frac{1}{2}\left|\sqrt{\frac{c^{\underline{1}}}{c^{\underline{2}}}} + \sqrt{\frac{c^{\underline{2}}}{c^{\underline{1}}}}\right|; \tag{E.50}$$

$$|\beta| = \frac{1}{2}\left|\sqrt{\frac{c^{\underline{1}}}{c^{\underline{2}}}} - \sqrt{\frac{c^{\underline{2}}}{c^{\underline{1}}}}\right|. \tag{E.51}$$

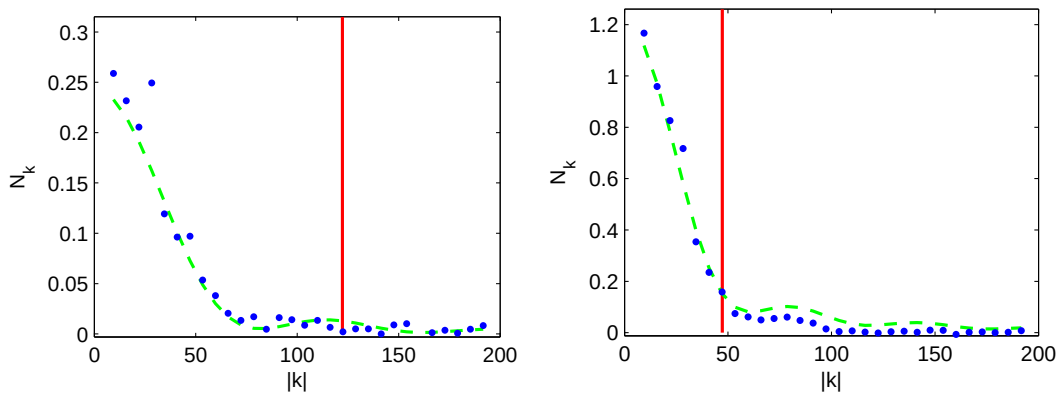
In short, this appendix has served to verify that the key technical parts of the calculation in Chapter 5 can mathematically be carried out in a number of different ways that ultimately lead to the same physical result.

APPENDIX F

Numerical results for rainbow inflation

The graphs in this appendix are bases on numerical work carried out by *Piyush Jain* as part of a close collaborative effort between the current author, Piyush Jain, Professor Crispin Gardiner, and Professor Matt Visser.

F.1 | Quasi-particle production during rainbow inflation for $t_s = 1 \times 10^{-4}$



(a) $t = 0.25 \times t_f$; $t_s = 1 \times 10^{-4}$.

(b) $t = 0.50 \times t_f$; $t_s = 1 \times 10^{-4}$.

(c) $t = 0.75 \times t_f$; $t_s = 1 \times 10^{-4}$.

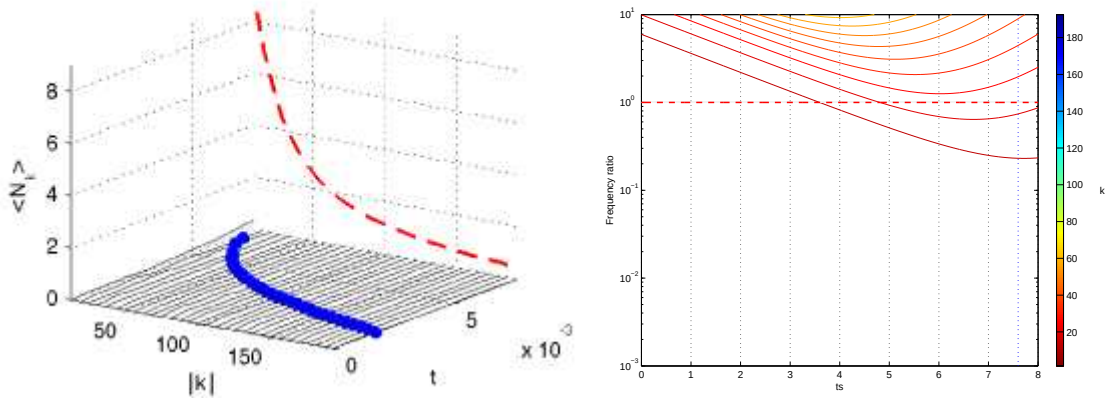
(d) $t = 1.00 \times t_f$; $t_s = 1 \times 10^{-4}$.

Figure F.1: The four figures show time-slices of the "quasi-particle" production N_k in a de Sitter like spacetime, for $t_s = 1 \times 10^{-4}$. The blue dots represent the actual data obtained from the simulations for a realistic Bose gas with time-dependent interaction-strength [113]. The dashed green line are the theoretical results for a finite de Sitter calculation obtained in the hydrodynamic limit, as presented in Sec. (6.4.3). The vertical red line indicates the borderline between the nature of the excitations: Everything to the left of the red line is phononic, while everything to right is trans-phononic/ free-particle like.

.

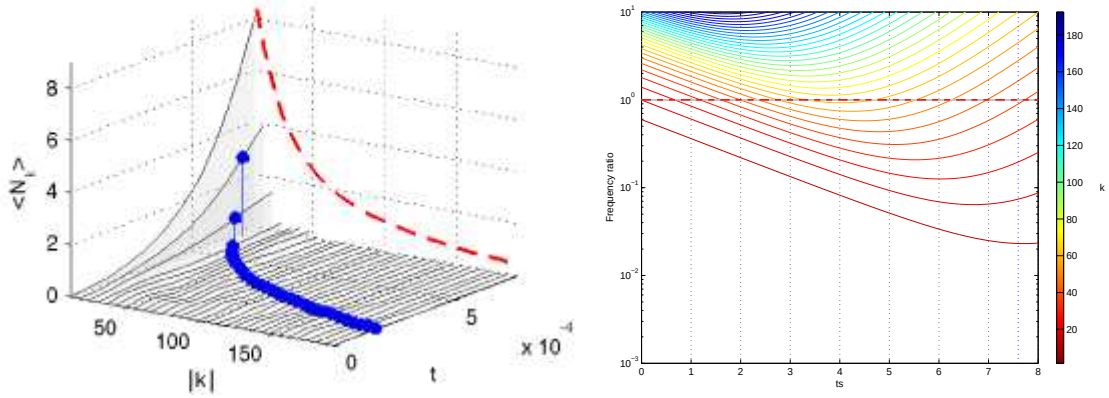
F.2 | Qualitative particle production in Bose gas

Figs. F.2 - F.5 compare the change in the mode occupation number in each mode on the left side (a), with frequency ratio $\mathcal{R}_k(t)$ of the mode on the right side (b). The different rows express different scaling times t_s. Each black line on the right hand side indicates the occupation number in the mode k as a function of time. (The red dashed line on the left had side indicates the sudden limit.) On the right hand side we have plotted the frequency ratio $\mathcal{R}_k(t)$ for each of those modes with a different color (online only) to indicate the energy difference of the modes; gradually changing from infrared modes (dark red), to ultraviolet modes (dark blue). The horizontal (red dashed) indicates where the frequency ratio $\mathcal{R}_k(t)$ is equal to one, while the vertical (blue dashed) line indicates end of the expansion time in our simulations. The blue dots in the figures to the left indicate when the modes cross over from phononic to trans-phononic behavior, or in other words start to decouple from the emergent spacetime. Roughly we can see that the blue dots are located where the frequency ratio has its minimum.



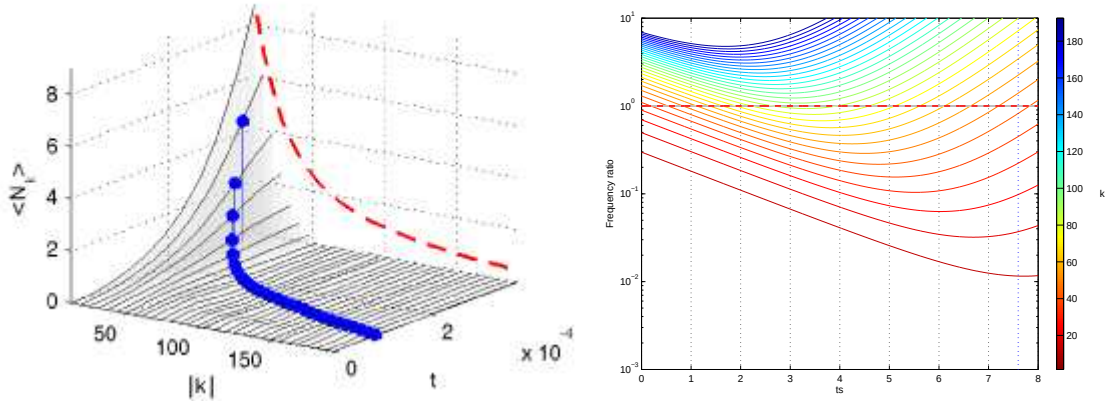
(a) (b)

Figure F.2: $t_s = 1 \times 10^{-3}$



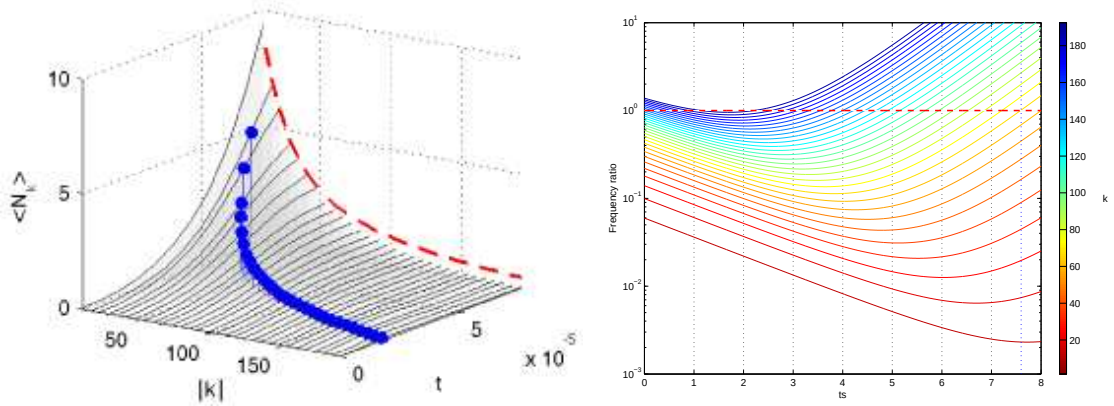
(a) (b)

Figure F.3: $t_s = 1 \times 10^{-4}$



(a) (b)

Figure F.4: $t_s = 5 \times 10^{-5}$



(a) (b)

Figure F.5: $t_s = 5 \times 10^{-5}$

Curriculum Vitae

2003-2007 PhD student at Victoria University of Wellington, New Zealand;
Project: *Emergent spacetimes*;
Supervisor: Prof. M. Visser;

2006 PhD completion scholarship from the Victoria University of Wellington.

2005 New Zealand Postgraduate Study Abroad Award, from Education New Zealand.

2003 Deutscher Akademischer Austauschdienst (DAAD) Gegenstipendium zur wissenschaftlichen Aus- und Fortbildung im Ausland. (Partial stipend for overseas studies.)

2003 Hartle Prize of the International Society on General Relativity and Gravitation. For one of the best student presentations at the 17th international conference on general relativity and gravitation (Dublin, Ireland).

2002-2003 Diplom thesis at the Max-Plank-Quantumoptics, Garching, Germany;
Thesis: *Simulation von Gravitationsobjekten im Bose-Einstein-Kondensat*;
Supervisor: Prof. J. I. Cirac;

1997-2002 Technical University of Munich, Germany undergraduate and graduate studies: General relativity, advanced quantum mechanics and theory of condensed matter physics.

Publications

Publications in Journals

- **Analogue model of an expanding FRW universe in Bose–Einstein condensates: Application of the classical field method**
 P. Jain, S. Weinfurtner, M. Visser, and C. Gardiner
 Accepted for publication in Phys. Rev. A
 [arXiv:gr-qc:cond-mat/0705.2077]

- **Naturalness in emergent spacetime**
 S. Liberati, M. Visser and S. Weinfurtner
 Phys. Rev. Lett. **96**, 151301 (2006)
 [arXiv:gr-qc/0512139]

- **Analogue quantum gravity phenomenology from a two-component Bose-Einstein condensate**
 S. Liberati, M. Visser and S. Weinfurtner
 Class. Quant. Grav. **23**, 3129 (2006)
 [arXiv:gr-qc/0510125]

- **Massive Klein-Gordon equation from a BEC-based analogue spacetime**
 M. Visser and S. Weinfurtner
 Phys. Rev. D **72**, 044020 (2005)
 [arXiv:gr-qc/0506029]

- **Generating perfect fluid spheres in general relativity**
 P. Boonserm, M. Visser and S. Weinfurtner
 Phys. Rev. D **71**, 124037 (2005)
 [arXiv:gr-qc/0503007]

- **Effective refractive index tensor for weak field gravity**
 P. Boonserm, C. Cattoen, T. Faber, M. Visser and S. Weinfurtner
 Class. Quant. Grav. **22**, 1905 (2005)
 [arXiv:gr-qc/0411034]

- **Vortex geometry for the equatorial slice of the Kerr black hole**
 M. Visser and S. E. C. Weinfurtner
 Class. Quant. Grav. **22**, 2493 (2005)
 [arXiv:gr-qc/0409014]

Articles under review

- **Trans-Planckian physics and signature change events in Bose gas hydrodynamics**
 S. Weinfurtner, A. White and M. Visser
 [arXiv:gr-qc/0703117]

- **Solution generating theorems for the TOV equation**
 P. Boonserm, M. Visser and S. Weinfurtner
 [arXiv:gr-qc/0607001]

Conference Proceedings

- **Analogue spacetime based on 2-component Bose-Einstein condensates**
 S. Weinfurtner, S. Liberati and M. Visser
 Lecture Notes in Physics **718**, (2006) [arXiv:gr-qc/0605121]

- **Solution generating theorems: perfect fluid spheres and the TOV equation**
 P. Boonserm, M. Visser and S. Weinfurtner
 [arXiv:gr-qc/0609099]
 To appear in the proceedings of 11th Marcel Grossmann Meeting on Recent Developments in Theoretical and Experimental General Relativity, Gravitation, and Relativistic Field Theories, Berlin, Germany, 23-29 Jul 2006

- **Solution generating theorems for perfect fluid spheres**
 P. Boonserm, M. Visser and S. Weinfurtner
 [arXiv:gr-qc/0609088]
 To appear in the proceedings of 12th Conference on Recent Developments in Gravity (NEB XII), Nafplio, Greece, 29 Jun - 2 Jul 2006

- **Modelling Planck-scale Lorentz violation via analogue models**
 S. Weinfurtner, S. Liberati and M. Visser
 J. Phys. Conf. Ser. **33**, 373 (2006) [arXiv:gr-qc/0512127]

- **Analogue model for quantum gravity phenomenology**
 S. Weinfurtner, S. Liberati and M. Visser
 J. Phys. A **39**, 6807 (2006) [arXiv:gr-qc/0511105]

Bibliography

[1] Milton Abramowitz and Irene A. Stegun. *Handbook of Mathematical Functions with Formulas, Graphs, and Mathematical Tables*. Dover, New York, ninth Dover printing, tenth GPO printing edition, 1964.

[2] Andreas Albrecht, Paul J. Steinhardt, Michael S. Turner, and Frank Wilczek. Reheating an inflationary universe. *Phys. Rev. Lett.*, 48:1437, 1982.

[3] G. Amelino-Camelia, J.R. Ellis, N.E. Mavromatos, D.V. Nanopoulos, and S. Sarkar. Potential sensitivity of gamma-ray burster observations to wave dispersion in vacuo. *Nature*, 393:763–765, 1998.

[4] Giovanni Amelino-Camelia and Tsvi Piran. Planck-scale deformation of Lorentz symmetry as a solution to the ultrahigh energy cosmic ray and the TeV-photon paradoxes. *Phys. Rev. D*, 64(3):036005, 2001.

[5] R. Balbinot, S. Fagnocchi, and A. Fabbri. Quantum effects in acoustic black holes: The back-reaction. *Phys. Rev.*, D71:064019, 2005.

[6] Roberto Balbinot, Serena Fagnocchi, Alessandro Fabbri, Sara Farese, and Jose Navarro-Salas. On the quantum stress tensor for extreme 2D Reissner–Nordstroem black holes. *Phys. Rev.*, D70:064031, 2004.

[7] Roberto Balbinot, Serena Fagnocchi, Alessandro Fabbri, and Giovanni P. Procopio. Backreaction in acoustic black holes. *Phys. Rev. Lett.*, 94:161302, 2005.

[8] B. Bao, S. S. Chern, and Z. Shen. *Finsler geometry*, volume 196. AMS Contemporary Mathematics, 1996.

[9] B. Bao, S. S. Chern, and Z. Shen. *An Introduction to Riemann–Finsler Geometry*. Springer-Verlag, 2000.

[10] Carlos Barceló, Stefano Liberati, Sebastiano Sonego, and Matt Visser. Causal structure of acoustic spacetimes. *New Journal of Physics*, 6:186, 2004.

[11] Carlos Barceló, Stefano Liberati, Sebastiano Sonego, and Matt Visser. Quasi-particle creation by analogue black holes. *Class. Quant. Grav.*, 23:5341–5366, 2006.

[12] Carlos Barceló, Stefano Liberati, and Matt Visser. Analog gravity from Bose-Einstein condensates. *Class. Quant. Grav.*, 18:1137, 2001.

[13] Carlos Barceló, Stefano Liberati, and Matt Visser. Analog gravity from field theory normal modes? *Class. Quant. Grav.*, 18:3595–3610, 2001.

[14] Carlos Barceló, Stefano Liberati, and Matt Visser. Refringence, field theory, and normal modes. *Class. Quant. Grav.*, 19:2961–2982, 2002.

[15] Carlos Barceló, Stefano Liberati, and Matt Visser. Analogue models for FRW cosmologies. *Int. J. Mod. Phys.*, D12:1641–1650, 2003.

[16] Carlos Barceló, Stefano Liberati, and Matt Visser. Probing semiclassical analogue gravity in Bose–Einstein condensates with widely tunable interactions. *Phys. Rev.*, A68:053613, 2003.

[17] Carlos Barceló, Stefano Liberati, and Matt Visser. Towards the observation of Hawking radiation in Bose–Einstein condensates. *Int. J. Mod. Phys.*, A18:3735, 2003.

[18] Carlos Barceló, Stefano Liberati, and Matt Visser. Analogue gravity. *Living Rev. Rel.*, 8:12, 2005.

[19] Carlos Barceló, Matt Visser, and Stefano Liberati. Einstein gravity as an emergent phenomenon? *Int. J. Mod. Phys.*, D10:799–806, 2001.

[20] James M. Bardeen. Gauge-invariant cosmological perturbations. *Phys. Rev. D*, 22(8):1882–1905, Oct 1980.

[21] Soumen Basak. Analog of superradiance effect in BEC. gr-qc/0501097, 2005.

[22] Soumen Basak and Parthasarathi Majumdar. Reflection coefficient for superresonant scattering. *Classical and Quantum Gravity*, 20:2929, 2003.

[23] Soumen Basak and Parthasarathi Majumdar. 'Superresonance' from a rotating acoustic black hole. *Classical and Quantum Gravity*, 20:3907, 2003.

[24] Mar Bastero-Gil and Laura Mersini-Houghton. Equation of state of the transplanckian dark energy and the coincidence problem. *Phys. Rev.*, D67:103519, 2003.

[25] J. D. Bekenstein. Black holes and the second law. *Nuovo Cim. Lett.*, 4:737–740, 1972.

[26] Jacob D. Bekenstein. Black holes and entropy. *Phys. Rev.*, D7:2333–2346, 1973.

[27] Francesco Belgiorno, Stefano Liberati, Matt Visser, and Dennis W. Sciama. Sonoluminescence: Two-photon correlations as a test of thermality. *Phys. Lett.*, A271:308–313, 2000.

[28] Jeremy Bernstein and Scott Dodelson. Relativistic Bose gas. *Phys. Rev. Lett.*, 66(6):683–686, Feb 1991.

[29] N. D. Birrell and P. C. W. Davies. *Quantum fields in curved space*. Cambridge Monographs on Mathematical Physics. Cambridge University Press, Cambridge, 1984.

[30] Immanuel Felix Bloch. *Atomlaser und Phasenkohärenz atomarer Bose–Einstein-Kondensate*. in german, LMU Munich: Faculty of Physics, 2000.

[31] Petarpa Boonserm, Celine Cattoen, Tristan Faber, Matt Visser, and Silke Weinfurtner. Effective refractive index tensor for weak field gravity. *Class. Quant. Grav.*, 22:1905–1916, 2005.

[32] Petarpa Boonserm, Matt Visser, and Silke Weinfurtner. Generating perfect fluid spheres in general relativity. *Phys. Rev.*, D71:124037, 2005.

[33] Petarpa Boonserm, Matt Visser, and Silke Weinfurtner. Solution generating theorems: perfect fluid spheres and the TOV equation. *gr-qc/0609099*, 2006.

[34] Robert H. Boyer and Richard W. Lindquist. Maximal analytic extension of the Kerr metric. *J. Math. Phys.*, 8(265-281), 1967.

[35] Robert Brandenberger, Ronald Kahn, and William H. Press. Cosmological perturbations in the early universe. *Phys. Rev. D*, 28(8):1809–1821, Oct 1983.

[36] R. Brout, S. Massar, R. Parentani, and P. Spindel. Hawking radiation without trans-Planckian frequencies. *Phys. Rev.*, D52:4559–4568, 1995.

[37] C.P. Burgess, J.M. Cline, E. Filotas, J. Matias, and G.D. Moore. Loop-generated bounds on changes to the graviton dispersion relation. *J. High Energy Phys.*, 2002(03), 2002.

[38] E. A. Calzetta and B. L. Hu. Bose–Einstein condensate collapse and dynamical squeezing of vacuum fluctuations. *Phys. Rev. A*, 68(043625), 2003.

[39] E. A. Calzetta and B. L. Hu. Early universe quantum processes in BEC collapse experiments. *Int. J. Theor. Phys.*, 44:1691–1704, 2005.

[40] B. J. Carr and S. W. Hawking. Black holes in the early universe. *Mon. Not. Roy. Astron. Soc.*, 168:399–415, 1974.

[41] E. Cartan. Les espaces de Finsler. *Act. scient. et ind.*, 79, 1934.

[42] Yvan Castin. Bose–Einstein condensates in atomic gases: Simple theoretical results. *cond-mat/0105058*, page 1, 2001.

[43] Celine Cattöen and Matt Visser. Cosmography: Extracting the Hubble series from the supernova data. *gr-qc/0703122*, 2007.

[44] S. Chandrasekhar. *Liquid Crystals*. Cambridge University Press, 1992.

[45] Peter J. Collings and Michael Hird. *Introduction to Liquid Crystals: Chemistry and Physics*. Taylor & Francis, 1997.

[46] John Collins, Alejandro Perez, Daniel Sudarsky, Luis Urrutia, and Hector Vucetich. Lorentz invariance and quantum gravity: An additional fine-tuning problem? *Physical Review Letters*, 93(19):191301, 2004.

[47] R. Courant and D. Hilbert. *Methods of Mathematical Physics*, volume 2. Wiley-Interscience, 1989.

[48] Tapas K. Das. Analogue Hawking radiation from astrophysical black hole accretion. *Classical and Quantum Gravity*, 22:2971, 2005.

[49] Tapas Kumar Das. Transonic black hole accretion as analogue system. gr-qc/0411006, 2004.

[50] R. A. D'Inverno. *Introducing Einstein's relativity*. Oxford University Press, 1992.

[51] Scott Dodelson. *Modern cosmology*. Academic Press, 2003. 440 pp.

[52] Elizabeth A. Donley, Neil R. Claussen, Simon L. Cornish, Jacob L. Roberts, Eric A. Cornell, and Carl E. Wieman. Dynamics of collapsing and exploding Bose–Einstein condensates. *Nature*, 412(6844):295–299, 2001.

[53] Chris Doran. A new form of the Kerr solution. *Physical Review D*, 61:067503, 2000.

[54] T. Dray, C. A. Manogue, and R. Kulkarni. Scalar field quantization in stationary, nonstatic space- times. *Gen. Rel. Grav.*, 24:1255–1266, 1992.

[55] T. Dray, C. A. Manogue, and R. W. Tucker. Particle production from signature change. *Gen. Rel. Grav.*, 23:967–971, 1991.

[56] Tevian Dray. Einstein's equations in the presence of signature change. *J. Math. Phys.*, 37:5627–5636, 1996.

[57] Tevian Dray. General relativity and signature change. In *Advances in Differential Geometry and General Relativity*, volume 359. American Mathematical Society, 2004.

[58] Tevian Dray, George Ellis, and Charles Hellaby. Note on signature change and colombeau theory. *Gen. Rel. Grav.*, 33:1041–1046, 2001.

[59] Tevian Dray, George Ellis, Charles Hellaby, and Corinne A. Manogue. Gravity and signature change. *Gen. Rel. Grav.*, 29:591–597, 1997.

[60] Tevian Dray and Charles Hellaby. The patchwork divergence theorem. *J. Math. Phys.*, 35:5922–5929, 1994.

[61] Tevian Dray and Charles Hellaby. Comment on 'smooth and discontinuous signature type change in general relativity'. gr-qc/9610062, 1996.

[62] Tevian Dray, Corinne A. Manogue, and Robin W. Tucker. The scalar field equation in the presence of signature change. *Phys. Rev.*, D48:2587–2590, 1993.

[63] Tevian Dray, Corinne A. Manogue, and Robin W. Tucker. Boundary conditions for the scalar field in the presence of signature change. *Class. Quant. Grav.*, 12:2767–2778, 1995.

[64] R. A. Duine and H. T. C. Stoof. Quantum evaporation of a Bose–Einstein condensate. *cond-mat/0204529*, 2002.

[65] Albert Einstein. The field equations of gravitation. *Sitzungsber. Preuss. Akad. Wiss. Berlin (Math. Phys.)*, 1915:844–847, 1915.

[66] Albert Einstein. On the general theory of relativity. *Sitzungsber. Preuss. Akad. Wiss. Berlin (Math. Phys.)*, 1915:778–786, 1915.

[67] Albert Einstein. The foundation of the general theory of relativity. *Annalen Phys.*, 49:769–822, 1916.

[68] G Ellis, A Sumeruk, D Coule, and C Hellaby. Change of signature in classical relativity. *Classical and Quantum Gravity*, 9(6):1535–1554, 1992.

[69] J.R. Ellis, N.E. Mavromatos, and D.V. Nanopoulos. Probing models of quantum space-time foam. gr-qc/9909085, 1999.

[70] Petr O. Fedichev and Uwe R. Fischer. Gibbons–Hawking effect in the sonic de Sitter space-time of an expanding Bose–Einstein-condensed gas. *Physical Review Letters*, 91:240407, 2003.

[71] Petr O. Fedichev and Uwe R. Fischer. 'Cosmological' particle production in oscillating ultracold Bose gases: The role of dimensionality. *Phys. Rev.*, A69:033602, 2004.

[72] Petr O. Fedichev and Uwe R. Fischer. Observing quantum radiation from acoustic horizons in linearly expanding cigar-shaped Bose–Einstein condensates. *Phys. Rev.*, D69:064021, 2004.

[73] P. Finsler. Über Kurven und Flächen in allgemeinen Räumen. *The Mathematical Gazette*, 36(318):292–293, Dec. 1952.

[74] Uwe R. Fischer. Quasiparticle universes in Bose–Einstein condensates. *Mod. Phys. Lett.*, A19:1789–1812, 2004.

[75] Uwe R. Fischer and Ralf Schützhold. Quantum simulation of cosmic inflation in two-component Bose–Einstein condensates. *Phys. Rev.*, A70:063615, 2004.

[76] Uwe R. Fischer and Matt Visser. On the space-time curvature experienced by quasiparticle excitations in the Painléve–Gullstrand effective geometry. *Ann. Phys.*, 304:22–39, 2003.

[77] Stephen A. Fulling. *Aspects of quantum field theory in curved space-time*, volume 17 of *London Mathematical Society Student Texts*. Cambridge University Press, Cambridge, 1989.

[78] R. Gambini and J. Pullin. Nonstandard optics from quantum space-time. *Phys. Rev. D*, 59:1–4, 1999.

[79] Alcides Garat and Richard H. Price. Nonexistence of conformally flat slices of the Kerr space-time. *Phys. Rev. D*, 61(12):124011, May 2000.

[80] L. J. Garay. Private comunications.

[81] L. J. Garay, J. R. Anglin, J. I. Cirac, and P. Zoller. Black holes in Bose–Einstein condensates. *Phys. Rev. Lett.*, 85:4643–4647, 2000.

[82] L. J. Garay, J. R. Anglin, J. I. Cirac, and P. Zoller. Sonic black holes in dilute Bose–Einstein condensates. *Phys. Rev.*, A63:023611, 2001.

[83] Crispin Gardiner and Peter Zoller. *Quantum Noise*. Springer Series in Synergetics. Springer, Berlin, 2nd edition, 2000.

[84] J. Gariel, M. A. H. MacCallum, G. Marcilhacy, and N. O. Santos. Kerr geodesics, the Penrose process and jet collimaton by a black hole. *gr-qc/0702123*, 2007.

[85] G.W. Gibbons and S.W. Hawking. Cosmological event horizons, thermodynamics, and particle creation. *Phys. Rev. D*, 15(10):2738, May 1977.

[86] Kostas Glampedakis and Nils Andersson. Scattering of scalar waves by rotating black holes. *Class. Quant. Grav.*, 18:1939–1966, 2001.

[87] Hock-Seng Goh, Markus A. Luty, and Siew-Phang Ng. Supersymmetry without supersymmetry. *Journal of High Energy Physics*, 2005(01):040, 2005.

[88] Alan H. Guth. Inflationary universe: A possible solution to the horizon and flatness problems. *Phys. Rev. D*, 23(2):347–356, Jan 1981.

[89] Andrew J. S. Hamilton and Jason P. Lisle. The river model of black holes. gr-qc/0411060, 2004.

[90] J. B. Hartle and S. W. Hawking. Wave function of the universe. *Phys. Rev. D*, 28(12):2960–2975, Dec 1983.

[91] S. W. Hawking. Black hole explosions. *Nature*, 248:30–31, 1974.

[92] S. W. Hawking. The development of irregularities in a single bubble inflationary universe. *Phys. Lett.*, B115:295, 1982.

[93] B. L. Hu. Can spacetime be a condensate? *Int. J. Theor. Phys.*, 44:1785–1806, 2005.

[94] B. L. Hu and E. A. Calzetta. BEC collapse, particle production and squeezing of the vacuum. cond-mat/0208569, 2002.

[95] S. Inouye, M. R. Andrews, J. Stenger, H. J. Miesner, D. M. Stamper-Kurn, and W. Ketterle. Observation of Feshbach resonances in a Bose–Einstein condensate. *Nature*, 392:152–154, 1998.

[96] C. J. Isham. Quantum gravity. *Proceedings of the Royal Society of London. Series A, Mathematical and Physical Sciences*, 368(1732):33–36, sep 1979.

[97] C. J. Isham, R. Penrose, and D. W. Sciama, editors. *Quantum Gravity — an overview.* Quantum Gravity: an Oxford Symposium, Clarendon Press, Oxford, England, 1975.

[98] B R Iyer and A Kumar. The Kerr black hole in thermal equilibrium and the ν vacuum. *Journal of Physics A: Mathematical and General*, 12(10):1795–1803, 1979.

[99] T. Jacobson, S. Liberati, and D. Mattingly. A strong astrophysical constraint on the violation of special relativity by quantum gravity. *Nature*, 424:1019–1021, March 2003.

[100] T. Jacobson, S. Liberati, and D. Mattingly. Threshold effects and Planck scale Lorentz violation: Combined constraints from high energy astrophysics. *Phys. Rev. D*, 67(12):124011, Jun 2003.

[101] T. Jacobson, S. Liberati, D. Mattingly, and F. W. Stecker. New limits on Planck scale Lorentz violation in QED. *Physical Review Letters*, 93(2):021101, 2004.

[102] T. A. Jacobson and G. E. Volovik. Effective spacetime and Hawking radiation from moving domain wall in thin film of He-3-A. *Pisma Zh. Eksp. Teor. Fiz.*, 68:833–838, 1998.

[103] T. A. Jacobson and G. E. Volovik. Event horizons and ergoregions in he-3. *Phys. Rev.*, D58:064021, 1998.

[104] Ted Jacobson. Black hole radiation in the presence of a short distance cutoff. *Phys. Rev.*, D48:728–741, 1993.

[105] Ted Jacobson. Thermodynamics of space-time: The Einstein equation of state. *Phys. Rev. Lett.*, 75:1260–1263, 1995.

[106] Ted Jacobson. Trans-Planckian redshifts and the substance of the space-time river. *Prog. Theor. Phys. Suppl.*, 136:1–17, 1999.

[107] Ted Jacobson. Introduction to quantum fields in curved spacetime and the Hawking effect. gr-qc/0308048, 2003.

[108] Ted Jacobson and Gungwon Kang. Conformal invariance of black hole temperature. *Classical and Quantum Gravity*, 10:L201, 1993.

[109] Ted Jacobson and Tatsuhiko Koike. Black hole and baby universe in a thin film of He-3-A. *cond-mat/0205174*, 2000.

[110] Ted Jacobson, Stefano Liberati, and David Mattingly. Tev astrophysics constraints on planck scale lorentz violation. *Phys. Rev. D*, 66(8):081302, Oct 2002.

[111] Ted Jacobson, Stefano Liberati, and David Mattingly. Lorentz violation at high energy: Concepts, phenomena and astrophysical constraints. *Annals Phys*, 321:150, 2006.

[112] Theodore Jacobson. Black hole evaporation and ultrashort distances. *Phys. Rev.*, D44:1731–1739, 1991.

[113] Piyush Jain, Silke Weinfurtner, Matt Visser, and Crispin Gardiner. Analogue model of an expanding FRW universe in Bose–Einstein condensates: Application of the classical field method. arXiv:0705.2077, 2006.

[114] Stewart D. Jenkins and T. A. B. Kennedy. Dynamic stability of dressed condensate mixtures. *Phys. Rev. A*, 68(5):053607, Nov 2003.

[115] Stewart D. Jenkins and T. A. Brian Kennedy. Spin squeezing in a driven Bose–Einstein condensate. *Phys. Rev. A*, 66(4):043621, Oct 2002.

[116] Qing-Quan Jiang and Shuang-Qing Wu. Hawking radiation from rotating black holes in anti-de Sitter spaces via gauge and gravitational anomalies. *Physics Letters B*, 647:200, 2007.

[117] Simon Judes and Matt Visser. Conservation laws in doubly special relativity. *Phys. Rev.*, D68:045001, 2003.

[118] Roy P. Kerr. Gravitational field of a spinning mass as an example of algebraically special metrics. *Phys. Rev. Lett.*, 11(5):237–238, Sep 1963.

[119] V.A. Kostelecký and S. Samuel. Spontaneous breaking of Lorentz symmetry in string theory. *Phys. Rev. D*, 39:683–685, 1989.

[120] J. A. Valiente Kroon. Asymptotic expansions of the Cotton–York tensor on slices of stationary spacetimes. *Classical and Quantum Gravity*, 21:3237, 2004.

[121] Juan A. Valiente Kroon. On the nonexistence of conformally flat slices in the Kerr and other stationary spacetimes. gr-qc/0310048, 2003.

[122] Ulf Leonhardt. Space-time geometry of quantum dielectrics. physics/0001064, 2000.

[123] Samuel Lepe and Joel Saavedra. Quasinormal modes, superradiance and area spectrum for 2+1 acoustic black holes. *Phys. Lett.*, B617:174–181, 2005.

[124] S. Liberati, F. Belgiorno, Matt Visser, and D. W. Sciama. Sonoluminescence as a QED vacuum effect. *J. Phys.*, A33:2251–2272, 2000.

[125] S. Liberati, Matt Visser, F. Belgiorno, and D. W. Sciama. Sonoluminescence and the QED vacuum. quant-ph/9904008, 1998.

[126] S. Liberati, Matt Visser, F. Belgiorno, and D. W. Sciama. Sonoluminescence: Bogolubov coefficients for the QED vacuum of a collapsing bubble. *Phys. Rev. Lett.*, 83:678–681, 1999.

[127] S. Liberati, Matt Visser, F. Belgiorno, and D. W. Sciama. Sonoluminescence as a QED vacuum effect. 1: The physical scenario. *Phys. Rev.*, D61:085023, 2000.

[128] S. Liberati, Matt Visser, F. Belgiorno, and D. W. Sciama. Sonoluminescence as a QED vacuum effect. 2: Finite volume effects. *Phys. Rev.*, D61:085024, 2000.

[129] Stefano Liberati, Sebastiano Sonego, and Matt Visser. Interpreting doubly special relativity as a modified theory of measurement. *Phys. Rev.*, D71:045001, 2005.

[130] Stefano Liberati, Matt Visser, and Silke Weinfurtner. Analogue quantum gravity phenomenology from a two-component Bose–Einstein condensate. *Class. Quant. Grav.*, 23:3129–3154, 2006.

[131] Stefano Liberati, Matt Visser, and Silke Weinfurtner. Naturalness in emergent spacetime. *Phys. Rev. Lett.*, 96:151301, 2006.

[132] James E. Lidsey. Cosmic Dynamics of Bose–Einstein Condensates. *Classical and Quantum Gravity*, 21:777, 2004.

[133] A.P. Lightman and D.L. Lee. Restricted proof that the weak equivalence principle implies the Einstein equivalence principle. *Phys. Rev. D*, 8:364–376, 1973.

[134] A. D. Linde. *Particle Physics and Inflationary Cosmology*. Harwood Academic Publishers, Chur, Switzerland, 1990.

[135] Joao Magueijo and Lee Smolin. Gravity's rainbow. *Classical and Quantum Gravity*, 21:1725, 2004.

[136] R. Mansouri and R.U. Sexl. A test theory of special relativity. i - simultaneity and clock synchronization. *Gen. Relativ. Gravit.*, 8:497–513, 1977.

[137] Jerome Martin and Robert Brandenberger. On the dependence of the spectra of fluctuations in inflationary cosmology on trans-Planckian physics. *Phys. Rev.*, D68:063513, 2003.

[138] David Mattingly. Modern tests of Lorentz invariance. *Living Reviews in Relativity*, 8(5), 2005.

[139] Laura Mersini-Houghton, Mar Bastero-Gil, and Panagiota Kanti. Relic dark energy from trans-Planckian regime. *Phys. Rev.*, D64:043508, 2001.

[140] Charles W. Misner, Kip S. Thorne, and John A. Wheeler. *Gravitation*. W. H. Freeman, September 1973.

[141] V. F. Mukhanov and S. Winitzki. *Introduction to Quantum Fields in Classical Backgrounds*. Cambridge University Press, 1 edition, July 31 2007.

[142] Robert C. Myers and Maxim Pospelov. Ultraviolet modifications of dispersion relations in effective field theory. *Phys. Rev. Lett.*, 90(21):211601, May 2003.

[143] Jens C. Niemeyer. Inflation with a high frequency cutoff. *Phys. Rev.*, D63:123502, 2001.

[144] M. Novello, M. Visser, and G. Volovik. *Artificial Black Holes*. World Scientific, Singapore; River Edge, U.S.A., 2002.

[145] L. Parker. Particle creation in expanding universes. *Phys. Rev. Lett.*, 21(8):562–564, Aug 1968.

[146] Leonard Parker. Quantized fields and particle creation in expanding universes. 1. *Phys. Rev.*, 183(5):1057–1068, Jul 1969.

[147] Leonard Parker. Quantized fields and particle creation in expanding universes. 2. *Phys. Rev. D*, 3(10):2546, May 1971.

[148] R. Penrose. Gravitational collapse: The role of general relativity. *Riv. Nuovo Cim.*, 1:252–276, 1969.

[149] Santiago Esteban Perez Bergliaffa, Katrina Hibberd, Michael Stone, and Matt Visser. Wave equation for sound in fluids with vorticity. *Physica D*, 191:121–136, 2004.

[150] Michael E. Peskin and Daniel V. Schroeder. *An introduction to quantum field theory*. Addison-Wesley Publishing Company Advanced Book Program, Reading, MA, 1995. Edited and with a foreword by David Pines.

[151] C. J. Pethick and H. Smith. *Bose–Einstein Condensation in Dilute Gases*. Cambridge University Press, 2001.

[152] Allan D. Pierce. Wave equation for sound in fluids with unsteady inhomogeneous flow. *The Journal of the Acoustical Society of America*, 87(6):2292–2299, 1990.

[153] Eric Poisson. *A relativist's toolkit*. Cambridge University Press, Cambridge, 2004. The mathematics of black-hole mechanics.

[154] B Riemann. Ueber die hypothesen, welche der geometrie zu grunde liegen. *Abhandlungen der Königlichen Gesellschaft der Wissenschaften zu Göttingen*, 13, 1867.

[155] B Riemann. On the hypotheses which lie at the bases of geometry. *Nature, Vol. VIII. Nos. 183, 184, pp. 14–17, 36, 37.*, (Translater: W. K. Clifford), 1873.

[156] J. L. Roberts, N. R. Claussen, S. L. Cornish, E. A. Donley, E. A. Cornell, and C. E. Wieman. Controlled collapse of a Bose–Einstein condensate. *Phys. Rev. Lett.*, 86(19):4211–4214, May 2001.

[157] H. Robertson. Postulate versus observation in the special theory of relativity. *Rev. Mod. Phys.*, 21:378, 1949.

[158] Tony Rothman and George F. R. Ellis. Lost horizons. *Am. J. Phys.*, 61(93), 1993.

[159] H. Rund. *The differential geometry of Finsler spaces*. Springer- Verlag, 1959.

[160] A. D. Sakharov. Vacuum quantum fluctuations in curved space and the theory of gravitation. *Sov. Phys. Dokl.*, 12:1040–1041, 1968.

[161] R. Schützhold and W.G. Unruh. Hawking radiation in an electromagnetic waveguide? *Phys. Rev. Lett.*, 95:1–4, 2005.

[162] Ralf Schützhold. Dynamical zero-temperature phase transitions and cosmic inflation / deflation. *Phys. Rev. Lett.*, 95:135703, 2005.

[163] Ralf Schützhold. On the detectability of quantum radiation in Bose–Einstein condensates. *quant-ph/0602180*, 2006.

[164] Ralf Schützhold, Michael Uhlmann, Yan Xu, and Uwe R. Fischer. Quantum back-reaction in dilute Bose–Einstein condensates. *Phys. Rev.*, D72:105005, 2005.

[165] Ralf Schützhold and W. G. Unruh. Quantum analogues: From phase transitions to black holes and cosmology. *Lecture Notes in Physics*, 718, 2007.

[166] Ralf Schützhold and William G. Unruh. Gravity wave analogs of black holes. *Phys. Rev.*, D66:044019, 2002.

[167] Z. Shen. *Lectures on Finsler Geometry*. World Scientific, 2001.

[168] T. R. Slatyer and C. M. Savage. Superradiant scattering from a hydrodynamic vortex. *Classical and Quantum Gravity*, 22:3833, 2005.

[169] M. Trippenbach, K. Goral, K. Rzazewski, B. A. Malomed, and Y. B. Band. Structure of binary Bose–Einstein condensates. *J.PHYS.B*, 33:4017, 2000.

[170] Michael S. Turner, Martin White, and James E. Lidsey. Tensor perturbations in inflationary models as a probe of cosmology. *Phys. Rev. D*, 48(10):4613–4622, Nov 1993.

[171] Michael Uhlmann, Yan Xu, and Ralf Schützhold. Aspects of cosmic inflation in expanding Bose–Einstein condensates. *New J. Phys.*, 7:248, 2005.

[172] W. G. Unruh. Notes on black hole evaporation. *Phys. Rev.*, D14:870, 1976.

[173] W. G. Unruh. Experimental black hole evaporation. *Phys. Rev. Lett.*, 46:1351–1353, 1981.

[174] W. G. Unruh. Dumb holes and the effects of high frequencies on black hole evaporation. gr-qc/9409008, 1994.

[175] W. G. Unruh. Sonic analogue of black holes and the effects of high frequencies on black hole evaporation. *Phys. Rev. D*, 51(6):2827–2838, Mar 1995.

[176] W. G. Unruh and R. Schützhold. On slow light as a black hole analogue. *Phys. Rev.*, D68:024008, 2003.

[177] William G. Unruh and Ralf Schützhold. On the universality of the Hawking effect. *Physical Review D*, 71:024028, 2005.

[178] Matt Visser. Acoustic propagation in fluids: An unexpected example of Lorentzian geometry. *gr-qc/9311028*, 1993.

[179] Matt Visser. Acoustic black holes. gr-qc/9901047, 1998.

[180] Matt Visser. Acoustic black holes: Horizons, ergospheres, and Hawking radiation. *Class. Quant. Grav.*, 15:1767–1791, 1998.

[181] Matt Visser. Hawking radiation without black hole entropy. *Phys. Rev. Lett.*, 80:3436–3439, 1998.

[182] Matt Visser. Some general bounds for 1-D scattering. *Phys. Rev.*, A59:427–438, 1999.

[183] Matt Visser. Sakharov's induced gravity: A modern perspective. *Mod. Phys. Lett.*, A17:977–992, 2002.

[184] Matt Visser. Essential and inessential features of Hawking radiation. *Int. J. Mod. Phys.*, D12:649–661, 2003.

[185] Matt Visser, Carlos Barceló, and Stefano Liberati. Acoustics in Bose-Einstein condensates as an example of broken Lorentz symmetry. hep-th/0109033, 2001.

[186] Matt Visser, Carlos Barceló, and Stefano Liberati. Bi-refringence versus bi-metricity. *gr-qc/0204017*, 2002.

[187] Matt Visser and S. E. Ch. Weinfurtner. Vortex geometry for the equatorial slice of the Kerr black hole. *Class. Quant. Grav.*, 22:2493–2510, 2005.

[188] Matt Visser and Silke Weinfurtner. Massive phonon modes from a BEC-based analog model. *cond-mat/0409639*, 2004.

[189] Matt Visser and Silke Weinfurtner. Massive Klein–Gordon equation from a BEC-based analogue spacetime. *Phys. Rev.*, D72:044020, 2005.

[190] J. M. Vogels, C. C. Tsai, R. S. Freeland, S. J. J. M. F. Kokkelmans, B. J. Verhaar, and D. J. Heinzen. Prediction of Feshbach resonances in collisions of ultracold rubidium atoms. *Phys. Rev. A*, 56:1067, 1997.

[191] G. E. Volovik. Is there analogy between quantized vortex and black hole? gr-qc/9510001, 1995.

[192] G. E. Volovik. Cosmology, particle physics and superfluid he-3. *Czech. J. Phys.*, 46:3048, 1996.

[193] G. E. Volovik. Superfluid analogies of cosmological phenomena. *Phys. Rept.*, 351:195–348, 2001.

[194] Grigory Volovik. From quantum hydrodynamics to quantum gravity. gr-qc/0612134, 2006.

[195] Grigory E. Volovik. *The universe in a Helium droplet*. International Series of Monographs on Physics. Oxford University Press, Jun 1 2003.

[196] R. M. Wald. *General Relativity*. Chicago university press, Chicago, 1984.

[197] Robert M. Wald. The thermodynamics of black holes. *LIVING REV.REL.*, 4:6, 2001.

[198] Silke Weinfurtner. Simulation of gravitational objects in Bose–Einstein condensates. (In German). gr-qc/0404022, 2004.

[199] Silke Weinfurtner. Analogue model for an expanding universe. *General Relativity and Gravitation*, 37(9):1549–1554, 2005.

[200] Silke Weinfurtner, Stefano Liberati, and Matt Visser. Analogue model for quantum gravity phenomenology. *J. Phys.*, A39:6807–6814, 2006.

[201] Silke Weinfurtner, Stefano Liberati, and Matt Visser. Analogue spacetime based on 2-component Bose–Einstein condensates. In R. Schützhold and W. G. Unruh, editors, *Quantum Analogues: From Phase Transitions to Black Holes and Cosmology*, volume 718. Lecture Notes in Physics, 2006.

[202] Silke Weinfurtner, Stefano Liberati, and Matt Visser. Modelling Planck-scale Lorentz violation via analogue models. *J. Phys. Conf. Ser.*, 33:373–385, 2006.

[203] Silke Weinfurtner, Angela White, and Matt Visser. Trans-Planckian physics and signature change events in Bose gas hydrodynamics. gr-qc/0703117, 2007.

[204] Reva Kay Williams. Extracting X rays, γ rays, and relativistic e^-e^+ pairs from supermassive Kerr black holes using the Penrose mechanism. *Phys. Rev. D*, 51(10):5387–5427, May 1995.

[205] Reva Kay Williams. Collimated escaping vortical polar e^-e^+ jets intrinsically produced by rotating black holes and Penrose processes. *The Astrophysical Journal*, 611:952, 2004.

[206] Elizabeth Winstanley. On classical super-radiance in Kerr–Newman-anti-de Sitter black holes. *Phys. Rev.*, D64:104010, 2001.

[207] A. Zee. *Quantum field theory in a nutshell*. Princeton University Press, Princeton, NJ, 2003.